NOVA SCHOOL OF SCIENCE & TECHNOLOGY

DEPARTMENT OF CIVIL ENGINEERING

# ECO-EFFICIENT PLASTERS FOR INCREASED INDOOR AIR QUALITY AND COMFORT

ALESSANDRA RANESI

Master in Architecture and Building Engineering

DOCTORATE IN CIVIL ENGINEERING

NOVA University Lisbon

OCTOBER 2023

NOVA SCHOOL OF SCIENCE & TECHNOLOGY

DEPARTMENT OF CIVIL ENGINEERING

# ECO-EFFICIENT PLASTERS FOR INCREASED INDOOR AIR QUALITY AND COMFORT

**ALESSANDRA RANESI**

Master in Architecture and Building Engineering

**Adviser:** Maria Paulina Santos Forte de Faria Rodrigues
*Associate Professor, NOVA School of Science and Technology, NOVA University Lisbon*

**Co-advisers:** Maria do Rosário da Silva Veiga
*Principal Researcher, Nacional Laboratory for Civil Engineering*

**Examination Committee:**

**Chair:** Rodrigo de Moura Gonçalves
*Full Professor, NOVA School of Science and Technology, NOVA University Lisbon*

**Rapporteurs:** Nuno Manuel Monteiro Ramos
*Associate Professor with Habilitation, University of Porto*

Ana Luisa Lomelino Velosa
*Associate Professor with Habilitation, University of Aveiro*

**Adviser:** Maria Paulina Santos Forte de Faria Rodrigues
*Associate Professor, NOVA School of Science and Technology, NOVA University Lisbon*

**Members:** António Santos Silva
*Senior Researcher, Nacional Laboratory for Civil Engineering*

Rodrigo de Moura Gonçalves
*Full Professor, NOVA School of Science and Technology, NOVA University Lisbon*

Luís Gonçalo Correia Baltazar
*Assistant Professor, NOVA School of Science and Technology, NOVA University Lisbon*

Maria Teresa Freire
*Head of R&D, CERIS and SIVAL - Gessos Especiais*

DOCTORATE IN CIVIL ENGINEERING

NOVA University Lisbon
October 2023

Eco-efficient Plasters for Increased Indoor Air Quality and Comfort



This document was created with Microsoft Word text processor and the NOVAthesis Word template [1].

A mio padre, mia madre e mia sorella.

# ACKNOWLEDGMENTS

Sometimes, I have the feeling that despite my attempts to distance myself from research, it always found its way back to me. I tend to relate this fact to my natural curiosity, for sure triggered and fed by my father since early childhood. Thus, he is the first person I have to thank for having inspired and challenged me about all the fields of knowledge (literally from cosmos to ants) ever since I remember. With the same gratitude, a big "grazie" goes to my mother, for always being there for me, in everyday life, and ready to show me how to be an independent, brave woman. She taught me how to persist and be careful. To my little sister, Marta, goes my deep thankfulness for supporting, motivating, and inspiring me every day. And to my extended family I also need to say thank you, to those who are still here to support me and to those who are no longer here but would have loved to be part of this.

Special thanks go to my first mentor, prof. Francesca Romana, for inspiring me and giving me confidence in my research skills. I am also grateful for the personal support received from my friends Claudia, Andrea, Francesca, Emilia, Francesca, Marion, Salomé, Anna, Luis, who were there to listen and sometimes distract me, when necessary.

I want to thank my hosting institutions, the NOVA School of Science and Technology of the NOVA University of Lisbon and the Portuguese National Laboratory for Civil Engineering (LNEC), and the funding institution, the Portuguese Foundation for Science and Technology (FCT), and the research unit CERIS, for making this work possible.

Among all the people involved in this work and, consequently, in my professional growth during the past 4 years, the biggest acknowledgment goes to my supervisors, Prof. Paulina and Dr. Rosario, who have always been available, engaged, and helpful.

I also want to thank Dr. Elliott for having accepted and hosted me in his Healthy Building Research Laboratory at Portland State University, where I learned many interesting new things. Thinking about my "Portland period" a special thank you goes to Aurélie and Tom, for the personal and scientific support they gave me.

Thanks to SIVAL-Gessos Especiais Lda, Embarro Srl and American Clay Enterprises LLC for providing their products. Thanks to Dr. Teresa for jumping onto this and to Prof. Margarida for providing the *Acacia dealbata* and many thanks to both for getting interested and involved in the research work.

A big thank you goes to my colleagues of LNEC and FCT-NOVA, who several times helped me with experiments and data interpretation, and/or have been great company during our lunch break. Namely I thank Bento, Acácio, Ana Maria, Otília, Ana Rita, Ana Marques, Catarina, Cinthia, Giovanni, Sofia, Anabela, Leo, Cláudio, Tânia, Joana and - of course - my "shipmates" Magda and Eleonora with whom I was lucky to share difficult moments and beautiful achievements.

I hope I didn't miss anyone but if I did it was unintentional, and I hope you will consider yourself included in my acknowledgment if you have been there at least one time to listen to some research speculation. Thank you.

L’un lito e l’altro vidi infin la Spagna,
fin nel Morrocco, e l’isola d’i Sardi,
e l’altre che quel mare intorno bagna.

Io e’ compagni eravam vecchi e tardi
quando venimmo a quella foce stretta
dov’Ercule segnò li suoi riguardi

acciò che l’uom più oltre non si metta;
da la man destra mi lasciai Sibilia,
da l’altra già m’avea lasciata Setta.

"O frati," dissi, "che per cento milia
perigli siete giunti a l’occidente,
a questa tanto picciola vigilia

d’i nostri sensi ch’è del rimanente
non vogliate negar l’esperïenza,
di retro al sol, del mondo sanza gente.

Considerate la vostra semenza:
fatti non foste a viver come bruti,
ma per seguir virtute e canoscenza".

*(Dante Alighieri, Divina commedia - Inferno canto XXVII).*

# ABSTRACT

Indoor walls and ceilings are often coated with plasters. Due to the large surface in contact with indoor air, the plasters can passively contribute to moisture regulation and pollutant removal. The work presented intends to better understand this contribution, while enhancing, when possible, the plasters formulations for the purpose. The first step was to analyze the hygroscopic response of traditional and modern binder-based plasters. To do so, a first study was run to quantify the relative humidity fluctuations indoor. Then, the methods fitting the most the real indoor microclimates were selected for testing. The campaign was run along with bibliographic research, to match laboratory results with those ones present in literature. The compatibility with the preexisting materials and products and the eco-efficiency of the plasters are two parameters that were kept in mind during the work. According to that, clay and gypsum based plastering mortars were selected as the most promising materials. Both, in fact, are present in traditional architecture, besides being suitable solutions for new construction, and have low embodied energy. However, while the clay-based plasters showed a high hygroscopic behavior, the gypsum-based ones showed a lower one. For this reason, the latter was modified through the addition of biomass and the clay-based plasters were kept as a benchmark along the study. The plant selected for the scope is *Acacia dealbata*, an invasive species that plays a role in the spread of wood fires in Portugal. The biowaste addition was aimed at enhancing the moisture buffering of gypsum-based plasters without jeopardizing other properties or their carbon footprint. Good results were obtained, increasing the moisture buffering ability of the gypsum plaster up to double, even if still lower than the clay-based ones. The ozone reactivity and primary and secondary emission rates (VOCs) of the innovative gypsum-based plaster and the clay-based ones were also analyzed. The ozone removal ability of the gypsum-based plaster was improved by the biomass addition, the primary emissions increased a little, but the secondary ones were very low. Clay-based plasters overall confirmed their low emissions and ozone removal activity.

**Keywords**: sustainable mortars, gypsum, earth, clay, air lime, passive moisture regulation, hygroscopic behavior, biomass, *Acacia dealbata*, bark, pollutant removal, ozone, volatile organic compounds (VOCs), primary and secondary emissions.

# RESUMO

As paredes e os tetos interiores são frequentemente revestidos com rebocos. Devido à grande superfície em contacto com o ar interior, os rebocos podem contribuir passivamente para a regulação da humidade e remoção de poluentes. O trabalho apresentado pretende compreender melhor esta contribuição; ao mesmo tempo, e quando possível, quer melhorar as formulações dos mesmos rebocos para o efeito. O primeiro passo foi analisar a resposta higroscópica de rebocos tradicionais e modernos com base em diferentes ligantes. Com esse propósito foi realizado um primeiro estudo para quantificar as flutuações da humidade relativa no interior. Assim, os métodos mais representativos dos microclimas internos monitorizados foram selecionados para ensaiar os rebocos. A campanha experimental foi realizada em conjunto com uma pesquisa bibliográfica, para combinar os resultados laboratoriais com a literatura. Os parâmetros de compatibilidade com os materiais e produtos preexistentes e de ecoeficiência dos rebocos foram tidos em conta ao longo do trabalho de tese. Dessa forma, argamassas com base em gesso e com base em terra argilosa foram selecionadas como mais promissoras. De facto, ambas fazem parte da arquitetura tradicional além de serem soluções adequadas para novas construções e têm baixa energia incorporada. No entanto, enquanto os rebocos com base em terra argilosa apresentam um comportamento higroscópico elevado, os com base em gesso apresentam um comportamento higroscópico mais baixo. Por esta razão, o estudo avançou com a modificação da formulação de rebocos de gesso através da adição de biomassa, enquanto os rebocos de terra foram mantidos como referência ao longo do estudo. A planta selecionada para a adição foi a *Acácia dealbata*, uma espécie invasora responsável pela propagação de incêndios florestais em Portugal. A adição de biorresíduos teve como objetivo aumentar a resposta higroscópica dos rebocos de gesso sem comprometer outras propriedades e sem aumentar as respetivas emissões de carbono. Foram obtidos bons resultados, com o aumento da capacidade de *buffer* de humidade do gesso até ao dobro, embora sendo ainda inferior à capacidade dos rebocos de terra. Também foram analisadas a reatividade ao ozono e as taxas de emissão primária e secundária de compostos orgânicos voláteis de rebocos com base em gesso formulados e de rebocos de terra. A capacidade de remoção de ozono do reboco de gesso foi melhorada pela adição de biomassa, as emissões primárias aumentaram um pouco, mas as secundárias foram muito baixas. Os rebocos de terra confirmaram, em geral, as baixas emissões e a atividade de remoção de ozono.

**Palavras chave:** rebocos sustentáveis, gesso, terra, argila, cal aérea, regulação passiva da humidade, comportamento higroscópico, biomassa, *Acacia dealbata*, casca, remoção de poluentes, ozono, compostos orgânicos voláteis (COVs), emissões primárias e secundárias.

# CONTENTS

# LIST OF FIGURES

# LIST OF TABLES

# 1

# GENERAL INTRODUCTION

## 1.1 Context of the Study

The building products studied by this PhD work are plasters. Plastering mortars are a mix of "one or more binders, water, aggregates and sometimes additions" (EN 998-1, 2003), commonly used to coat indoor walls and ceilings. Plasters' moisture buffering and potential to passively remove pollutants are here investigated for being important factors to increase occupants indoor air quality and comfort. The plasters selected for the research project are further described both as traditional and modern ones and were all identified as common plasters in Portugal, during different historical periods.

During the Arabic domination of the Iberian Peninsula, gypsum was added in different proportions (Freire et al., 2015) to give different properties to the mortars. Gypsum has been commonly used in Portugal since the stucco technique became popular, namely from the second half of the 18$^{th}$ century until the end of the 19$^{th}$ century, because it was responding the most to decorative style requirements of the period. Traditional gypsum plaster was prepared mixing calcium hydroxide, calcium sulphate hemihydrate and sand or marble powder in different volumetric proportions, from 3:1:1 to 1:0:0 (gypsum: lime: sand), depending on its function (undercoat, preparation or finishing coat), the architectural and artistic period and the local know-how (Malta da Silveira et al., 2007). Technologies with earth as main construction material were also very used in the vernacular architecture in Portugal. Rammed earth and adobe masonry are common from the southern coast of Portugal (between Faro and Vila Real de Santo António) to Lisbon southern area, to Aveiro (Mestre, 2007). Other earth-based technologies were also used to build walls. Clay-based mortars are compatible either with earth

or stone walls, then with modern masonry (Santos et al., 2019). Indeed, clay-based mortars were often used to plaster these earth-based constructions, often rendered by air lime mortars (Fernandes, 2008) due to the good compatibility of both binders with the substrates. Air lime mortars were a common choice until the first decades of the 20$^{th}$ century, performing both protective and decorative functions. In Portugal, for instance, the use of air lime as a binder for structural or protective functions was often verified on study cases from the 1$^{st}$ to the 20$^{th}$ century (Damas et al., 2016) and, thus, can be the most adequate solution in many cases of conservation and rehabilitation (Veiga, 2017). Traditional air lime-based plasters can differ in many aspects: the composition (Faria et al., 2008); the application technology; the environmental conditions at the time of application (weather before and after application, which can strongly influence carbonation process (Balksten & Klasén, 2005; Santos et al., 2018; Rosell et al., 2014). Several of the previous elements involve human decisions and for this reason bring high heterogeneity between air lime mortars. For Instance, in Roman Empire times lime mortars were frequently enriched with natural or artificial pozzolans, such as ceramic dust from crushed bricks, to provide them hydraulic properties (Matias et al., 2014). According to Elsen et al., (2010) there was some uncertainty about the definition of hydraulic lime, for its chemical and mineralogical composition. The concept of natural hydraulic lime was clarified with the 2010 update of EN 459-1 (2015) defining what can be called natural hydraulic lime, hydraulic lime and formulated lime. Nevertheless, the use of natural hydraulic lime as it is currently available (excluding the air lime + pozzolana mixture spread since antiquity) interests all the 19$^{th}$ century. The 20$^{th}$ century, instead, was dominated by the use of Portland cement as a binder (Candeias et al., 2006).

All the presented binders can be used when designing plasters for a new building or an intervention on existing buildings, but particularly in that case it is important to select the binders addressing the compatibility criteria with the substrate. For this reason, a good intervention should always check the compatibility of chemical, mechanical, and physical properties with the preexisting materials and products (Veiga & Faria, 2018).

Besides compatibility, the sustainability of the binders was also considered in the present study to inform the choices. For instance, clay-based plastering mortars respond to requirements of low embodied energy and low environmental impact if considering the energy used in the manufacturing process is only for grinding and sieving and that, if not chemically stabilized, they can be directly reused. Some authors measured many indicators of the environmental impact comparing a clay-based plaster with other plastering mortars. Melià et al. (2014)

reported that for 1 Functional Unit (FU) of plaster, the Cumulative Energy Demand (CED) is 22.7 MJ for clay and 52,8 MJ and 45,5 MJ for hydraulic lime and cement, respectively. CED is the measure of direct and indirect energy requested for the entire cycle of the product, which in this case corresponds to an analysis *cradle to gate* for the boundaries chosen. Advantages for clay-based plastering mortars were also highlighted by Santos et al. (2021). Gypsum plasters also present low embodied energy mostly due to the low calcination temperature of the binder (120-180ºC). However, there are many factors influencing this evaluation. For example, a higher volume of production can lower the environmental impact per ton of material (Damas et al., 2016; Pedreño-Rojas, 2020), while transportation can clearly increase it. Air lime plasters compared to earth and gypsum, show higher embodied energy, due to the higher temperatures required for production (~900ºC), but anyway lower than cement (Moropoulou et al., 2011). However, the durability and predicted lifetime of these plasters are different, as well as de-construction impact, and these differences should be considered in a complete LCA. Summing up, even if the Life Cycle Assessment tool is still under development and there are many uncertainties (Santos et al., 2021), different authors are focusing their research on the evaluation of the sustainability of different binders, either comparing modern with traditional ones (Diaz-Basteris et al., 2022; Marcelino-Sadaba et al., 2017; Bumanis et al., 2020) or quantifying the accessible gain obtained with a replacement/addition of demolition/industrial/agricultural wastes (Brazão Farinha et al., 2019; Bumanis et al., 2022). Clay and gypsum, according to the referred literature, have the lowest global warming potential and a very low environmental impact. Therefore, these binders represent the most sustainable choices for eco-efficient plasters.

Due to the high amount (90%) of time people spend indoors (Diffey, 2011), the Indoor Environmental Quality (IEQ) is a very much discussed topic nowadays. The research on indoor thermal comfort (Frontczak & Wargocki, 2011; Fanger, 1967; Humphreys & Nicol 1998), air quality (Arundel et al., 1986), perceived air quality (Fang et al., 1998), and the correlation of air quality with human health (Wolkoff, 2018) is gaining more and more interest. The regulation of indoor hygrothermal (temperature and relative humidity, RH) conditions can contribute to the assessment of healthier indoors (Arundel et al., 1986; Xiong et al., 2015). Indeed, the study of passive moisture regulation performed by coating products has got increasing attention since the beginning of the 21st century (Padfield, 1999) and nowadays represents a research topic of great interest. Plastering mortars are commonly used to coat large surfaces and, thus, their ability to act as passive moisture buffers can be very favorable (Liuzzi & Stefanizzi, 2016;

Ferreira et al., 2020). This behavior interests traditional and modern plasters, often enhanced to be highly performing for the scope (Lima & Faria, 2016; McGregor et al., 2016; Pawełkowicz et al., 2022; Gentile et al., 2023; Li et al., 2023; Yang et al., 2022; Gbekou et al., 2022). Highly hygroscopic coating products are expected to adsorb and release moisture when the RH increases or decreases (Posani et al., 2021). The indoors that can take the most advantage of these passive regulations are the ones with natural and non/low air exchanges (Rode et al., 2005) and high moisture production (like the case of a bedroom during the night occupied by two people sleeping). Nevertheless, the moderation of the RH peaks and the reduction of operational energy (Barbosa et al., 2020; Wargocki & Wyon, 2013) can also be targeted while designing a space with a HVAC system. It seems important to highlight that plasters often can be coated with a finishing system, such as a finer finishing paste, wallpapers, paints, etc., that can have an impact on their moisture buffering.

The exposure to unhealthy levels of RH is one of the aspects to consider when evaluating the IEQ. The exposure of people indoor and outdoor to different pollutants, such as molds, airborne particulate matter ($PM_{2.5}$ and $PM_{10}$), sulfur dioxide ($SO_2$) carbon monoxide (CO) and carbon dioxide ($CO_2$), nitrogen oxides (NOx), Volatile Organic Compounds (VOCs) and ozone ($O_3$) is nowadays a big concern between researchers (Kelly and Fussell, 2011; Trasande and Thurston, 2005; Apte et al., 2008). Ozone is a harmful secondary pollutant. It represents one of the principal constituents of photochemical gas and is associated with the occurrence of chronical respiratory diseases such as asthma and Sick Building Syndrome (SBS) symptoms (Apte et al., 2008; Weschler, 2006; Kelly & Fussel, 2011; Trasande & Thurston, 2005). In some studies, this pollutant was found also responsible for increased mortality risk (Bell et al., 2004; Bell et al., 2006; Gryparis et al., 2004). The ozone formation outdoors depends on meteorological factors combined with the presence of VOCs and nitrogen oxides, mainly related to the combustion of hydrocarbon fuels (primary pollutant) in urban areas. The ozone levels are increasing all over the world and represent nowadays a problem everywhere and not only in highly polluted countries like China (Li et al., 2020). For instance, in the Lisbon region (Portugal) the threshold of 180 $\mu g \cdot m^3$ on one hour average for ozone was exceeded during five months in 2001-2003, most of the time (86% of the cases) during the afternoon (13h to 17h) in summer (Ferreira et al., 2004). Although the ozone concentration indoor is mainly a function of the outdoor concentration (Weschler, 2000) there are other indoor sources and sinks that turn possible to have higher concentration indoor than outdoor (Huang et al., 2019). Moreover, the ozone can react with some volatile organic compounds (VOCs) doubling their initial

concentration. The byproducts of the oxidation of these compounds (that present unsaturated carbon-carbon bond) are typically aldehydes, organic acids, and ketones. The inhalation of high concentrations of VOCs (most famous of them is formaldehyde) has dangerous effects on human health and has been correlated with the increase of the risk in developing diseases like leukemia, asthma, and low birth weight (Liu et al., 2022). There are several measures that can be adopted to increase indoor air quality and prevent high indoor pollutant concentration such as mechanical filtration systems (Nazaroff & Weschler, 2022; Hyttinen et al., 2006; Lee & Davidson, 1999). These solutions are energy demanding and can be coupled (in a more sustainable design) with passive mitigation strategies that rely on the use of plants (Abbass et al., 2017; Berardi et al., 2014; Abbass et al., 2018) or passive removal materials (PRM) (Jing & Wang, 2022; Shen & Gao, 2018).

For all the listed reasons, the hygroscopic behavior of traditional binder-based plasters (based on gypsum, air lime, clay) and more modern ones (based on cement, natural hydraulic lime), was investigated to assess the plasters potential to act as passive moisture regulators. Results point out that there is a substantial difference between the two greenest binder-based plasters (clay and gypsum): very high adsorption/desorption capacity for the clay-based but lower for the gypsum plasters. To enhance the performance of gypsum plasters, the addition of a biobased waste product was considered. The biowaste selected is a byproduct of another supply chain that would not jeopardize the carbon footprint of the gypsum plastering mortar. Instead, it would turn it more "eco-competitive" decreasing its embodied energy. The thesis work presents the research steps given in this direction up to the formulation of a higher hygroscopic plastering mortar based on gypsum. The clay-based plasters were kept as a baseline due to their high hygroscopicity. Moreover, the primary emissions of both the clay and gypsum-based plastering mortars were evaluated (VOCs emissions) together with their ozone reactivity in terms of deposition velocities (ability to uptake the ozone from air) and secondary emissions (VOCs emissions as byproducts of oxidation).

## 1.2 Research Objectives and Methodology

The indoor surfaces covered by plaster are commonly large areas and, if they can act as passive moisture regulators and pollutants removal, their contribution to indoor air quality and comfort, and to the health of occupants, can be important, especially in absence of Heating Ventilating and Air Conditioning (HVAC) systems and during the most extreme seasons when

the natural indoor ventilation is poor. The main objective of the present work is to understand the different contribution that common traditional and modern plasters can give to indoor air quality and comfort and, thereby, try to enhance optimized mortars formulations (respecting the criteria of eco-efficiency and compatibility with both built heritage and new buildings) to improve this contribution. Thus, according to all the exposed considerations, the main goal of the PhD work here presented - Eco-efficient plasters for increased indoor air quality and comfort - is to address the following research questions:

- How can plasters contribute to indoor air quality and comfort?
- How to assess this contribution?
- For this purpose, are there significative differences between different binder-based plasters?
- Is it possible to improve the hygroscopic behaviour of a traditional low-embodied-energy plaster, such as gypsum-based one and how?

Thus, the study was implemented according to the following steps:

- Monitoring indoor hygrothermal conditions (RH and temperature) in some study cases of Lisbon area, Portugal (section 2.2);
- Simulation of the response of four modern and traditional plastering mortars (based on cement, natural hydraulic lime, air lime and clay) in winter (worst case scenario) for the previously monitored indoors (section 2.2);
- Comparison and discussion of the existing methods to test RH dependent properties (section 2.2);
- Assessment of ranges for hygroscopic behaviour of traditional and modern plasters in literature, building a state-of-the-art dataset (section 2.2);
- Assessment of hygroscopic behaviour for traditional and modern plastering mortars and pastes through tests, building an experimental dataset (section 3.2);
- Study of the influence of the application of two paint systems (one specific for indoor application) on the hygroscopic properties of the previously characterized plasters (section 3.3);
- Studying the influence of the addition of different biomass content (0, 5 and 10% by volume) and fractions from an invasive species (flowers, leaves, branchlets, wood and bark from *Acacia dealbata*) on fresh and hardened state of gypsum plaster and their hygroscopic behaviour (sections 4.2 and 4.3);
- Investigation on the effect of thermal treatment (of a selected biomass fraction - bark) and addition of air lime on biological growth (section 5.1);
- Assessment of the hygroscopic behaviour of the optimized gypsum-based plastering mortars and comparison with clay-based plasters (section 5.2);

- Assessment of the ozone deposition velocity, primary and secondary emissions of the optimized mortars and comparison with clay-based plasters (section 5.3).

## 1.3 Document Organization and Graphical Abstract

The document is a collection of eight articles: five already published and three under submission.

The structure is the same for all the chapters (apart from the present chapter *Introduction*):

- Preamble to introduce the content of the chapter and link the previous study to the next.
- Article addressing research questions.
- Additional considerations (when appropriate).

After the chapters presenting the research (from chapters 2 to 5), the Conclusions summarize the findings and include proposals for future studies and perspectives. The references are presented in alphabetical order (excluding those only reported in the Articles, with the format of the publishing journal) and, in the Annex, the scientific dissemination performed so far (articles under submission not included yet) and laboratories where the work took place are listed.

The 2nd chapter presents the preliminary investigation. A hygrothermal microclimatic monitoring campaign opens the dissertation. The main objective of the study was to observe the real range of variation of RH and temperature in residential indoors of Lisbon area in Portugal, presented as an example of a Southern European country where HVAC systems are not very commonly installed. The study was useful to match the monitored conditions with the ones suggested by the existing standards and protocols to test hygroscopic behavior of building materials. Moreover, a simulation of the effect of four common traditional and modern plasters under the monitored hygrothermal conditions was run, to quantify the potential contribution of each plaster to passive regulation. The second chapter continues presenting a state-of-the-art of test methods to quantify the RH dependent properties and a collection of results of traditional and modern binder-based plasters from literature.

In the 3rd chapter results from the first experimental campaign are presented and discussed. Eight different plastering mortars and pastes used as plaster finishings, based on clay, gypsum, air lime, natural hydraulic lime, cement (and some combinations of them) underwent the RH dependent properties characterization. The properties included in the study are the ones related to the moisture adsorption/desorption mechanism under static and dynamic

conditions and water vapor permeability, responsible for the moisture penetration depth. The effect of the application of two paint systems (acrylic and vinylic) on the same bare plasters' hygroscopic behavior is presented and discussed in the second study of the chapter.

The 4th chapter introduces a specific study on gypsum plasters. From the previous studies the plasters based on gypsum showed a hygroscopic behavior significantly poorer than clay-based ones. Considering the compatibility of gypsum plasters with the built heritage and the low embodied energy, they were found to be a very interesting product to be enhanced. The enhancement was designed to improve their potential as passive moisture regulator coatings. New plastering mortars were formulated, based on gypsum with the addition of five biowaste fractions of *Acacia dealbata* (an invasive species) in two quantities (5% and 10% by vol. of a ready-mix plastering product). The biowastes were used as byproducts, after extraction of nutraceutical compounds for other industries. Eleven mortars were formulated and characterized at fresh and hardened state, with special focus on RH dependent properties.

The 5th chapter presents the optimized mortars formulations. The bark fraction was selected and added at 10% by vol., although it was not possible to use it after the extraction of the compounds. To avoid some biological growth observed on the former modified plasters, a small percentage of air lime was also added to the ready-mixed product. Besides the raw bark addition, an additional formulation was run with thermally treated bark (heated at 250 ºC for 1 hour). The optimized mortars underwent fresh and hardened state characterization. Their moisture buffering capacity was compared with two premixed clay-based plasters. To conclude the study, the ozone deposition velocities, primary and secondary emissions of the three gypsum-based mortars were assessed and compared with clay-based plasters (highly performing according to literature).

The following graphical abstract tries to summarize the research performed.

## Graphical Abstract

2|3

### THE CHOICE OF THE PROTOCOL

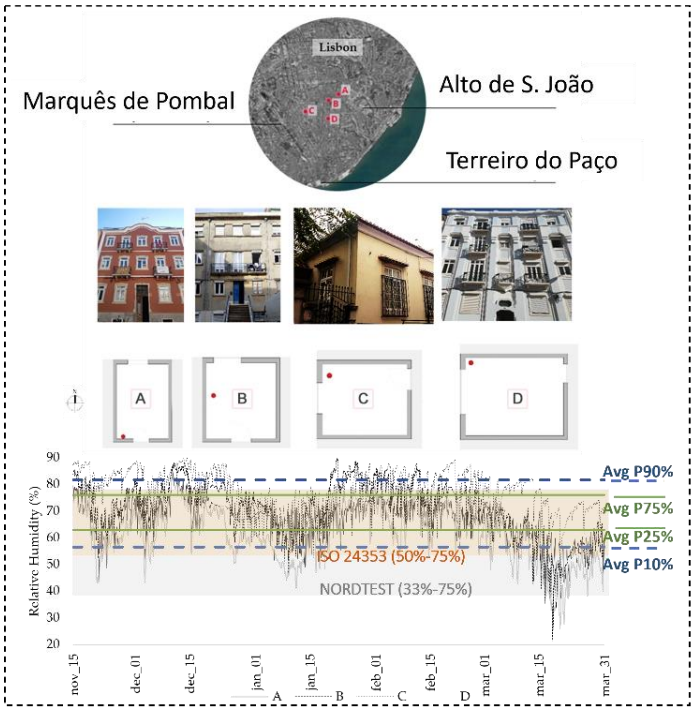


### PASSIVE MOISTURE REGULATION OF PLASTERS

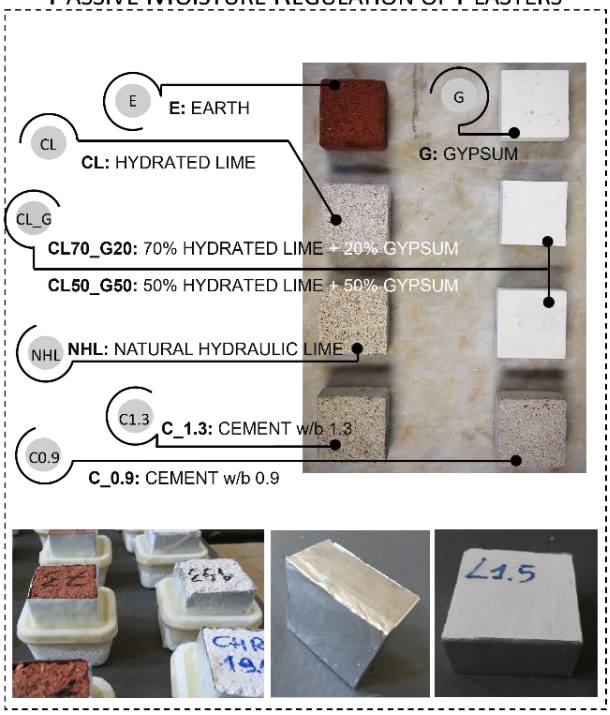


4|5

### ADDITION OF *A. DEALBATA*

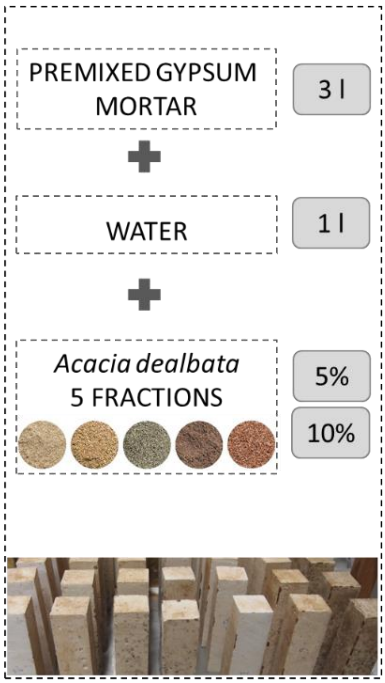


### | ADDRESSING THE BIOLOGICAL PROBLEM |

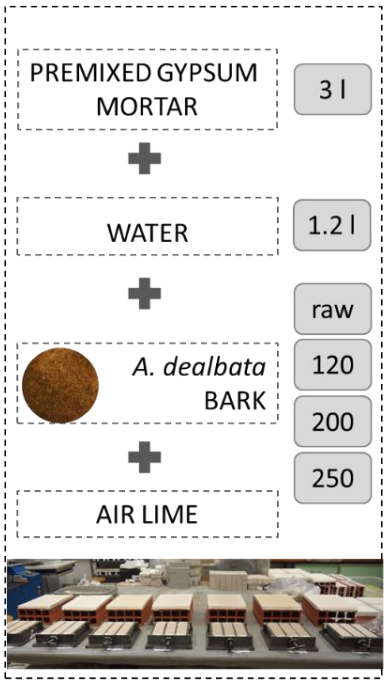


### THE FINAL PRODUCTION

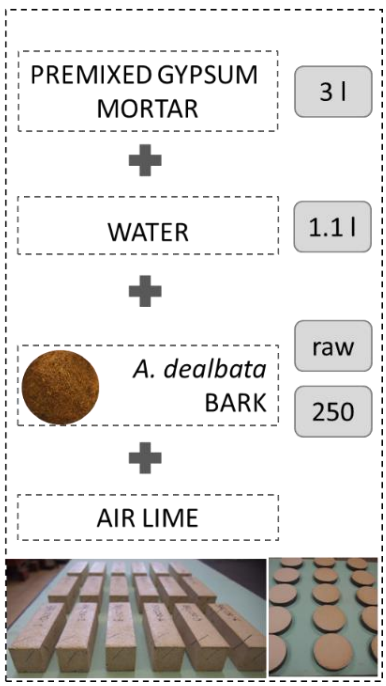

4|5

## LABORATORY CHARACTERIZATION


5

## OZONE REACTIVITY

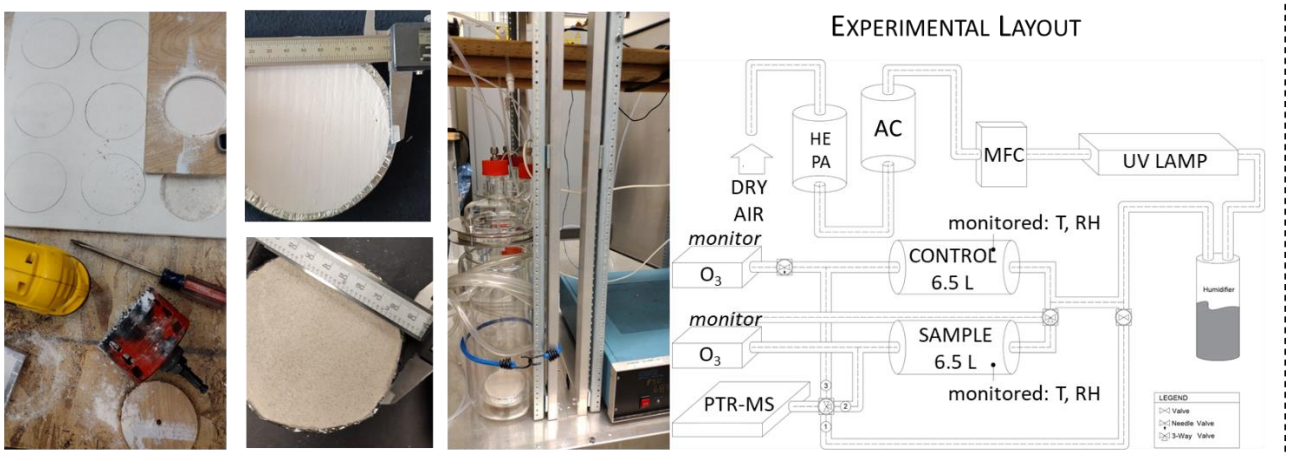

# 2

# INDOOR HYGROTHERMAL CONDITIONS AND RELATIVE HUMIDITY RELATED METHODS

## 2.1 Preamble

As previously mentioned, the hygrothermal indoor conditions are mainly responsible for user's comfort. For this reason, the first study presented here (section 2.2) is the result of a monitoring campaign. The campaign interested four bedrooms, differently located in the city of Lisbon, Portugal. The design prioritized rooms with the same use (bedrooms) in buildings from different constructive techniques, ages, and locations. The monitoring was run from November 2020 to November 2021. The article presents and analyzes the less favorable period - winter - and four bedrooms representative of different layouts. The aim of the study was not to characterize the hygrothermal conditions of the bedrooms in their specificity, e.g., the kind of plasters and eventually the paint system applied in the rooms, the constructive details of the buildings, the presence or not of traditional window frames and windows, etc., but to have a general understanding of the fluctuation range for the considered parameters under common operational conditions of bedrooms in residential buildings in Lisbon. Moreover, the Lisbon residential situation can be a moderate one when compared with others from the same country. Nevertheless, the article refers to Southern European countries because, despite the local climate that can be observed in Portugal (IPMA), the country is generally included in the temperate climate of Southern Europe (Arriazu-Ramos et al., 2023) and differs from Northen

European countries for the frequent shortage of continuous heating systems, often related with energy poverty. For instance, Antepara et al. (2020) observed that, in Spain, Portugal and Greece, consumes for residential buildings are below the 50% of theoretical energy needs. Indeed, monitored real hygrothermal conditions (in the four study cases) were compared with those suggested for ensuring indoor comfort and they were found out of the comfort zone at least 50% of the times. Moreover, the observed indoor hygrothermal fluctuations were compared with temperature (T) and ranges of relative humidity (RH) recommended for testing building materials by the two most widespread protocols: ISO 24353 (2021) and Rode et al. (2005), the latter developed for Northen Europe countries.

According to results, an informed choice on testing methods could be made when testing moisture buffering of materials for applications in intermittently heated or unheated indoors located in temperate climates. Moreover, the same study (section 2.2) investigates the improvement that the application of traditional and modern plasters (based on clay, cement, air lime and natural hydraulic lime) could bring. The hygroscopic behavior of the plasters was laboratory characterized and data introduced into a model. The simulation was calibrated with real values of T and RH from the monitoring and the modelled plasters were applied (in the simulation) in the four study cases. The different contribution of each coating was quantified, pointing out the clay-based plaster as the most promising for passive RH regulation.

The second article here presented (section 1.1) is a literature review on testing methods and responses of different binder-based plasters. The RH dependent properties which are included in the review are: sorption isotherms, moisture buffering and water vapor permeability (the latter to establish the moisture penetration depth). The microstructure analysis is not included, despite being very important for justifying results from physical characterization, because it was not commonly associated, in literature, to relative humidity dependent properties and presented only if a complementary characterization was needed (i.e., to have a better understanding of the hysteresis phenomenon). All the articles matching the inclusion criteria were analyzed and the methods presented by the authors were included in the review in a systematic way, according to their percentage distribution.

The aim of the systematic review was to collect data on testing conditions (area and thickness of the specimens, hygrothermal conditions, duration of the tests), but also to build a dataset of results (quantifying these properties for different binder-based plasters) as the starting point for the next study. Mortars included are based on air lime, clay, gypsum, natural hydraulic lime (NHL), cement, and combinations of these binders. The study concluded that, for testing moisture buffering, the NORDTEST method (Rode et al., 2005) is chosen in most of the studies

(*71.8%*) above the ISO 24353 (2021), but eventually the conditions adopted the most are not very representative of some climates (as also observed in the previous study 2.2). In terms of materials' response, the clay-based plasters are very promising for the purpose of moisture passive regulation for increasing users' comfort while reducing energy consumption (both operational and embodied).

## 2.2 Article A1 - A study on the Indoor Hygrothermal Conditions

(the article has been published in the journal *Infrastructures* 2022, 7 (3), 38;
https://doi.org/10.3390/infrastructures7030038)

# A discussion on winter indoor hygrothermal conditions and hygroscopic behaviour of plasters in Southern Europe

## Abstract

In Southern European countries, due to the specific climate, economy and culture, a permanent heating practice during winter is not widely adopted. This may have a significant effect on the performance of indoor coating materials, typically tested considering hygrothermal conditions in the range 33–75% relative humidity (RH) and 20–25 °C, which are common in continuously heated buildings. In this study, the indoor climate of four bedrooms located in Lisbon, Portugal, was monitored under operational conditions. Based on the data monitored in the case studies, characteristic ranges of indoor hygrothermal conditions were defined and compared to those considered in standard test procedures. In addition, numerical simulations were adopted to compare the hygroscopic performance of four plasters under operational conditions observed on-site. Results show that the four rooms, intermittently heated or unheated, do not provide comfort conditions over 50% of the wintertime, with temperature lower and RH higher than the ones recommended by the standards. The MBVs resulting from simulations (under operational conditions) are qualitatively in agreement with the MBVs obtained under standard testing conditions. Nonetheless, future studies are recommended to evaluate if standard tests are quantitatively representative of the hygroscopic performance of coating materials in the Southern European scenario.

## Keywords

Hygrothermal comfort; Indoor climate; Moisture Buffering; Hygroscopic behaviour, Southern Mediterranean countries, Hygrometric regulation.

### 2.2.1 Introduction

The importance of indoor environmental quality (IEQ) is nowadays largely acknowledged, due to the extended amount of time people spend indoors [1]. Consequently, the study of parameters like indoor thermal comfort [2–4], indoor air quality [5], perceived quality [6] and the correlation with human health [7] gained importance in research. In this context, increasing attention has been paid to the use of building materials [8] and hygroscopic coating systems [9,10] that can help to passively regulate indoor relative humidity (RH). The idea is to exploit

the moisture buffering ability of the materials to regulate indoor hygrometric conditions. Indeed, hygroscopic materials tend to adsorb moisture when RH rises and then release it when the air gets drier [11], thus moderating the peaks in indoor RH and reducing operational energy demands [12,13] while passively improving indoor comfort [14].

To evaluate and compare the moisture buffering ability of materials, the NORDTEST protocol [15, 16] is often adopted. This test procedure was defined by a research group working on the specific scenario of North European countries [17] and it is based on the hypothesis of continuously heated buildings (e.g., indoor set-point temperature of 23°C [18]). The methodology was defined considering an occupancy of 8 hours per day, which is typical of offices and bedrooms [19]. Three possible ranges of RH were proposed, and the one normally adopted spans from 33% to 75%. Even though some other procedures exist, for instance ISO 24353 [20], the NORDTEST method is the most largely adopted one, because it provides a quantitative evaluation of the moisture buffering capacity [17] through a single parameter: the practical Moisture Buffering Value (MBV). Hence, this test procedure allows to compare the potential effectiveness of different hygroscopic materials and coating systems through their MBVs.

Despite the great contribution provided by the introduction of the NORDTEST procedure, some doubts may arise when it is adopted in the context of Southern European countries. In fact, in Southern Europe, a permanent heating practice is not commonly adopted, especially in residential buildings [21]. On one hand, this is a consequence of the milder winter conditions. On the other, the combination of low incomes and high energy costs leads to a general "Lack of Motivation to Heat", which is extremely high in Portugal, Romania and Greece, and lower but still relevant in other Southern European countries like Spain, Croatia and Italy [21]. In this context, a relevant share of the population is found to be unable to keep the house adequately warm [22, 23]. Due to the low indoor temperatures (T), high RH levels can be expected. The scenario of Southern Europe may thus require a complementary approach that differs from the standard test conditions defined for the case of Northern Europe by the NORDTEST protocol.

This study aims to evaluate the indoor hygrothermal conditions in four case studies located in Lisbon (Portugal) and intends to open a discussion on the applicability of standard tests on moisture buffering ability of building materials, in the context of Southern Europe. The detailed methodology is schematized in **Figure 2.1**.

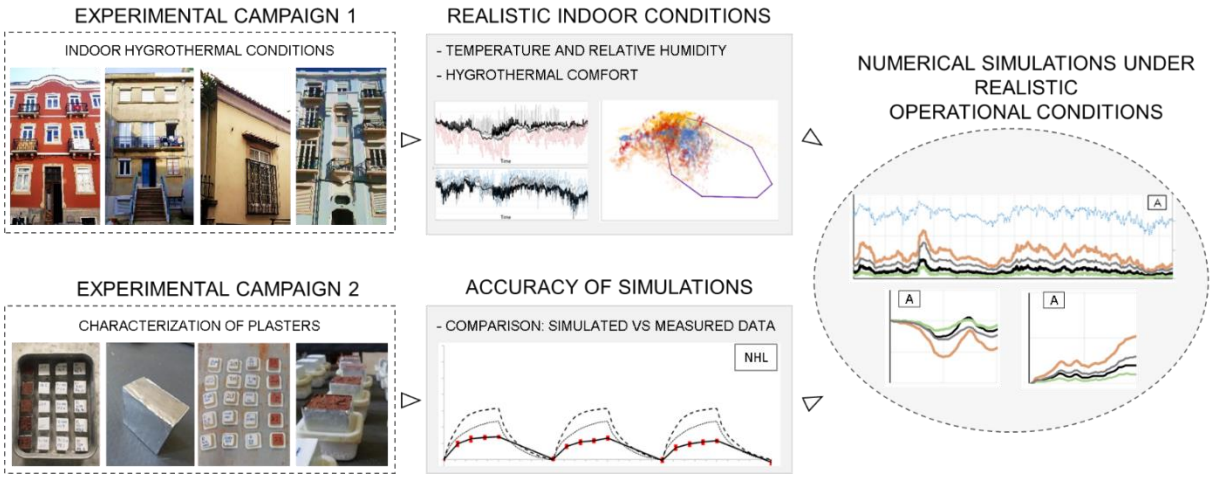


**Figure 2.1.** Schematic representation of the methodology followed in the study.

The monitoring was performed during winter, when the passive relative humidity regulation can be significant since windows are kept closed for most of the time. Moreover it was possible to verify the complaints of the bedrooms' users, who reported the spaces to be cold and moist during winter. The dataset, thus obtained, was examined to evaluate the fluctuation of indoor RH to be compared to the scenario adopted in the NORDTEST. To facilitate the comparison between real conditions and testing ones, the data were recorded in bedrooms which better represent (for residential) the type of space (occupation for 1/3 of the day) considered in the NORDTEST. The indoor climate data obtained on-site were then used as input in numerical simulations, to evaluate the hygroscopic behaviour of different plasters under realistic operational conditions. Results were compared to the MBVs of the plasters obtained under standard conditions (via laboratory tests), to assess if they were representative of their potential hygroscopic behaviour under the observed real conditions.

## 2.2.2 Materials and methods

### 2.2.2.1 Case studies selected and indoor monitoring campaign

Four case studies were selected for the experimental indoor monitoring campaign. In each one, the air temperature (T) and relative humidity (RH) were continuously recorded during winter 2021. The four buildings are located in the core of the city of Lisbon, and their location is displayed in **Figure 2.2**. All the buildings were built before the first Portuguese regulation on thermal requirements for buildings was published [24]. This is a very common condition in the Portuguese building stock, where 85% of the building stock, reported in 2011, dated back to

before the 1990s [25]. The bedrooms under study are subjected to one-person occupancy and they are intermittently heated by the users with electric-heating devices, or not heated at all.


**Figure 2.2.** Selected case studies: location in the map of Lisbon, building facades, and plans of the monitored bedrooms (openings: interior door and outdoor-facing window). In each room, a red dot indicates the position of the data-logger used to monitor the indoor hygrothermal conditions.

Case study A (**Figure 2.2**a) is located in a three-floor building whose envelope was recently refurbished. The bedroom considered is on the 1st floor, and it has an area of about 7.5 m2. It has one external wall, which is North-oriented, and a balcony. Case study B (**Figure 2.2**b) is located in a building that looks like the result of a social housing project of the second half of the 20th century. The bedroom selected is on the upper ground floor and has an area of about 8.4 m2. It has one external wall, North-oriented, with one window. Case study C (**Figure 2.2**c) is a room of a detached house with an individual owner. The bedroom analysed is on the upper ground floor and it has an area of about 7.5 m2. The bedroom has one external wall, West-oriented, with a window. Case study D (**Figure 2.2**d) is located on the 3rd and last floor of an apartment building. It has a floor area of about 11 m2 and one external wall with a balcony, West-oriented.

The indoor monitoring campaign was performed by means of two data-loggers HOBO UX100-003 (accuracy: ±0.21°C, ±3.5% for 25- 85% RH and 5% out of this range) and two HOBO U12-013 (accuracy: ±0.35°C, ±2.5% for 10- 90% RH and 5% out of this range). The sampling interval

adopted was 10 minutes and the final hygrothermal data were defined as the hourly average values of T and RH obtained from the recordings, as in previous studies [26, 27]. The data-loggers were positioned inside paper boxes (open on the top) to avoid the interference of drafts and solar radiation in the measurements. Furthermore, the equipment was located on the top of different pieces of furniture, at 70 –180 cm from the floor, to minimize direct interactions between the bedrooms users and the sensors. Finally, a minimum distance of 10 cm was kept between the walls and the data-loggers. The hourly data of outdoor T and RH were provided by the Portuguese Institute of Sea and Atmosphere (IPMA) [28], from a local meteorological station.

The monitoring campaign was performed during winter because it is the period when a passive regulation of RH can be very beneficial for improving hygrothermal comfort. Indeed, during winter the air change rates are low because windows are kept closed for most of the time, and the lower the air change rates the higher the potential impact of the materials on indoor RH [10]. In addition, due to the typically moderate use of heating in Southern Europe, high RH levels can occur. Wintertime was approximated considering the period November 15 – March 31, based on the degree days' calculation. Since the Portuguese legislation [29] that defines the degree days does not include a specific identification for the starting and ending date of the heating period (which is hereby considered to define wintertime), an Italian standard was taken as a reference [30]. This choice was considered suitable for the scope since both Portugal and Italy are South-European countries, and the selected period appeared representative of wintertime in Lisbon.

#### 2.2.2.2 Statistical analysis of indoor hygrothermal conditions and indoor comfort

Once the set of hygrothermal data from the case studies was acquired, it was statistically evaluated through cumulative frequency plots. The 25th and 75th percentiles, also known as the upper and lower quartiles [31], were considered to identify a typical range of indoor conditions. Similarly, a wider range was defined by using the 10th and 90th percentiles.

To evaluate whether the indoor environments were cold and moist, as reported by the bedroom users, the data obtained in the monitoring were compared to the comfort requirements found in the literature. Indoor comfort depends on a variety of factors that can be difficult to forecast for residential buildings, due to the uncertainty on the activities performed, the variability of clothing, the uncontrolled use of the windows, and so forth. Thus, calculations concerning the Predicted Mean Vote (PMV) and Predicted Percentage of Dissatisfied (PPD), as indicated in standards ISO 7730 [32] and ASHRAE 55 [33] are disregarded

in favour of a more simplified evaluation. A zone of acceptable hygrothermal comfort was defined according to the following observations. During winter the temperature should be higher than 16°C to guarantee neutral or comfort sensation for the occupants, as referred by Peeters et al. [34] for bedrooms. Standard EN 16798-1 [35] indicates a maximum temperature of 25°C for bedrooms belonging to category III (acceptable, moderate level of expectation on indoor comfort). In addition, standard EN 15251 [36] suggests a RH level within the range 20-70%, for buildings in category III. Anyway, in order to account for an additional indication of the literature, the minimum acceptable RH level is increased to 30% [7], to avoid excessive drying out of the skin and of the mucous membranes.

#### 2.2.2.3 Plasters characterization

Four plastering mortars were selected to be used in the simulations. The mortars were prepared by mechanical mixing and water was added to achieve suitable workability (assessed through flow table test [37]). The mortars and their consistence were the following:

E – commercial plaster based on clayish earth produced by EMBARRO [38] with a consistence by flow table of 170±10 mm;
CL – 1:3 volumetric ratio of hydrate air lime CL 90-S and siliceous sand (0-4 mm) with a consistence by flow table of 151±5 mm;
NHL – 1:3 volumetric ratio of natural hydraulic lime NHL3.5 and siliceous sand (0-4 mm) with a consistence by flow table of 150±5 mm;
Cem – 1:4 volumetric ratio of CEM II/B-L 32.5N and siliceous sand (0-2 mm) with a consistence by flow table of 140±3 mm.

A detailed description and characterization of the plastering mortars can be found in a previous study [39]. The Moisture Buffering Values (MBVs) were calculated considering the experimental results obtained following the NORDTEST protocol [17] and the ISO 24353 standard [20]. MBVs were calculated on the average of five specimens for each plaster (40x40x20 $mm^3$). According to the NORDTEST protocol [17], the specimens were cyclically exposed to steps of RH 33% (16 hours) – 75% (8 hours) until quasi-steady-state equilibrium was reached. When tested according to the ISO 24353 [20], the cyclic condition of middle humidity level (12 hours at 75% RH followed by 12 hours at 50% RH) was chosen. Temperature was fixed at 23±0.5 °C during the entire test in both cases. The difference between the two methods lies in the range of RH considered (minimum of 33% or 50%) and in the period of exposure to different hygrometric conditions (12-12 h; 16-8 h). The MBV results are reported in **Table 2.1**.

**Table 2.1.** Plasters MBVs [g/m$^{2}$·%RH] according to the NORDTEST and ISO 24353 testing protocols.

| Plaster | NORDTEST | ISO 24353 |
|---|---|---|
| E | 1.493 ± 0.09 | 1.327 ± 0.08 |
| CL | 0.416 ± 0.04 | 0.267 ± 0.03 |
| NHL | 0.799 ± 0.03 | 0.537 ± 0.02 |
| Cem | 0.843 ± 0.07 | 0.660 ± 0.05 |

The physical and hygric characterization of the plasters was performed in previous studies [39 – 42]. The materials properties needed for the simulations were defined following the indication of Posani, Veiga and Freitas [43], based on the results of the experimental campaigns. Thermal properties were considered of minor importance in this study and they were thus approximated using the values provided in WUFI data-base [46] for similar materials. The main data adopted for the simulations are summarized in **Table 2.2**.

**Table 2.2.** Plasters properties adopted in numerical simulations.

| Plaster | $P_o$ [%] | $\rho_{Dry}$ [kg /m$^3$] | μ [–] | $A_w$ [kg/m$^2$s$^{0.5}$] | *$\lambda_{Dry}$ [W/(mK)] |
|---|---|---|---|---|---|
| E | 29.9 | 1743 | 9.07 | 0.50 | 0.5 |
| CL | 25.8 | 1720 | 7.43 | 1.71 | 0.7 |
| NHL | 26.2 | 1779 | 9.32 | 2.40 | 0.7 |
| Cem | 20.2 | 1919 | 20.42 | 0.43 | 1.2 |

Notation: Po – open porosity, $\rho$ Dry – dry bulk density, μ - water resistance factor, Aw – capillary water absorption, $\lambda$ Dry – thermal conductivity, *not measured but approximated considering values from WUFI database.

The sorption isotherm is recognized to be one of the most important material properties when simulating the impact of hygroscopic materials on indoor RH [44]. They were defined for both the adsorption and desorption phases, according to standard ISO 12571 [45]. Five specimens (40x40x20 mm$^3$) for each plaster were tested. They were first dried at 60 °C, then they were kept under constant hygrothermal conditions until equilibrium was reached, using a climatic chamber FITOCLIMA 700EDTU. The steps of RH considered were the following: 30%, 50%, 70%, 80%, 95% RH, while the temperature was constantly kept at 23±0.5°C.

#### 2.2.2.4 Numerical Simulations

The Software adopted for mono-dimensional hygrothermal simulations is WUFI Pro 5 [46], which allows performing mono-dimensional hygrothermal simulations of multi-layered walls cross-section under realistic climatic conditions. This software was chosen for several reasons. First, it offers a detailed calculation model of combined heat and moisture transport, which includes liquid transport, vapour diffusion, and hygroscopic behaviour of porous materials [46].

Furthermore, WUFI Pro has been validated through several years of field and laboratory testing [47–51], and it is widely adopted to investigate passive regulation of humidity due to hygroscopic building materials [52–55]. In addition, the software allows introducing materials properties as input data, thus plasters can be modelled according to the information obtained in laboratory tests. Additionally, the software accounts for hourly data of boundary conditions, thus the indoor climate can be introduced in the model based on the microclimate monitoring performed in the case studies.

In this study, numerical simulations are first adopted to reproduce the standard test on moisture adsorption/desorption defined by ISO 24353 [20]. The results numerically obtained are compared to the experimental results observed in the laboratory. The accuracy of the model for representing the hygroscopic behaviour of the plasters is consequently discussed. The plasters are then simulated considering the indoor climatic conditions measured onsite and the results are discussed in comparison with MBV experimentally obtained. The comparison aims to evaluate if standard test conditions are representative of materials adopted in the context of Southern Europe, where indoor climatic conditions can become colder and moister than in Northern countries, due to the different heating habits.

##### *2.2.2.4.1 Simulations under standard conditions*

Dynamic numerical simulations have been largely applied to study the hygroscopic behaviour of building materials. Nonetheless, modelling hygroscopic materials requires some simplifications, in particular concerning their sorption isotherm. Building materials can show a residual moisture content at the end of desorption, due to the effect of capillary forces which make the uptake of water molecules in the porous network easier than its removal [56]. This behaviour is also known as moisture hysteresis [57]. Thus, the curves obtained during the adsorption and desorption phases can be quite different from each other.

In WUFI software, the sorption isotherm is assumed as a bijective function, thus two separate curves cannot be introduced for adsorption and desorption, and a simplification must be adopted. In the literature, two approaches emerge for operating this simplification: some studies consider the adsorption isotherm only [58], and others use the average values obtained combining adsorption and desorption curves [59]. Both simplifications are applied in this research and evaluated. The materials modelled according to the two approaches are simulated under the standard conditions adopted in the laboratory test as in ISO 24353 [20]. Then the results obtained with the two simplifications are compared to those measured in the laboratory. Based on the outcomes of this comparison, the simplification offering more

accurate results is chosen for the forthcoming simulations. The NORDTEST procedure was not replicated via numerical simulation due to the very little data available, namely only one measurement after each phase of adsorption or desorption. Consequently, it was of minor interest for the sake of comparing measured and simulated values.

More in detail, this first set of simulations is performed as follows. First, the materials were modelled as horizontal components, having a thickness of 2 cm, and a sealing material is applied on the bottom (a vapour barrier with a Sd=1500m). The lateral sealing is not modelled since the simulations run under the hypothesis of an infinite plane component, thus the conditions at the border do not influence the results. The upper and lower boundary conditions adopted are those of the experimental test, namely a constant temperature of 23 °C and cycles of 12h of constant RH, which is alternatively kept at 75% or 50%. To replicate the test performed in the laboratory, the initial condition of the material is 23 °C and moisture content stabilized at 63% RH. The results of the first 4 cycles, i.e. a total of 48h, are not represented, while the following ones are reported in comparison to those measured in the laboratory, in terms of moisture content per unit of surface in the samples.

##### *2.2.2.4.2 Simulations under realistic operational conditions*

The plasters are then simulated under realistic operational conditions, considering the indoor data recorded on-site and a typical Portuguese wall assembly.

Since all case studies have different walls, a typical configuration is adopted to have comparable results, while being representative of the Portuguese building stock. The geometry consists of a whole-brick structure, 34cm-thick, as characteristic of traditional Portuguese brick-masonry walls with medium thickness [60]. On the exterior side, 2 cm of lime-cement render is considered, finished with acrylic paint, to account for a typically refurbished façade. At the indoor-facing side of the wall, a 2cm-thick layer of plaster is adopted (E, CL, NHL, and Cem, alternatively). The initial conditions in the plasters are assumed as in equilibrium with air at 20°C and 60% RH, which is considered to be a realistic assumption, based on the indoor hygrothermal data observed on-site. Outdoor boundary conditions are defined using typical weather data of Lisbon, namely those provided in the Test Reference Year from WUFI database. At the interior side of the walls, the microclimate adopted is the one recorded on-site during winter, in the four case studies, alternatively.

Results are evaluated in terms of moisture content in the plaster, per unit of surface. Then, the variation of moisture content in the plasters is observed in detail during a 2- day period. Based

on the results, the hygroscopic behaviour observed under realistic operational conditions is discussed and compared to the results obtained in terms of MBV in standard tests.

## 2.2.3 Results and discussion

### 2.2.3.1 Indoor climate

**Figure 2.3** shows the hourly data of T and RH obtained in the indoor environmental monitoring, versus the ones recorded by IPMA for the outdoor climate, from November 2020 to March 2021. According to the collected data, during winter the outdoor temperature and relative humidity were in the ranges 1–26°C and 40–100% RH, respectively, with T being lower than 16 °C for most of the time and RH being generally above 75%. Regarding indoor climates, hygrothermal conditions were in the ranges 10–28°C and 21–90% RH in the period considered.

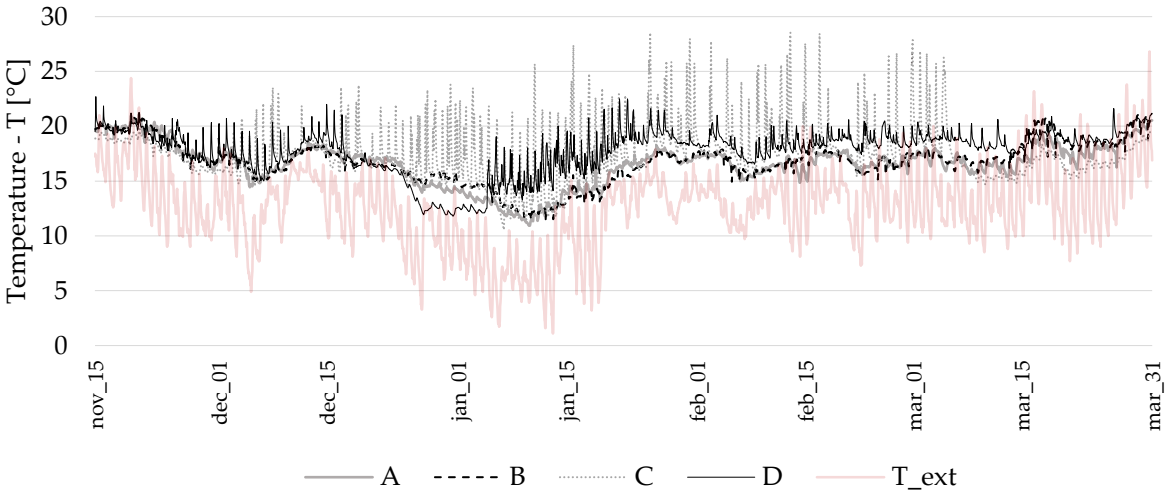

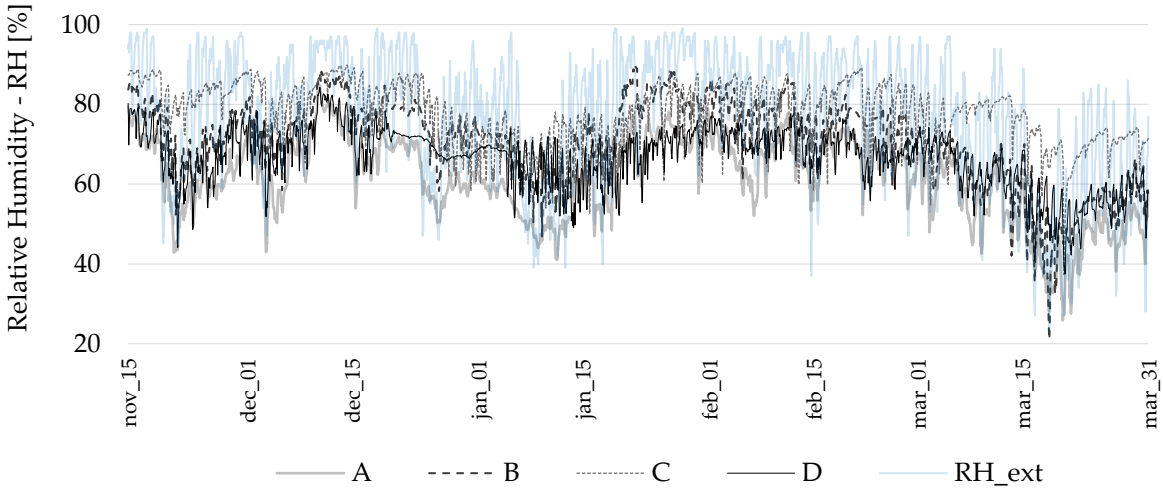


**Figure 2.3.** Hourly average air temperature (°C) and relative humidity (%) data recorded by IPMA in the city of Lisbon and the same parameters recorded in the four bedrooms (A, B, C and D), for the period 15th November 2020 – 31st March 2021.

#### 2.2.3.2 Statistical evaluation

To analyse the typical range of variation of indoor T and RH, a statistical evaluation was performed, and the results are shown in **Figure 2.4**.

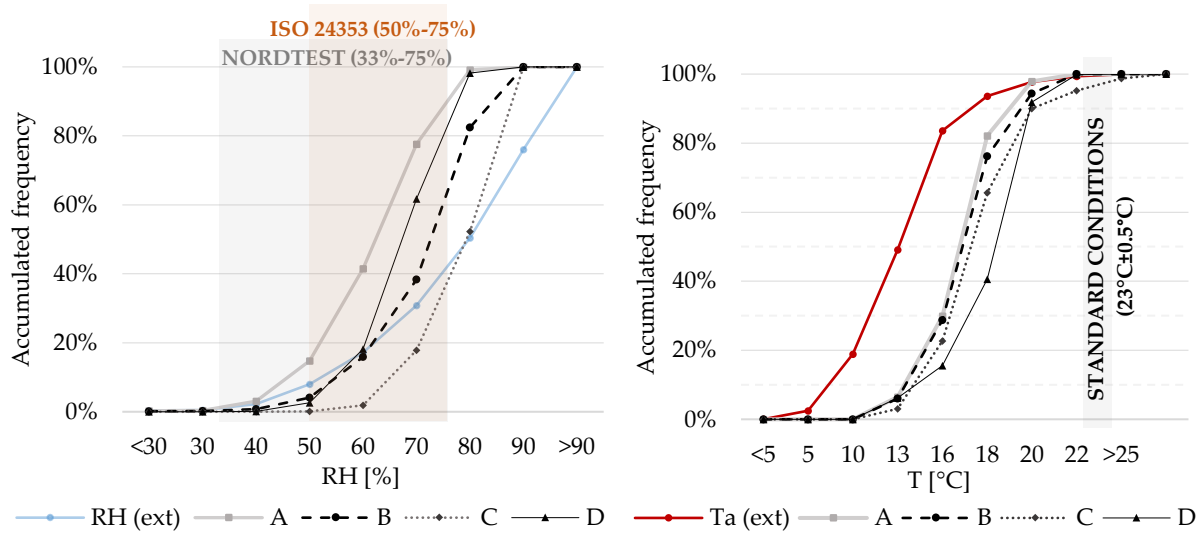


**Figure 2.4.** Frequency distribution of hourly RH and T data recorded in the four bedrooms under study in Lisbon and in the outdoor climate, from November 2020 to March 2021.

The curve of accumulated frequency shows that the lower threshold value considered in the NORDTEST is not very representative of the indoor hygrometric conditions analysed. Indeed, this condition was never reached in case studies C and D, while such low levels of RH, namely below 35%, are obtained for less than 5% of the time in the other 2 case studies. This result

indicates that a RH level around 33% is not representative of a typical daily low point of RH, but it is more of an exceptional condition, in the case studies considered. This outcome is coherent with the heating strategy adopted in the case studies. While continuous heating may lead to low levels of RH, intermittent or absent heating leads to lower indoor temperatures, with consequently higher RH levels.

As far as the upper limit value of the NORDTEST is concerned, i.e. 75% RH, it seems quite representative of a typical condition of high RH in case studies A and D. In these two rooms, indoor hygrometric conditions are below this value at least 80% of wintertime. On the contrary, much higher RH levels can be found in case studies B and C, where a RH above 75% is detected during 60% and 40% of the winter period, respectively. Even for temperature, the standard range considered in laboratory testing (23°C ± 0.5°C) does not seem to represent typical indoor conditions in the analysed bedrooms. Indeed, temperatures below 22.5°C are found for more than 90% of the time in all the rooms taken into analysis.

The outcomes of the monitoring seem consistent with previous indoor monitoring campaigns performed in buildings located in Portugal. Indeed, in a study on a prototype of an unrefubished classroom [3], on social housing [68], and on residential apartments [63], RH levels were frequently falling in the range 50%–80% RH during winter. In addition, in the three studies, indoor temperature was found to be below 22.5°C for almost the whole winter period considered in the monitoring (entire winter in [3] and [63], and only February in [68]).

In order to have a representation of a typical range for indoor RH and T fluctuations, two intervals are hereby considered: the 90th – 10th percentile (P90% – P10%) and the more restrictive interval 75th – 25th percentile (P75%, P25%). Considering all case studies, the average values of P25% and P75% are 63% - 16°C and 76% - 18.5°C, whereas the average values obtained for P10% and P90% are 56% - 14.5°C and 82% - 19.5°C, as reported in **Figure 2.5**.

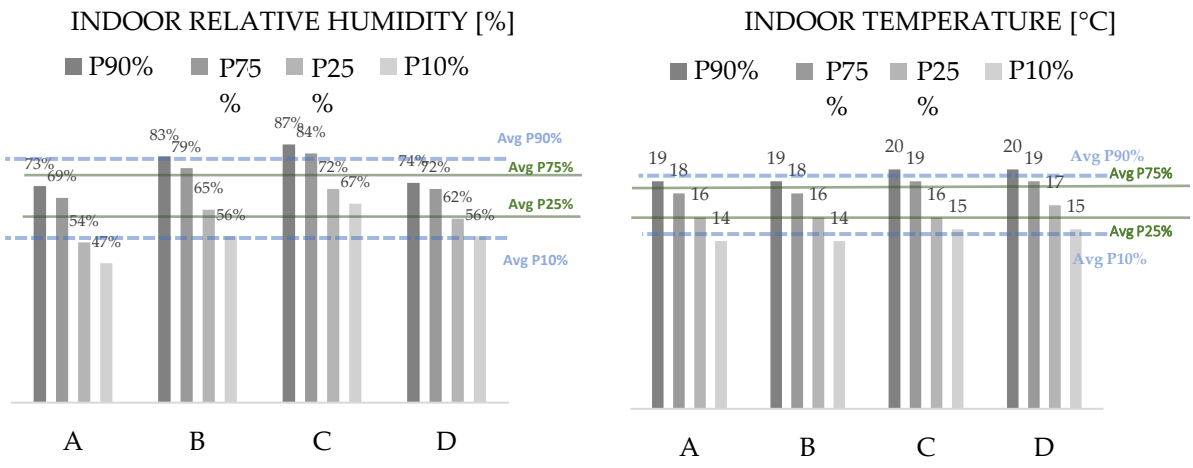


**Figure 2.5**. Values of the 90th, 75th, 25th, and 10th percentiles in the dataset of indoor relative humidity and temperature recorded in each case study, during winter. The blue and green lines indicate the average values obtained from the percentiles of the 4 case studies.

According to this analysis, a typical range of fluctuation would be 63-76% RH and 16-18.5°C (considering 25th – 75th percentiles) or 56%-82% for RH and 14.5-19.5°C (accounting for 10h – 90th percentiles). The proposed ranges are hereby assumed as representative of the indoor climates considered, and they are compared to the indication of ISO 24353 [20] and NORDTEST [17] for the RH range to consider during the tests.

From the qualitative comparison provided in **Figure 2.6**, the step 50-75% RH suggested by ISO 24353 [20] for a "middle humidity level" appears to better estimate the indoor data-sets than the NORDTEST. In the latter, the minimum RH appears extremely lower than the values of indoor RH registered, and it is significantly below the limits estimated with P10% and P25%. This difference between typical testing conditions and real climates might result in an overestimation of the potential benefits of hygroscopic materials applied in the Southern European context. In fact, the conditions of the NORDTEST have a greater range of RH and a much lower minimum value, which would probably result in higher MBV of the materials than at "more realistic conditions". For this reason, it could be valuable to have further studies aimed to evaluate the scenario of Southern European countries and a possible complementary approach to adopt for applications of hygroscopic materials within this context. Regarding the temperature, both the methods (ISO and NORDTEST) account for a T of 23±0.5°C, which is quite far from the ranges hereby observed (16-18.5°C and 14.5-19.5°C). Even though the effect of T on the moisture buffering capacity of building materials is hardly ever investigated, according to Mazhoud et al. [61] a linear correlation between T and MBV exists, probably for the effect of T on saturation vapour pressure [62]. The possibility of considering a specific

temperature for Southern European countries might be an option to consider in future investigations.

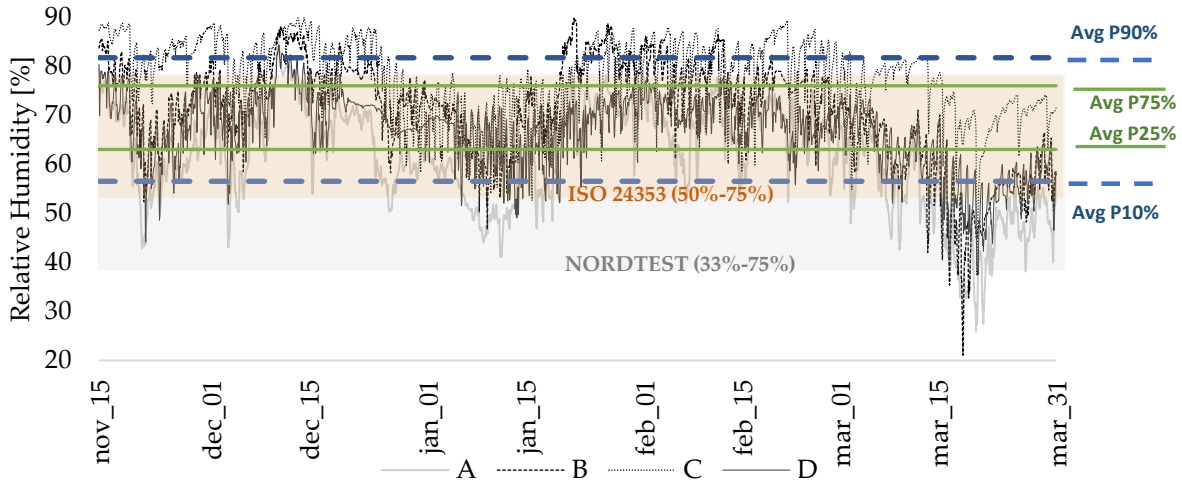


**Figure 2.6.** Indoor RH in each of the four bedrooms. The blue and green lines indicate the average values found in the case studies, in terms of 10th, 25th, 75th and 90th percentile of RH. For comparison, the ranges of RH considered in the NORDTEST [17] and the ISO 24353 [20] are also reported, in grey and orange hatches respectively.

#### 2.2.3.3 Indoor Comfort

Comparing the datasets obtained via indoor monitoring with the comfort zone roughly defined through four points (**Figure 2.7**), it emerges that all case studies are out of the hygrothermal comfort area for a large share of wintertime. In case studies A and D indoor RH and T are out of the comfort zone for at least 50% of wintertime, a percentage that increases to 75% and about 90% in case studies B and C, respectively.

The comparison reported in Figure 7 shows that discomfort conditions are mainly due to high RH and/or low T. This result is in agreement with the feedback given by the users and with the observation raised in the literature concerning the typical lack of comfort in Southern European residential spaces.

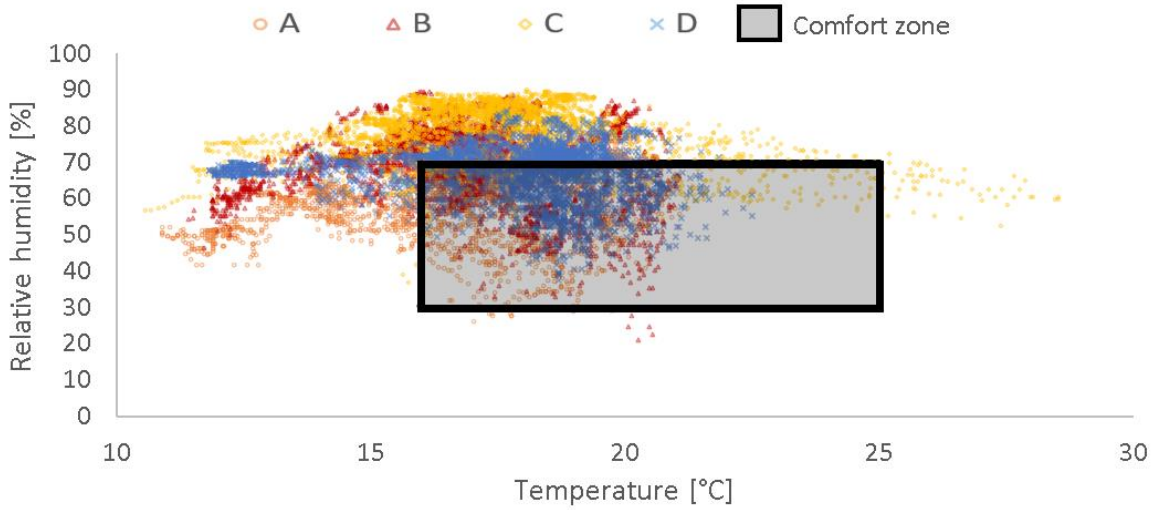


**Figure 2.7.** Graphic comparison between the hygrothermal datasets registered on-site in case studies A to D, and the comfort zone defined through 4 points (16;30); (16;70); (25;30); (25;70).

#### 2.2.3.4 Sorption isotherms of the plasters

The sorption isotherms of the plasters are shown in **Figure 2.8**. For each plaster, the adsorption and the desorption phases are represented by a continuous and a dotted line, respectively. All the plasters present some hysteresis, showing a residual moisture content at the end of the desorption phase. For E and NHL plasters, the hysteresis is very low and the adsorption and desorption curves almost overlap. The other two plasters, CL and Cem, have higher hysteresis.

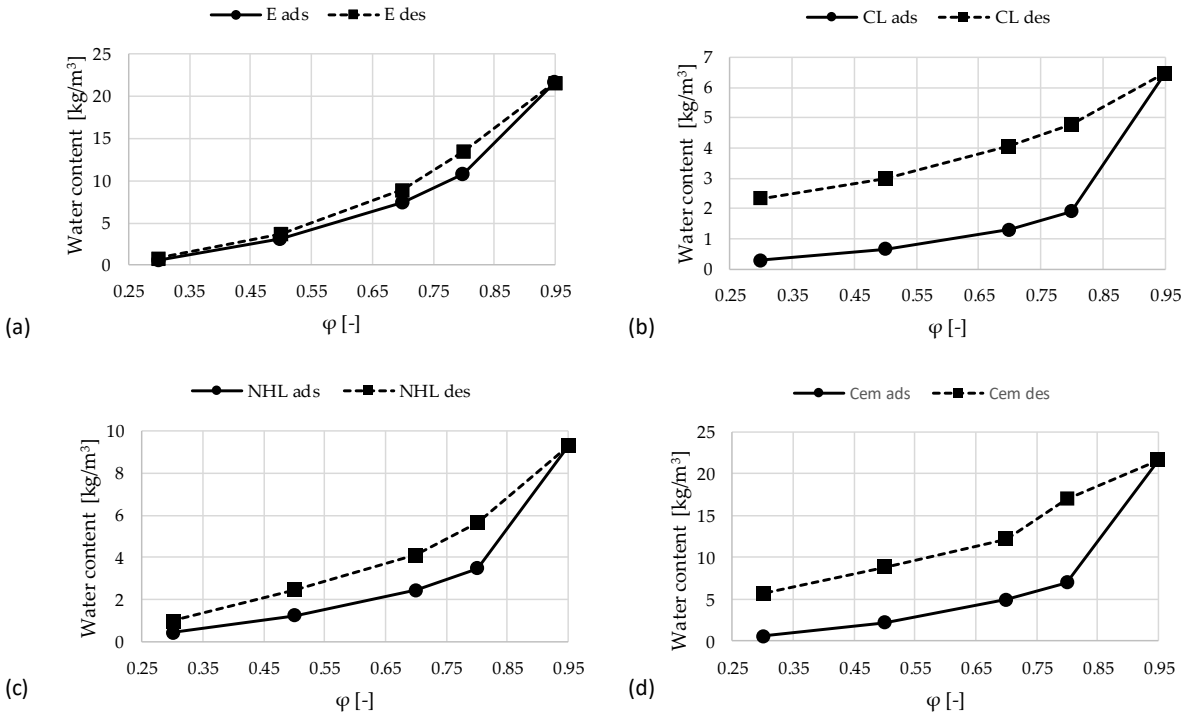


**Figure 2.8.** Sorption isotherms of the mortars based on: (a) earth; (b) air lime CL90-S; (c) natural hydraulic lime NHL 3.5 and (d) cement II/B-L 32.5N.

## 2.2.4 Simulations

### 2.2.4.1 Simulations under standard conditions

**Figure 2.9** shows the results of numerical simulations compared to those obtained in the experimental characterization of the plasters. Numerical simulations were run both considering the average of adsorption and desorption curves – simulated (AVG) – and only accounting for the adsorption curve – simulated (ADS). For E and Cem the two curves (AVG and ADS) are almost overlapped. On the contrary, CL and especially NHL show more relevant differences when different assumptions are made to simplify their sorption isotherms. Namely, more accurate results were obtained considering only the adsorption curve. Thus, for the simulations presented in the following section, this simplification (ADS) is adopted to model the sorption isotherm of the four plasters considered.

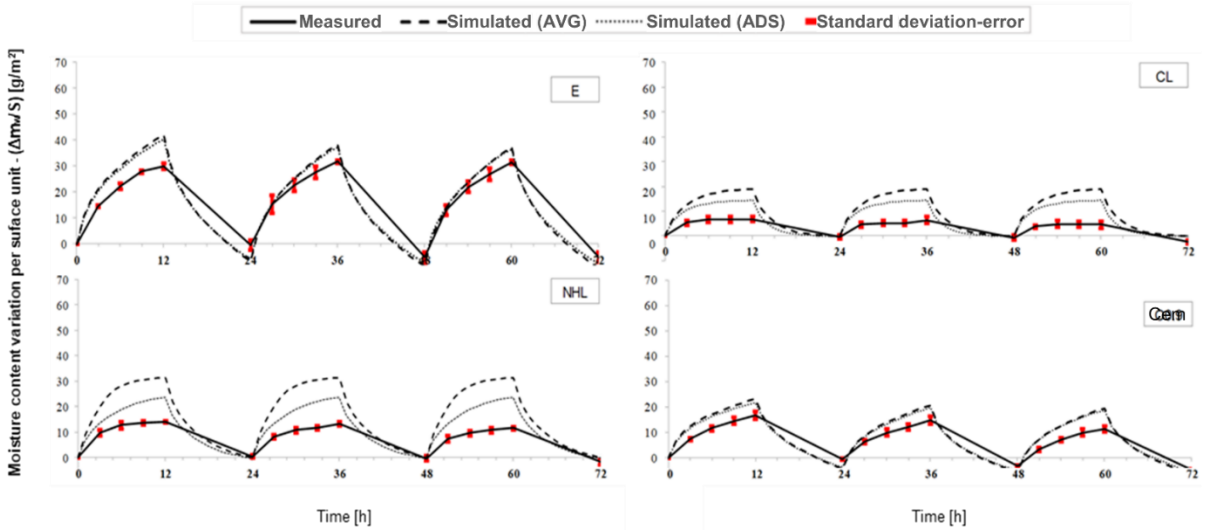


**Figure 2.9.** Three cycles of moisture content variation per unit of surface, displayed among time for each plaster: E – earth, CL – air lime, NHL – natural hydraulic lime and Cem – cement-based; *Continuous* - plasters laboratory results tested according to ISO 24353 [20] and relative standard deviation; *Dashed* - hourly measures on simulation based on sorption/desorption average curve; *Dotted* - hourly measures on simulation based on adsorption.

Moreover, all simulations appear to overestimate the moisture content in the materials during the adsorption process. This outcome seems less relevant for E and Cem, and more significant for CL and NHL. Nonetheless, simulations still appear representative of the different behaviour of materials, meaning that materials showing higher moisture content variation in the laboratory do also have higher changes of moisture content in the simulations. For this reason, the model adopted is considered suitable for a qualitative comparison of the hygroscopic behaviour of the plasters under realistic operational conditions.

Finally, similar differences between measured and simulated water content in building materials, during alternated cycles of high and low humidity, were also observed in previous studies [64–66].

#### 2.2.4.2 Simulations under realistic operational conditions

The results obtained via dynamic hygrothermal simulations under realistic operational conditions are presented in **Figure 2.10**. In the first four graphics (**Figure 2.10**a), the moisture content per unit area is represented with different colours for each plaster, for the indoor conditions of case studies A, B, C and D. The initial moisture content of plasters is assumed as the one at 60% RH, which corresponds to a different value depending on the sorption isotherm of each material. Although this difference in initial water content is noticeable, it is not relevant

for the discussion on RH regulation. On this regard, what matters is the variation in the moisture content of the plaster, not its absolute value. Results shown in **Figure 2.10**a suggest that the variation of moisture content is stronger in plasters E and Cem, rather than in CL and NHL.

The fluctuation of moisture content is shown more in detail for two periods of 2 days and the results are displayed in **Figure 2.10**b. The eight graphics reported in the figure confirm the previous observations. In all the scenarios considered, the largest fluctuations of moisture content are observed in the earthen plaster (E), followed by plasters based on cement (Cem), natural hydraulic lime (NHL) and hydrated air lime (CL), in this order. An exception is observable in the graphic on the right referring to case C, where the difference between E and Cem, and between NHL and CL does not seem relevant. The ranking observed is in agreement with the MBVs experimentally obtained following the standard ISO 24353 [20] and the NORDTEST procedure [17]. The simulation results obtained under operational conditions show that in Southern European countries with low heating habits, the analysed standard tests used to quantify moisture buffering are qualitatively representative of the hygroscopic performance of materials under real operational conditions.

Finally, the earth-based plaster, E, seems to be the most promising for further studies on indoor air quality improvement. This outcome is consistent with the observations in Cascione et al. [15], where an experimental campaign conducted at the room level showed that a clayey earth plaster was more effective than a lime-based one, for stabilizing indoor RH. Thus earth-based plasters appear extremely appealing thanks to the additional benefits given by the low environmental impact and infinite recycling possibilities of earth [67].

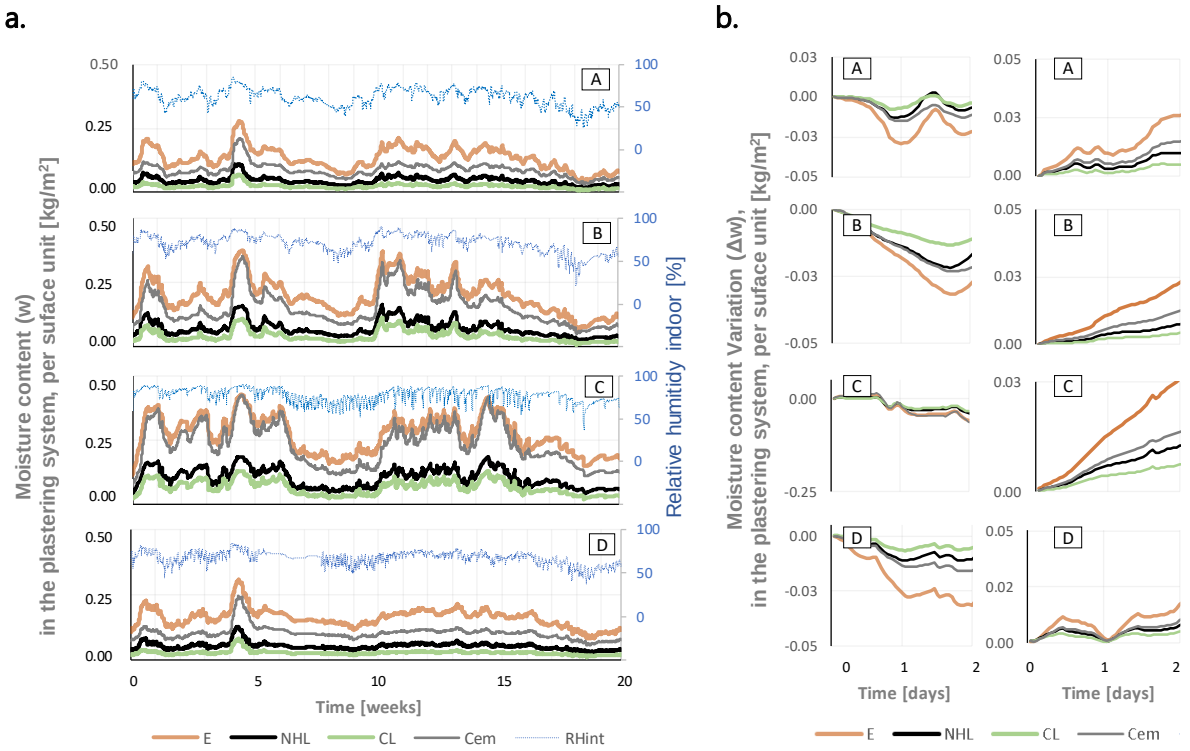


**Figure 2.10.** Simulation results of the moisture behaviour of the four plasters for each study case: (a) moisture content per unit of surface (mw/S) during the entire winter period; (b) moisture content variation per unit of surface (Δmw/S) during two periods of 2 days each, respectively starting on February 20 and March 21. From top to bottom, the graphics correspond to the results obtained considering the indoor climate recorded in case studies A, B, C and D.

### 2.2.5 Conclusions

This study presents the results obtained in an indoor hygrothermal monitoring campaign performed in four bedrooms of different buildings in Lisbon, during winter-time. The datasets obtained were analyzed, and characteristic ranges of temperature and relative humidity were defined. Mono-dimensional dynamic hygrothermal simulation tools were adopted to simulate the hygroscopic performance of four plasters, under the operational conditions measured on-site.

The outcomes of the indoor monitoring campaign allowed to define the following conclusions:

- The microclimates of the four case studies are found to be well represented by the hygrothermal ranges of 63–76% RH and 17.5±1.5°C, which were defined considering the 25th and 75th percentiles of the dataset distributions.
- In terms of RH, the ISO 24353 sets the closest values to the characteristic ranges defined for the four case studies according to the monitoring. The standard adopts the condition

50% to 75% RH, differently to the NORDTEST procedure, which is typically used considering the range 33-75% RH. Overall, the humidity range adopted in the ISO standard appears more representative of the microclimates observed on-site. Indeed, the lower RH value adopted in the NORDTEST (33%) is rarely reached in the datasets presented in this study. RH below this value is observed for less than 5% of the time and only in two case studies.

- Considering the temperature, the values prescribed in both the ISO 24353 standard and the NORDTEST protocol (22.5-23.5°C) are higher than those observed in the case studies during almost the entire wintertime.
- In terms of indoor comfort, it was observed that the case studies are often out of the comfort area – over 50% of wintertime – mainly due to high relative humidity and low temperature. This outcome is consistent with the complaints of the bedrooms users. Furthermore, it is aligned with the literature concerning the inability of keeping residential spaces sufficiently warm in Southern Europe.

Dynamic hygrothermal simulations allowed to give a rough evaluation of the moisture buffering ability of the plasters, under realistic operational conditions. The main remarks defined from the simulations results are the following:

- The fluctuation in the moisture content of the plasters was qualitatively in agreement with the ranking based on the MBV determined by both the NORDTEST procedure, ISO 24353 standard. Thus, the standard test procedures for evaluating the moisture buffering capacity of building materials might be representative also for the context of Southern European housing, despite its colder and moister indoor conditions. Further studies are needed to evaluate this point more in depth, accounting for the more accurate results obtainable through whole-building simulation models.
- The earth-based plaster, above all, showed the widest fluctuations in water content under realistic operational conditions. This result suggests that this material could be promising for passive regulation of indoor relative humidity.

Forthcoming studies will be focused to quantitatively evaluate the effect of the plasters on indoor RH regulation, by means of whole-building simulation tools. These evaluations will be used to further assess the suitability of standard tests to represent the hygroscopic behaviour of plasters in intermittently-heated/unheated spaces, typical of Southern European countries.

**Author Contributions**: Conceptualization, investigation, writing—original draft preparation A.R.; conceptualization, software, writing—original draft preparation M.P.; supervision,

writing—review and editing, R.V. and P.F. All authors have read and agreed to the published version of the manuscript.

**Funding**: This research is funded by the Portuguese Foundation for Science and Technology: PD/BD/150399/2019, PD/BD/135192/2017 (1st and 2nd authors are part of the Doctoral Training Programme EcoCoRe) and UIDB/04625/2020 (Civil Engineering Research and Innovation for Sustainability Unit – CERIS).

**Acknowledgments**: The authors would like to acknowledge the support provided by CONSTRUCT-LFC (Institute of R&D in Structures and Construction at FEUP) and also by the National Laboratory for Civil Engineering, through projects PRESERVe and REuSE, as well as the help offered by IPMA, who provided for the outdoor climate dataset considered in the study.
Conflicts of Interest: The authors declare no conflict of interest.

## References

1. Diffey, B.L. An overview analysis of the time people spend outdoors. British journal of dermatology 2011, 164, pp. 848-854. DOI: 10.1111/j.1365-2133.2010.10165.x.
2. Curado, A.; Freitas, V.P.; Ramos, N.M. Variability assessment of thermal comfort in a retrofitted social housing neighborhood based on "in situ" measurements. Energy Procedia 2015, 78, pp. 2790–2795.
3. Barbosa, F.C.; Freitas, V.P.; Almeida, M. School building experimental characterization in Mediterranean climate regarding comfort, indoor air quality and energy consumption. Energy and Buildings 2020, 212, 109782.
4. Caro, R.; Sendra, J. J. Are the dwellings of historic Mediterranean cities cold in winter? A field assessment on their indoor environment and energy performance. Energy and Buildings 2021, 230, 110567.
5. Almeida, R.M.; Freitas, V.P. IEQ assessment of classrooms with an optimized demand controlled ventilation system. Energy procedia 2015, 78, pp. 3132–3137.
6. Darling, E.K.; Cros, C.J; Wargocki, P.; Kolarik, J.; Morrison, G.C.; Corsi, R.L. Impacts of a clay plaster on indoor air quality assessed using chemical and sensory measurements. Building and Environment 2012, 57, pp. 370–376.
7. Wolkoff, P. Indoor air humidity, air quality, and health – An overview. International Journal of Hygiene and Environmental Health 2018, 221, pp. 376–90. DOI: 10.1016/j.ijheh.2018.01.015.

8. McGregor, F.; Heath, A.; Maskell, D.; Fabbri, A.; Morel, J. C. A review on the buffering capacity of earth building materials. In Proceedings of the Institution of Civil Engineers-Construction Materials, October 2016, 169(5), pp. 241-251
9. Liuzzi, S.; Stefanizzi, P. Experimental study on hygrothermal performances of indoor covering materials. International Journal of Heat and Technology 2016, 34 (2), pp. S 365–70. DOI: 10.18280/ijht.34S225.
10. Ferreira, C.; de Freitas, V. P.; Delgado, J.M.P.Q. The influence of hygroscopic materials on the fluctuation of relative humidity in museums located in historical buildings. Studies in Conservation 2020, 65 (3), pp. 127-41. DOI: 10.1080/00393630.2019.1638666.
11. Posani, M.; Veiga, M.R.; de Freitas, V.P. Towards resilience and sustainability for historic buildings: A review of envelope retrofit possibilities and a discussion on hygric compatibility of thermal insulations. International Journal of Architectural Heritage 2021, 15, 5, pp. 807-823. DOI: 10.1080/15583058.2019.1650133.
12. Ramos, N.M.; de Freitas, V.P. The evaluation of hygroscopic inertia and its importance to the hygrothermal performance of buildings. In Heat and Mass Transfer in Porous Media. Springer: Berlin, Germany, 2012; pp. 25-45.
13. Wargocki, P.; Wyon, D.P. Providing better thermal and air quality conditions in school classrooms would be cost-effective. Building and Environment 2013, 59, pp. 581-89. DOI: 10.1016/j.buildenv.2012.10.007.
14. Cintura, E.; Nunes, L.; Esteves, B.; Faria, P. Agro-industrial wastes as building insulation materials: A review and challenges for Euro-Mediterranean countries. Industrial Crops and Products 2021, 171, 113833. DOI: 10.1016/j.indcrop.2021.113833.
15. Cascione, V.; Maskell, D.; Shea, A.; Walker, P.; Mani, M. Comparison of moisture buffering properties of plasters in full scale simulations and laboratory testing. Construction and Building Materials 2020, 252, 119033. DOI: 10.1016/j.conbuildmat.2020.119033.
16. Gonçalves, H.; Gonçalves, B.; Silva, L.; Vieira, N.; Raupp-Pereira, F.; Senff, L.; Labrincha, J.A. The influence of porogene additives on the properties of mortars used to control the ambient moisture. Energy and Buildings 2014, 74, 61-68. DOI: 10.1016/j.enbuild.2014.01.016.
17. Rode, C.; Peuhkuri, R.H.; Mortensen, L.H.; Hansen, K.K.; Time, B.; Gustavsen, A.; Ojanen, T.; Ahonen, J.; Svennberg, K.; Harderup, L.E.; Arfvidsson, J. Moisture buffering of building materials. Technical University of Denmark, Department of Civil Engineering, 2005. BYG Report, R-127.

18. Rode, C.; Peuhkuri, R. The concept of moisture buffer value of building materials and its application in building design. In Proceeding of the 8th International Conference and Exhibition on Healthy Buildings, Lisbon, Portugal, 4-8 June 2006.
19. Rode, C.; Peuhkuri, R.H.; Time, B.; Svennberg, K.; Ojanen, T. Moisture buffer value of building materials. In Heat-Air-Moisture Transport: Measurements on Building Materials, ASTM International 2007; STP 1945, pp 111–122.
20. ISO 24353. Hygrothermal performance of building materials and products - Determination of moisture adsorption/desorption properties in response to humidity variation. International Organization for Standardization: Geneva, Switzerland, 2008.
21. Magalhães, S. A.; de Freitas, V. P. A complementary approach for energy efficiency and comfort evaluation of renovated dwellings in Southern Europe. In Proceedings of 11th Nordic Symposium on Building Physics, Trondheim, Norway, 11-14 June 2017.
22. Magalhães, S. A.; de Freitas, V. P.; Alexandre, J.L. Energy certification label vs. passive discomfort index for existing dwellings. In Proceedings of the XIII International Research-Technical Conference on the Problems of Designing, Construction and Use of Low Energy Housing, Krakow, Poland 11–13 September 2018, IOP Conference Series: Materials Science and Engineering, 2018, 415, 01202. DOI: 10.1088/1757-899X/415/1/012021.
23. Atanasiu, B.; Kontonasiou, E.; Mariottini, F. Alleviating fuel poverty in the EU – Investing in home renovation, a sustainable and inclusive solution. Buildings Performance Institute Europe (BPIE): Brussels, Belgium, 2014.
24. Portuguese Republic. Portuguese Regulation of thermal behaviour characteristics of buildings – Decreto-Lei n° 40/90, de 6 de Fevereiro, 1990. RCCTE – Regulamento das Características de Comportamento Térmico de Edifícios (revised version 80/2006).
25. INE and LNEC. The housing stock and its rehabilitation - Analysis and evolution (in Portuguese), 2011. Ed: 2013; Statistics Portugal - INE; National Laboratory for civil engineering - LNEC, Lisbon, Portugal. ISBN 978-989-25-0246-5
26. Posani, M.; Veiga, M.R.; de Freitas, V.P.; Kompatscher, K.; Schellen, H. Dynamic hygrothermal models for monumental, historic buildings with HVAC systems: complexity shown through a case study. In Proceedings of 12th Nordic Symposium on Building Physics – NSB2020, Tallinn, Estonia, 6-9 September 2020, E3S Web of Conference, 172, 15007. DOI: 10.1051/e3sconf/20201721.
27. Posani, M.; Veiga, M.R.; de Freitas, V.P. Thermal retrofit for historic massive walls in temperate climates: risks and opportunities. In Proceedings of the 4º Encontro de

Conservação e Reabilitação de Edifícios – ENCORE 2020, Lisbon, Portugal, 3-6 November 2020.

28. Portuguese Institute for Sea and Atmosphere (Instituto Português do Mar e da Atmosfera) - IPMA, 2021. Available online: http://www.ipma.pt/pt/. (Accessed: June 2021).
29. Portuguese Republic. Portuguese energy regulation of buildings ¬– Diário da República, Despacho n° 15793-K/2013 (Portuguese), 2013.
30. Italian Republic. Italian energy regulation of buildings – Decreto del Presidente della Repubblica n° 74 del 16 aprile 2013 (Italian), 2013.
31. Chambers, J. M.; Cleveland, W. S.; Kleiner, B.; Tukey, P. A. Graphical methods for data analysis, 1st ed.; Chapman and Hall/CRC: Boca Raton, Florida, 2017.
32. ISO 7730. Ergonomics of the thermal environment - Analytical determination and interpretation of thermal comfort using calculation of the PMV and PPD indices and local thermal comfort criteria. International Organization for Standardization, Geneva, 2005.
33. ASHRAE 55. Thermal environmental conditions for human occupancy. American Society of Heating, Refrigerating and Air-conditioning Engineers, U.S.A., 2020.
34. Peeters, L.; de Dear, R.; Hensen, J.; D'haeseleer W. Thermal comfort in residential buildings: comfort values and scales for building energy simulation. Applied Energy 2009, 86, pp. 772-80. DOI: 10.1016/j.apenergy.2008.07.011.
35. EN 16798-1. Energy performance of buildings - Ventilation for buildings - Part 1: Indoor environmental input parameters for design and assessment of energy performance of buildings addressing indoor air quality, thermal environment, lighting and acoustics. European Committee for Standardization, Brussels, 2019.
36. EN 15251. Indoor environmental input parameters for design and assessment of energy performance of buildings addressing indoor air quality, thermal environment, lighting and acoustics. European Committee for Standardization, Brussels, 2007.
37. EN 1015-3. Methods of test for mortar for masonry - Part 3: Determination of consistence of fresh mortar (by flow table). European Committee for Standardization, Brussels, 1999.
38. Embarro Universal. https://www.embarro.com/en/ (Accessed on 04/02/2022).
39. Ranesi, A.; Faria, P.; Veiga, M.R. Traditional and modern plasters for built heritage: sustainability and contribution for passive relative humidity regulation. Heritage, 2021, 4(3), pp. 2337–2355.
40. Santos, A. R. The influence of natural aggregates on the performance of replacement mortars for ancient buildings: the effects of mineralogy, grading and shape. PhD thesis, Instituto Superior Técnico, Lisbon, 2019.

41. Santos, A.R.; Veiga, R.; Santos Silva, A.; de Brito, J.; Álvarez, J.I. Evolution of the microstructure of lime based mortars and influence on the mechanical behaviour: The role of the aggregates. Construction and Building Materials, 2018, 187, 907–922. DOI: 10.1016/J.CONBUILDMAT.2018.07.223.
42. Pederneiras, C.; Veiga, R.; de Brito, J. Physical and mechanical performance of coir fiber-reinforced rendering mortars. Materials, 2021, 14, pp. 823. DOI: 10.3390/ma14040823.
43. Posani, M.; Veiga, R.; de Freitas, V. P. Thermal mortar-based insulation solutions for historic walls: An extensive hygrothermal characterization of materials and systems. Construction and Building Materials, 2022, 315, 125640. DOI: 10.1016/j.conbuildmat.2021.125640.
44. Ferreira, C.; de Freitas, V. P.; Ramos, N. M. Quantifying the influence of hygroscopic materials in the fluctuation of relative humidity in museums housed in old buildings. In Proceedings of the 10th Nordic Symposium on Building Physics, Lund, Sweden, 15-19 June 2014.
45. ISO 12571. Hygrothermal performance of building materials and products - Determination of hygroscopic sorption properties. International Organization for Standardization, Geneva, 2013.
46. Fraunhofer Institute for Building Physics IBP. Available online: https://wufi.de/en/software/product-overview/ (Accessed on 29 March 2021).
47. Mundt Petersen, S.; Arfvidsson, J. Comparison of field measurements and calculations of relative humidity and temperature in wood framed walls. In Proceedings of the 15th International Meeting of Thermophysical Society, Valtice, Czech Republic, 3-5 November 2010.
48. Mundt Petersen, S.; Harderup, L.H. Validation of a one-dimensional transient heat and moisture calculation tool under real conditions. In Proceedings of the Thermal Performance of the Exterior Envelopes of Whole Buildings XII International Conference, 1-5 December 2013, Clearwater, Florida, USA.
49. Alev, Ü.; Targo K.; Marko T.; Martti-Jaan M. Air leakage and hygrothermal performance of an internally insulated log house. In Proceedings of the 10th Nordic Symposium on Building Physics–NSB 2014, Lund, Sweden, 15-19 June 2014.
50. Stöckl, B.; Daniel Z.; and Hartwig M. K. Hygrothermal simulation of green roofs-new models and practical application. In Proceedings of the 10th Nordic Symposium on Building Physics–NSB 2014, Lund, Sweden, 15-19 June 2014.
51. Villmann, B.; Slowik, V.; Wittmann, F.H.; Vontobel, P.; Hovind, J. Time-dependent moisture distribution in drying cement mortars – results of neutron radiography and inverse analysis

of drying tests. Restoration of Buildings and Monuments, 2014, 20, pp. 49-62. DOI:10.12900/rbm14.20.1-0004.

52. Ferreira, C.; Freitas V.P.; Delgado, J.M.P.Q. The influence of mass tourism and hygroscopic inertia in relative humidity fluctuations of museums located in historical buildings. In Building Pathology, Durability and Service Life.; Delgado J.M.P.Q; Springer, Cham, 2020; Volume 12, pp. 121–144.
53. Cascione, V; Maskell, D.; Shea, A.; Walker, P.; Mani, M. Comparison of moisture buffering properties of plasters in full scale simulations and laboratory testing. Construction and Building Materials, 2020, 252, 119033. DOI: 10.1016/j.conbuildmat.2020.119033
54. Liuzzi, S.; Rubino, C.; Martellotta, F.; Stefanizzi, P.; Casavola, C.; Pappalettera, G. Characterization of biomass-based materials for building applications: The case of straw and olive tree waste. Industrial Crops & Products 2020, 147, 112229. DOI: 10.1016/j.indcrop.2020.112229.
55. Evrard, A.; De Herde, A. Hygrothermal performance of lime-hemp wall assemblies. Journal of building physics 2010, 34(1), 5-25. DOI: 10.1177/1744259109355730.
56. Claude, S.; Ginestet, S.; Bonhomme, M.; Escadeillas, G.; Taylor, J.; Marincioni, V.; Korolija, I.; Altamirano, H. Evaluating retrofit options in a historical city center: Relevance of bio-based insulation and the need to consider complex urban form in decision-making. Energy and Buildings, 2019, 182, pp. 196–204. DOI: 10.1016/j.enbuild.2018.10.026.
57. Libralato, M.; De Angelis, A.; D'Agaro, P.; Cortella, G.; Qin, M.; Rode, C. Damage risk assessment of building materials with moisture hysteresis. In Proocedings of the 8th International Building Physics Conference, Copenhagen, Denmark, 25-27 August 2021. DOI: 10.1088/1742-6596/2069/1/012043.
58. Kunzel, H. M. Simultaneous heat and moisture transport in building components. Fraunhofer Institute of building physics, Germany, 1995. ISBN 3-8167-4103-7.
59. Rode, C. Combined heat and moisture transfer in building constructions. PhD thesis, Technical University of Denmark, Lyngby, 1990.
60. Pina dos Santos, C.A.; Rodrigues, R. ITE54—Thermal transmission coefficients of opaque elements of building envelope (in Portuguese). National Laboratory of Civil Engineering: Lisboa, Portugal, 2009.
61. Mazhoud, B.; Collet, F.; Pretot, S.; Chamoin, J. Hygric and thermal properties of hemp-lime plasters. Building and Environment 2016, 96, pp. 206–16. DOI: 10.1016/j.buildenv.2015.11.013.

62. Ramos, N.M.M.; Delgado, J.M.P.Q.; de Freitas, V.P. Influence of finishing coatings on hygroscopic moisture buffering in building elements. Construction and Building Materials 2010, 24, pp. 2590–97. DOI: 10.1016/j.conbuildmat.2010.05.017.
63. Magalhães, S. A. Comparison between the passive discomfort index and the energy class of rehabilitated residential buildings in Southern Europe (Original title, in Portuguese: Comparação do índice de desconforto passivo com a classe energéticade edifícios de habitação reabilitados do sul da Europa). PhD thesis, Faculty of Engineering of the University of Porto, Portugal, 2020. (pp.85)
64. Kaczorek, D. Moisture buffering of multilayer internal wall assemblies at the micro scale: Experimental study and numerical modelling. Applied Sciences 2019, 9(16), 3438.
65. Colinart, T.; Lelièvre, D.; Glouannec, P. Experimental and numerical analysis of the transient hygrothermal behavior of multilayered hemp concrete wall. Energy and Buildings 2016, 112, pp. 1–11.
66. Goto, Y.; Wakili, K.G.; Frank, T.; Stahl, T.; Ostermeyer, Y.; Ando, N.; Wallbaum, H. Heat and moisture balance simulation of a building with vapor-open envelope system for subtropical regions. Building simulation 2012, 5(4), pp. 301–314.
67. Du, Y.; Habert, G.; Brumaud, C. Influence of tannin and iron ions on the water resistance of clay materials. Construction and Building Materials 2022, 323, 126571.
68. Ramos, N.M.; Almeida, R.M.; Simões, M.L.; Delgado, J.M.; Pereira, P.F.; Curado, A.; Soares S.; Fraga, S. Indoor hygrothermal conditions and quality of life in social housing: A comparison between two neighborhoods. Sustainable cities and society 2018, 38, pp. 80–90.

## 2.3 Article A2 - Relative Humidity Dependent Properties

(the article has been published in the journal *Construction and Building Materials* 2021, 304, 124595; https://doi.org/10.1016/j.conbuildmat.2021.124595)

### Laboratory characterization of relative humidity dependent properties for plasters: a systematic review

### Abstract

An informed choice of plasters can contribute to improving the comfort and health of buildings users. Therefore, knowing the relative humidity dependent properties to consider when analysing the behaviour of different plasters appears as a fundamental for the selection process, as well as their hygroscopic intrinsic characteristics. A review was conducted on both the test methods and data obtained in literature for a benchmark of more than *200* mineral compositions based on clay, lime, gypsum, cement and combination of those binders. Overall, ranges of response for different plasters, gaps and differences in widespread methods and most common practices of characterization observed in literature were identified and discussed.

### Keywords

Clay, gypsum, lime, moisture adsorption, moisture buffering, water vapour permeability.

#### 2.3.1 Introduction

For almost 50 years, a big impulse on the study of all the elements of influence for Indoor Air Quality (IAQ) has been given due to the link found between a poor IAQ and people's health [1], recognizing effects on occupants like the sick-building-syndrome and building-related illnesses. Relative Humidity (RH) of indoor environment influences thermal sensation and comfort, well-being and health of occupants, from irritation or drying of the mucous membranes to asthma, vocal problems and chronicle respiratory diseases. The desired level of indoor RH for ensuring the best conditions has been identified within the range of *40 - 60%* [2]. In case of RH values above *80%*, a higher risk of biological growth has been pointed out, which can not only be negative for occupant's health or induce distress, but also reduce, in some cases, the expected life time of the building [3]. Furthermore, a passive RH regulation is required in a scenario demanding more and more frequently low energy consumption, embodied and operational. RH indoors depends on several parameters, such as outdoor hygrothermal conditions, occupancy (i.e., period, number of people, kind of activities),

ventilation rate, specific constructive solutions, rain penetration, rising dump or built-in moisture. RH regulation can be controlled passively by natural ventilation but, during heating season, this ventilation is commonly minimized not to lose heat. There are evidences that coating materials can be used to moderate the amplitude of RH fluctuation. For these reasons, RH dependent properties of building materials [4] have been studied in the last decades.

Plastering mortars, that based on EN 998-1 [5] are "a mix of one or more inorganic binders, aggregates, water and sometimes admixtures and/or additions" for indoor applications, have an important role both for being widely used and for covering large areas in contact with indoor air. Plastering mortars are commonly composed by a binder, an aggregate and water. Therefore, plasters are building composites. Sometimes their composition includes the presence of bio-products, such as natural fibers, and other additions to improve their properties. A plaster can be applied in one or more layers, with different thicknesses, and often it is coated with finishings, such as a paint system [6-8]. All these factors have influence on the hygroscopic behaviour and permeability of the all-coating system, together with boundary conditions related to the substrate where it is applied, and indoor environment of exposure.

The present study aims to analyse applied methods and respective results for laboratory characterization of RH dependent properties for plasters since in literature a considerable heterogeneity of procedures was detected. For example, hygroscopic behaviour of plasters is related to intrinsic properties of materials like porosity, pore size distribution and bulk density, to properties like surface texture, that are related to application, as well as to RH dependent properties. The latter properties are of more uncertain assessment due to their dependence to indoor microclimatic conditions (RH, T) and time of exposure. The lack of an only protocol for plasters does not promote their homogeneous analysis and, in some cases, affects comparability of results. How to comprehensively characterize plasters response to RH? Which are the methods currently applied and procedures most performed by researchers? What results do we have from literature for different plasters? Are the tendencies of each characteristic similar for the same type of mortars when evaluated by different methods? Therefore, after stating the research questions, eligibility criteria are set to decide inclusion or exclusion of each study. At the end of the selection step, data from 42 articles have been extracted and analysed. Results from about two hundred different plasters were processed and conclusions about the state of art and gaps in literature were lastly presented.

### 2.3.2 Review criteria of selection

This study collects and analyses articles responding to the following criteria:

- Year of publication - Although previous studies exist long ago, it was decided to collect from the publication of *Moisture Buffering of Building Materials,* by Rode et al. [9] in 2005, which set the NORDTEST method, until June 2020.
- Topic - Studies on plasters based on mineral binders such as lime, clay, gypsum and cement, or a combination of those binders were selected. Plaster with special additions like Phase Changing Materials or Super-Absorbent Polymers were excluded since results are considered out of range when compared with plasters with no special addition.
- Methods - If the study met the previous criteria, a laboratory test to determine one or more RH dependent parameters must had been run, to definitively include the article in the review.

The research was conducted on *Web of Science* database with the keywords *plaster*, *experimental*, *moisture*, *MBV*, *WVP*, *adsorption*. According to these search settings, *137* results were found. Applying the referred criteria of selection, *20* of the *137* screened articles were finally selected. To include a larger number of studies, then, the reference list of the already selected articles was checked and, according to the same criteria of exclusion, *22* more articles were included. This implementation method is less time-consuming and permits to include a higher number of articles, although the risk of bias was not assessed. For example, some of the articles included were referenced in other articles of the same research group. Although the risk of slightly affecting statistics, all articles have been included as far as they met the referred criteria. **Table 2.3** presents a synthesis of the *42* articles finally included in the review.

**Table 2.3.** Synthesis of articles characterizing plasters for RH dependent properties selected for the review.

| n | Journal/conference proceeding | Year | Country of 1st author | Main binder | Tested properties | Testing methods |
|---|---|---|---|---|---|---|
| [9] | *Technical University of Denmark. BYG Report* | 2005 | Denmark | gypsum | MBV | NORDTEST |
| [10] | *Experimental Thermal and Fluid Science* | 2005 | Italy | cement | WVP | EN 12086 |
| [11] | *Construction and Building Materials* | 2006 | Czech Republic | lime | S.I.<br>WVP | ISO 12571<br>ISO 12572 |
| [12] | *1st Historical Mortars Conference* | 2008 | Portugal | lime | WVP | EN 1015-19 |
| [13] | *Building and Environment* | 2009 | Estonia | clay | S.I. | - |
| [14] | *Construction and Building Materials* | 2010 | Portugal | gypsum | S.I. | ISO 12571 |

| | | | | | | |
|---|---|---|---|---|---|---|
| | | | | lime | MBV | NORDTEST |
| | | | | | WVP | ISO 12572 |
| [15] | *Applied Thermal Engineering* | 2011 | Egypt | clay | S.I. | ISO 12571 |
| [16] | *XII DBMC- International Conference on Durability of Building Materials and Components* | 2011 | Portugal | gypsum | S.I. | - |
| | | | | lime | WVP | EN 1015-19 |
| [17] | *Construction and Building Materials* | 2012 | Czech Republic | lime | WVP | - |
| [18] | *Construction and Building Materials* | 2012 | Czech Republic | lime | WVP | - |
| [19] | *Building and Environment* | 2013 | Italy | clay | S.I. | - |
| | | | | | WVP | ISO 1015-19 |
| [20] | *4th European Conference of Mechanical Engineering*, | 2013 | Czech Republic | lime | WVP | - |
| [21] | *HMC13 - 3rd Historic Mortars Conference* | 2013 | Portugal | lime | WVP | ISO 12572 |
| [21] | *Energy and Buildings* | 2014 | Portugal | cement | MBV | NORDTEST |
| | | | | lime | WVP | EN 1015-19 |
| [22] | *5th International Conference on Non-conventional Materials and Technologies* | 2015 | U.K. | clay | MBV | ISO 24353 |
| [23] | *Construção magazine* | 2015 | Portugal | clay | S.I. | DIN 18947 |
| | | | | | WVP | - |
| [24] | *Building and Environment* | 2016 | France | lime | S.I. | ISO 12571 |
| | | | | | MBV | NORDTEST |
| | | | | | WVP | ISO 12572 |
| [25] | *International Journal of Heat and Technology* | 2016 | Italy | clay | S.I. | ISO 12571 |
| | | | | | WVP | EN 1015-19 |
| [26] | *Applied Clay Science* | 2016 | Italy | clay | S.I. | UNI 11086 |
| [27] | *Key Engineering Materials* | 2016 | Portugal | clay | S.I. | DIN 18947 |
| [28] | *Journal of Materials in Civil Engineering* | 2016 | Portugal | clay | S.I. | DIN 18947 |
| | | | | | WVP | - |
| [29] | *RILEM Bookseries* | 2016 | Portugal | clay | S.I. | DIN 18947 |
| [30] | *II Simpósio de Argamassas e Soluções Térmicas de Revestimento* | 2016 | Portugal | clay | S.I. | DIN 18947 |
| [31] | *Energy and Buildings* | 2016 | Czech Republic | cement | MBV | - |
| | | | | | WVP | - |
| [32] | *Building and Environment* | 2016 | Spain | clay | MBV | NORDTEST |
| | | | | | WVP | ISO 12572 |
| [33] | *4th Historic Mortars Conference (HMC 2016)* | 2016 | U.K. | lime | WVP | EN 12086 |
| [34] | *Materials and Structures/Materiaux et Constructions* | 2017 | France | clay | S.I. | ISO 12571 |
| | | | | | WVP | ISO 12572 |

| | | | | | | |
|---|---|---|---|---|---|---|
| [35] | *Energy Procedia* | 2017 | Estonia | clay | S.I.<br>MBV<br>WVP | ISO 12571<br>-<br>EN 1015-19 |
| [36] | *Materials* | 2017 | Italy | cement | MBV<br>WVP | NORDTEST<br>EN 1019-15 |
| [37] | *International Journal of Architectural Heritage* | 2017 | Italy | clay | WVP | - |
| [38] | *Cold Climate HVAC 2018* | 2018 | Estonia | clay | S.I.<br>WVP | ISO 12571<br>EN 1015-19 |
| [39] | *Building and Environment* | 2018 | U.K. | clay | MBV<br>WVP | ISO 24353<br>ISO 12572 |
| [40] | *Construction and Building Materials* | 2018 | Italy | clay | S.I.<br>WVP | ISO 12571<br>EN 1015-19 |
| [41] | *Building and Environment* | 2019 | China | gypsum | S.I.<br>MBV<br>WVP | ISO 12571<br>NORDTEST<br>ISO 12572 |
| [42] | *3rd International Conference on Bio-Based Building Materials* | 2019 | France | clay | MBV | NORDTEST<br>ISO 24353 |
| [43] | *IOP Conference Series: Materials Science and Engineering* | 2019 | France | clay | MBV | NORDTEST |
| [44] | *IOP Conference Series: Materials Science and Engineering* | 2019 | Czech Republic | cement<br>lime | WVP | ISO 12572 |
| [46] | *Construction and Building Materials* | 2020 | U.K. | clay | S.I.<br>MBV | DIN 18947<br>NORDTEST |
| [47] | *Construction and Building Materials* | 2020 | U.K. | clay<br>gypsum<br>lime | S.I.<br>MBV<br>WVP | -<br>NORDTEST<br>ISO 12572 |
| [48] | *Construction and Building Materials* | 2020 | Portugal | clay<br>cement<br>gypsum | S.I. | DIN 18947 |
| [49] | *International Journal of Architectural Heritage* | 2020 | Portugal | clay | S.I. | DIN 18947 |
| [50] | *Materials Letters* | 2020 | Italy | gypsum | WVP | ISO 12572 |

Notation: S.I. – sorption isotherms; MBV – moisture buffering value; WVP – water vapour permeability.

The journal with higher number of publications included in the review is *Construction and Building Materials*, covering *19%* of the studies, followed by *Building and Environment* with *14%*. Still, *26%* of the studies are from conferences proceedings. Moreover, *29%* of affiliation institution of the first author are located in Portugal, *20%* in Italy, *15%* in Czech Republic, *12%* in UK, *10%* in France and *7%* in Estonia. A predominance of European Mediterranean countries

exists, that may be linked to energy poverty as those countries have a large number of buildings with lack of thermal insulation. The number of articles testing the considered properties has increased mostly from 2016 on, as displayed in **Figure 2.11**(a), most probably related with increased concern with indoor comfort and energy efficiency.

The characterization of RH dependent properties for plasters commonly passes through the evaluation of adsorption and desorption mechanisms, moisture buffering capacity and WVP. Other connected characteristics are sometimes investigated, such as pore size distribution, surface film resistance [35], moisture penetration depth [40] or moisture diffusivity [25]. Although not all the studies consider all mechanisms at once, they frequently report a combination of several of those.

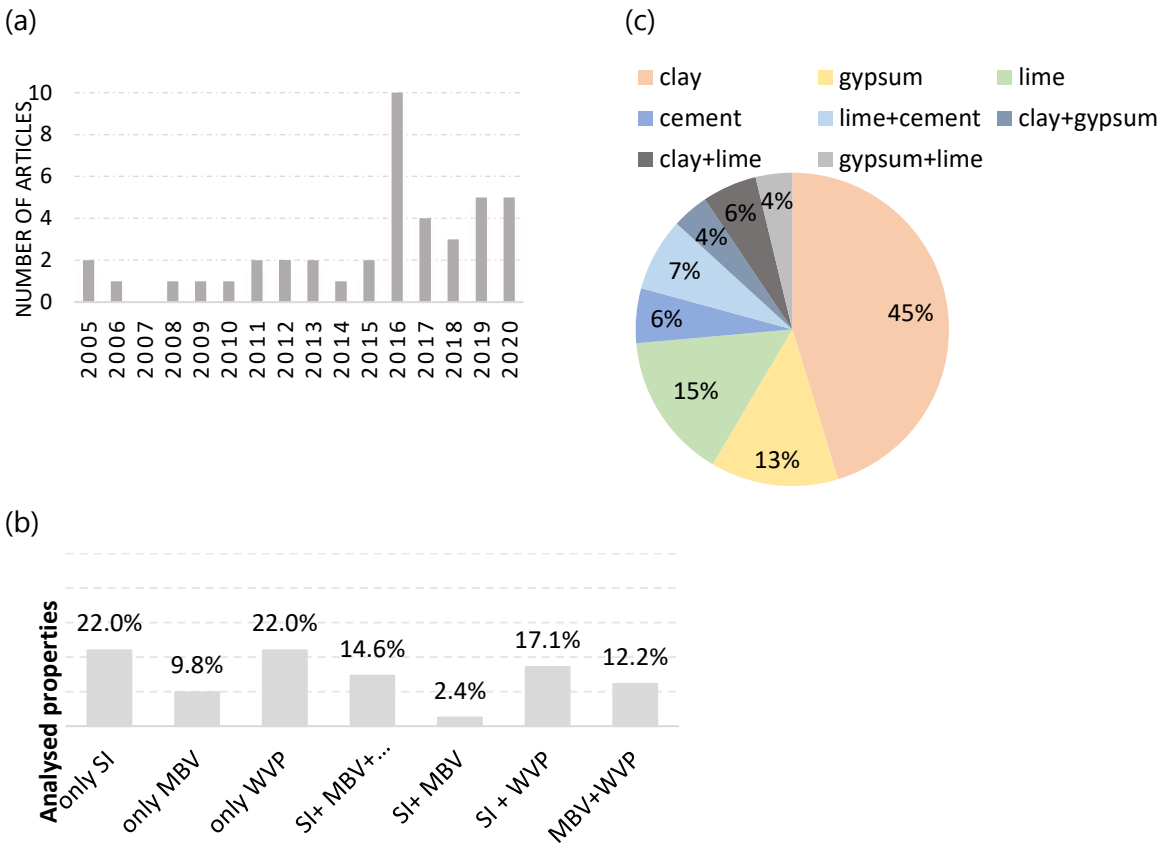


**Figure 2.11**. Temporal distribution of selected articles (a); analysed properties: SI – sorption isotherms; MBV – moisture buffering value; WVP – water vapour permeability (b); percentage distribution of detected plastering mortar by binders (c)

As displayed in **Figure 2.11**(b), around *22%* of considered articles test only adsorption mechanism (in some cases combined with desorption), the same percentage of articles only WVP, *17%* both these properties, and circa *15%* water vapour adsorption, permeability and

moisture buffering together. Regarding the binders selected by authors, the percentage distribution is displayed in **Figure 2.11**(c): plasters based on clay are prevalent, covering *45%* of the studies though gypsum and lime-based plasters are observed at *13%* and *15%*, respectively. Stabilized earth plasters and multi-binder based ones cover only small percentages. The clay plaster is observed in a high number of studies probably due to its acknowledged high hygroscopic capacity, already discussed by Padfield [51] 20 years ago.

### 2.3.3 Observed methods for characterization

The response of plastering mortars to indoor air RH fluctuations in isothermal conditions can be investigated and described through several methods. Sorption isotherms display moisture adsorption and desorption as a function of the exposure time or of the increasing RH. The procedure would test adsorption for an increase of RH and, otherwise, desorption. Methods apply a RH variation to a specimen already stabilized at another RH stage and quantify the moisture content adsorbed or desorbed. These procedures would give a partial information about the hygroscopic behaviour of the material. In the attempt to approximate real conditions, also stress must be included in the study. This parameter is introduced by the characterization of moisture buffering. The ability of the material to adsorb and desorb moisture in this case is tested through cycles repeated several times. One cycle consists in adsorption and desorption. The methods prescribe a determined duration for each cycle phase, the RH conditions and the minimum number of cycles. Thus, through moisture buffering it is possible to know which would be the response of the material under repeated phases of adsorption and desorption, namely if hysteresis occurs. The moisture behaviour of a plaster would depend on many intrinsic properties, i.e. dry bulk density, porosity, pore size distribution, but to be tested in a correct way it is important to evaluate the thickness involved in the mechanism of moisture penetration. In fact, the specimen has to be thick enough to allow the mechanism being fully activated. The water vapour permeability will give knowledge of the thickness involved in the moisture penetration mechanism. Thus, this property is also considered specific of hygroscopic behaviour. More details on the methods and discussion will be presented.

#### 2.3.3.1 Sorption isotherms

The sorption isotherms are curves displaying the moisture adsorption and desorption of a material tested at a fixed temperature. Moreover, it is possible to test the material at one RH increase (and vice versa) for a determined period of time or at multiple increasing RH steps,

each one kept until constant mass is achieved. The first procedure can be referred as a one-step or single-cycle method, the second one as a multi-step. Although both procedures aim to describe sorption behaviour of materials, the duration of the test is fixed in one-step method and unknown (depends on materials' response) in multi-step procedure. This first difference can have, eventually, an impact on the choice of one method or the other, i.e. in case of short time available for laboratory characterization, one-step can be more suitable. Even if single and multi-step methods are both used for testing moisture sorption, they cannot be considered equivalent as a direct result. They are rather complementary since one sets out equilibrium moisture content for given RH stages and the other permit to know the moisture content after a determined period of exposure to one selected RH step. Usually these last two parameters (time of exposure and RH conditions) depend on the environment. A short description of existing methods is here presented to enable the comparison.

The DIN 18947 [52], was found in *34.8%* of the cases, the ISO 12571 [53] was adopted by *43.5%* of the studies and the ISO 24353 [54] was not observed in the selected literature. Moreover, *8.7%* of the articles did not specify the standard adopted and the rest (*13%*) referred to other methods. Approximately *70%* of works testing adsorption also perform desorption. Furthermore, in the section 3.1.2 some differences of execution for the same test method are referred.

##### 2.3.3.1.1 Methods for sorption isotherms

*DIN 18947*

The German standard DIN 18947 [52] describes a one-step procedure specifically defined for earth plasters. After preconditioning the specimens at 50% and 23°C, temperature is kept constant and RH is set at 80% and maintained for the exposure time of 12 h. During the 12 h the standard prescribes five weighing at different, specified, times, and the class of plasters´ hygroscopicity is achieved by comparing the mass increase of the specimens, 15 mm x 200 mm x 500 mm, on metallic moulds, per exposed area (of 1000 $cm^2$) with limits defined by the standard along the period of test.

*ISO 24353 – part for one step method*

The ISO 24353 [54] standard describes a single cycle procedure. The prescribed dimension for specimens is at most 250 mm x 250 mm but not less than 100 mm x 100 mm. Thickness is not specified, deferring to the thickness of the product under test. The standard considers three RH conditions: low, middle and high RH. Temperature should be set at 23±0.5 °C and RH for

preconditioning can be 30%, 50% or 70% depending on the RH condition chosen for the test. After a period of preconditioning, when constant mass is reached (the rate of increase in mass does not exceed 0.01g in 24 hours), the adsorption process can start (55%, 75% or 95% RH) and lasts 12 hours. At the end of the 12 hours the desorption process should start with RH set at lower levels (namely 30%, 50% and 70%). Consecutive weighing (10 min intervals) is prescribed. The water vapor surface resistance when running the test should be set equal to 13.3 ±1.3 $m^2$·h·Pa/µg. This parameter was found strongly influencing the response of bio-based and earth-based building materials [35] and its inclusion in the standard has a relevant role in homogenizing results.

*ISO 12751*

The ISO 12751 [53] standard is addressed to building materials and products for the determination of hygroscopic sorption properties. The prescribed dimension for specimens is a minimum mass of 10 g and, for materials with low dry density, a minimum area of 100 mm x 100 mm is defined for specimens. Two conditioning methods are accepted: desiccator and climatic chamber. Results can be expressed as moisture content mass by mass, mass by volume and volume by volume. Starting conditions of specimens is constant dried mass for adsorption phase and 95% RH for desorption. A minimum of four steps in the range of 30% to 95% RH is prescribed, each one kept until constant mass of the specimen is reached. Desorption process is ended with specimens dried to constant mass. Temperature of testing is 23±0.5 °C or 27±0.5 °C in tropical countries although other temperatures are accepted for testing specific conditions.

#### 2.3.3.1.2 Discussion on sorption isotherms

One-step methods are chosen from *39%* of the selected literature testing sorption mechanism. The majority of the collected articles applying one-step methods adopts a modified version of DIN 18957 [52], adding the same procedure (inverted) to test also desorption [30] evidencing a lack of the standard. Another important adjustment observed regards the duration of moisture loading phase (and unloading, when tested): nearly half of the sources are keeping RH level for 24 h instead of only 12 h. Probably the reason is that testing clayish plasters their hygroscopic capacity is not saturated after the prescribed 12 h and neither after 24 hours [24]. This detected practice can indicate that the adsorption period must be extended to completely describe earth plasters potential moisture adsorption. However, the duration of the loading phase can depend on observed indoor RH fluctuations (namely 12 h as a maximum), in which

case the introduction of the desorption phase and other RH conditions may be suggested. Adsorption results of one-step method found in literature are all expressed in $g/m^2$ and dimensions of the specimens are mostly 500 mm x 200 mm x 15 mm with only one face of 1000 $cm^2$ exposed [52]. These are big specimens, that occupy large space in climatic chambers and that need stable molds not to be damaged when handling. In **Table 2.4** some parameters referring to experimental setting conditions are summarized.

Multi-step methods are chosen by *60%* of the authors, *71%* of which follow the ISO 12571 [53] test procedure. The curve is displayed starting from dry state [25,35,47] or equilibrium at 30% RH [14,16,41] and the highest RH is observed in the range 80-97% [41,42]. The duration of the test mainly depends on the specimen (size and plaster composition). Observed specimens are very heterogeneous in terms of thickness, shape and dimensions of the exposed exchanging surface: cylinder with diameter of 100 mm and thickness of 24 mm [36] or diameter and thickness measuring the same (70 mm) [25], prisms of 60 mm side and 6 mm thickness [14] or 40 mm side and 10 mm thickness [26]. The methods adopted to run the test are indistinctly desiccator and climatic chamber, at times together (very high and low RH levels reached by desiccator and middle ranges by climatic chamber). When water vapor film resistance is not considered the wide variation of specimens' size as well as the free interchanging of equipment can affect results. Also, heterogeneous expression of results has been reported. The observed outputs are moisture content percentage (%) in *53.3%* of the studies, mass by volume ($kg/m^3$) in *26.7%* of the cases, mass by surface ($g/m^2$) in *13.3%* of the studies, and mass by mass (kg/kg) in the remaining *6.7%* cases.

**Table 2.4**. One-step and Multi-step methods observed conditions (referenced in **Table 2.3**).

| | | $Area_{specimen}$ [$mm^2$] | $Dimension_{specimen}$ [mm] | $Thickness_{specimen}$ [mm] | T [°C] | RH [%] | Duration [h] |
|---|---|---|---|---|---|---|---|
| *One-step* | *min* | 6362 | ø 90 | 10 | 20 | 50 | 12 |
| | *max* | 100000 | 500x200 | 20 | 23 | 80 | 36 |
| | *mode* | 100000 | 500x200 | 15 | 23 | - | 12 |
| *Multi-step* | *min* | 300 | 10x30 | 6 | 20 | 0.0 | Until steady-state |
| | *max* | 24025 | 155x155 | 70 | 25 | 97.3 | Until steady-state |
| | *mode* | 7854 | ø 100 | 10 | 23 | 97.0 | Until steady-state |

#### 2.3.3.2 Moisture buffering

The moisture buffering performance of a plaster in an indoor environment is the ability of the building material to capture and release water vapor from the air. It is related to the exposed

surface and thickness of the material combined with the moisture production of the room and air change ratio [9]. To test this performance, many procedures have been developed: the NORDTEST [9] which has been adopted for the majority of the studies (*71.8%*); the Japanese standard JIS A 1470-1 [56], not observed in selected articles; the standard ISO 24353 [54] used in *15.6%* of the cases.

2.3.3.2.1 Methods for moisture buffering

*NORDTEST protocol*

The method was developed running a round-robin test in laboratories of four universities partners of a project, proving the reliability of the procedure. The test applies RH variation from 33% (16 hours) to 75% (8 hours) with a temperature fixed at 23°C, simulating the daily use of a room (8 hours sleeping; 16 hours woke up) in North European countries. The test requires a minimum of three stable cycles (mass variation not exceeding 5% from one day to another) to calculate the final value. Furthermore, the protocol points out 5 different levels of MBV classification, from negligible to excellent, producing a simple scale for comparison (**Table 2.5**). Besides this cyclic test to calculate MBV in a practical way, the protocol developed a method, based on heat transport theory, to calculate an ideal MBV through some material properties (dry density, water vapour permeability) determined at equilibrium under stationary conditions. The ideal MBV is calculated from moisture effusivity bm (kg/(m2·Pa·s1/2), which depends on WVP. Additionally, when calculating MBVideal the thickness must be higher than moisture penetration depth and, to guarantee that ideal and practical MBV are similar, it is recommended that the tested material is homogeneous and thickness exceeds penetration depth in both cases.

**Table 2.5.** MBV classification from NORDTEST [9] method.

| MBV class | Negligible | Limited | Moderate | Good | Excellent |
|---|---|---|---|---|---|
| Minimum MBV [g/($m^{2}$· %RH)] | 0 | 0.2 | 0.5 | 1.0 | 2.0 |
| Maximum MBV [g/($m^{2}$· %RH)] | 0.2 | 0.5 | 1.0 | 2.0 | >2.0 |

For that, preliminary data on penetration depth of different binder-based plasters will be needed. The protocol also gives prescription on the surface film resistance, recommended to be 5.0 x $10^{7}$ $m^{2}$·s·Pa/kg.

*ISO 24353 – part for moisture buffering*

For cyclic test the standard follows the same prescriptions for specimens, apparatus and water vapour surface resistance described for single test in section 3.1.1. Temperature should be set at 23±0.5 °C and RH for preconditioning can be chosen between 43%, 63% or 83% corresponding to low, middle and high RH levels, respectively. According to RH condition chosen, adsorption should be run at 55%, 75% and 95% RH and desorption at 30%, 50% and 70% RH. Each cycle must be performed at constant temperature and keeping each RH level during 12 hours' adsorption and 12 hours' desorption. The standard prescribes to run four cycles. Weighing follows the same prescriptions than the single cycle procedure. Results are expressed as moisture adsorption content (kg/m$^2$), desorption content (kg/m$^2$) and difference between these two contents (kg/m$^2$). Thus, only the desorption of the third cycle and adsorption and desorption of the fourth are considered by the standard and only under the three RH conditions referred.

*JIS A 1470-1*

The Japanese Industrial Standard JIS A 1470-1 [56] firstly introduces loading/unloading phases of the same duration (24 hours each) and specifies three alternative humidity conditions. It gives prescriptions about the material surface film resistance to be equal to 4.8±0.48 ·10$^7$ m$^2$.s.Pa/kg [4] and thickness of specimen to be the same as the recommended application thickness of the tested product. Preconditioning is the same than for ISO 24353 [54] and, keeping constant temperature, RH steps can be 33-53%, 53-75% or 75-93%, according to the chosen RH condition.

2.3.3.2.2 Discussion on moisture buffering methods

The NORDTEST protocol introduced the moisture buffering value and its classification scale. Moreover, it is the only method that provided a way to calculate a practical value for every chosen step of RH. Thus, following this protocol, the results are expressed as moisture adsorption or desorption content referenced to the ΔRH applied. The moisture buffering value is, therefore, less influenced by the chosen RH conditions and comparison of values is easier. Furthermore, it needs to be investigated if the mechanism of moisture behaviour is similar when tested at different RH steps for plasters. The totality of the articles when applying NORDTEST [9] used the same RH conditions than the protocol (33-75% RH) which correspond to low humidity according to ISO 24353 [54], representative of indoor for Nord European countries. Another innovation introduced by the protocol is the prescription for the specimens' thickness to be fitting its moisture penetration depth. To know the moisture penetration depth of specimens, some researchers run NORDTEST at different thickness [35,43,46] and results are

discussed in section 4.2. From the analysed literature, thickness and exposed area of the plaster samples are found quite variable from an experiment to another. The most common dimensions for plasters are squared area of 150 mm side and thickness of 20 mm (**Table 2.6**). The ISO 24353 [54] is observed in less cases and, when followed, the middle RH condition is the most commonly used. The shape and size of specimens are found homogeneously as squares of 150 mm side (**Table 2.6**). The thickness is found quite variable and the same discussion on optimal thickness introduced by NORDTEST can be found [40]. Moreover, one of the analysed articles [43] applied both NORDTEST [9] and ISO 24353 [54] methods, recording some differences in results: for the same clay-based plaster, MBV values correspond to *1.5* g/(m$^2$·%RH) if run by NORDTEST and *1.9* g/(m$^2$·%RH) when run by ISO procedures.

**Table 2.6.** NORDTEST [9] and ISO 24353 [54] methods observed conditions (referenced in **Table 2.3**).

| | | $A_{sample}$ [mm$^2$] | Dimensions $_{sample}$ [mm] | Thickness $_{sample}$ [mm] | T [°C] | RH [%] | n° cycles |
|---|---|---|---|---|---|---|---|
| NORDTEST | *max* | 62500 | 250x250 | 80 | 23 | 75 | 20 |
| | *min* | 7854 | ø 100 | 10 | 11 | 33 | 4 |
| | *mode* | 22500 | 150x150 | 20 | 23 | - | 4 |
| ISO 24353 | *max* | 22500 | 150x150 | 40 | 23 | 75 | 4 |
| | *min* | 22500 | 150x150 | 2 | 23 | 50 | 4 |
| | *mode* | 22500 | 150x150 | 20 | 23 | - | 4 |

Some studies apply a controlled airflow rate when testing moisture buffering of materials, as referred in **Table 2.7**. In fact, this parameter could affect MBV. Cascione et al. [47] refer important differences between laboratory steady-state conditions and real ones (simulated by modelling) where ventilation, moisture transport and other mechanisms are considered. Shi et al. [42] analyze different responses obtained undergoing four different airflow settings (*0.0* m/s, *0.5* m/s, *1.0* m/s, *1.5* m/s) with horizontal or vertical oriented specimens. Adsorption for the vertical group of specimens was higher than for the horizontal ones, especially under maximum airflow conditions. Also, desorption process was influenced by the airflow rate: the higher the flow, the higher the desorption, whereas no big differences between horizontal and vertical position were detected in this phase. For testing plasters, mainly used on vertical surfaces except the ones on ceilings, the experience of Shi et al. [42] should be taken into account as vertical position and controlled settings of airflow rate could lead to different values of adsorption and desorption.

**Table 2.7.** Air velocity with plaster specimens placed horizontally, vertically or undefined, in literature studies.

| Reference | | (Rode et al. 2005) | | | | (Mazhoud et al. 2016) | (Jiang et al. 2020) | (Cascione et al. 2020) | (Shi et al.,2019) | (Thomson et al. 2015) |
|---|---|---|---|---|---|---|---|---|---|---|
| Vair,h [m/s] | Vair | 0.05-0.10 | 0.6 | 0.50-0.59 | 0.1-0.3 | 0.1–0.4 | 0.1–0.4 | < 0.1 | 0.0; 0.5; 1.0; 1.5 | 0.1 |
| Vair,v [m/s] | [m/s] | | | | | 0.07–0.14 | < 0.15 | | | |

### 2.3.3.3 Water vapour permeability

Considering the water vapour transport mechanisms in plasters, WVP (δ) is combined with the analysis of the hygroscopic behaviour nearly in *46%* of the total considered studies. The standards more often referred are ISO 12572 [57] and EN 1015-19 [58], present respectively in about *39%* and *28%* of the articles. The remaining *33%* is divided between some articles not specifying which standard is used and others referring to EN 12086 [59] or to EN 15803 [60] [24,33]. The last two European standards are specific for thermal insulating products and cultural property and will be no further discussed. Thus, for the numbers of data available, only testing procedures of ISO 12572 and EN1015-19 have been here summarized.

#### 2.3.3.3.1 Methods for water vapour permeability

*ISO 12572*

Standard ISO 12572 [57] aims to determine water vapour permeance and/or permeability of building materials and products. It describes the cup test method performed in wet or dry conditions. Circular or square specimens with thickness similar to plasters are used, placed on a cup and sealed. The interior side of the specimen is exposed to a wet or dry conditions, while the assembly is placed in climatic chamber and the other side of the specimen is exposed to a specified RH condition. The exposed area is prescribed to be at least 0.005 $m^2$ and twice the thickness of the specimen. The thickness can be the same of the recommended application thickness of the product, and in case of homogeneous materials not exceeding 100 mm. The expression of results could be reported as water vapour: permeance w (kg/($m^2$·Pa·s), permeability δ (kg/(m·Pa·s)), resistance factor μ (-) and diffusion-equivalent air layer thickness $S_d$ (m). Furthermore, it has been observed that the ISO 12572 [57] refers to Schirmer formula to calculate the WVP of the air, $\delta_a$, required to calculate the water vapour resistance factor ($\mu=\delta_a/\delta$), as equation 1:

$$\delta_a = \frac{0.083 \cdot p_0}{R_V \cdot T \cdot p} \cdot \left(\frac{T}{273}\right)^{1.81} \quad (1)$$

where $p_0$ is the standard barometric pressure, 1013.25 hPa; $R_v$ is the gas constant for water vapour, 462 N·m/(kg·K); $T$ is the temperature of the experiment, expressed in K; $p$ is the mean barometric pressure, expressed in hPa.

The ISO 12572 [57] also provides a graph for deducing $\delta_a$ at 23°C as function of the barometric pressure.

Nevertheless, in the analysed studies the procedure to calculate $\delta_a$ is not always expressed and, when it is, sometim

es other equations are reported, as the equation 2 from Künzel [64] defined by McGregor *et al.* [35]:

$$\delta_a \approx 2 \cdot 10^{-7} \frac{T^{0.81}}{p_0} \quad (2)$$

or equation 3 from ASTM E96/E96M-10 [61] or EN 15803[60]:

$$\delta_a = \frac{2.3056 \cdot 10^{-5} \cdot p_0}{R \cdot T \cdot p} \left(\frac{T}{273}\right)^{1.81} \quad (3)$$

where $p_0$, $T$ and $p$ are the same parameters than in equation 1 and R is the gas constant for water vapour, 462 N·m/(kg·K).

The value of $\delta_a$ calculated using the referred equations, with conditions of 296 K temperature and standard barometric pressure, would be floating between *1.95* and *2.05* $E^{-10}$ kg/(m·Pa·s).

*EN 1015-19*

The European standard [58] specifies a method for evaluating water vapour permeability of hardened rendering and plastering mortars, unlike the methods introduced so far. Sampling, preparation and storage of specimens is accurately described, due to its specificity for mortars. The specimen is set in test cup and sealed. The area of the circular cup has to be approximately 0.02 $m^2$ that correspond to approximately 16 cm diameter. Test is run at 20±2°C and 50±5% RH inside a climatic chamber, while inside the cup a saturated solution of $KNO_3$ (93.2%) for upper hygroscopic range in wet conditions or of LiCl (12.4%) for lower hygroscopic range in dry conditions is used. An air gap of 15±5 mm should be left between the specimen and the surface of the solution. No prescriptions are given about thickness of the test specimen. The assembly (cup + specimen) is weighed at appropriate time intervals until the quantity of water

vapour passing through the specimen is constant. Calculation and expression for permeance and permeability are reported in the standard.

#### 2.3.3.3.2 Discussion on water vapour permeability methods

The ISO 12572 [57] was found equally performed in dry or wet cup, with only few works publishing results for both. In **Table 2.8** the experimental conditions for various studies are reported. The most common RH used in the dry cup test is 0-50% and in the wet cup is 93-50% (interior-exterior of the cup). The shape and dimension of specimens was observed mainly as circular with a diameter of 100 mm but also square specimens of various size were found. The characterization following EN 1015-19 [58] shows always circular specimens with big differences in specimens´ dimensions (area and thickness, that may be justified by the specimen dimensions defined in a previous version of the standard, where smaller specimens were used) and RH settings among published articles (**Table 2.8**). Following one standard or the other, the dry or wet cup test procedures are considered equally valid, representing different test methods to calculate the same material property. However, what happens in the open pores of the specimen from a sorption point of view is not the same: the mechanism changes from molecular adsorption at lower RH levels to capillary condensation at high RH. Exposure at 0-50% or 95-50% RH can introduce differences in response of some hygroscopic plasters, also if based on the same binder [35]. Therefore, results using the wet and dry cups should not be directly compared.

**Table 2.8.** ISO 12572 [57] and EN 1015-19 [58] observed conditions (referenced in **Table 2.3**).

| | | $A_{specimen}$ [$mm^2$] | $Dimension_{specimen}$ [mm] | $Thickness_{specimen}$ [mm] | T[°C] | $\Delta RH_{dry}$ [%] int-ext | $\Delta RH_{wet}$ [%] int-ext |
|---|---|---|---|---|---|---|---|
| ISO 12572 | *max* | 44100 | 210x210 | 50 | 23 | 23-60 | 95-50 |
| | *min* | 7854 | ø 100 | 10 | 20 | 0-23 | 85-60 |
| | *mode* | 7854 | ø 100 | 20 | 23 | 0-50 | 93-50 |
| EN 1015-19 | *max* | 17671 | ø 150 | 38 | 23 | 12.4-50 | 100-40 |
| | *min* | 7854 | ø 100 | 10 | 20 | 0-50 | 93.2-50 |
| | *mode* | - | - | - | 20 | - | 93.2-50 |

The values of WVP of air ($\delta_a$) calculated from the literature are found as minimum *1.675* $E^{-10}$ and maximum *2.052* $E^{-10}$ kg/(m·s·Pa)). The highest and lowest water vapour resistance factor corresponding to each value of permeability has been therefore displayed through error bars in **Figure 2.12**. The lowest the water vapour permeability of the material, the widest the error when expressing water vapour resistance factor.

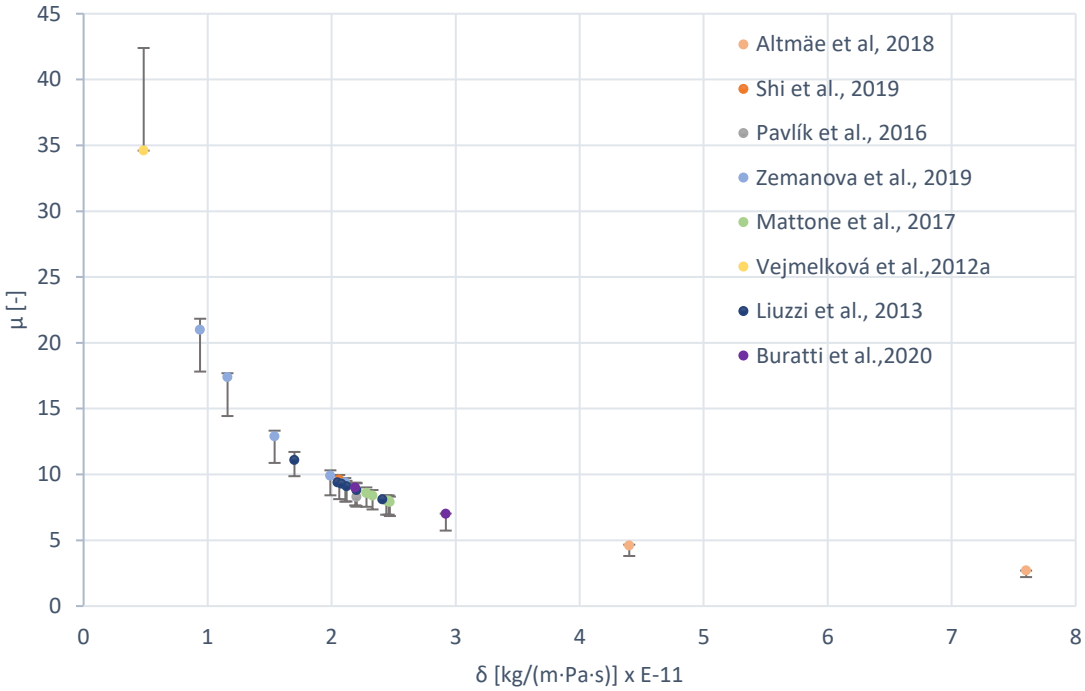


**Figure 2.12.** Correlation between water vapour permeability and resistance factor.

Results obtained from dry and wet cup tests for the same specimens of air lime or clay-based plasters [41, 17,18-20] are considerably different, probably due to capillary condensation in the pores when performing the wet cup test. **Figure 2.13** presents in light grey values obtained running the wet cup test, compared with full columns in dark grey representing results of the same experiment but with dry cup. The closest pair of values observed for water vapour resistance factor run in both test methods is *9.1-15.1* (about *165%* of increase in the dry cup) and the furthest is *10.95–37.12* (about *340%* of increase in the dry cup). Nevertheless, two out of the three studies here referred were conducted by the same research team on plasters based on lime with additions (metakaolin or grinded bricks) but a greater number of studies is desirable to validate the hypothesis that the two methods are not equivalent for plasters.

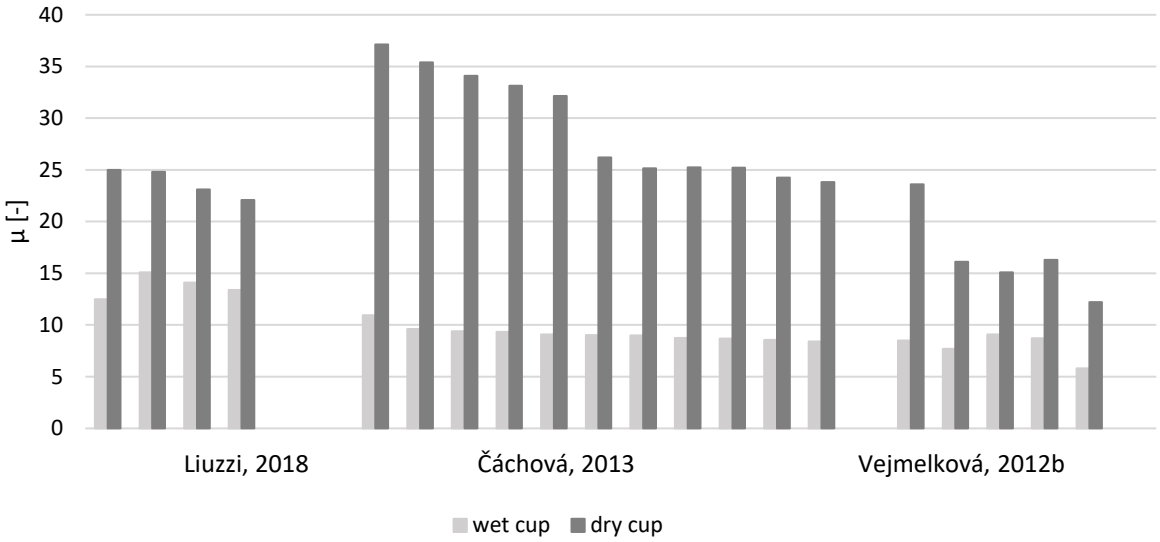


**Figure 2.13.** Water vapour resistance factor (μ) for wet and dry cup test procedures.

## 2.3.4 Data meta-analysis

### 2.3.4.1 Sorption isotherms

The one-step method is mainly used for clay plasters since the DIN 18947 [52] is addressed to this type of plasters but, within the references, also some other binder-based plasters have been tested for comparison [48]. In **Figure 2.14**(a), results (in g/m$^2$) are reported together with DIN [52] limits for different time of adsorption exposure (6h, 12h, and further for 24h and 36h). In Table A.1 of Supplementary materials more information is reported about considered studies for sorption isotherms. Inside the group of clay plasters there are important differences in terms of compositions. Differences could depend on clay mineralogy [49], addition of bio-aggregates as plant powder [46] or fibers [30,13], sand grain size distribution [28] or added content of other binders [30]. Moreover, some studies were testing the same plaster prepared in different shapes or dimensions [29] or combining more than one of the referred factors [24]. In literature the effect of binders' addition to clay based plasters was found to reduce their adsorption and desorption capacity. Thus, the results reported are in agreement with the expected behaviour, displaying a higher moisture capacity of the unstabilized clay based plaster compared with the stabilized ones. Furthermore, the displayed values of adsorption do not represent the maximum moisture content of clay plasters neither at 36 hours, when the material is still not saturated. Gypsum and cement based plasters, on the contrary, were no

longer adsorbing after 12 hours. Maybe 36 hours' duration of loading phase is not considered a realistic simulation, but in winter season under free running conditions in specific areas of unheated buildings in Mediterranean countries, it could happen that RH level is kept around 80% for longer periods [62].

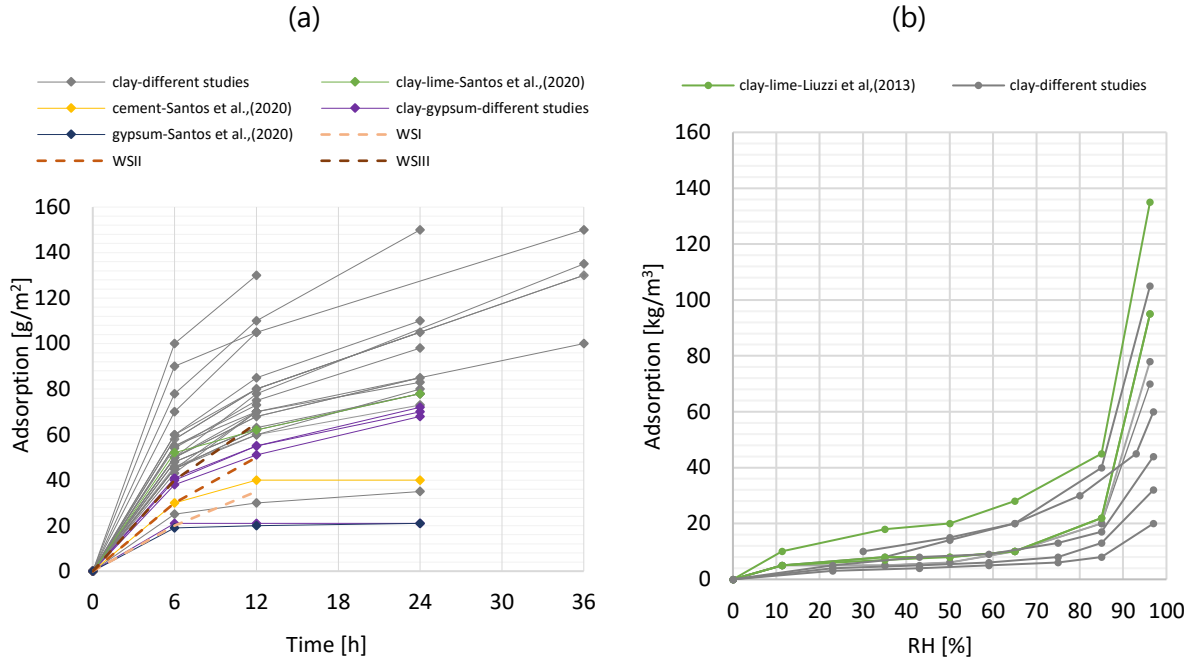


**Figure 2.14.** Adsorption of plasters with different binders for: (a) one-step method and limits of DIN 18947 [52] classes WSI to WSIII at different exposure time; (b) multi-step methods at different RH.

Multi-step tests are run with different levels of RH, chosen by each author from the range suggested by the standard. In some cases a real *scenario* of indoor environment [36] with different occupation and ventilation settings is considered; in other cases standard prescriptions are followed and RH is pushed to 95-97%, values hardly observed in common indoor environment. Values of uptaken moisture (kg/m$^3$) at successive RH steps of stabilized and unstabilized earth plasters are reported in **Figure 2.14**(b). There is an evident rise in the slope of the curves above 80% RH, emphasized when lime is added, probably due to the activation of another mechanism besides adsorption. Indeed, adding a 5% wt. of lime to a clay based plaster results in an increase of moisture adsorbed, namely about a 30% higher than in the plaster without any lime, when the step 85 to 96% RH is considered [19]. The change in the slope often involves hysteresis in desorption, when tested [41,25,35]. This phenomenon, mainly observed for lime or gypsum plasters, has been related by some authors to capillary condensation and possibly to change of microstructure due to additional carbonation of lime [47,14,25]. Moreover, the influence of temperature on the mechanism was rarely investigated; Ashour et *al.* [15] tested various formulations of plasters based on clay with fibers addition, all

showing equilibrium moisture content as inversely proportional to temperature. Thus, a small addition of gypsum or lime in plasters can be considered to improve adsorption behaviour of those exposed to high RH and T environmental conditions. Nevertheless, the desorption behaviour should always be tested to ensure there is no decay in moisture buffering capacity when continuous cycles are run.

#### 2.3.4.2 Moisture buffering

Dimension of exposed surfaces and RH settings are more homogenous within the analysed literature for MVB evaluations in comparison to all other procedures analysed. A linear correlation between temperature and MBV is observed [25] probably due to the influence of temperature on saturation vapour pressure [14]. To profit all the plaster capacity and provide a correct estimation of MBV, the thickness of the specimens has to be equal or higher than their moisture penetration depth. Laboratory characterization [40] is often conducted to determine the optimal thickness of a plaster. Phelipot-Mardelé et al. [43], testing clay-based plasters with addition of hemp powder and pumice sand, conclude that in specimens *70* mm thick, the phenomenon of moisture penetration is still uncompleted, demanding to further testing campaign. On the contrary, according to Jiang et al. [46], a clay-based plaster incorporating hemp powder shows only plus *15%* of MBV when its thickness is increased from *10* mm to *70* mm, concluding that the first 10 mm of material are responsible for the biggest part of the mechanism. McGregor at al. [35], also testing clay-based plasters, referred the optimal MPD for "fine calcareous-clay" in between *20* and *40* mm and for "kaolinitic clay" in between 10 and 20 mm. Since thicknesses of the tested specimen influences the moisture buffering, in Fig. 5 the MBV (practical) and $MBV_{ideal}$ of observed plasters are presented in function of it. The ideal value of MBV is presented only in five of the considered studies [14,19,32,41,42] following the method proposed from Rode et al. [9]. Despite the limited data, $MBV_{ideal}$ was however included and its values are found in the range of the corresponding practical ones. Based on the literature results, MBV of gypsum plasters is greater for 20 than 10 mm thicknesses, making the former preferable. Instead, lime based plasters keep the same value both for thicknesses of 20 mm as of 80 mm. Thus, 20 mm for application would be advisable to optimize their moisture buffering using the lowest thickness. The same choice applies to clay based plasters, which highest values of moisture buffering are observed for thicknesses of 20 mm. Thus, 20 mm of thickness corresponds to common application practice for a plaster and for the three binders referred can be consider the optimal one for moisture buffering, unless MPD is calculated.

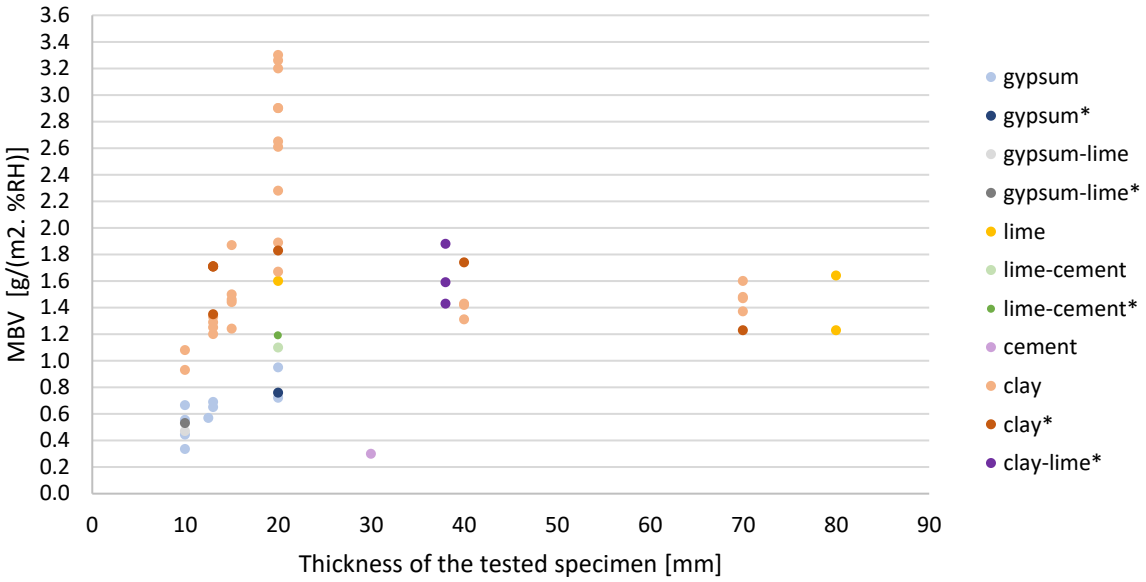


**Figure 2.15.** MBV and MBVideal (*) for plaster specimens with different thicknesses.

According to NORDTEST [9] classification (**Table 2.5**) and based on **Figure 2.15**, it appears that, within the referred literature, there are no plasters with *negligible* MBV; plasters based on gypsum and gypsum-lime have mainly a *moderate* behaviour whereas based on lime and clay-lime correspond to *good* behaviour according to the classification. From the collected significant amount of data regarding clay-based plasters, it is visible that it covers different classes of behaviour, but it is the only material reaching *excellent* classification.

#### 2.3.4.3 Water vapour permeability

The WVP test is used in some articles to determine MPD, as referred in the previous paragraphs, or to investigate the property itself as another RH dependent-one. Permeability (δ) and resistance factor (μ) observed are resumed in **Figure 2.16**. Some of the reported values have been calculated from the published data available, using a WVP of air ($\delta_a$) of 19.50 $E^{-11}$ kg/(m·Pa·s). The addition of lime or gypsum to the clay based plaster appear to slow down its water vapour permeability. Instead, combination of cement and air lime, often taken with a weight ratio 1:1 [21,44], shows an enhancement of WVP. Thus, the addition of lime can be a tool to improve the poor permeability of cement. Not many results were found for blended binder-based plasters, requiring further investigation.

(a) (b)

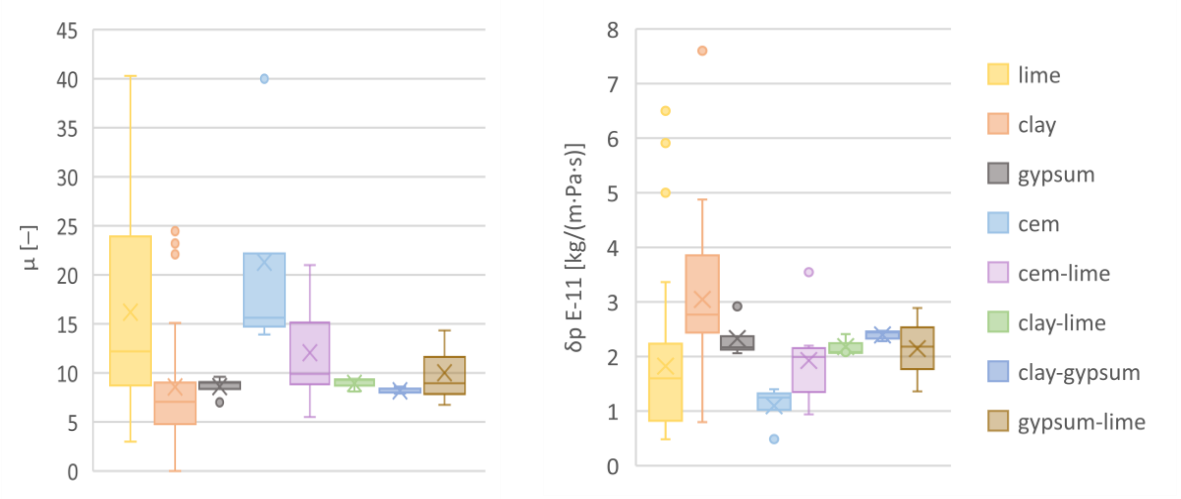


**Figure 2.16.** Water vapour resistance factor μ (a) and permeability δ (b) for different binder plasters (referenced in **Table 2.3**).

### 2.3.5 Results and discussion

A resume of existing test methods for characterization of RH dependent properties, their most common practices of application and a meta-analysis of results present in literature, has been presented. Moreover, a database of results has been created (Table A.1 - A.3 of Supplementary Materials). Methods have been presented and discussed in section 3 and some strengths and errors have been identified.

DIN 18947 [52] and ISO 24353 [54] were presented as one-step methods, addressed to evaluate the materials' moisture adsorption in a determined period of time and for a chosen RH variation. The ISO standard is considered the most suitable to describe the moisture behaviour of plasters because it admits three different humidity conditions, gives prescriptions on the surface film resistance and includes adsorption and desorption. The German standard, instead, only admit adsorption for a duration of 12 hours. Desorption is not covered by the standard. Thus, the duration of moisture release and the eventual residual moisture content are not investigated when using the DIN18947 [52]. However, the mechanisms of desorption and possible hysteresis of the material are important to fully understand its response to RH fluctuations and were, indeed, implemented in many of the studies. Moreover, only one range of RH condition is considered by the DIN standard (most probably common in German buildings) whereas indoor microclimate can present many different scenarios in other countries. Nevertheless, a more detailed prescription on thickness of the tested product in case of plasters, recommending it to be higher than the moisture penetration depth, should be added to the recommendations of both standards. Moreover, to facilitate comparison of results

from different studies it could be preferable the expression of results in terms of gained mass per volume (rather than area). Multi-step methods aim to describe the moisture behaviour at equilibrium moisture content of materials. The ISO 12571 [53] prescribes the range of RH exposure 0-95% and admit the use of climatic chamber or desiccator indiscriminately. Nevertheless, to reach low and high stages of RH, is common practise the use of desiccator due to technical difficulties in reaching this values of RH by the climatic chamber. This turns the use of both in the same laboratory characterization a widespread practice, although in climatic chamber the air velocity would be higher than in desiccator and it was already observed [55] that the air flow can have big effects on adsorption and desorption properties of some hygroscopic materials. A prescription on the air flow inside the chamber would be recommended to ensure a better comparison of the test results. The characterization of moisture buffering introduces the material stress factor in the study. Both NORDTEST protocol [9] and ISO 24353 [54] observed in the analysed literature consider the surface film resistance but NORDTEST implemented prescription on the thickness of the specimen, not present in the international standard. Moreover, the calculation of the value introduced by the protocol, makes the results independent from the chosen RH conditions and gives a tool of easy comparison. Thus, the NORDTEST protocol is considered the most accurate of the two. This method, on the other side, is set on indoor hygrothermal conditions of Northern European Countries where, during winter, indoor temperature is considered 23°C and RH fluctuation in between 33% and 75%. However, there are many different situations, according to regional climate and access to energy, that the method may not represent, namely when energy poverty occurs and heating is not continuous during Winter. If water vapour loading and unloading time is considered a fixed parameter (16 hours of activity and 8 hours of sleeping at least for developed countries) the minimum and maximum indoor values of RH and temperature could variate from country to country. Representativeness of the test is questioned for different conditions and eventually different RH ranges. Testing water vapour permeability, both the two methods (ISO 12572 [57] and EN 1015-19 [58]) allow the use of dry or wet cup procedures indistinctly. When testing plasters, the two procedures were found to give different results. Although the ISO introduces the information that "at higher humidities the material pores start to fill with water" [57] and transport of liquid water increases, it seems reasonable that for plasters dry cup procedure should be recommended as conservative approach. The European standard [58] is addressed to hardened rendering and plastering mortars and, for this reason, contains more specifications on sampling, preparation and storage of the tested mortars. The circular shape prescribed from this standard seems more accurate for avoiding edges and

easily applicable to plasters, cast in moulds. On the other side calculation and expression of results is less meticulously described than in the ISO [57].

Furthermore, the application procedures of each method in the selected literature has been analysed and some heterogeneity observed. In **Table 2.9** a summary of the parameters considered for the comparison is reported. Experimental conditions (T and RH), duration of the experiment and dimensions of specimens (surface and thickness) are the main variables considered. Comparability of results is calculated as the combination of the three previous parameters. The NORDTEST method [9] is the most homogeneous for hygrothermal conditions, test duration and dimensions of specimens. The poorest comparability is reported for hygroscopicity tested according to ISO 12751 [13], where shape, exchanging surface and thickness of the specimens vary a lot from one study to another, and a big diversity of RH steps is observed. All the other methods result mildly comparable.

**Table 2.9.** Resume of characteristics for observed applications of methods to test RH dependent properties of plasters.

| Method | Property | Conditions | Duration | Dimensions | Comparability | Representativeness |
|---|---|---|---|---|---|---|
| DIN 18947 | hygroscopicity | + | - | + | *moderate* | *clay* |
| ISO 12571 | | - | n.a. | - | *poor* | *diverse* |
| NORDTEST | MBV | + | + | + | *good* | *diverse* |
| ISO 24353 | | + | + | - | *moderate* | *diverse* |
| ISO 12572 | WVP | - | n.a. | + | *moderate* | *diverse* |
| EN 1015-19 | | + | n.a. | - | *moderate* | *diverse* |

**Table 2.10** reports ranges of results for the various plasters, as found in the reviewed literature. According to the German standard DIN 18947 [52] modified to 24 hours' duration, clay plasters show the highest adsorption of *140* g/m$^2$ [63].

From the few results available on not-only clay based plasters, it appears interesting that the lowest value of adsorption (*73* g/m$^2$) for a specific clay plaster with *20%* addition of gypsum [40] results 2 times higher than the lowest value of adsorption for another clay plaster with no addition. The variability of clays' response largely depends on the different mineralogy, turning the observed range of results for this material quite wide. Moreover, expression of results does not consider the thickness of the tested specimen with the risk of providing an inaccurate data. Clay-based plasters show very good adsorption capacity at steady state too, although the highest value is observed for the hemp-lime plasters tested by Mazhoud *et al.* [25], with a hemp-lime mass ratio of 0.15. These plasters show a moisture content of *10%* when stabilized at 97% RH. Without addition of hemp powder, lime plasters show lower hygroscopicity, thus

for this binder base it is observed the widest range in between all the reported plasters. Furthermore, it is important to remark the hysteresis phenomenon referred by many researchers particularly for lime-based plasters. Further investigation is suggested for gypsum-lime plasters, once few data were found available and adsorption values appear too low compared with the range of plasters based on single gypsum and single lime. MBV values are all above *0.2* as referred already in section 4.2, with no plaster classified as *negligible* according to the NORDTEST [9] (**Table 2.5**). Still, as expected from adsorption results, clay-based plasters show the highest MBV. Ranges are very varied: more than *2* g/(m$^2$·%RH) for clay, *1* g/(m$^2$·%RH) for air lime and about *0.50* g/(m$^2$·%RH) for gypsum plasters. Just one result was found for cement plasters, whereas really small ranges are observed for plasters with more than one binder due to the small number of case studies. WVP is determined for all the different types of plasters, giving the opportunity of a fairer comparison. According to results here reported, the highest value of WVP is observed in clay-based plasters, followed by air lime, lime-cement, gypsum, gypsum-lime, clay-gypsum, clay-lime and cement. Cement shows the lowest WVP. As the low WVP of cement is commonly assumed, the improvement obtained from the combination with lime could be deeper investigated to increase its compatibility with traditional buildings. The lower range limit for gypsum, clay-lime and clay-gypsum plasters are all above *2* E$^{-11}$kg/(m·Pa·s), that once more could be due to a lack of number of results or to a consistently permeable behaviour.

**Table 2.10**. Value or range of values for adsorption, MBV and WVP from literature (referenced in **Table 2.3**).

| Property | Unit | | C | AL | G | CE | C-AL | C-G | G-AL | AL-CE |
|---|---|---|---|---|---|---|---|---|---|---|
| Adsorption* | [g/m$^2$] | max | 140 | - | 22 | 40 | 24 | 82 | - | - |
| | | min | 35 | | | | | 73 | | |
| Adsorption** | [%] | max | 6.30 | 10 | 3.10 | - | - | - | 0.98 | - |
| | | min | 0.10 | 0.03 | 0.08 | | | | 0.16 | |
| MBV | [g/(m$^2$·%RH)] | max | 3.3 | 1.64 | 0.95 | 0.30 | - | - | 0.47 | 1.19 |
| | | min | 0.93 | 0.67 | 0.33 | | | | 0.42 | 1.10 |
| WVP*' | E$^{-11}$[kg/(m·Pa·s)] | max | 7.60 | 6.50 | 2.92 | 1.40 | 2.41 | 2.47 | 2.89 | 3.55 |
| | | min | 0.8 | 0.48 | 2.06 | 0.49 | 2.05 | 2.28 | 1.36 | 0.94 |

AL - air lime; C - clay; CE - cement; G - gypsum; L - lime; *according to DIN 18947 [52] adsorption at 24 hours; **according to ISO 12571 [53]; *' according to ISO 12572 [57] and EN 1015-19 [58] by wet and dry cup all together.

The methods and results until here discussed pave the way for some considerations. The thickness of specimens should be set according to moisture penetration depth. For clay based specimens the thickness is found equal or above *20* mm [35], compatible with common plaster thickness. The referred value could be chosen also for other based plasters where MPD is

proved lower or equal than the value and no specific design purposes occur. The round shape attends standard prescription for WVP and remove possible dispersions in sealing the edges while testing adsorption/desorption mechanisms in static and/or dynamic settings. A diameter of 100 mm is here suggested, since it is widely used for WVP and for adsorption/desorption isotherms in multi-step method tests. Moderating and unifying the dimensions of the specimen can improve the efficiency of production and simplify the execution of the tests, i.e. a higher number of specimens can be simultaneously placed in a climatic chamber, quicker response to each step in case of multi-step adsorption/desorption test, higher manoeuvrability. When a dynamic test is run the surface film resistance should be set according to ISO 24353 [54].

### 2.3.6 Conclusion

Indoor moisture passive control performed by plasters is considered nowadays an important goal to improve comfort of occupants, avoid health diseases linked with bad quality of indoor air, and save energy. Thus, it is desirable to consolidate the methods used to characterize plasters in that regard. The present study analyses the principal existing methods for characterization of relative humidity dependent properties, points out variability in the procedures most performed in literature and synthetizes ranges of results for different binder-based plasters.

ISO 24353 and DIN 18947 are the two standards used to characterize adsorption/desorption behaviour by one-step procedure. The first is recommended, as it is found more complete, preferably adding the calculation and use of the optimal specimen thickness. The standard ISO 12571 is used to describe equilibrium moisture content at steady state. Doubts are raised on the representativeness of real conditions for some of the steps prescribed by the standard as they are found really low or high. Furthermore, the standard allows using climatic chamber and desiccator methods indistinctly. This indication results in having the two methods adopted within the same test procedure in common practice, which may provide a poor accuracy of results because of the different air velocity affecting the two environments. For testing moisture buffering the most suitable method is the NORDTEST although further investigations are believed to be necessary to evaluate the validity of this method for different environmental conditions (different duration of exposure and RH levels) that can be typical of non-Northern European Countries. Methods for water vapour permeability are found quite similar, although the European standard EN 1015-19 is addressed to hardened rendering and plastering mortars,

thus providing more detailed specifications for plasters. On the other side, the ISO 12572 accurately describes all results calculation and properties that can be determined in relation to the permeability or resistance of building materials to water vapour diffusion. Both standards allow for the use of wet and dry cup indiscriminately. The dataset obtained from literature clearly indicates that for hygroscopic materials the results from one procedure or the other are very different. Hence, the dry cup is preferable as it gives the results in the worst case scenario, i.e. the lowest vapour permeability among the two cup tests. Anyway, it seems that some indication should be provided in both standards, concerning which type of cup should be used or defining that the results must always be provided together with the specific indication of the test condition used, namely the RH inside the cup or, at least, the type of test-cup.

Results from one-step and multi-step methods confirm the high adsorption capacity of clay-based plasters. Cement and gypsum based plasters, instead, show the lowest value of adsorption and the quickest saturation. The influence of the addition of low content of lime or gypsum in clay plasters should be further investigated. Indeed, if it may appear to slightly reduce adsorption capacity when exposed to 80% RH, for higher RH exposures it can introduce an increase in moisture adsorption. Nevertheless, desorption of stabilized clay plasters should be more investigated since the lime and/or gypsum added can cause hysteresis and reduce the moisture buffering. However, most analysed plasters are classified as *good* according to the NORDTEST classification. For clay, lime and gypsum based plasters a thickness equal to *20* mm is found suitable, in case the moisture penetration depth is not calculated. Water vapour permeability of clay, gypsum and lime was found, as expected, better than cement. Thus, cement shows the lowest permeability, which can be significantly improved by adding lime, according to some results.

In order to have consistent results for the most significant RH dependent properties of plasters, apart from the methods selection and improvement suggested, some homogenization of test methods and shapes of specimens should be considered. Specimens with cylinder shape of about *100* mm diameter and *20* mm thickness, when greater than moisture penetration depth, could be adequate for the overall study of RH dependent properties of different types of plasters. However, the application of a plastering mortar on a substrate may change its microstructure and, therefore, its performance when tested for RH related properties. Thus, specimens demoulded after having being moulded in contact with a substrate should also be tested and validated.

Concluding, for reducing energy consumption while improving indoor air quality and comfort, the contribution of plasters for RH related properties can be considered. Furthermore, to

permit a fairer comparability of different plastering solutions, it emerges the need of a standardised protocol designed to fully describe plasters in their dependence on the considered RH conditions. Finally, the use of clay-based plasters appears very promising in this regard.

### Acknowledgements

### Funding

This research was founded by Portuguese Foundation for Science and Technology: PD/BD/150399/2019 – 1st author Doctoral Training Programme EcoCoRe - and UIDB/04378/2020 - Civil Engineering Research and Innovation for Sustainability Unit-CERIS.

## References

1. Jones AP (1999) Indoor air quality and health. *Atmospheric Environment* 33(28), 4535–64.
2. Arundel AV, Sterling EM, Biggin JH, Sterling TD (1986) Indirect health effects of relative humidity in indoor environments. *Environmental Health Perspectives* 65, 351.
3. Viitanen H, Ritschkoff AC, Ojanen T, Salonvaara M (2004) Moisture and bio-deterioration risk of building materials and structures. In *2nd International Symposium ILCDES 2003, Integrated Life-time Engineering of Buildings and Civil Infrastructures*, 151-156.
4. Kreiger BK, Srubar III WV (2019) Moisture buffering in buildings: A review of experimental and numerical methods. *Energy and Buildings* 202, 109394.
5. CEN (European Commetee for Standardization) EN 998- 1: Specification for mortar for masonry - Part 1: Rendering and plastering mortar. Brussels, Belgium, 2016.
6. Faria P, Tavares M, Menezes M, Veiga R, Margalha G (2010) Traditional portuguese techniques for application and maintenance of historic renders. In HMC2010 - *2nd Historic Mortars Conference and RILEM TC 203-RHM Final Workshop*, 609-617.
7. Brito V, Diaz Gonçalves T, Faria P (2011) Coatings applied on damp building substrates: Performance and influence on moisture transport. *Journal of Coatings Technology and Research* 8(4), 513–25.
8. Parracha JL, Pereira AS, Velez da Silva R, Almeida N, Faria P (2019) Efficacy of iron-based bioproducts as surface biotreatment for earth-based plastering mortars. *Journal of Cleaner Production* 237, 117803.

9. Rode C, Peuhkuri RH, Mortensen LH, Hansen KK, Time B, Gustavsen A, Ojanen T, Ahonen J, Svennberg K, Harderup LE, Arfvidsson, J (2005) Moisture buffering of building materials. *Technical University of Denmark, Department of Civil Engineering. BYG Report*, R-127.
10. Frattolillo A, Giovinco G, Mascolo M C, Vitale A (2005) Effects of hydrophobic treatment on thermophysical properties of lightweight mortars. *Experimental Thermal and Fluid Science* 29 (6), 733-741. DOI: 10.1016/j.expthermflusci.2004.12.002
11. Černý R, Kunca A, Tydlitát V, Drchalová J, Rovnaníková P (2006) Effect of pozzolanic admixtures on mechanical, thermal and hygric properties of lime plasters. *Construction and Building Materials*, 20(10), 849 – 857.
12. Margalha MG, Appleton J, Carvalho F, Veiga R, Santos Silva A, de Brito J (2008) Traditional lime kilns - Industry or archaeology? In *HMC08 – 1st Historical Mortars Conference*.
13. Maddison M, Mauring T, Kirsimäe K, Mander Ü (2009) The humidity buffer capacity of clay-sand plaster filled with phytomass from treatment wetlands. *Building and Environment*, 44(9), 1864–68.
14. Ramos N M M, Delgado J M P Q, De Freitas V P (2010) Influence of finishing coatings on hygroscopic moisture buffering in building elements. *Construction and Building Materials* 24(12), 2590–97. DOI:10.1016/j.conbuildmat.2010.05.017
15. Ashour T, Georg H, Wu W (2011) An experimental investigation on equilibrium moisture content of earth plaster with natural reinforcement fibres for straw bale buildings. *Applied Thermal Engineering* 31 (2-3), 293-303.
16. Freire T, Veiga M d R, Santos Silva A, de Brito J (2011) Improving the durability of Portuguese historical gypsum plasters using compatible restoration products. In *XII DBMC- International Conference on Durability of Building Materials and Components*, Vol. II, 905- 913.
17. Vejmelková, E, Koňáková D, Čáchová M, Keppert M, Černý R (2012) Effect of hydrophobization on the properties of lime-metakaolin plasters. *Construction and Building Materials* 37, 556–61.
18. Vejmelková E, Keppert M, Keršner Z, Rovnaníková P, Černý R (2012) Mechanical, fracture-mechanical, hydric, thermal, and durability properties of lime-metakaolin plasters for renovation of historical buildings. *Construction and Building Materials* 31, 22–28.
19. Liuzzi S, Hall M R, Stefanizzi P, Casey S P (2013) Hygrothermal behaviour and relative humidity buffering of unfired and hydrated lime-stabilised clay composites in a Mediterranean climate. *Building and Environment* 61, 82-92. DOI: 10.1016/j.buildenv.2012.12.006.

20. Čáchová M, Vejmelková E, Koňáková D, Keppert M (2013) Influence of finely ground brick on hydric properties of lime plasters. In *Proceedings of the 4th European Conference of Mechanical Engineering*, Paris: WSEAS Press, 117–121.
21. Matias G, Faria P, Torres I (2013) Viability of ceramic residues in lime-based mortars. In *HMC13 - 3rd Historic Mortars Conference.*
22. Gonçalves H, Gonçalves B, Silva L, Vieira N, Raupp-Pereirac F, Senff L, Labrincha J A (2014) The influence of porogene additives on the properties of mortars used to control the ambient moisture. *Energy and Buildings*, 74, 61-68.
23. Thomson A, Maskell D, Walker P, Lemke M, Shea A, Lawrenceet M (2015) Improving the hygrothermal properties of clay plasters. In *NOCMAT 2015 - 15th International Conference on Non-conventional Materials and Technologies*.
24. Santos T, Silva V, Faria P (2015) Earthen mortars – Hygrotermal behaviour as a function of grain size distribution of sand (in Portuguese). *Construção Magazine* 68, 28 - 30.
25. Mazhoud B, Collet F, Pretot S, Chamoin J (2016) Hygric and thermal properties of hemp-lime plasters. *Building and Environment* 96, 206–16.
26. Liuzzi S, Stefanizzi P (2016) Experimental study on hygrothermal performances of indoor covering materials. *International Journal of Heat and Technology* 34, (Special Issue 2), S365-70.
27. Randazzo L, Montana G, Hein A, Castiglia A, Rodonò G,Donato DI (2016) Moisture absorption, thermal conductivity and noise mitigation of clay based plasters: The influence of mineralogical and textural characteristics. *Applied Clay Science*, 132-133, 498-507. DOI: 10.1016/j.clay.2016.07.021.
28. Lima J, Faria P, Santos Silva A (2016) Earthen plasters based on illitic soils from barrocal region of Algarve: Contributions for building performance and sustainability. *Key Engineering Materials*, 678, 64–77.
29. Faria P, Santos T, Aubert JM (2016) Experimental characterization of an earth eco-efficient plastering mortar. *Journal of Materials in Civil Engineering*, 28(1), 04015085.
30. Lima J, Faria P (2016) Eco-efficient earthen plasters: The influence of the addition of natural fibers. In Natural Fibres: Advances in Science and Technology Towards Industrial Applications. From Science to Markets, Fangueiro, Raul, Rana, Sohel (Eds.). Springer, *RILEM Bookseries*, 12, 315–27.
31. Lima J, Correia D, Faria P (2016) Earthen plasters: The influence of the addition of gypsum and of the grain size distribution of sand (in Portuguese). In *ARGAMASSAS 2016 – II Simpósio de Argamassas e Soluções Térmicas de Revestimento*, ITeCons, 119–130.

32. Pavlík Z, Fořt J, Pavlíková M, Pokorný J, Trník A, Černý R (2016) Modified lime-cement plasters with enhanced thermal and hygric storage capacity for moderation of interior climate. *Energy and Buildings* 126, 113-127. DOI: 10.1016/j.enbuild.2016.05.004.
33. Palumbo M, McGregor F, Heath A, Walker, P (2016) The influence of two crop by-products on the hygrothermal properties of earth plasters. *Building and Environment*, 105, 245 – 252. DOI: 10.1016/j.buildenv.2016.06.004.
34. Pasian C, Secco M, Piqué F, Rickerby S, Artioli G, Cather S (2016) Performance of grouts with reduced water content: the importance of porosity and related properties. In HMC2016 - *4th Historic Mortars Conference*
35. McGregor F, Fabbri A, Ferreira J, Simões T, Faria P, Morel JC (2017) Procedure to determine the impact of the surface film resistance on the hygric properties of composite clay/fibre plasters. *Materials and Structures/Materiaux et Constructions* 50(4), 193. DOI: 10.1617/s11527-017-1061-3.
36. Vares O, Ruus A, Raamets J, Tungel E (2017) Determination of hygrothermal performance of clay-sand plaster: Influence of covering on sorption and water vapour permeability. *Energy Procedia* 132, 267–72.
37. Giosuè C, Pierpaoli M, Mobili A, Ruello M L, Tittarelli F (2017) Influence of binders and lightweight aggregates on the properties of cementitious mortars: From traditional requirements to indoor air quality improvement. *Materials*, 10(8), 978. DOI:10.3390/ma10080978.
38. Mattone M, Rescic S, Fratini F, Manganelli Del Fa R (2017) Experimentation of earth-gypsum plasters for the conservation of earthen constructions. *International Journal of Architectural Heritage*, 11(6), 763-772. DOI: 10.1080/15583058.2017.1290850.
39. Altmäe A, Ruus A, Raamets J, Tungel E (2018) Determination of hygrothermal performance of clay-sand plaster: Influence of covering on sorption and water vapour permeability. In *Cold Climate HVAC 2018*, 78, v4. DOI: 10.1016/j.egypro.2017.09.719.
40. Maskell D, Thomson A, Walker P, Lemke M (2018) Determination of optimal plaster thickness for moisture buffering of indoor air. *Building and Environment* 130, 143–50.
41. Liuzzi S, Rubino C, Stefanizzi P, Petrella A, Boghetich A, Casavola C, Pappalettera G (2018) Hygrothermal properties of clayey plasters with olive fibers. *Construction and Building Materials* 158, 24–32. DOI: 10.1016/j.conbuildmat.2017.10.013.
42. Shi C, Zhang H, Xuan Y (2019) Experimental investigation of thermal properties and moisture buffering performance of composite interior finishing materials under different airflow conditions. *Building and Environment* 160, 106175.

43. Phelipot-Mardelé A, Collet F, Jiang Y, Lanos C, Lawrence M, Lemke M (2019) Moisture buffering capacity of clay-based plasters. In *3rd International Conference on Bio-Based Building Materials, AJCE - Special Issue* 37(2), 363-370.
44. Lagouin M, Laborel-Préneron A., Magniont C, Aubert J-E (2019) Development of a high clay content earth plaster. In *IOP Conference Series: Materials Science and Engineering* 660, 012068. DOI:10.1088/1757-899X/660/1/012068.
45. Zemanova L, Pokorny J, Pavlikova M, Pavlik Z (2019) Hygric properties of cement-lime plasters with incorporated lightweight mineral admixture. In *IOP Conference Series: Materials Science and Engineering*, 603 (2), 022046. DOI: 10.1088/1757-899X/603/2/022046.
46. Jiang Y, Phelipot-Mardele A, Collet F, Lanos C, Lemke M, Ansell M, Hussain A, Lawrence M (2020) Moisture buffer, fire resistance and insulation potential of novel bio-clay plaster. *Construction and Building Materials* 244, 118353. DOI: 10.1016/j.conbuildmat.2020.118353.
47. Cascione V, Maskell D, Shea A, Walker P, Mani M (2020) Comparison of moisture buffering properties of plasters in full scale simulations and laboratory testing. *Construction and Building Materials* 252, 119033. DOI: 10.1016/j.conbuildmat.2020.119033.
48. Santos T, Faria P, Santos Silva A (2020) Eco-efficient earth plasters: The effect of sand grading and additions on fresh and mechanical properties. *Journal of Building Engineering* 33, 101591. DOI: 10.1016/j.jobe.2020.101591.
49. Lima J, Faria P, Santos Silva A (2020) Earth Plasters: The influence of clay mineralogy in the plasters' properties. *International Journal of Architectural Heritage*. DOI: 10.1080/15583058.2020.1727064.
50. Buratti C, Belloni E, Merli F (2020) Water vapour permeability of innovative building materials from different waste. *Materials Letters*, 265, 127459. DOI: 10.1016/j.matlet.2020.127459.
51. Padfield T (1999) Humidity buffering of the indoor climate by absorbent walls. In 5*th Symposium Building Physics in the Northern Countries* 2, 637–644.
52. DIN (Deutsches Institut fur Normung), DIN 18947: Earth plasters - Requirements, test and labelling. Berlin, Germany, 2018.
53. ISO (International Standards Organization), ISO 12571: Hydrothermal performance of building materials and products - Determination of hygroscopic sorption properties., ISO, Geneva, Switzerland, 2013.

54. ISO (International Standards Organization), ISO 24353: Hygrothermal performance of building materials and products - Determination of moisture adsorption/desorption properties in response to humidity variation., ISO, Geneva, Switzerland, 2008.
55. Cascione V, Cavone E, Maskell D, Shea A, Walker P (2019) The effect of air velocity on moisture buffering. In *Central European Symposium of Building Physics* 282, 02007. DOI: 10.1051/matecconf/201928202007.
56. JIS (Japanese Industrial Standard), A1470: Test method of adsorption/desorption efficiency for building materials to regulate an indoor humidity part 1: Response method of humidity, JIS, Tokyo, Japan, 2002.
57. ISO (International Standards Organization), ISO 12572: Hygrothermal performance of building materials and products - Determination of water vapour transmission properties - Cup method., ISO, Geneva, Switzerland, 2016.
58. CEN (European Commetee for Standardization), EN 1015-19: Methods of test for mortar for masonry - Part 19: Determination of water vapour permeability of hardened rendering and plastering mortars. Brussels, Belgium,1998.
59. CEN (European Commetee for Standardization), EN 12086: Thermal insulating products for building applications - Determination of water vapour transmission properties. Brussels, Belgium, 2013.
60. CEN (European Commetee for Standardization), EN 15803: Conservation of cultural property - Test methods - Determination of water vapour permeability (δp). Brussels, Belgium, 2009.
61. ASTM International, ASTM E96 / E96M-10: Standard test methods for water vapor transmission of materials, West Conshohocken , PA, 2010.
62. Fernandes J, Pimenta C, Mateus R, Monteiro Silva S, Bragança L (2015) Contribution of portuguese vernacular building strategies to indoor thermal comfort and occupants' perception. *Buildings* 5(4), 1242–64.
63. Santos T, Gomes MI, Santos Silva A, Ferraz E, Faria P (2020) Comparison of mineralogical, mechanical and hygroscopic characteristic of earthen, gypsum and cement-based plasters. *Construction and Building Materials* 254, 119222.
64. Künzel HM (1995) Simultaneous heat and moisture transport in building components, one-and two-dimensional calculation using simple parameters. IRB-Verlag, Stuttgart.

## 2.4 Additional Considerations

From the first study (section 2.2) emerged that passive moisture regulation can be an important tool for contributing to users' comfort in intermittently heated and/or unheated indoors, very common in Southern European Countries. The general outcome put emphasis on the comparison between real RH fluctuation and tests conditions. The research question behind the study is, thus, designed: is the hygroscopic response of plasters, evaluated through widespread methods and protocols, representative of their behavior under real conditions indistinctly? Namely, which possibility these coatings would have to act as described by the methods if the RH range is different from what expected? A higher low level of RH under real conditions (63% instead of 33%) could affect the release of moisture and the successive uptake, decreasing the real moisture control? Nevertheless, comparisons between various binder-based plasters according to different testing methods are consistent even if absolute values are changing. Results point the middle humidity level condition (ΔRH 50%-75%) of ISO 24353 (2021) as the closest one to the monitored microclimates. The simulations run applying clay, air lime, NHL and cement (calibrated using results from mortars' laboratory characterization) under real microclimatic conditions (in the four monitored study cases) are consistent with results expected from the MBV calculated with both methods. The (simulated) clay-based plaster shows the highest variation in moisture content under real RH fluctuations. Indeed, in terms of reactivity to moisture variations, it is confirmed a very promising plastering mortar.
Moreover, from the literature review (section 1.1) emerged the need of a greater homogenization of test methods. In fact, it was found that, due to methodological differences, results from different studies (of the same property) cannot always be directly compared among them. Nevertheless, the use of ranges seemed reasonable for the scope and a synthesis of them is presented in **Table 2.11**.

**Table 2.11.** Synthesis of results for mortars RH dependent properties from literature.

| Property | Unit | | C | AL | G | CE | C-AL | C-G | G-AL | AL-CE |
|---|---|---|---|---|---|---|---|---|---|---|
| Adsorption* | [%] | max | 6.30 | 10 | 3.10 | - | - | - | 0.98 | - |
| | | min | 0.10 | 0.03 | 0.08 | | | | 0.16 | |
| MBV** | [g/(m$^2$·%RH)] | max | 3.3 | 1.64 | 0.95 | 0.30 | - | - | 0.47 | 1.19 |
| | | min | 0.93 | 0.67 | 0.33 | | | | 0.42 | 1.10 |
| WVP*** | E$^{-11}$[kg/(m·Pa·s)] | max | 7.60 | 6.50 | 2.92 | 1.40 | 2.41 | 2.47 | 2.89 | 3.55 |
| | | min | 0.8 | 0.48 | 2.06 | 0.49 | 2.05 | 2.28 | 1.36 | 0.94 |

Notation: C - MBV - moisture buffer value; WVP - water vapor permeability; clay; AL - air lime; G - gypsum; CE - cement; * ISO 12571 (2013); ** NORTEST (Rode et al., 2005); *** ISO 12572 (2016) and EN 1015-19 (1998) by both wet and dry cup

# 3

# PASSIVE MOISTURE REGULATION OF PLASTERS

## 3.1 Preamble

The next study presented (section 3.2) is intended to better understand differences between plastering mortars based on gypsum, air lime, natural hydraulic lime, cement and clay. A fair comparison is given from results obtained applying the same test methods to all materials. The main objective is to build a dataset of values that includes plasters based on both traditional and modern binders. The studied properties are, according to the previous study (section 1.1), the relative humidity dependent properties of mortars: sorption isotherms, moisture buffering value and water vapor permeability. Results pointed out that some binders (like clay) are much more hygroscopic than others (gypsum or air lime).

It is common practice to apply a paint system for coating indoor plasters and it is possible that the system impacts the properties here object of study. So, once all the different binder-based plasters were classified according to their potential to act as passive regulator of relative humidity, a complementary study (section 3.3) was included to quantify the effect of two paint systems on previous results, one specific for indoor application and other for comparison. The conclusions of the study pointed out a significative different effect of different binder-based paints applications on mortars' hygroscopic behavior and opened the way to multiple research questions for further studies. For example, which factors influence the hygroscopic behavior and water vapor permeability of the final system (plaster-paint)? The whole paint chemical composition? The kind of binder? Does the volume solid have a role in this? Why different

mortars are influenced differently by the same paint application? Is it linked to surface properties or to physical properties of the mortars, such as roughness or as open porosity? Is it more a matter of surface chemical reactivity to the paint? Further studies are needed to seek for answers.

## 3.2 Article B1 - Relative Humidity Passive Regulation of Plasters

(the article has been published in the journal *Heritage* 2021, 4, 2337–2355;
https://doi.org/10.3390/heritage4030132)

### Traditional and modern plasters for built heritage: contribution for relative humidity passive regulation

### Abstract

Plasters cover wide surface areas of buildings since ancient time with the main purpose to indoor protection of the substrate on which they are applied. When no longer functional, they might need to be substituted by solutions which can combine compatibility with the substrate with the nowadays need of mitigating buildings emissions. Indeed, plasters can contribute to lowering buildings energy demands while improving indoor air quality and comfort of buildings' users, as they can be used as passive regulators of relative humidity (RH). Hence, this study presents the relative humidity dependent properties of different plastering mortars based on clay, air lime and natural hydraulic lime, and plastering finishing pastes based on gypsum and gypsum-air lime, in all cases tested through small size specimens. A cement-based plaster is also analysed for comparison. The clay based plaster is the most promising material for RH passive regulation and can be applied to repair and replace plasters in different types of buildings. Pastes based on air lime-gypsum can be applied as finishing layers, namely on traditional porous walls. The sorption behaviour of cement plaster appeared interesting; however, its water vapour permeability was found the lowest, as expected, discouraging its application on historic walls.

### Keywords

Air lime; Clay; Gypsum; Hygroscopicity; Moisture passive regulation; Mortar; Natural hydraulic lime; Paste; Plaster; Water vapour permeability.

#### 3.2.1 Introduction

Plasters are "a mix of one or more binders, sand, water and sometimes additives" [1] that have been used for covering interior walls and ceilings since ancient times. Thus, traditional plasters cover a large surface of historical buildings and represent themselves part of the built heritage. The old plasters were commonly based on clayey earth, air lime and gypsum [2,3]. Only in the late 19th century those materials started to be replaced with hydraulic binders, as hydraulic lime, natural cement and Portland cement [4]. Thus, during the 20th century, many interventions oriented to the repair and conservation of old buildings were carried out with

complete substitution of original mortars by new binders-based ones [5], which frequently contributed to speed up the degradation process of the built heritage.

The main role of plasters is to protect the substrate they are applied on, but also to improve living conditions. Nowadays, aspects related to respect the eco-efficiency of interventions are also demanded. Hence, the intervention on historical buildings must consider compatibility criteria, i.e. physical, chemical and mechanical compatibility [6], but include also the aim to improve indoor air quality and to decrease energy demand of buildings. The passive regulation of relative humidity (RH) performed by plasters [7-9] has been largely discussed during the present century, since the interest on human health [10], indoor air quality (IAQ) [11] and perceived air quality [12] has spread together with the aim of adapting historical buildings to climate change [13]. Moreover, the optimization of passive RH regulation represents an opportunity for improving indoor comfort while reducing the need for HVAC systems, thus improving energy efficiency in historic buildings [14,15] and lowering their environmental impact and operational costs, which is fundamental to mitigate climate change [16] and reach a climate-neutral Europe by 2050 [17].

The assessment of the hygroscopic behaviour of plasters depends on some intrinsic properties of the plasters like bulk density, pore size distribution and porosity, combined with others like the surface texture (partially related to application) and to some properties that can be quantified only as a function of the RH fluctuation. To better understand the response of plasters when exposed to a change of hygrothermal conditions for a given period, the present study tests the RH dependent properties of eight different plastering mortars and pastes, based on traditional binders and newer hydraulic ones.

It is well-known that cement-based plasters present low compatibility with built heritage, due to their high mechanical resistance, low capillarity, low water vapour permeability, and also high soluble salt content [18,19]. Moreover, while many studies have been run on the contribution that innovative plasters might provide to occupants' health and comfort, the same has been rarely assessed for traditional ones. Thus, the aim of the study is to characterize and quantify the response to RH variations of mortars and pastes based on traditional and contemporary binders, in order to assess compatibility and define possibilities of RH passive regulation.

## 3.2.2 Materials and methods

### 3.2.2.1 Materials and fresh state characterization

In order to assess RH dependent properties of a wide variety of plasters, seven different mortars and pastes were tested using specimens resulting from previous experimental campaigns [14–17] together with one clay-based plaster specifically produced for this campaign. The characterization of the clay-based plaster is presented and compared with the other plasters as described by their authors. Hence, the mortars and pastes included in the study are:

- A commercially available earthen plastering mortar (*E*) made of clayish earth, mixed grade sand of 0-2 mm and barley straw fibers cut with less than 30 mm [20] mechanically mixed in laboratory with addition of 20% by mass of water (Fig.1a), as recommended by the producer (Embarro).
- Three pastes designed as finishing restoration products [21] for ancient Portuguese interior finishings based on hydrated lime powder CL90-S (CL) and calcium sulphate hemi-hydrate - gypsum (G): *CL70_G20, CL50_G50* and *G*. The CL70_G20 was formulated with 70% of hydrated lime, 20% of gypsum, 10 % of calcitic aggregate (< 45 μm) and an addition of 0.1% of a water-retaining agent methylcellulose-based and of 0.02% of set retarder to assess a required workability. The same retarder, in the same proportions, was added to CL50_G50 (50% of hydrated lime and 50% of gypsum) designed to mould on-site elements for gypsum plasters decoration. G was produced for restoration of precast elements with 100% of calcium sulphate hemi-hydrate. All the percentages are by mass.
- One plastering mortar made of hydrated lime (*CL*) and one made of natural hydraulic lime 3.5 (*NHL*), both mixed with siliceous sand from Tagus river (0-4 mm) with volumetric ratio 1:3, corresponding to 1:13 and 1:6.7 by mass, respectively [22].
- Two cement plastering mortars [23,24] produced with CEM II/B-L 32.5 N and siliceous sand from Tagus river (0-2 mm) with volumetric ratio 1:4, corresponding to 1:6 (*C_1.3*) and 1:5 (*C_0.9*) by mass.

The fresh characterization of the earthen mortar and of all the other mortars and pastes, as reported by each author [21-24], is summarized in **Table 3.1**.

The amount of mixing water was determined by each author in order to ensure the good workability of the mortar. The water content defined by the producer and used for the E plaster has shown a flow within the limits of DIN 18947 [25] for earth plasters. The plaster/water ratio of the gypsum paste (*G*) was decided according to EN 13279-2 [26] while for lime-gypsum pastes (*CL_Gs*) and all the mortars the flow table consistency method [27] was used [21]. Santos

[22] refers that the amount of water added to *CL* and *NHL* mortars was quantified to ensure a flow table consistency of 150 ± 5 mm [27].

**Table 3.1.** Synthesis of fresh characterization of selected plastering mortars and pastes.

| Pastes and mortars | Ref | Month-year of production | Binder | Aggregate | b/a ratio | w/b ratio | Flow [mm] | BD [kg/dm³] |
|---|---|---|---|---|---|---|---|---|
| G | [21] | 04-2012 | G(100%) | – | – | 0.7 | 190 ± 5 | nf |
| CL50_G50 | [21] | 03-2012 | G(50%) CL(50%) | – | – | 0.8 | 165 ± 5 | nf |
| CL70_G20 | [21] | 03-2012 | G(20%) CL(70%) | CA(10%) | – | 1.0 | 165 ± 5 | nf |
| E | – | 02-2020 | IE | SS02 | nf | 0.2' | 171±10 | 1.95 |
| CL | [22] | 03-2016 | CL 90-S | TR04 | 1:3 | 2.8 | 151 ± 5 | nf |
| NHL* | – | 03-2016 | NHL 3.5 | TR04 | 1:3 | 1.4 | 150 ± 5 | nf |
| C_0.9 | [23] | 10-2018 | CEM II/B-L 32.5N | SS02 | 1:4 | 0.9 | 140 ± 3 | 2.00 |
| C_1.3 | [24] | 07-2017 | CEM II/B-L 32.5N | SS02 | 1:4 | 1.3 | 161 ± 1 | 1.97 |

Notation: b/a – binder/aggregate; w/b – water/binder; Flow – flow table consistency; BD – wet bulk density; G – Hemihydrate gypsum; CL – calcitic hydrated air lime; CA – fine calcitic aggregate; IE – illitic clay earth; SS02 – natural siliceous sand 0-2 mm; TR04 – Tagus river sand 0-4 mm; nf – not found; % values are by mass; * – unpublished result; ' – water/mix ratio; ± values for standard deviation.

The flow table consistency was fixed at 140 ± 2 mm for *C_0.9*, that is quite a low value for cement plasters, and 165 ± 5 mm for *C_1.3*. Only the earth plaster *E* and the cement *C_0.9* [28] and *C_1.3* [24] were characterized also at fresh bulk density [29].

#### 3.2.2.2 Hardened state general test methods

All the selected mortars and pastes were cast in prismatic moulds of 40 mm x 40 mm x 160 mm and cured. As reported by the respective authors: cements and NHL mortars were moulded and cured according to EN 1015-11 [30]; the *G* and *CL_Gs* were moulded according to EN 13279-2 [26]; the air lime mortar CL was cured five days at 20 ± 2 °C and 65 ± 5 % RH and after demoulding was kept in the same conditions. The *E* specimens were cured seven days in the moulds at 20 ± 2 °C and 65 ± 5 % RH, then demoulded and kept in the same environment for four months (**Figure 3.1**a).

After drying, the bulk density was geometrically determined [31]. Flexural strength was evaluated for three prismatic specimens with a 2 kN loading cell and 10 N/s loading speed. Compressive strength of the six semi-prisms of approximately 40 mm x 40 mm x 80 mm derived from the flexural test (**Figure 3.1**b) was performed [30] with a 2 kN loading cell and 50 N/s loading speed.


(a) (b)

**Figure 3.1.** Clay-based mortar samples: **(a)** when drying; **(b)** after flexural test.

A universal force equipment ETI - HM-S/CPC from PROETI was used for the tests. Dynamic modulus of elasticity was assessed according to EN 14146 [32] using an equipment of frequency of resonance ZRM ZEUS 2005 on prismatic specimens. The dry bulk density, flexural, compressive strength and dynamic modulus of elasticity of all the other plasters and pastes [21–24] were tested following the same standards used for the earth plaster with loading cells and speeds suitable for each plaster. Open porosity for cement and lime mortars were measured [22–24] by hydrostatic method [33] and for *CL_G* and *G* [21] by Mercury Intrusion Porosimetry (MIP). Capillarity by water absorption was tested based on EN 1015-18 [34] by Freire [21], Pederneiras et al. [23], Farinha et al. [24] and EN 15801 [35] by Santos [22].

#### 3.2.2.3 Preparation of the specimens

For each coating material, the hardened prismatic specimens were mechanically cut and five specimens of approximately 40 mm x 40 mm x 20 mm (**Figure 3.2**) obtained (**Table 3.2**).
Thereafter, the new specimens were prepared to be tested to water vapour permeability [36], adsorption/desorption [25,37] and moisture buffering [8]. The surfaces resulting from the cut were selected to be exposed during the tests.

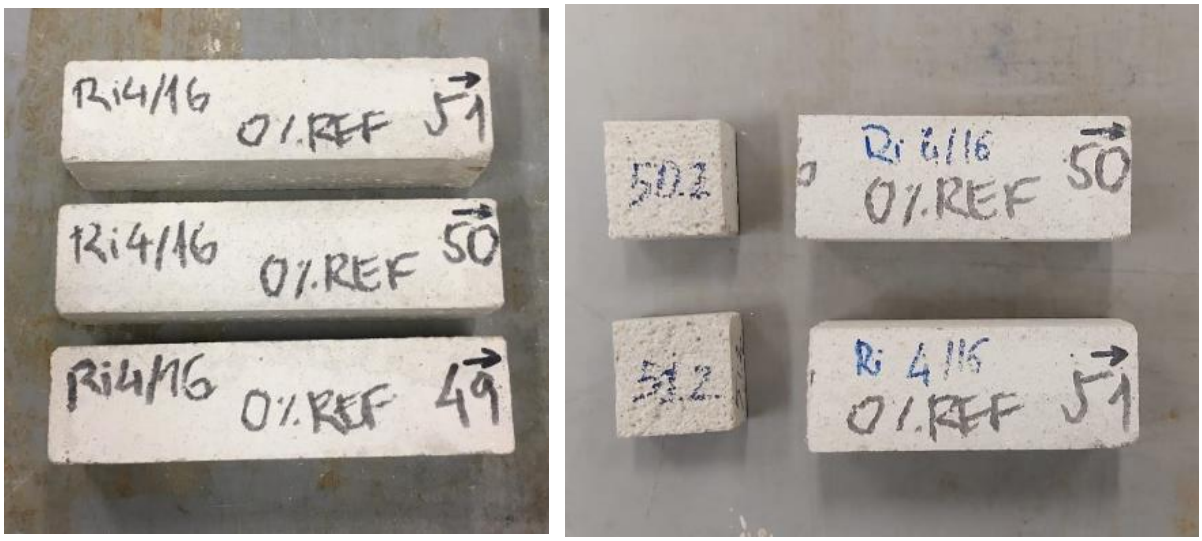


(a) (b)

**Figure 3.2. (a)** Prismatic samples of C_1.3; **(b)** sliced to obtain specimens 40x40x20 mm$^3$.

**Table 3.2.** Dimensions and mass (average value of 5 specimens) of plaster specimens at the beginning of the experimental campaign.

| Pastes and mortars | Specimens | | | |
|---|---|---|---|---|
| | $S_1$ [mm] | $S_2$ [mm] | $d$ [mm] | *Mass* [g] |
| G | 40 | 40 | 21 | 34 |
| CL50_G50 | 40 | 40 | 21 | 34 |
| CL70_G20 | 38 | 38 | 21 | 29 |
| E | 39 | 40 | 22 | 58 |
| CL | 40 | 40 | 23 | 57 |
| NHL | 40 | 40 | 21 | 55 |
| C_0.9 | 40 | 40 | 22 | 64 |
| C_1.3 | 40 | 40 | 22 | 60 |

Notation: S1 – side 1; S2– side 2; d – thickness mean value.

#### 3.2.2.4 Relative Humidity dependant properties test methods

##### 3.2.2.4.1 Water Vapour Permeability

Five specimens for each mortar and paste, preconditioned at 20±2 °C and 65±5 % RH, were sealed on their thickness by aluminium tape and then placed on top of plastic boxes (65 mm x 55 mm x 40 mm) in which a cut of 35 mm x 35 mm was performed. The basis (40 mm x 40 mm) of the specimens was then sealed by paraffin with the top of the box (**Figure 3.3**a). Dry cup method according to ISO 12572 [36] was followed and 0% of RH inside each box was obtained with 30 ml of calcium chloride ($CaCl_2$) as desiccant, ensuring the 15±5 mm air space between the desiccant and the lower surface of the specimen. The closure of the box was sealed by paraffin (**Figure 3.3**b). Before starting the experiment, the assembly (box + specimen) was

weighed and the starting mass, $m_0$, determined. Balance of 0.001 g resolution was used. The specimens were put into the climatic chamber FITOCLIMA 700EDTU at 50±5 % RH and 23±5 °C and weighed every 24 h until three successive daily determinations of the weight agree to within 5% and the curve of change in mass against time displayed a constant mass change rate.

3.2.2.4.2 Adsorption/desorption

The same specimens were used to perform adsorption/desorption according to a simplified version [38] of DIN 18947 [25]. After preconditioning in a climatic chamber (FITOCLIMA 700EDTU) at 50±5 % RH and 23±5 °C until constant mass, the specimens were weighed and the starting mass, $m_0$, determined. A balance of 0.001 g resolution was used. RH was increased to 80±5 % and specimens were weighed after 1, 3, 6, 12 and 24 h. The weighing at 0.5 h prescribed from the standard was not performed to ensure the chamber was stabilized at 80% RH a substantial period of time before the weighing. The adsorption phase was extended until 24 h, according to the amplified version, to better understand the adsorption behaviour of the highly hygroscopic plasters. After 24 h, the climatic chamber was set at 50±5 %, 23±5 ºC, and desorption was run following the same weighting intervals. The results are displayed in $g/m^2$ against time.

3.2.2.4.3 Sorption Isotherms

The hygroscopic curve was determined according to ISO 12571 [37]. Five specimens for each plaster were sealed on their thickness and their basis by aluminium tape (**Figure 3.3**c), ensuring only one exchanging surface exposed. They were dried at 60 °C until constant mass and then placed in a climatic chamber. During adsorption, five RH steps (30%, 50%, 70%, 80%, 95%) until equilibrium of the specimens were performed at the constant temperature of 23±5 °C. Equilibrium at each stage was reached when the change in mass of three successive weighting, every 24 hours, was less than 0.1%. Once completed adsorption, desorption was performed fallowing the same RH steps from 95% to 30%. Sorption isotherms were obtained from the equilibrium moisture content of each step.

3.2.2.4.4 Moisture Buffering Value

Determination of Moisture Buffering Value (MBV) followed the NORDTEST protocol [8]. The same five specimens for each plaster were dried at 60° and starting mass, $m_0$, was determined. The specimens were then placed in a climatic chamber inside a laboratory tray (**Figure 3.3**d) to avoid direct air flow. Temperature was fixed at 23±5 ºC and four daily cycles of 33–75% RH were run. The last three cycles were considered to calculate the value. According to the method,

loading and unloading phases were kept respectively 8 h and 16 h, simulating the daily use of one bedroom. MBV was then calculated as the average value of the last three cycles of adsorption and desorption. Results are expressed in g/(m$^2$·%RH).

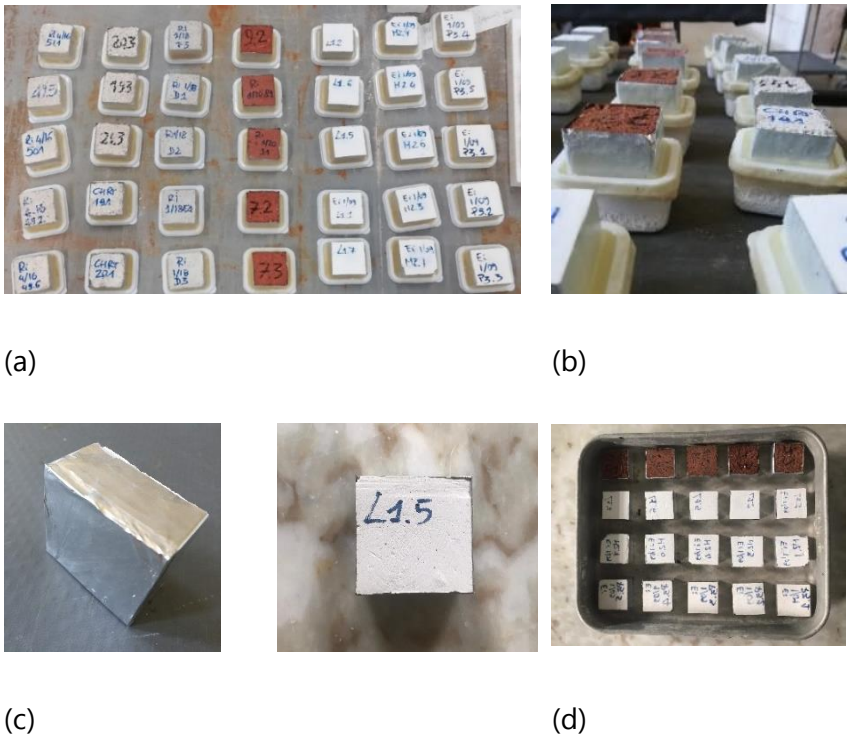


(a) (b)

(c) (d)

**Figure 3.3.** Specimens: **(a)** sealed on the top of the plastic boxes filled with the desiccant; **(b)** zoom of the sealing for the water vapour test; **(c)** sealed by aluminium tape; **(d)** placed in a laboratory tray.

## 3.2.3 Results

### 3.2.3.1 Plasters general characteristics

**Table 3.3** shows the synthesis of the general characteristics of the three pastes and five mortars and refers general requirements for compatible plastering substitution mortars for ancient buildings [18]. The ranges referred are meant to be used for a first assessment of compatibility when no deeper knowledge of the substrate and/or the plaster to replace is available.

The open porosity (OP) and dry bulk density (BD) of the pastes and the mortars differ very much. According to the WTA directive 2-9-04/D (cited by Pavlíková *et al.* [39]) for restoration renders the dry bulk density should be guaranteed below 1400 kg/m$^3$ and the open porosity above 40%. Thus, if applying these limits to the analyzed plasters, only the three pastes would fulfil the requirements. Moreover, the cement-based mortars present the highest values of compressive strength, as expected, followed by the gypsum-based pastes, the clay, the air lime and the natural hydraulic lime mortars. All the plastering mortars fulfil general requirements of

compressive strength [1] within different classes except the *NHL* plaster which is slightly below the lowest class CSI (0.4 to 2.5 N/mm$^2$).

**Table 3.3.** Synthesis of hardened characterization of plasters.

| Pastes and mortars | Ref | Test age | OP [%] | BD [kg /m$^3$] | Fs [MPa] | Cs [MPa] | DME [GPa] | CC [kg/(m$^2$ min$^{0.5}$)] | $W_{24h}$[1] [kg/m$^2$] |
|---|---|---|---|---|---|---|---|---|---|
| G | [21] | 2 y | 46.1 | 1128 | 2.42±0.11 | 5.19±0.27 | 5.04±0.01 | 6.42 | 71.26 |
| CL50_G50 | [21] | 2 y | 48.4 | 1104 | 1.61 | 3.24±0.31 | 2.35±0.01 | 6.23 | 76.26 |
| CL70_G20 | [21] | 2 y | 50.7 | 1031 | 1.55 | 3.03±0.40 | 1.87±0.00 | 4.49 | 78.92 |
| E | – | 120 d | – | 1743±0.01 | 0.45±0.04 | 0.82±0.05 | 3.50±0.01 | – | – |
| CL | [22] | 90 d | 25.8 | 1720 | 0.39 | 0.55 | 2.72 | 1.71 | 31.00 |
| NHL * | – | 90 d | 26.2 | 1780 | 0.15±0.02 | 0.35±0.002 | 1.86±0.07 | 2.4 | 36.50 |
| C_0.9 | [23] | 28 d | 20.2 | 1919 | 2.56±0.21 | 9.66±0.11 | 16.2±0.9 | 0.43* | 24.30* |
| C_1.3 | [24] | 2 y | 22.4 | 1875 | 2.00±0.31 | 5.98±0.79 | 10.1±0.8 | 1.55 (1y) | 17.47[2] (1y) |
| **Requirements** | **[18]** | **–** | **–** | **–** | **0.20–0.70** | **0.40–2.50** | **2.00–5.00** | **–** | **–** |

Notation: OP – open porosity; BD – bulk density; Fs – flexural strength; Cs – compressive strength; DME – dynamic modulus of elasticity; CC – capillary water absorption; $W_{24h}$ – water absorption at 24 hours; d – days; y – years; ± values for standard deviation; * – unpublished result; 1 – dimensions 40 x 40 x 160 (mm); 2 – dimensions 40 x 40 x 80 (mm).

If considered to be used as restoration products, instead, only *E* and *CL* would fit the compatibility range, with *NHL* placed slightly below and all the other pastes and mortars above the range. As for the compressive strength, the highest value of dynamic modulus of elasticity is observed for the *C* plasters and the lowest for the *NHL* one. Only the *CL_G* pastes present a lower value than expected from the observation of their mechanical properties. The values could depend on their different pores structure. The pastes capillary water absorption coefficient is very high and so is the free water saturation. The predominance of the capillary pores in their pore structure, characteristic of the permeable binders used and linked to the absence of sand, may justify the high capillary rise. Between the mortars, the highest capillary water absorption coefficient is observed for the *NHL* and the lowest for the cement mortar. Considering the range of values suggested for compatibility, mechanical behaviour of *E*, *CL* and *NHL* plasters fulfil the requirements unlike both cement plasters, as expected. Hence, if applying these cement mortars as substitutive interior plasters, they could transmit to the pre-existing material a higher stress and speed up degradation phenomena. The physical compatibility concerns the behaviour to the liquid and vapour phases of water, once retention of water in the substrate or in the pre-existing mortars could trigger new degradation mechanisms, especially if soluble salts are introduced with the repair mortar. Capillary water

absorption and water vapour permeability should be high enough to guarantee water migration and evaporation. Thus, considering the inferior limit of 1.0 kg/($m^2 min^{0.5}$) of capillary water absorption suggested for renders [18], the *C_0.9* would not fulfil requirement of physical compatibility, being the less feasible choice for substitution in ancient buildings.

#### 3.2.3.2 Water Vapour Permeability

**Table 3.4** shows the main values for water vapour permeability (WVP) of the analysed coating materials and for resistance factor calculated as the ratio between WVP of air and plaster ($\delta_a/\delta_p$). The WVP of air ($\delta_a$) refers to Shirmer formula, equal to 1.951 $E^{-10}$. The combinations of air lime and gypsum, namely *CL70_G20* and *CL50_G50*, show the highest value of WVP ($\delta_p$), followed by gypsum and air lime based ones. The high WVP of gypsum and gypsum-lime agree with the study of Ramos *et al.* [9], in which the same test procedure was applied to bigger specimens (210 mm x 210 mm, with a thickness of 20 mm and 10 mm respectively). Lower WVP is observed in mortars based on NHL and illitic earth. The lowest values refer to cement mortars. The *C_1.3*, with higher w/b ratio and longer curing, shows higher permeability than the *C_0.9,* that can be justified by a more porous microstructure of the former. Furthermore, considering the limit of 0.10 m thickness of equivalent air layer (Sd, d=10mm) recommended for substitution plasters in ancient buildings [18], none of the cement-based plasters is suitable for this kind of application.

**Table 3.4.** Synthesis of results of WVP for all the plasters.

| Pastes and mortars | d [mm] | ΔM 24h [g] | Q [(kg/s ) x $10^{-9}$] | Wp [ng/$m^2$·s·Pa] | WVP [kg/(m·s·Pa)]·$10^{-12}$ | μ [-] | Sd [m] |
|---|---|---|---|---|---|---|---|
| G | 20.69 | 0.30 | 3.43 | 1718 | 35.53 | 5.49 | 0.055 |
| CL50_G50 | 21.06 | 0.30 | 3.54 | 1775 | 37.36 | 5.22 | 0.052 |
| CL70_G20 | 20.91 | 0.29 | 3.38 | 1802 | 37.68 | 5.18 | 0.051 |
| E | 22.43 | 0.15 | 1.69 | 960 | 21.50 | 9.07 | 0.091 |
| CL | 22.52 | 0.20 | 2.31 | 1166 | 26.24 | 7.43 | 0.074 |
| NHL | 21.12 | 0.17 | 1.97 | 991 | 20.92 | 9.32 | 0.093 |
| C_0.9 | 22.01 | 0.07 | 0.86 | 434 | 9.55 | 20.42 | 0.204 |
| C_1.3 | 21.59 | 0.11 | 1.25 | 624 | 13.48 | 14.48 | 0.144 |

Notation: d – thickness; ΔM – daily change in mass; Q – water vapour flow; Wp – water vapour permeance; WVP – water vapour permeability; μ – water vapour resistance factor; Sd – thickness of the equivalent air layer (for d 10 = mm).

Also the EN 998-1 [1] and WTA directive 2-9-04/D (cited by Pavlíková *et al.* [39]) define a limit for WVP, requiring a water vapour resistant factor (μ) ≤ 15 and < 12, respectively, for renovation

mortars. Hence, the requirement would not be fulfilled by both cement mortars if considering the directive and only by *C_0.9* according to the standard.

The dimensional variation of specimens from the WVP standards´ [36] requirements mostly concerns the exposed area. Indeed, the prescription is to use a specimen of diameter or side at least two times its thickness and with a minimum exposed area of 5000 $mm^2$. The 20 mm thick and nearly 40 mm side specimens produced for the study complied with the first prescription. The exposed area, i.e. "the arithmetic mean of the upper and lower free surface areas" [36], instead, is roughly 3000 $mm^2$. However, the dimension of specimens hugely differs from study to study, where the same testing method is applied and the exposed surface varies from a minimum of about 17318 $mm^2$ [40] to a maximum of nearly 88200 $mm^2$ [9]. The possibility of introducing uncertainties of measurement is higher for smaller specimens, thus the number of specimens was increased from three to five and comparison with previous studies was run to confirm accuracy of results. Hence, **Table 3.5** reports values of WVP and resistance factor by dry cup from literature [40–50]. For clay and air lime-based plasters, the consistent difference between dry and wet methods has been already shown by some authors [43, 45-47], with values of resistance factor by dry cup two times higher than by wet cup, but no evidence of this difference was found for cement mortars.

**Table 3.5.** Comparison with literature of water vapour permeability and resistance factor obtained by dry cup test method.

| Pastes and mortars | WVP [$10^{-12}$ kg/(m·Pa·s)] | | | Resistance factor μ [–] | | |
|---|---|---|---|---|---|---|
| | Result | | Range* | Result | | Range* |
| Gypsum | **35.5** | ▲ | 21.9 – 29.2 | **5.5** | ▼ | 7.0 – 9.1 |
| Gypsum + lime | **37.4** | ▲ | 28.9 | **5.2** | ▼ | 6.7 |
| | **37.7** | ▲ | | **5.2** | ▼ | |
| Clay | **21.5** | ▲ | 7.8 – 8.8 | **9.1** | ▼ | 22.1 – 25.0 |
| CL90 | **26.2** | ▲ | 5.3 – 16.0 | **7.4** | ▼ | 12.2 – 37.1 |
| NHL3.5 | **20.9** | ▲ | 9.9 | **9.3** | ▼ | 19.6 |
| Cement ** | **9.5** | | 4.9 – 14.0 | **14.5** | | 13.9 – 40.0 |
| | **13.5** | | | **20.4** | | |

Notation: * Values from literature [33-44], due to the lack of results, permeability or resistance factor in some cases was calculated using δa of 19.50 E-11 [kg/(m·Pa·s)]; ▲ value above the range; ▼ value below the range; ** range from literature for cement is referred to wet cup.

Therefore, due to the lack of results from dry cup found in literature, the cement mortar range refers to the wet cup test method. From the comparison, the WVP of the tested plasters is higher than the referred range (or value where only one study was found) and, consequently,

the resistance factor is lower except for cement. However, the composition of the mortars and pastes from literature show a consistent heterogeneity even if based on the same binders, due to additions of diverse materials and/or natural fibers, or even due to different w/b ratios.
The pastes *G*, *CL50_G50* and *CL70_G20* are compared in **Table 3.6** with values reported by Freire [21] testing WVP according to EN 1015-19 [51] by wet cup, at 90 days and 2 years of curing of the same. It is expected that wet cup gives higher values of WVP than the dry cup but pastes with presence of lime showed a higher permeability in the later test probably related to an increase in porosity over the time. Nevertheless, the equivalent air layer for 10 mm of thickness (Sd) complies with the limit of 0.10 m [18] either by wet and dry cup.

**Table 3.6.** Comparison with results from the study of Freire [21] of water vapour permeability and equivalent air layer for a thickness of 10 mm tested by wet cup [51].

| Pastes | Test age | WVP [kg/(m·Pa·s)] · E-11 | | Sd [m] (d=10 mm) | |
|---|---|---|---|---|---|
| | | wet cup | dry cup (8y) | wet cup | dry cup (8y) |
| G | 90 days | 4.915 | 3.553 | 0.035 | 0.055 |
| | 2 years | 3.169 | | 0.057 | |
| CL50_G50 | 90 days | 2.036 | 3.736 | 0.100 | 0.052 |
| | 2 years | 2.397 | | 0.083 | |
| CL70_G20 | 90 days | 3.282 | 3.768 | 0.054 | 0.051 |
| | 2 years | 2.269 | | 0.081 | |

Notation: WVP – water vapour permeability; Sd –equivalent air layer; d – specimen thickness.

#### 3.2.3.3 Adsorption/desorption

**Figure 3.4** displays the mean curve of adsorption and desorption for each plaster and limits of the three classes defined by DIN 18947 [25]. The clay plaster *E* shows high hygroscopic behaviour adsorbing 74.4 g/m$^2$ at 12 h, about 15 g/m$^2$ higher than the highest class of the standard WSIII (≥60 g/m$^2$). The maximum adsorption, at 24 hours, was found 99.3 g/m$^2$ in accordance with another study testing the same premixed clay plaster [52]. The residual moisture content at the end of the test was 16.1 g/m$^2$. The test was therefore extended and, after additional 48 h (96 h from the beginning of sorption phase), the residual moisture content was 4.7 g/m$^2$. The temporal relation between adsorption and desorption could be 1 to 3 or more. The pastes based on air lime and gypsum (*CL70_G20, CL50_G50*) show higher hygroscopicity than pure *G* paste and *CL* mortar but a similar curve after the first 6 h. The low hygroscopic behaviour of the air lime mortar (*CL*) is evident, mainly when compared with the *CL70_G20* paste. That should be due to the absence of sand and the different microstructure. The slope of their curve at the end of adsorption is lower than the cement based mortars,

probably able to adsorb more if longer loaded. After 48 h, at the end of desorption process, all the tested coatings show a residual value of uptaken moisture. *C_0.9* and *C_1.3* specimens show the slowest desorption, confirming a low hygroscopic performance of cement plasters.

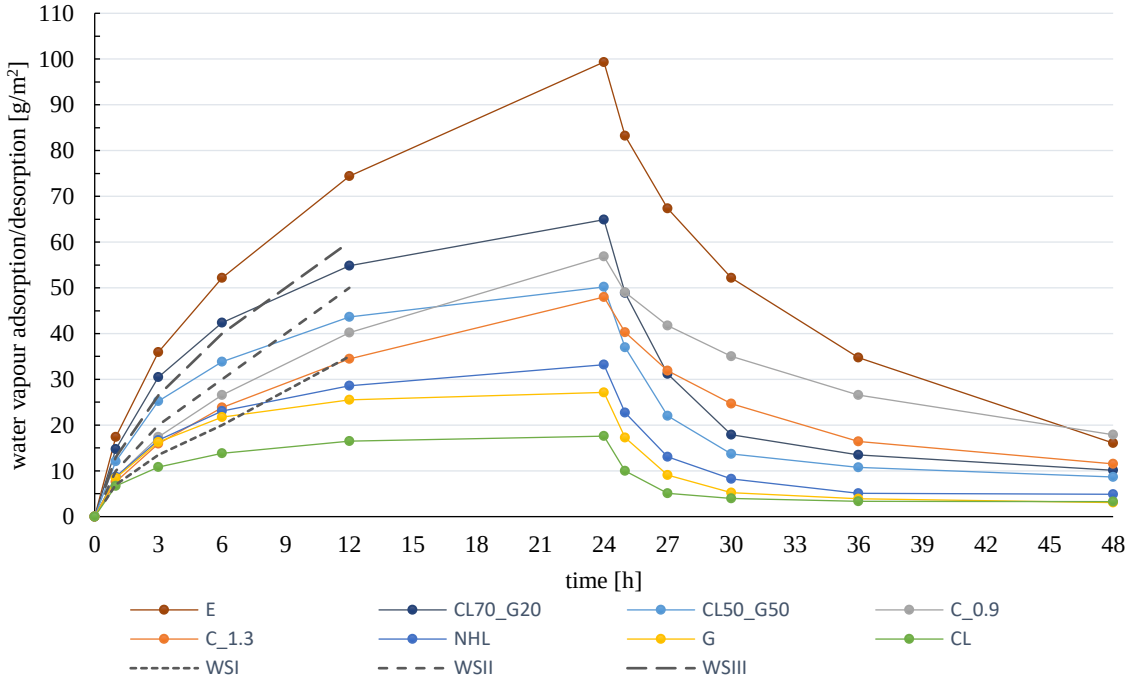


**Figure 3.4.** Sorption and desorption curve of plasters and hygroscopic classes WS defined by DIN 18947 [25].

In the test, not significative coefficient of variation (CV) was observed between specimens except for *G* and *CL*. The air lime specimens present a maximum CV of 14% at the end of 24 h of adsorption and the gypsum specimens of 61%. Thus, the gypsum paste displays a significative dispersion between the 5 specimens. The test was run two times and similar results were obtained. Based only on the similar response of three specimens, the average values of adsorption would be 17.6 g/m$^2$ at 24 h and final moisture content at 24 h of desorption would be 2.1 g/m$^2$, which would agree with studies of other authors [52]. The possible explanation is that the highest hygroscopic performance corresponds to specimens obtained from the top closest regions of the original sample, where the lowest corresponds to specimens obtained from the core of the prism. According to that, the highest value would better represent a real application. Anyway, an operational error has been excluded with the support of the repetition of the test, thus the average curve of **Figure 3.4** includes all the samples. **Table 3.7** compares results among several authors testing adsorption and desorption according to DIN 18947 [25] or the modified version of it (adsorption extended to 24 hours and inverse process for desorption).

**Table 3.7.** Synthesis of adsorption and desorption results (with standard deviation) and comparison with other studies from literature.

| Plaster | | Adsorption [g/m²] | | Desorption [g/m²] | | Ref |
|---|---|---|---|---|---|---|
| | | *(12h)* | *(24h)* | *(12h)* | *(24h)* | |
| Clay | Ep | **74.43 ± 4.42** | **99.35 ± 4.89** | **34.76 ± 1.56** | **16.10 ± 1.51** | Present study |
| | | <80 | 104 | >10 and <20 | <10 | [52] |
| | | >60 | – | ≈ 0 | – | [53] |
| | | <130 | – | ≈ 60 | – | [53] |
| | | 67,7 | – | – | – | [54] |
| | | 68.5 | – | – | – | [54] |
| | | 105,3 | – | – | – | [54] |
| | Ef | >60 and <80 | – | – | – | [55] |
| | | >80 and <100 | – | <20 | – | [53] |
| | | <70 | ≈ 80 | ≈ 12 | ≈ 5 | [56] |
| | | >21 and <38 | - | 0 | - | [57] |
| | E | >60 | 76 | <10 | <5 | [52] |
| | | ≈ 80 | – | ≈ 0 | – | [53] |
| | | ≈100 | | ≈20 | | [53] |
| | | ≈60 | >70 | >10 | <15 | [58] |
| | | ≈70 | ≈85 | ≈18 | >10 | [58] |
| | | ≈80 | <100 | <25 | >10 | [58] |
| | | ≈85 | ≈110 | ≈30 | | [58] |
| | | <70 | ≈ 85 | ≈ 20 | ≈ 10 | [56] |
| | | ≈80 | ≈83 | ≈ 10 | ≈ 0 | [59] |
| | | ≈60 | ≈78 | | | [59] |
| | | 60 | 70 | >10 and <20 | < 10 | [38] |
| | | 30 | – | 0 | – | [57] |
| | $E_K$ | 30 | 35 | ≈ 0 | 0 | [38] |
| | $E_B$ | 110 | 140 | >30 and <40 | ≈ 10 | [38] |
| Cement | C | **34.49 ± 3.02** | **47.99 ± 7.79** | **16.45 ± 2.13** | **11.54 ± 2.14** | Present study |
| | | **40.21 ± 3.45** | **56.84 ± 5.27** | **26.59 ± 3.15** | **17.89 ± 2.06** | Present study |
| | | 40 | 40 | ≈ 0 | ≈ 0 | [52] |
| Gypsum | G | **25.54 ± 13.42** | **27.15 ± 16.62** | **3.90 ± 2.54** | **3.03 ± 1.96** | Present study |
| | G | 22 | 22 | ≈ 0 | ≈ 0 | [52] |

Notation: E – illitic clay mortar; Ef – illitic clay mortar with natural fibers; Ep – premixed illitic clay mortar; $E_K$ – kaolinitic clay mortar; $E_B$ – montmorillonitic clay mortar; C – cement mortar; G – gypsum mortar. Values reported using symbols ">"; " <"; "≈" are taken from graphs; ± values for standard deviation.

As the standard is addressed to earth plasters, only one study was found [52] testing premixed gypsum and cement mortars. All the other values are from earth-based plasters differing in clay mineralogy, sand granulometry and fibers. The largest part of the studies used specimens

with similar thickness (15–20 mm) and very different exposed area (500 mm x 200 mm) when compared to the present study. Although the difference in specimen dimensions, results obtained from the campaign are in agreement with the ones found in literature, inducing that using smaller specimens may be a viable option.

#### 3.2.3.4 Sorption Isotherms

The average change in mass (u) of each plaster for every RH step is presented in **Figure 3.5**. The dry state was chosen as starting point for adsorption but in desorption phase 0% RH was not possible to be reach, thus the curves are not closed. Results of *CL70_G20* and *CL50_G50* are shown separately (**Figure 3.5**b), due to the consistently higher values of water vapour adsorbed during the last RH stage (95%) and residual moisture content at 30% RH. The clay-based plaster (**Figure 3.5**a) shows the highest hygroscopicity at each step, if compared with mortars based on cement, gypsum, air lime and natural hydraulic lime. After 80% RH, the slope of the equilibrium moisture content curve of cement mortars *C_0.9* and *C_1.3* and air lime–gypsum pastes *CL70_G20, CL50_G50* slightly rises. The presence of air lime in *CL_G* pastes, if compared with pure gypsum paste, show a significant increase of adsorption after 80% RH and hysteresis in desorption. *CL_G* specimens were analysed by MIP after 90 days and 2 years of curing [21] and a direct connection was found between the lime content and the amount of smaller pores in the range of 0.1-0.5 micron. Given that this range was found more sensitive to condensation of water adsorbed (Houst & Wittmann, 1994 cited by Freire [21]), the high adsorption at 95% RH is probably due to capillary condensation, as also observed by other authors [9]. The presence of liquid water in pores could have possibly given access for $CO_2$ in dissolved state to react with $Ca(OH)_2$ initiating the precipitation of $CaCO_3$. Furthermore, the slices cut from prismatic specimens could have exposed the inner core still not completely carbonated. Although samples with CL were aged previously to testing, pH test could not be performed for confirmation. The long-time taken to reach equilibrium at high RH level and the change in mass kept from these two plasters after the test suggest that a faster carbonation of calcium hydroxide occurred, probably promoted by high RH [60].

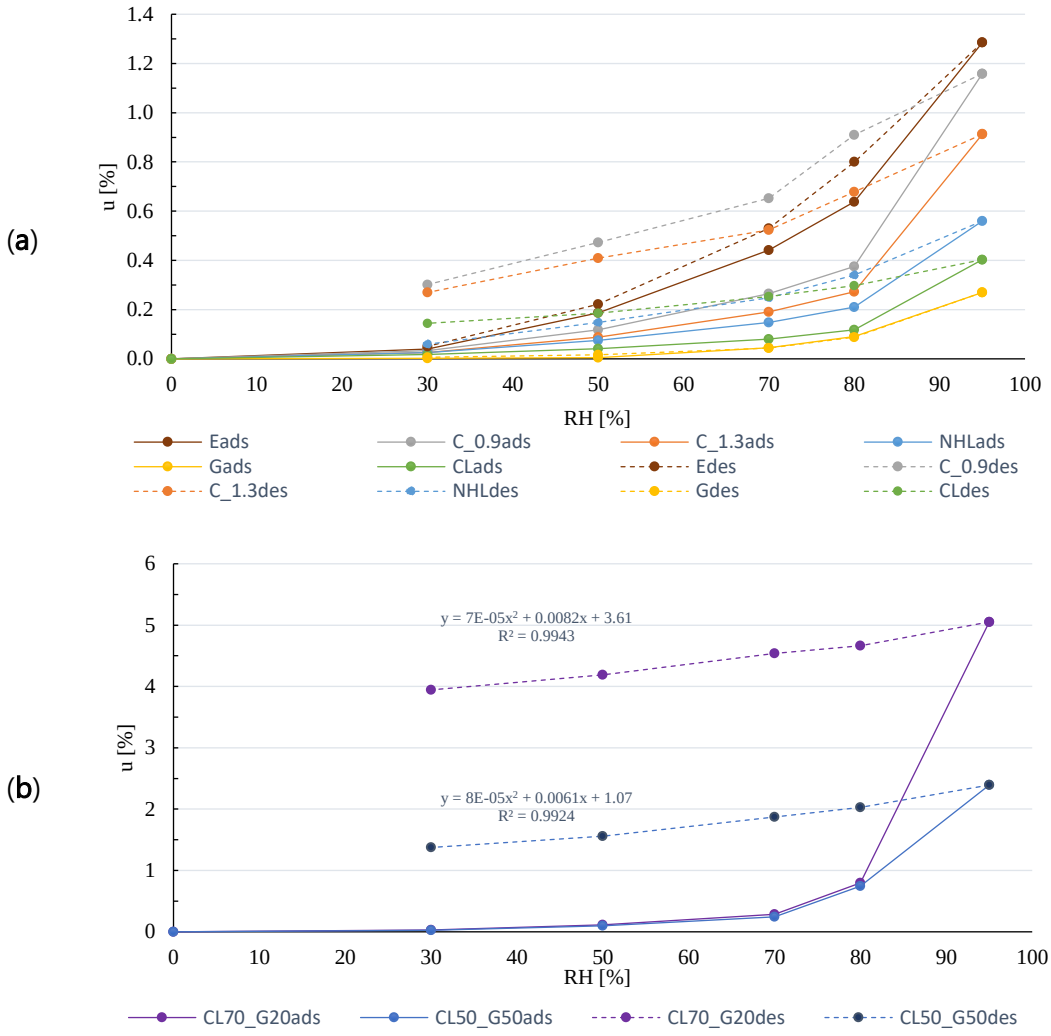


**Figure 3.5.** Average change in mass for each mortar and paste per RH step, tested according ISO 12571 [37].

Values of standard deviation are not high, except for *CL* and *G*, as expected according to the previous test of adsorption/desorption. The air lime mortar (*CL*) presents high variation in adsorption only after 80% RH exposure and during the entire desorption phase. The response of the *G* specimens is similar to the one observed in the previous section, confirming the hypothesis of the heterogeneity of the original prismatic sample and, for the same reasons presented above, all specimens were considered reliable.

Results of hygroscopic behaviour of *G, CL70_G20* and *CL50_G50* are compared with the ones obtained by Freire [21] using the same methodology on the same pastes after 2 years curing (instead of 8 years), although in that study RH passed from 70% to 90% while in the present study passed to 80% and after to 95% RH. Furthermore, the specimens tested at 2 years were unsealed circular truncated cones with bottom diameter of 50–55 mm, top diameter of 55–60

mm and thickness of 15–18 mm. The results (**Table 3.8**) are given in % by mass. Major differences were observed for the highest step of RH reached. The difference of 5% between highest RH stages tested by the two studies seems to widely affect the equilibrium moisture content of all the pastes that, at 95% RH, pass to be approximately 2.5 times the value registered at 90% RH (in bold in **Table 3.8**), together with a sudden increase of standard deviation. This effect is evident in **Figure 3.6**: the curves of the two studies are almost overlaid for RH levels below 80%. Instead, above 80% RH, the highest the content of air lime, the highest the increase of the moisture adsorbed and, thereby, of the residual moisture content. The pure gypsum paste does not show the same adsorption capacity than the air lime–gypsum pastes. In both studies (2 years and 8 years) hygroscopicity of *G* is quite low and a slight rise of the curve is observed in the oldest paste.

**Table 3.8.** Synthesis of adsorption and desorption results (8 years) and comparison with the study of Freire [21] (2 years).

| MC [%] | CL70_G20 | | | | CL50_G50 | | | | G | | | |
|---|---|---|---|---|---|---|---|---|---|---|---|---|
| RH [%] | 8y | | 2y | | 8y | | 2y | | 8y | | 2y | |
| | AV | SD | AV | SD | AV | SD | AV | SD | AV | SD | AV | SD |
| 30 | 0.03 | 0.003 | 0.05 | 0.004 | 0.02 | 0.002 | 0.06 | 0.004 | 0.02 | 0.002 | 0.03 | 0.003 |
| 50 | 0.11 | 0.004 | 0.09 | 0.049 | 0.10 | 0.002 | 0.11 | 0.005 | 0.06 | 0.005 | 0.06 | 0.003 |
| 70 | 0.28 | 0.004 | 0.16 | 0.059 | 0.24 | 0.006 | 0.19 | 0.003 | 0.14 | 0.046 | 0.08 | 0.003 |
| 80 | 0.80 | 0.074 | – | – | 0.74 | 0.036 | – | – | 0.21 | 0.090 | – | – |
| 90 | – | – | **1.67** | 0.037 | – | – | **1.30** | 0.094 | – | – | **0.18** | 0.009 |
| 95 | **5.05** | 0.129 | – | – | **2.39** | 0.172 | – | – | **0.48** | 0.270 | – | – |
| 80 | 4.66 | 0.180 | – | – | 2.03 | 0.185 | – | – | 0.25 | 0.088 | – | – |
| 70 | 4.54 | 0.237 | 1.44 | 0.036 | 1.87 | 0.185 | 1.09 | 0.096 | 0.17 | 0.044 | 0.10 | 0.008 |
| 50 | 4.19 | 0.260 | 1.33 | 0.037 | 1.56 | 0.176 | 1.00 | 0.094 | 0.08 | 0.017 | 0.07 | 0.007 |
| 30 | 3.94 | 0.267 | 1.17 | 0.035 | 1.37 | 0.179 | 0.84 | 0.092 | 0.03 | 0.006 | 0.04 | 0.008 |

Notation: MC – moisture content; y – years of curing; AV – average value; SD – standard deviation.

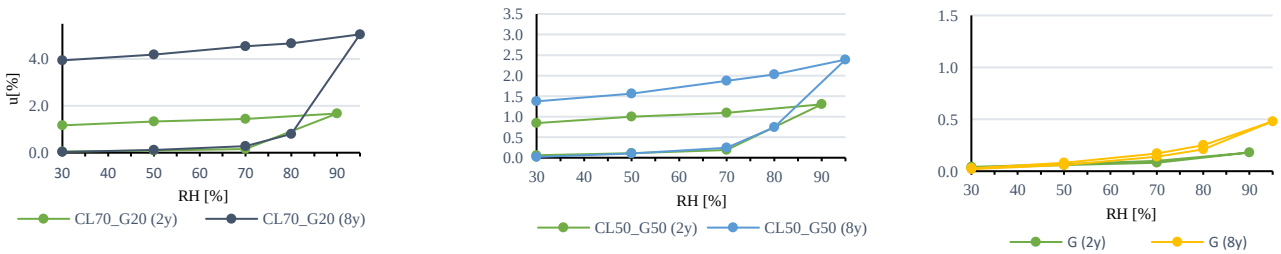


(**a**) (**b**) (**c**)

**Figure 3.6.** Synthesis of adsorption and desorption results (8 years) and comparison with the study of Freire [21] (2 years) for: (**a**)CL70_G20; (**b**) CL50_G50; (**c**) G pastes.

### 3.2.3.5 Moisture Buffering Value

The mean values of MBV for adsorption and desorption calculated on the last three cycles for all the tested plasters are presented in **Figure 3.7**.

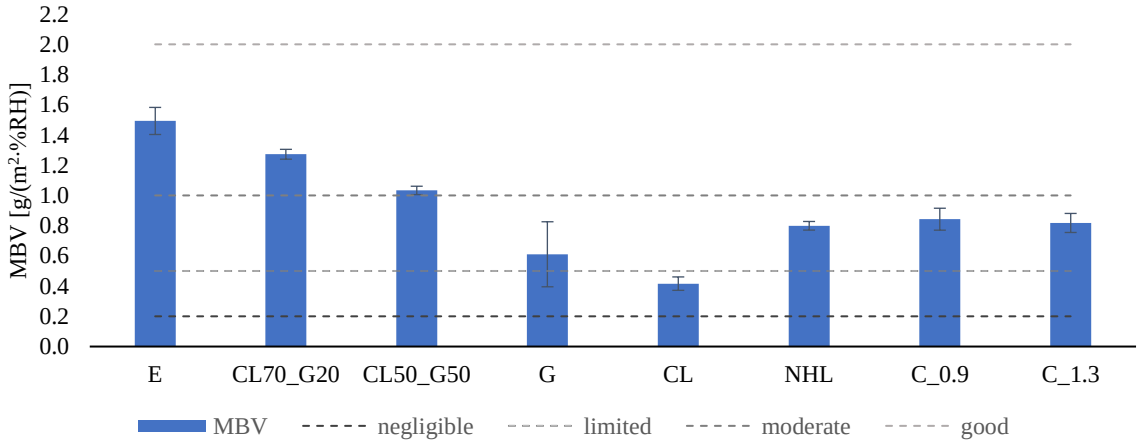


**Figure 3.7.** MBV of tested plasters (and standard deviation) and limits from NORDTEST [8].

Classes of MBV proposed by Rode *et al.* [8] are useful to have a quick comparison of different materials. Above 2 g/(m$^2$·%RH) the behaviour is classified excellent, here not referred as none of the considered materials was exceeding the *good* grade. The highest values of moisture buffering observed are from clay plaster and air lime–gypsum pastes, which show a *good* behaviour (1<MBV<2 g/(m$^2$·%RH)) according to the limits suggested by Rode *et al.* [8]. *NHL* and cement plasters show similar MBV classified as *moderate* (0.5<MBV<1 g/(m$^2$·%RH)). The lowest values are observed for *G,* still classified as *moderate* although showing a very high standard deviation, and *CL* ranked as *limited* (0.2<MBV<0.5 g/(m$^2$·%RH)).

Several other studies used the NORDTEST method to test plasters' MBV. A finishing coating paste based on gypsum and another made of 50% gypsum and 50% air lime (by weight) were tested by Ramos *et al.* [9] with specimens of 210 mm x 210 mm x 20 mm and 210 mm x 210 mm x 10 mm, respectively. Values of MBV at 23°C were 0.47 g/(m$^2$·%RH) for gypsum-lime pastes and 0.72 g/(m$^2$·%RH) for gypsum pure pastes. The MBV found for *CL50_G50*, 1.03 g/(m$^2$·%RH), is consistently higher than the one referred by Ramos *et al.* [9] while for *G* (0.61 g/(m$^2$·%RH)) the values are closer. Cascione *et al.* [42] tested a clay, a light-weight gypsum and a NHL3.5 plasters. The tested clay was kaolinitic and the mortar had 20% mass of water, the binder:aggregate ratio of the NHL plaster was 1.2:5 and the hemihydrate gypsum mortar had 30% mass of water. The dimensions of specimens were 150 mm x 150 mm x 20 mm. Results obtained were 1.67, 1.60 and 0.95 g/(m$^2$·%RH), respectively for clay, gypsum and NHL plasters. Values for clay and NHL are slightly higher than the results obtained in the present study, 1.49

and 0.80 g/(m$^2$·%RH) respectively, but the gypsum is almost three times higher. Unknown complete composition of the light-weight gypsum tested by Cascione [42] may justify the different response of two gypsum-based coatings. According to Roels *et al.* [61], for a gypsum plaster the thickness involved in the mechanism of moisture buffering is approximately 33 mm and when thinner samples are tested the MBV drops. Thus, considering that results from Cascione *et al.* [42] and the ones tested in the present study are from specimens of about 20 mm thickness, it is expected that their thicknesses are completely involved in moisture buffering while showing a different percentage of the potential response of each plaster. The different composition and microstructure is, anyway, here considered the main responsible of the different behaviours. A cement CEM II A/LL 42.5 R plaster was tested from Giosuè *et al.* [49] with a volumetric binder: aggregate proportion of 1:3.5, by cylindrical specimens with diameter of 100 mm and a thickness of 30 mm. The MBV found was about 0.3 g/(m$^2$·%RH), quite lower than the values 0.82 and 0.84 g/(m$^2$·%RH) found in the present study and enough to get different ratings in the MBV classification. The cement plasters have similar composition, except the one tested from Giosuè *et al.* [49] which shows a slightly higher dry bulk density (2091 kg/m$^3$) and a lower flow table consistency (120 mm). Thus, the thickness, porosity and dry bulk density seem to be parameters of influence for this test rather than the dimension of specimens, contributing to confirm the reliability of the tests with small samples.

### 3.2.4 Discussion

A synthesis of the characterization of RH dependent properties for the eight analyzed plasters is presented in **Table 3.9**. The same test procedures were adopted for all the plastering mortars and pastes, guaranteeing comparability of results.

All the pastes show WVP higher than mortars: the *CL_G* pastes present a higher WVP than pure *G* and *CL* mortars. When RH passes from 50% to 80%, kept for 12 hours [25], the highest adsorption is performed by the clay mortar (74.4 g/m$^2$) followed by the *CL_G* pastes and *C* mortars. When tested at steady state from 50% RH to 80% RH (**Table 3.9**), the moisture content of the *E* mortar rises less than the *CL_G* pastes. Thus, considering also the MBV found, the plaster based on clay has a quicker response to adsorption. The clay plaster *E* shows results in agreement with literature for WVP and hygroscopic behaviour. The measured MBV confirms the good response to moisture buffering of clay. Cement mortars show the lowest WVP between the analysed plasters, in agreement with previous studies [50] performed by wet cup method, whereas adsorbed water vapour at 12 hours of 80% RH exposure is the highest after

*E* and *CL_G* plasters, and a high moisture content is displayed in sorption isotherms at 95% RH (still lower than *E* and *CL_G*).

**Table 3.9.** Synthesis of average results of WVP, adsorption/desorption, sorption isotherms and MBV.

| Pastes and mortars | WVP [kg/(m·s·Pa)] x$10^{-12}$ | $MC_{(12h)}$ [g/$m^2$] | $MC_{30}$ [%] | $MC_{50}$ [%] | $MC_{70}$ [%] | $MC_{80}$ [%] | $MC_{95}$ [%] | $MC_{80}$ [%] | $MC_{70}$ [%] | $MC_{50}$ [%] | $MC_{30}$ [%] | MBV [g/($m^2$·%RH)] |
|---|---|---|---|---|---|---|---|---|---|---|---|---|
| G | 35.53 | 25.5 | 0.02 | 0.06 | 0.14 | 0.21 | 0.48 | 0.25 | 0.17 | 0.08 | 0.03 | 0.61 |
| CL50_G50 | 37.36 | 43.6 | 0.02 | 0.10 | 0.24 | 0.74 | 2.39 | 2.03 | 1.87 | 1.56 | 1.37 | 1.03 |
| CL70_G20 | 37.68 | 54.8 | 0.03 | 0.11 | 0.28 | 0.80 | 5.05 | 4.66 | 4.54 | 4.19 | 3.94 | 1.27 |
| E | 21.50 | 74.4 | 0.04 | 0.19 | 0.44 | 0.64 | 1.29 | 0.80 | 0.53 | 0.22 | 0.05 | 1.49 |
| CL | 26.24 | 16.5 | 0.02 | 0.04 | 0.08 | 0.12 | 0.40 | 0.30 | 0.25 | 0.19 | 0.14 | 0.42 |
| NHL | 20.92 | 28.6 | 0.03 | 0.07 | 0.15 | 0.21 | 0.56 | 0.34 | 0.25 | 0.15 | 0.06 | 0.80 |
| C_0.9 | 9.55 | 40.2 | 0.03 | 0.12 | 0.26 | 0.38 | 1.16 | 0.91 | 0.65 | 0.47 | 0.30 | 0.84 |
| C_1.3 | 13.48 | 34.5 | 0.03 | 0.09 | 0.19 | 0.27 | 0.91 | 0.68 | 0.52 | 0.41 | 0.27 | 0.82 |

Notation: WVP – water vapour permeability; Δm – change in mass; A – exchanging surface; MC – moisture content; MBV – moisture buffering value; E – clay; G – gypsum; CL – air lime; NHL – natural hydraulic lime 3.5; C – cement.

As discussed in the previous section, the desorption of cement plasters is a slower process and they show hysteresis at the end of desorption. At steady state the residual moisture content of *C* is, after the *CL_Gs*, the highest. Values of moisture buffering found are in accordance with all other tests of hygroscopicity. The two cement and the *NHL* plasters display a similar value of adsorption after 8 h at high RH. Therefore, the similar MBV of these three plasters is related to the specific exposure time and RH prescribed by NORDTEST. *NHL* and *CL* present similar sorption isotherms, and only air lime shows high residual moisture content.

Between the two cement mortars, *C_1.3* with higher open porosity (+2.2%) displays the highest WVP but a lower hygroscopic behaviour and moisture buffering. The results are in agreement with what was expected considering kneading water more related to macro porosity than to sorption mechanism, which interests micro and meso pores [62]. The analysis of pore size distribution was not run in the present study, but **Figure 3.8** shows this property for the same binder-based plasters (not applied on any substrate, such as in the present study) together with IUPAC classification of pores and ranges of pores responsible for different mechanism, as presented by Thomson [62].

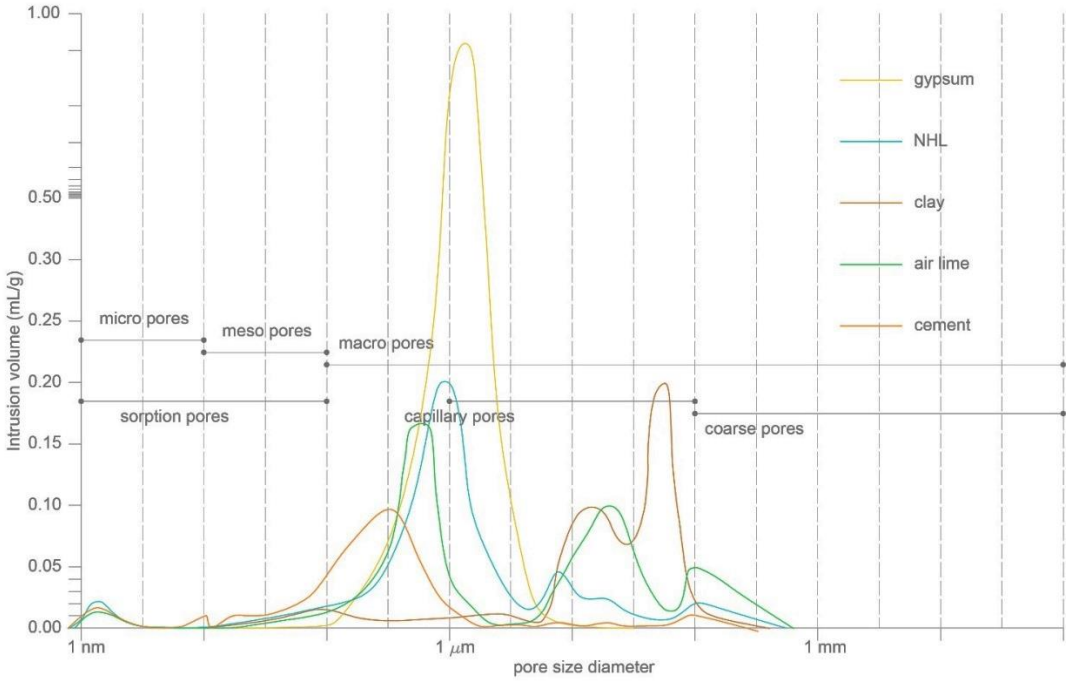


**Figure 3.8.** Pore size distribution from literature [22,63,64] of mortars based on gypsum, natural hydraulic lime, clay, air lime and cement and classification and ranges of pores (adapted from IUPAC (1972) and Thomson *et al.* [62]).

Although the pore size distribution displayed is not obtained from the analysed mortars, it is expected that the contribution of moisture buffering of the *Cs, NHL* and *CL* mortars is quite poor due to the similar and small amount of micro pores found for the same type of binder-based mortars [22]. However, the cement mortars showed the highest moisture capacity between them, probably related to their higher amount of meso pores (as in **Figure 3.8**). Thus, in this case meso pores of the cement mortars could be responsible of their higher moisture adsorption. Clay plasters [57] show higher pore size diameter (in the range $10^1$–$10^2$ μm) in a bimodal distribution although their dimension of pores does not influence in the same way the sorption since a chemical mechanism [58] is also responsible for moisture capacity.

### 3.2.5 Conclusions

In the present study, the assessment of RH dependant properties of five plastering mortars and three finishing pastes was run. The general characterization of the mortars and pastes was discussed and, where applicable, the requirements for substitution plasters for historic buildings were presented and the prescribed limits and ranges considered. The study was run on: two finishing pastes based on air lime and gypsum in different proportions (*CL70_G20* and *CL50_G50*), one gypsum paste (*G*), one plastering mortar based on clayish earth (*E*), one with

air lime (*CL*), one with natural hydraulic lime 3.5 (*NHL*) and two with cement (*C_0.9* and *C_1.3*). Apart from *E*, produced for the study, the samples of all the other mortars were received as leftover from previous experimental campaigns, thus with different curing ages, all higher than 2 years.

The results lead to the following conclusions:

- The three finishing pastes, designed for restoration of historic plaster finishings, show an open porosity and dry bulk density compatible with requirements for restoration plasters, a mechanical strength above the limit and a good water vapour permeability for that type of application. The high compressive and flexural strength decreases with the addition of air lime together with an increase in hygroscopicity. Hence, for moisture passive regulation the combinations of gypsum and air lime are more suitable than the pure gypsum paste. The latter, indeed, presents very low moisture capacity: in static condition, the maximum value of moisture adsorbed is the lowest between all the tested coatings; after the 12 h of adsorption, it is probably saturated and no additional moisture is adsorbed which is reflected in a *moderate* moisture buffering value. The *CL_Gs*, instead, present a *good* moisture buffering, being also very suitable for passive regulation.
- The earth plaster *E* fulfils requirements of mechanical compatibility together with some of the requirements for physical compatibility to water vapour. There is no doubt that this plaster is the most suitable for moisture passive regulation: it shows high hygroscopicity in dynamic and static conditions. Adsorption capacity exceeds the 24 h test and it is classified as *good* for moisture buffering.
- The *NHL* plaster in terms of compatibility complies with the same requirements as the earth plaster. For what concerns the RH dependant properties, when tested at adsorption/desorption in static and dynamic conditions its behaviour is moderately good. Moreover, it shows a moisture buffering value similar to the cement plasters.
- The *CL* plaster meets the mechanical requirement for compatibility and water vapour permeability is considered enough for application as restoration plaster. Its adsorption and desorption is the lowest when tested dynamically and still very low when tested at steady states. Furthermore, its moisture buffering value is the lowest, classified as *limited*.
- The cement plasters are the less suitable for application in historical buildings, as expected. They do not comply with any of the requirements, especially the *C_0.9*, which is considered the less compatible choice for substitution in ancient buildings. They show the lowest water vapour permeability and slow adsorption and desorption, but their moisture content at high RH is quite significant when tested at steady-state. The *moderate* classification for

moisture buffering makes of these plasters a possible choice for application in modern building where their passive regulation can be improved.

Further studies, namely on microstructure, may help to deeply understand the weak contribution of air lime and gypsum pure plastering mortars and finishing pastes.

### Author Contributions

Conceptualization, investigation, writing—original draft preparation, A.R.; supervision, writing—review and editing, P.F.; supervision, writing—review and editing, M.R.V.; All authors have read and agreed to the published version of the manuscript."


### Funding

This research was funded by PORTUGUESE FOUNDATION FOR SCIENCE AND TECHNOLOGY: 1st author Doctoral Training Programme EcoCoRe grant number PD/BD/150399/2019 and CIVIL ENGINEERING RESEARCH AND INNOVATION FOR SUS-TAINABILITY Unit-CERIS (UIDB/04378/2020).

### Acknowledgments

The authors would like to thank the National Laboratory for Civil Engineering of Portugal (LNEC) for the laboratory equipment and the support provided through the projects PRESERVe and REuSE; the technical team of NRI, especially Bento Sabala, and the researchers who donated their samples, namely Ana Rita Lopes dos Santos, Catarina Brazão Farinha, Cinthia Maia Pederneiras and Maria Teresa Freire.


### Conflicts of Interest

The authors declare no conflict of interest.

## References


1. EN 998-1 (2003) Specification for mortar for masonry – Part 1: Rendering and plastering mortar. CEN, Brussels.
2. Veiga R (2017) Air lime mortars: what else do we need to know to apply them in conservation and rehabilitation interventions? A review. Construction and Building Materials, 157, 132–40. DOI: 10.1016/j.conbuildmat.2017.09.080.
3. Freire M T, Veiga M R, Santos Silva A, de Brito J (2019) Studies in ancient gypsum based plasters towards their repair: physical and mechanical properties. Construction and Building Materials, 202, 319–31. DOI: 10.1016/j.conbuildmat.2018.12.214.

4. Candeias A E, Nogueira P, Mirão J, Santos Silva A, Veiga R, Gil Casal M, Ribeiro I, Seruya A I (2006) Characterization of ancient mortars: present methodology and future perspectives. In Proc. Workshop on Chemistry in the Conservation of Cultural Heritage: present and future perspectives. Retrieved from http://www.eu-artech.org/files/Ext_ab/candeias.pdf.
5. Gomes I, Faria P (2011) Repair mortars for rammed earth constructions. In Proceedings of the XII DBMC – 12th International Conference on Durability of Building Materials and Components, Porto, 2208. ISBN: 9789727521326.
6. Veiga R, Faria P (2018) The role of mortars in the durability of ancient walls (in Portuguese). In CirEA2018 - Conferência Inter-nacional sobre Reabilitação de Estruturas Antigas de Alvenaria, 1-15. ISBN: 978-972-8893-67-5.
7. Padfield T (1999) Humidity buffering of the indoor climate by absorbent walls. In 5th Symposium on Building Physics in the Nordic Countries, 2, 637–644.
8. Rode C, Peuhkuri RH, Mortensen LH, Hansen KK, Time B, Gustavsen A, Ojanen T, Ahonen J, Svennberg K, Harderup LE, Arfvidsson J (2005) Moisture buffering of building materials. Technical University of Denmark, Department of Civil Engi-neering. BYG Report R-127.
9. Ramos N M M, Delgado J M P Q, De Freitas V P (2010) Influence of finishing coatings on hygroscopic moisture buffering in building elements. Construction and Building Materials 24(12), 2590–97. DOI:10.1016/j.conbuildmat.2010.05.017.
10. Arundel A V, Sterling E M, Biggin J H, Sterling T D (1986) Indirect health effects of relative humidity in indoor environments. Environmental Health Perspectives, 65, 351-61.
11. Wolkoff P (2018) Indoor air humidity, air quality, and health – An overview. International Journal of Hygiene and Environmental Health, 221, 376-90. DOI: 10.1016/j.ijheh.2018.01.015.
12. Fang L, Clausen G, Fanger P O (1998) Impact of temperature and humidity on the perception of indoor air quality. Indoor air, 8, 80-90. DOI: 10.1111/j.1600-0668.1998.t01-2-00003.x.
13. Posani M, Veiga M D R, de Freitas V P (2019) Towards resilience and sustainability for historic buildings: a review of envelope retrofit possibilities and a discussion on hygric compatibility of thermal insulations. International Journal of Architectural Heritage, 15(5), 807–823. DOI: 10.1080/15583058.2019.1650133.
14. McGregor F, Heath A, Shea A, Lawrence M (2014) The moisture buffering capacity of unfired clay masonry. Building and En-vironment 82, 599–607. DOI: 10.1016/j.buildenv.2014.09.027.

15. Zhang M, Qin M, Rode C, Chen Z (2017) Moisture buffering phenomenon and its impact on building energy consumption. Applied Thermal Engineering 124, 337-345. DOI: 10.1016/j.applthermaleng.2017.05.173.
16. Sesana E, Gagnon A S, Bertolin C, Hughes J (2018). Adapting cultural heritage to climate change risks: perspectives of cultural heritage experts in Europe. Geosciences 8(8), 305. DOI: 10.3390/GEOSCIENCES8080305.
17. Posani M, Veiga M R, de Freitas V P, Kompatscher K, Schellen H (2020) Dynamic hygrothermal models for monumental, historic buildings with HVAC systems: complexity shown through a case study. E3S Web of Conference, 172, In 12th Nordic Symposium on Building Physics, NSB2020, 15007. DOI: 10.1051/e3sconf/20201721.
18. Veiga M R, Fragata A, Velosa A L, Magalhães A C, Margalha G (2010) Lime-based mortars: Viability for use as substitution renders in historical buildings. International Journal of Architectural Heritage, 4(2), 177–195. DOI: 10.1080/15583050902914678.
19. Ranesi A, Veiga M R, Faria P (2020) Plasters for rehabilitation – relevant requirements and characteristics (in Portuguese). In 4° Encontro de conservação e reabilitação de edifícios – ENCORE 2020, Lisbon, 551-561. DOI: 10.34638/yzys-hn57.
20. EMB01, clay plaster Embarro Universal thecnhical sheet. https://www.embarro.com/wp-content/uploads/1-CLAY-PLASTER-EMBARRO-UNIVERSAL.pdf.
21. Freire M T (2016) Restoration of ancient Portuguese interior plaster coatings: Characterization and development of compatible gypsum-based products. Instituto Superior Técnico, Universidade de Lisboa. PhD thesis.
22. Santos A R (2019) The influence of natural aggregates on the performance of replacement mortars for ancient buildings: the effects of mineralogy, grading and shape. Instituto Superior Técnico, Universidade de Lisboa. PhD thesis.
23. Pederneiras C, Veiga R, de Brito J (2019) Rendering mortars reinforced with natural sheep's wool fibers. Materials, 12, 3648. DOI: 10.3390/ma12223648.
24. Farinha C, de Brito J, Veiga R (2019) Assessment of glass fibre reinforced polymer waste reuse as filler in mortars. Journal of Cleaner Production, 210, 1579–1594. DOI: 10.1016/J.JCLEPRO.2018.11.080.
25. DIN 18947 (2018) Earth plasters - Requirements, test and labelling. DIN, Berlin.
26. EN 13279-2 (2004) Gypsum binders and gypsum plasters - Part 2: Test methods. CEN, Brussels (Replaced in 2014).
27. EN 1015-3 (1999) Methods of test for mortar for masonry - Part 3: Determination of consistence of fresh mortar (by flow table). CEN, Brussels.

28. Pederneiras C, Veiga R, de Brito J (2021) Physical and mechanical performance of coir fiber-reinforced rendering mortars. Materials, 14, 823. DOI: 10.3390/ma14040823.
29. EN 1015-6 (1998) Methods of test for mortar for masonry - Part 6: Determination of bulk density of fresh mortar. CEN, Brussels.
30. EN 1015-11 (1999) Methods of test for mortar for masonry - Part 11: Determination of flexural and compressive strength of hardened mortar. CEN, Brussels.
31. EN 1015-10 (1999) Methods of test for mortar for masonry - Part 10: Determination of dry bulk density of hardened mortar. CEN, Brussels.
32. EN 14146 (2004) Natural stone test methods - Determination of the dynamic modulus of elasticity (by measuring the funda-mental resonance frequency). CEN, Brussels.
33. EN 1936 (2006) Natural stone test method - Determination of real density and apparent density, and of total and open porosity. CEN, Brussels.
34. EN 1015-18 (2002) Methods of test for mortar for masonry - Part 18: Determination of water absorption coefficient due to capillary action of hardened mortars. CEN, Brussels.
35. EN 15801 (2009) Conservation of cultural property - Test methods - Determination of water absorption by capillarity. CEN, Brussels.
36. ISO 12572 (2016) Hygrothermal performance of building materials and products - Determination of water vapour transmission properties - Cup method. ISO, Geneva.
37. ISO 12571 (2013) Hygrothermal performance of building materials and products - Determination of hygroscopic sorption properties. ISO, Geneva.
38. Lima J, Faria P, Santos Silva A (2020) Earth Plasters: The influence of clay mineralogy in the plasters' properties. International Journal of Architectural Heritage, 678, 64–77. DOI: 10.1080/15583058.2020.1727064.
39. Pavlíková M, Kapicová A, Pivák A, Záleská M, Lojka M, JankovskýO, Pavlík Z (2021) Zeolite lightweight repair renders: effect of binder type on properties and salt crystallization resistance. Materials, 14, 3760. DOI: 10.3390/MA14133760.
40. Černý R, Kunca A, Tydlitát V, Drchalová J, Rovnaníková P (2006) Effect of pozzolanic admixtures on mechanical, thermal and hygric properties of lime plasters. Construction and Building Materials, 20(10), 849 – 857. DOI: 10.1016/J.CONBUILDMAT.2005.07.002
41. Mazhoud B, Collet F, Pretot S, Chamoin J (2016) Hygric and thermal properties of hemp-lime plasters. Building and Environment 96, 206–16. DOI: 10.1016/J.BUILDENV.2015.11.013
42. Cascione V, Maskell D, Shea A, Walker P, Mani M (2020) Comparison of moisture buffering properties of plasters in full scale simulations and laboratory testing. Construction and Building Materials 252, 119033. DOI: 10.1016/j.conbuildmat.2020.119033.

43. Liuzzi S, Rubino C, Stefanizzi P, Petrella A, Boghetich A, Casavola C, Pappalettera G (2018) Hygrothermal properties of clayey plasters with olive fibers. Construction and Building Materials 158, 24–32. DOI: 10.1016/j.conbuildmat.2017.10.013.
44. McGregor F, Fabbri A, Ferreira J, Simões T, Faria P, Morel JC (2017) Procedure to determine the impact of the surface film resistance on the hygric properties of composite clay/fibre plasters. Materials and Structures/Materiaux et Constructions 50(4), 193. DOI: 10.1617/s11527-017-1061-3.
45. Čáchová M, Vejmelková E, Koňáková D, Keppert M (2013) Influence of finely ground brick on hydric properties of lime plasters. In Proceedings of the 4th European Conference of Mechanical Engineering, Paris: WSEAS Press, 117–121.
46. Vejmelková, E, Koňáková D, Čáchová M, Keppert M, Černý R (2012a) Effect of hydrophobization on the properties of lime-metakaolin plasters. Construction and Building Materials 37, 556–61. DOI: 10.1016/j.conbuildmat.2012.07.097.
47. Vejmelková E, Keppert M, Keršner Z, Rovnaníková P, Černý R (2012b) Mechanical, fracture-mechanical, hydric, thermal, and durability properties of lime-metakaolin plasters for renovation of historical buildings. Construction and Building Materials 31, 22–28. DOI: 10.1016/j.conbuildmat.2011.12.084.
48. Buratti C, Belloni E, Merli F (2020) Water vapour permeability of innovative building materials from different waste. Materials Letters, 265, 127459. DOI: 10.1016/j.matlet.2020.127459.
49. Giosuè C, Pierpaoli M, Mobili A, Ruello M L, Tittarelli F (2017) Influence of binders and lightweight aggregates on the properties of cementitious mortars: From traditional requirements to indoor air quality improvement. Materials, 10(8), 978. DOI:10.3390/ma10080978.
50. Frattolillo A, Giovinco G, Mascolo M C, Vitale A (2005) Effects of hydrophobic treatment on thermophysical properties of lightweight mortars. Experimental Thermal and Fluid Science 29 (6), 733-741. DOI: 10.1016/j.expthermflusci.2004.12.002
51. EN 1015-19 (1998) Methods of test for mortar for masonry - Part 19: Determination of water vapour permeability of hardened rendering and plastering mortars. CEN, Brussels.
52. Santos T, Gomes MI, Santos Silva A, Ferraz E, Faria P (2020) Comparison of mineralogical, mechanical and hygroscopic characteristic of earthen, gypsum and cement-based plasters. Construction and Building Materials 254, 119222. DOI: 10.1016/j.conbuildmat.2020.119222.

53. Santos T, Silva V, Faria P (2015) Earthen mortars – Hygrotermal behaviour as a function of grain size distribution of sand (in Portuguese). Construção Magazine 68, 28 - 30.
54. Santos T, Faria P, Silva V (2014) Characterization of premixed earth mortars (in Portuguese). In Argmassas 2014 – Simpósio de Argamassas e Soluções Térmicas de Revestimento, ITeCons, 1–12.
55. Jiang Y, Phelipot-Mardele A, Collet F, Lanos C, Lemke M, Ansell M, Hussain A, Lawrence M (2020) Moisture buffer, fire resistance and insulation potential of novel bio-clay plaster. Construction and Building Materials 244, 118353. DOI: 10.1016/j.conbuildmat.2020.118353.
56. Lima J, Faria P (2016) Eco-efficient earthen plasters: The influence of the addition of natural fibers. In Natural Fibres: Advances in Science and Technology Towards Industrial Applications. From Science to Markets, Fangueiro, Raul, Rana, Sohel (Eds.). Springer, RILEM Bookseries, 12, 315–27.
57. Maddison M, Mauring T, Kirsimäe K, Mander Ü (2009) The humidity buffer capacity of clay-sand plaster filled with phytomass from treatment wetlands. Building and Environment, 44(9), 1864–1868. DOI: 10.1016/j.buildenv.2008.12.008.
58. Lima J, Faria P, Santos Silva A (2016) Earthen plasters based on illitic soils from barrocal region of Algarve: Contributions for building performance and sustainability. Key Engineering Materials, 678, 64–77. DOI: 10.4028/www.scientific.net/KEM.678.64
59. Lima J, Correia D, Faria P (2016) Earthen plasters: The influence of the addition of gypsum and of the grain size distribution of sand (in Portuguese). In ARGAMASSAS 2016 – II Simpósio de Argamassas e Soluções Térmicas de Revestimento, ITeCons, 119–130.
60. López-Arce P, Gómez-Villalba, LS, Martínez-Ramírez S, Álvarez de Buergo M, Fort R (2011) Influence of relative humidity on the carbonation of calcium hydroxide nanoparticlesand the formation of calcium carbonate polymorphs. Powder Technology 205, 263-69. DOI: 10.1016/j.powtec.2010.09.026.
61. Roels S, Janssen H (2005) Is the moisture buffer value a reliable material property to characterise the hygric buffering capacities of building materials? Working paper A41-T2-B- 05-7 for IEA Annex 41 project, Whole Building Heat air and Moisture Response.
62. Thomson M L, Lindqvist J-E, Elsen J, Groot C J W P (2004) Porosity of historic mortars. In 13th International Brick and Block Masonry Conference.
63. Freire M T, Veiga R, Santos Silva A, de Brito J (2019) Studies in ancient gypsum based plasters towards their repair: Physical and mechanical properties. Construction and Building Materials, 202, 319–331. DOI: 10.1016/j.conbuildmat.2018.12.214.

64. Santos T, Faria P, Silva V (2019) Can an earth plaster be efficient when applied on different masonries? Journal of Building En-gineering 23, 314–23. DOI: 10.1016/j.jobe.2019.02.011.
65. Osanyintola O F, Simonson C J (2006) Moisture buffering capacity of hygroscopic building materials: Experimental facilities and energy impact. Energy and Buildings, 38, 1270–1282. DOI: 10.1016/j.enbuild.2006.03.026.

## 3.3 Article B2 - The Influence of the Paint System

(the article was submitted on 28/10/2023 to the *Journal of Building Engineering;* reviews from the thesis advisory committee were applied)

# Paint systems on traditional and modern plasters: effect on passive contribution to indoor comfort

Alessandra Ranesi [1,2,*], M. Rosário Veiga [2], Paula Rodrigues[2], Paulina Faria [1].
[1] CERIS and Dep. Civil Engineering, NOVA School of Science and Technology, NOVA University of Lisbon, 2829-516 Caparica, Portugal
[2] National Laboratory for Civil Engineering, Avenida do Brasil 101, 1700-066 Lisbon, Portugal

[*] Corresponding author: a.ranesi@campus.fct.unl.pt

## Abstract

Plasters can be finished with paint systems that can affect their physical properties. A change in water vapor permeability and moisture buffering performance is expected in that case. To confirm that, eight traditional and modern plastering mortars and pastes – based on cement, natural hydraulic lime, air lime, earth and gypsum - were coated with a vinylic paint (A) and an acrylic paint (B) and underwent the same hygroscopic characterization of the bare mortar samples. Results showed that the studied properties were influenced by the paint systems. Overall, the water vapor permeability of all the plasters decreased after the paint A application. The effect of the same paint system A on water vapor adsorption and the moisture buffering was small, in some cases positive. The trend was not the same for all the plastering mortars and pastes, suggesting that, even with the application of the studied paint system, the different plastering substrates were still involved in the hygroscopic mechanism. The application of the paint system B, instead, significantly reduced the hygroscopic behavior of the mortars, leveling their responses. The two paints are produced for different applications, and it is reasonable to conclude that their formulations are designed for different scopes and, thus, have a diverse effect on these properties. Therefore, to optimize the passive contribution plasters may have to indoor comfort it is important to have a conscious choice when applying paint finishing systems.

## Keywords

Coating; Hygroscopicity; Moisture buffer; Water vapor permeability; Vinylic paint; Acrylic paint.

## 3.3.1 Introduction

The high amount (40%) of global energy consumed by the building sector (UNEP-SBCI, 2009) and the high amount (90%) of time people spend indoors (Frey et al., 2015) are two key factors to consider for indoors design. Coating materials can passively contribute to the indoor moisture control (Padfield 1999) diminishing the energy requirements of buildings (Zhang et al., 2017; Osanyintola and Simonson 2006; Li and Ran 2023) and preventing risk of inhabitants' exposure to unhealthy environments and the possible development of chronical diseases (Arundel et al., 1986; Jones, 1999; Wolkoff, 2018; Fang et al., 1998; Guarnieri et al., 2023).

Among many coating materials, plastering mortars and pastes are commonly used to cover walls and ceilings. Thus, they have a large surface in contact with indoor air and their potential to contribute to passive moisture control can be important. Traditional and modern binder-based plasters are found to have different relative humidity dependent properties (Ranesi et al., 2021a; Ranesi et al., 2021b). Plasters based on clay generally have a very high moisture capacity and for this reason their moisture behavior is often studied (Liuzzi et al., 2018; Randazzo et al., 2016, Ashour et al., 2011), but also other binder-based plasters have been the subject of interest in some research studies (Cascione at el., 2020; Santos et al., 2020), often in comparison with the clay-based ones.

Nevertheless, it is common practice to apply a finishing layer (or more) on plasters. The reasons can be related to the liquid water vulnerability of some plasters like clay or gypsum-based ones; their poor aesthetics as for cement and natural hydraulic lime-based plasters; habit use; social factors; or simply users' decision. Thus, it seems reasonable to consider possible the application of one additional finishing layer (or more).

Among all the possible finishings, the present study analyzes the application of two paints, A and B, produced and commercialized for indoor and for exterior use. The selected paints A and B are both water-based but with different common binders: a polyvinyl acetate resin (paint A) and an acrylic one (paint B). The application of both paints was made according to the same protocols and producer recommendations and their influence on the hygroscopic behavior of mortars was evaluated.

## 3.3.2 Materials and methods

### 3.3.2.1 The commercial paintings

- PAINT A

A commercial paint (A) for indoor use was selected for the study. The paint was not on the market yet and the laboratory characterization was run for the study. The binder was identified by Fourier-transform infrared spectroscopy (FT-IR) after an extraction with chloroform. The results showed that the paint binder is a polyvinyl acetate resin (**Figure 3.9**). The bulk density of the paint was determined by using a pycnometer and the non-volatile-matter content (NVMC) by drying at 105 °C in a ventilated oven for 1 hour (**Figure 3.10**).

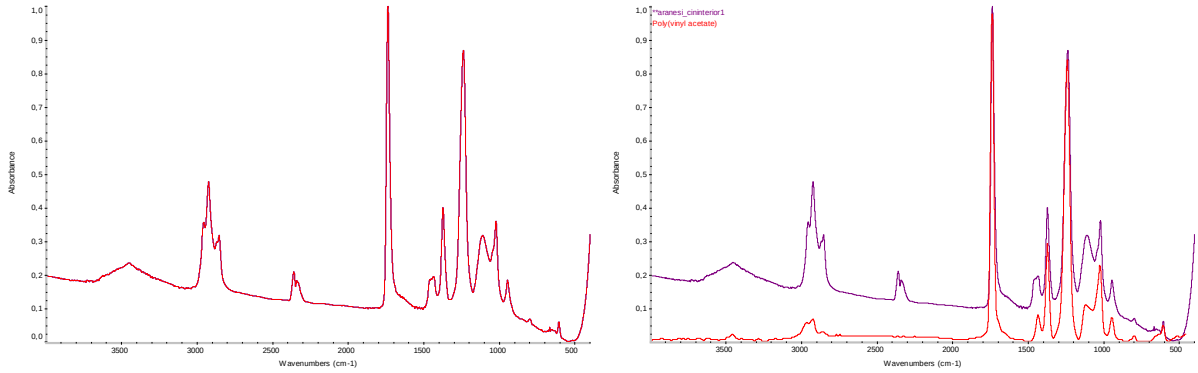


(a) (b)

**Figure 3.9.** FT-IR spectra of **(a)** binder of paint A and **(b)** binder of paint A (in purple) compared with a polyvinyl acetate (in red) from the literature.

**Figure 3.10.** Laboratory assessment of bulk density and SC of paint A.

The water vapour permeability (WVP) of the paint was tested on three specimens. The application was run on polytetrafluoroethylene sheets (PTFE or Teflon) (**Figure 3.11**a) in order to obtain a final thickness of 140 µm in two layers, brushed with 24-hours drying interval and dried at 23 ± 2 ºC e 50 ± 5 % RH for 30 days.

After curing, the dried paint films were detached from the PTFE sheet and cut in the shape of disks (approx. 80 mm diameter) (**Figure 3.11**b). Three film disks from the paint A were sealed with wax to the rims of the cups used for WVP tests (**Figure 3.11**c). A saturated solution of ammonium dihydrogen phosphate (300 ml) was used to obtain 93% RH environment inside the cups, based on EN ISO 7783 (2018). The circular test area of approx. 60 mm diameter was exposed to the test conditions inside a climatic chamber Aralab-Fitoclima 700 EDTU kept at 50 ± 5 % RH and 23 ± 2 °C until constant water vapor flux for at least five successive weighing

intervals (24 hours). The determination of the films´ thicknesses was done by using an electronic micrometer according to EN ISO 2808 (2019).

(a) (b) (c) (d)

**Figure 3.11.** Application of the paint on Teflon **(a)**; disks cut **(b)**; disks sealed on water vapor permeability cups **(c)**; thickness of the dried paint system measurement **(d)**.

A value of 158 µm was found, by averaging eight measurements (**Figure 3.11**d). This real thickness value was considered for calculating the diffusion-equivalent air layer thickness of 0.053 m that would correspond to the class $V_1$ – high water vapor transmission rate ($s_d$< 0.14 m) according to the standard (EN 1062-1, 2004) and is consistent with tabulated design values for paint emulsion referred in the standard ISO 10456 (2007).

- **PAINT B**

A second commercial paint (B) was already characterized by the Portuguese National Laboratory for Civil Engineering (LNEC) and classified as a coating for exterior surfaces. It was used in the study to allow some comparison in terms of type of binder and water vapour properties. Following the producer recommendations, it was applied in three layers to obtain around the same thickness as paint A. The main characteristics found from the analysis of the paint A and obtained by the LNEC technical sheet for the paint B are synthetized in **Table 3.10**.

**Table 3.10.** Synthesis of the paintings' characterization.

| | **BD [g/mL]** | **NVMC [%]** | **$s_d$ [m]** | **WVP class** |
|---|---|---|---|---|
| Paint A | 1.403 | 48.9 | 0.053 | $V_1$ |
| Paint B | 1.373 | 52 | >0.14 ;<1.4 | $V_2$ |

Notation: BD – bulk density; NVMC – non-volatile-matter content; sd – air layer of equivalent diffusion; WVP – water vapor permeability.

### 3.3.2.2 The plastering mortars

The products selected as substrates for the experimental campaign were five plastering mortars and three pastes used as plasters finishing layers (**Figure 3.12**). The plasters were elsewhere characterized by water vapor permeability and hygroscopic behavior (Ranesi et al., 2021a). The five mortars are based on different binders, namely: clayish earth (E), hydrated lime (AL), natural hydraulic lime (NHL) and cement (C), the latter produced with two different water:binder ratios (0.9 and 1.3). The pastes are based on calcium sulphate hemihydrate (G) and two combinations of the latter with hydrated lime (AL50_G50 and AL70_G20). For each product, three specimens of 40 mm x 40 mm x 20 mm approx. were used for the application of the paints. The apparent bulk density and open porosity of the plasters were obtained following EN 1936 (2006) by vacuum and hydrostatic weighing, except for the earth plasters which were geometrically determined as they would be damaged by water. **Table 3.11** presents a synthesis of the plasters and their characteristics, including their previous hygroscopic characterization.

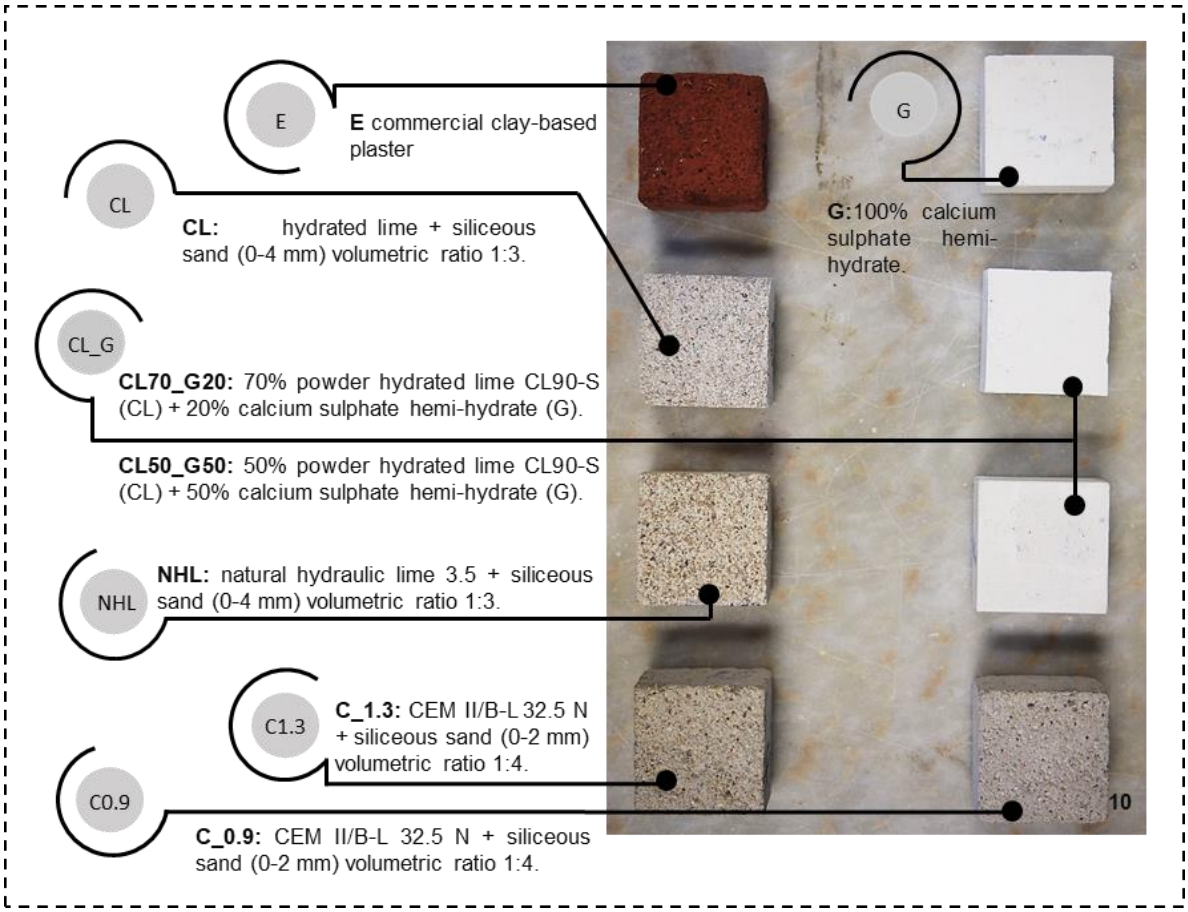


**Figure 3.12.** The plastering mortars and pastes ready for the application of the commercial paint system.

The two commercial paint systems A and B were applied on the substrate specimens following the same procedure described for the application on PTFE sheets (intended thickness of 140 µm in two layers for paint A and three layers for paint B, brushed with 24 hours drying interval and dried at 23 ± 2 °C and 50 ± 5 % RH for 30 days).

**Table 3.11.** Synthesis of characterization of the plastering mortars and finishing pastes selected as substrate for the study (Ranesi et al., 2021a).

| Property | E | AL | NHL | C0.9 | C1.3 | G | AL50_G50 | AL70_G20 |
|---|---|---|---|---|---|---|---|---|
| BD [kg/m$^3$] | 1770 | 1755 | 1852 | 1937 | 1891 | 1048 | 1048 | 1043 |
| OP [%] | - | 27.4 | 25.6 | 20.4 | 23.3 | 46.3 | 50.7 | 53.4 |
| µ [-] | 9.07 | 7.43 | 9.32 | 20.42 | 14.48 | 5.49 | 5.22 | 5.18 |
| MBV[g/(m$^2$%RH)] | 1.49 | 0.42 | 0.80 | 0.84 | 0.82 | 0.61 | 1.03 | 1.27 |
| $MC_{12h}$ [g/m$^2$] | 74.4 | 16.5 | 28.6 | 40.2 | 34.5 | 25.5 | 37.36 | 37.68 |

Notation: BD – Bulk Density; OP – Open porosity; µ – water vapor resistance factor; MBV – moisture buffering value by NORDTEST (Rode et al., 2005); $MC_{12h}$ – moisture content at 12 hours (DIN18947, 2018).

## 3.3.3 Test methods on the painted plasters

### 3.3.3.1 Water Vapor Permeability

After the application and drying of the paint A (as described in section 3.3.2.2), three specimens of each mortar and paste were tested for water vapor permeability. They were sealed with aluminum tape on the four lateral faces, to guarantee the mono-directionality of the water vapor flux, and with wax on the top of the cups containing calcium chloride, to ensure the ΔRH (0-50%) prescribed by the ISO 12572 (2016) for the dry cup conditions. The test procedure followed was the same described by Ranesi et al. (2021a) for the same, unpainted, specimens. For shortage of specimens (the ones used in the study were mainly collected as leftover from other campaigns) it was not possible to perform the test of WVP for the mortars and pastes coated by the paint B system. Results were expressed as thickness of the equivalent air layer for the bare plasters and for the coated systems (paint A), at the experiment hygrothermal conditions (0% RH, 23 °C; 50% RH, 23°). The water vapor permeability of air was calculated according Schirmer formula as prescribed by ISO 12572 (2016).

### 3.3.3.2 Sorption Isotherms

After the WVP test, the sorption isotherms of the painted plasters were determined according to ISO 12571 (2013). The specimens were sealed with aluminum tape on their four lateral faces and on the base. Once dried in an oven at 45 °C until constant mass (mass variation lower than 0.1% in 24 hours, for three consecutive weighing), they were placed in the same climatic

chamber used before at 23 ± 5 °C and RH following the steps 30%, 50%, 70%, 80% and 95%, keeping each until steady state. The slope of the curves was used to calculate the specific moisture capacity for *middle humidity levels* (50-70% RH). During the test on the specimens with the application of the paint B some technical issues prevented the climatic chamber from reaching the 95%. In order to show results compatible with the previous two tests, it was then decided to predict the curve based on a nonlinear regression analysis of the adsorption (0-80% RH) and the desorption (80%-0%RH) real data, available from the test.

The model selected has already been used by other authors (Ferreira et al., 2020) and retained a good choice for simulating the response of hygroscopic materials. The equation (1) here applied, was firstly proposed by Hansen in 1986 (Hansen, 1986):

$$u = a \cdot (1 - \frac{\ln \varphi}{b})^{-\frac{1}{c}} \quad (1)$$

with $u$ the moisture content [kg/kg], $\varphi$ the relative humidity [-] and $a, b, c$ the parameters to be calculated to fit the prediction curve to the experimental data. To obtain a better fit, it was decided to write two equations (one for adsorption and one for desorption) and calculate the $R^2$ for each segment (adsorption and desorption) to fit the curve the most. The moisture content at 95% RH was successively predicted as the maximum value between the adsorption and the desorption equations applied at 95% RH. In **Table 3.12** a synthesis of the calculated parameters and $R^2$ is shown.

**Table 3.12.** Synthesis of the nonlinear regression analysis parameters: a, b, c and $R^2$ fitting the Hansen equation (Hansen, 1986) for adsorption and desorption.

| Mortar | Adsorption | | | $R^2$ | Desorption | | | $R^2$ |
|---|---|---|---|---|---|---|---|---|
| | a | b | c | | a | b | c | |
| E | 0.006 | 24.742 | 0.024 | 0.99 | 0.006 | 0.724 | 0.827 | 0.98 |
| AL | 0.001 | 34.000 | 0.019 | 0.99 | 0.002 | 1.500 | 0.380 | 0.99 |
| NHL | 0.002 | 25.934 | 0.024 | 0.99 | 0.002 | 24.000 | 0.050 | 0.97 |
| C1.3 | 0.003 | 28.249 | 0.026 | 0.99 | 0.002 | 0.926 | 1.271 | 0.98 |
| C0.9 | 0.004 | 25.534 | 0.023 | 0.99 | 0.004 | 0.882 | 0.973 | 0.93 |
| AL70_G20 | 0.004 | 26.569 | 0.024 | 0.99 | 0.005 | 23.913 | 0.059 | 0.98 |
| AL50_G50 | 0.004 | 24.871 | 0.023 | 0.99 | 0.004 | 0.839 | 0.858 | 0.97 |
| G | 0.004 | 24.111 | 0.022 | 0.99 | 0.003 | 15.000 | 0.090 | 0.99 |

#### 3.3.3.3 Moisture Penetration Depth

The moisture penetration depth (MPD) was calculated for bare mortars and for the system mortars with paint A. The determination of this parameter for mortars with application of paint B was not possible for lack of experimental results of the system WVP. The MPD represents the

thickness of the material involved in the mechanism of moisture buffering. Thus, to determine correctly the moisture buffering value of any building material, it is necessary to test specimens with a higher thickness than the material's MPD. Two simplified methods of calculation for porous materials, present in literature (Rode et al., 2005; Woods et al., 2013), were followed.

The theoretical penetration depth calculated according to Rode (2005) as the "depth where the amplitude of moisture content variations is only 1% of the variation on the material surface", $d_{p,1\%}$, is given by equation (2):

$$d_{p.1\%} = 4.61\sqrt{\frac{D_w t_p}{\pi}} \quad (2)$$

being $t_p$ the time in seconds of duration of the daily cycle 86400 s, and $D_w$ the moisture diffusivity of the material depending on the water vapor permeability of the material ($\delta_p$), its dry bulk density ($\rho$), its specific moisture capacity ($\xi_u$) and the saturation vapor pressure ($p_s$), defined by equation (3):

$$D_w = \frac{\delta_p p_s}{\rho \xi_u} \quad (3)$$

The dry bulk density of the mortars was presented in section **3.2.2.2**, the water vapor permeability ($\delta_p$) of the plasters at ΔRH 0-50%, and the specific moisture capacity ($\partial u/\partial \varphi$) according to the values of moisture content ($u$) at 50% RH and 70% RH. The saturation water pressure was calculated by equation (4):

$$p_s = 610.5\, e^{\frac{17.269\, t}{237.3+t}} \quad (4)$$

where $t$ is the temperature [°C] of the experiment.

But, as observed by Maskell et al. (2018), the application of a model built for a semi-infinite or very thick material (as the one proposed by Rode et al. (2005)) may not be very suitable for plasters. Therefore, the model proposed by Woods et al., (2013) was also applied, considering 1/e (36.8% instead of 1%) as the ratio of the amplitude of moisture content variation (Maskell et al., 2018), and the theoretical penetration depth was calculated by equation (5):

$$d_{1/e} = \sqrt{\frac{D_w t_p}{\pi}} \quad (5)$$

#### 3.3.3.4 Moisture Buffering Value

The practical moisture buffering value (MBV) of the bare mortars and of the systems with paints A and B was obtained by tests, even if not simultaneously run. The specimens were sealed on their five faces with aluminum tape and preconditioned in a climatic chamber at 63 ± 5% RH

and 23 ± 0.5 °C. A balance with 0.001 g resolution was used. The test was run according to the *middle humidity level* condition of the international standard ISO 24353 (2008). Thus, the specimens were exposed cyclically at two steps, 12 h each, of 75% and 50% RH, at the fixed temperature of 23 ± 0.5 °C and weighted after 3, 6, 9, 12 and 24 hours. The last three cycles out of five were considered for calculating the average value in adsorption and desorption of practical MBVs, according to the NORDTEST prescriptions (Rode et al., 2005).

Moreover, for comparison, the ideal MBV of bare and painted A mortars was calculated as proposed by Rode et al. (2005) by equation (6). The determination of this parameter for mortars with application of paint B was not possible for lack of experimental results of WVP.

$$MBV_{ideal} = \frac{G_{(t)}}{\Delta RH} \tag{6}$$

being ΔRH the applied step in RH and $G_{(t)}$ the predicted moisture flux (uptaken and released), calculated by equation (7):

$$G_{(t)} = b_m \, \Delta_p \, h(\alpha) \sqrt{\frac{t_p}{\pi}} \tag{7}$$

being $\Delta_p = p_{s,50} - p_{s,0} = 1403.91$ Pa; $b_m$ the moisture effusivity of the material. The moisture effusivity ($b_m$) is function of water vapor permeability ($\delta_p$), dry bulk density ($\rho$), specific moisture capacity ($\xi_u$) and saturation water pressure ($p_s$) of the material, and was calculated by equation (8):

$$b_m = \sqrt{\frac{\delta_p \, \rho \, \xi_u}{p_s}} \tag{8}$$

were h(α) is a function of the fraction of the time-period where the RH is high (α). In the case of the present study, α was taken as ½ with h(α)=1.073 from equation (9):

$$h_{(\alpha)} \approx 2.252[\alpha(1-\alpha)]^{0.535} \tag{9}$$

turning the equation (6) for the predicted moisture flux for application of the cycle 12/24 prescribed by ISO 24353 (2008) into equation (10):

$$MBV_{(ideal)} = 0.00605 \, b_m \Delta_p \sqrt{t_p} \tag{10}$$

Thus, the ideal MBV of the unpainted and painted (A) mortars will mostly depend on their moisture effusivity ($b_m$), meaning that, under the same testing conditions, differences of results will mainly rely on materials water vapor permeability and moisture capacity.

## 3.3.4 Results and discussion

### 3.3.4.1 Water Vapor Permeability

An increase in thickness of the air layer with equivalent water vapor diffusion of the plastering mortars and pastes introduced by the application of the paint system A (**Figure 3.13**) is overall observed. The effect of paint A is more evident for the gypsum pastes (AL70_G20, AL50_G50, G) probably due to the higher permeability of the products. Ramos *et al.* (2010) also tested gypsum and gypsum-lime (50%-50%) finishing plasters coated by 50 μm layers of both vinyl and acrylic paints. The authors observed that the coatings water vapor resistance can be influenced by the base material, consistent with the results here found. Indeed, the different influence of the same paint on plastering mortars and pastes can also be related to their different surface properties, like the surface roughness and compactness, that can lead to a different final dried thickness of the paint film.

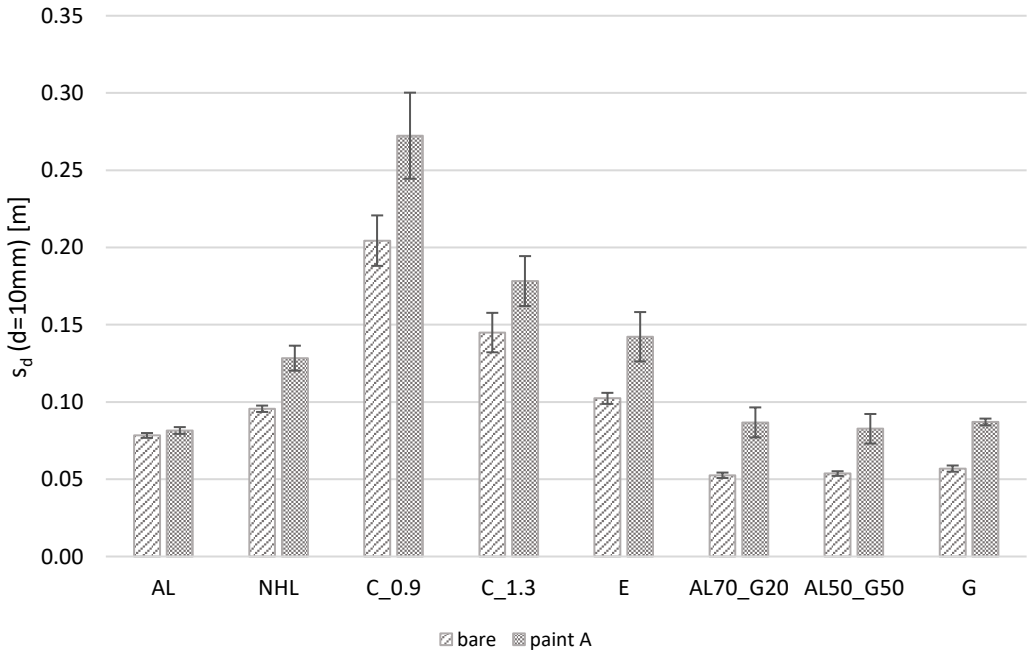


**Figure 3.13.** Thickness (m) of air layer with equivalent diffusion of water vapor for the plasters (10 mm thickness) with and without paint A application (average and standard deviation).

### 3.3.4.2 Sorption Isotherms

Sorption isotherms of the bare mortars (dashed black line), the painting system A (continuous grey line), the painting system B (only symbols, blue) and the predicted response of the painting system B (continuous blue line) are shown in **Figure 3.14**, with y axes differently scaled, according to the plaster-paint moisture content, for a better reading of results. The amount of moisture adsorbed for each RH step is calculated at steady states and, due to each thickness, the plaster is the main volume for storage. The expression of moisture content [%] is given mass by mass ($u=(m_i-m_0)/m_0$) with $m_i$ the i-th mass and $m_0$ de initial dry mass of the specimens. It is observed a difference between the two painting systems, with the paint B generally decreasing the hygroscopic behavior of the mortars, with some differences on different substrates, but bringing all the hygroscopic curves to range 0-0.5% moisture content. The paint A, instead, is overall not decreasing much the systems adsorptions.

Thus, to better analyze and quantify the moisture storage capacity of paint A, three applications on sheet glass were prepared to be dynamically tested at moisture buffering (ISO 24353:2008). The MBV of the paint A (calculated according to Rode at al., 2005) was found 0.06 ± 0.013 g/($m^2$·RH%) which still shows a hygroscopic response of the paint itself even if very small. This little moisture storage capacity of paint A combine with the little increase introduced by the same paint in the system thickness of equivalent air layer, probably contributed to the adsorption and desorption of the system.

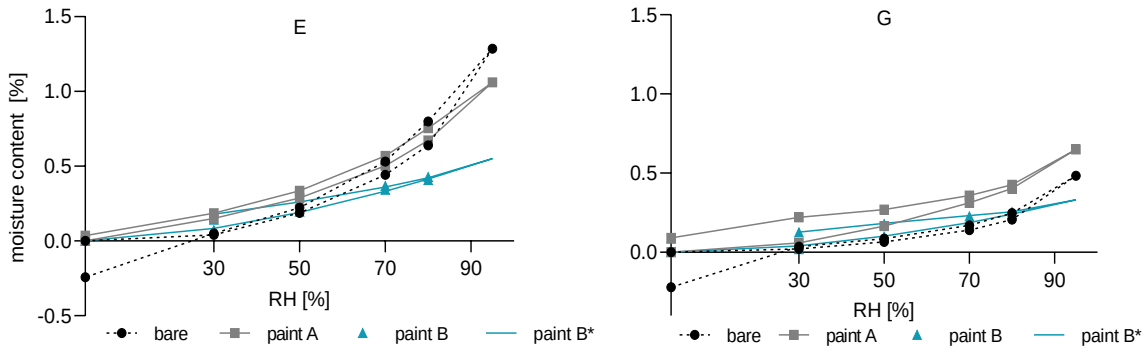

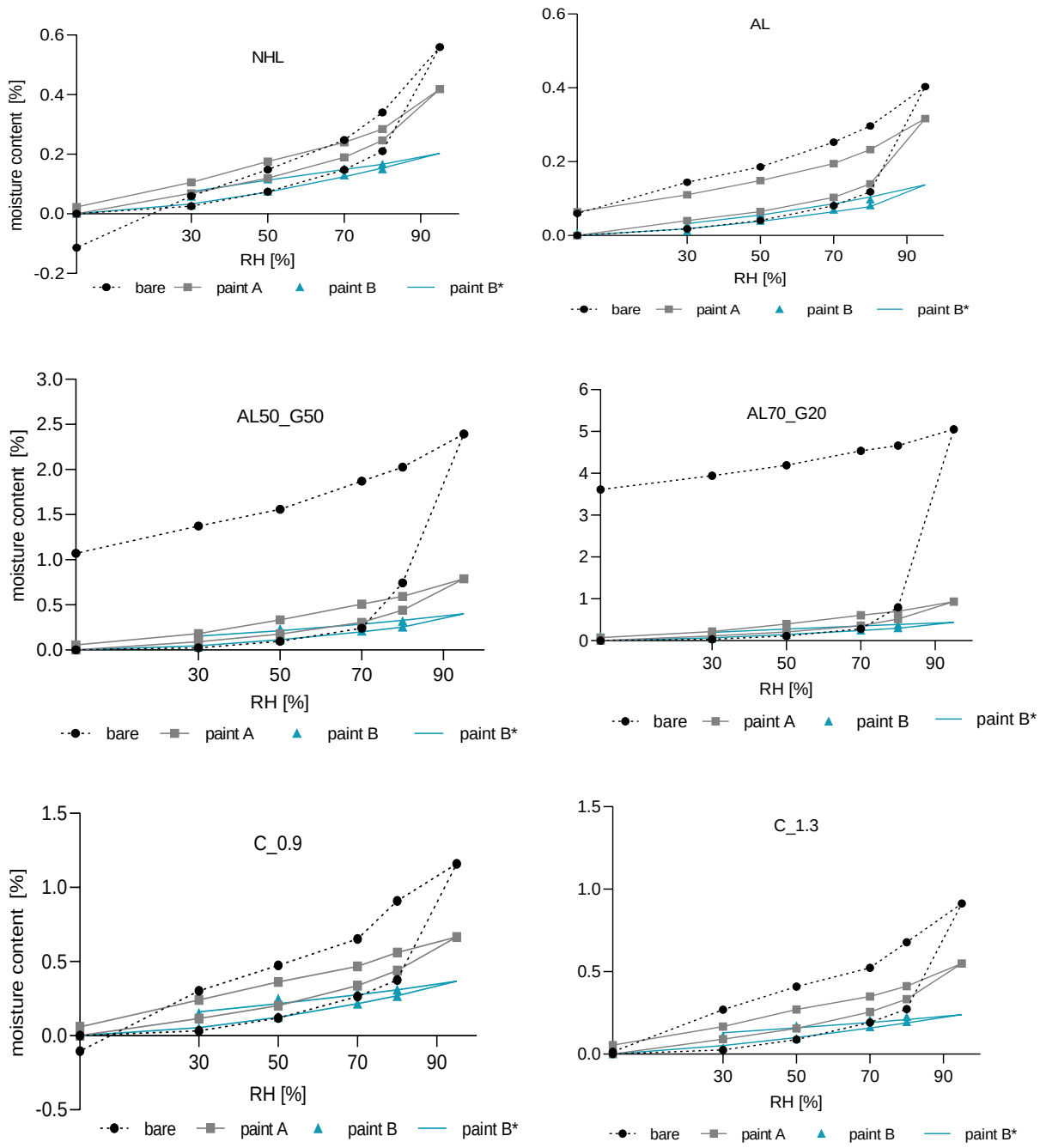


**Figure 3.14.** Sorption isotherms 0% -95% RH. In black (dashed) the bare mortars, in grey (continuous) the plasters + paint A, in blue (only symbols) the plasters + paint B and in blue (continuous) the predicted curves for plasters + paint B (*).

On desorption the effect of paint system A is also quite good, with a decrease of the hysteresis in the plastering pastes and, overall, a diminishment of the distance between the adsorption and the desorption curves. A small amount of residual moisture is introduced by paint A for mortars G, NHL, C_0.9, all showing without painting a negative moisture content when dried at the end of the test. It is supposed here that these mortars, and mortar E, were not completely

dried when the test started, so the $m_0$ accounted for calculation is higher than the real dry mass (final one). Nevertheless, the test was performed according to the standard (ISO ISO12571, 2013) and the dry specimens reached equilibrium before being moved to the climatic chamber to start the RH steps. The supposed real starting mass, lower than the one used here, would have brought to calculate higher values of moisture content for each RH step, in adsorption and desorption. It is reasonable, thus, to expect that with these corrections (the use of the final dried mass as $m_0$), the effect of the paint system A would have a different relative effect (**Figure 3.15**) on the plasters, with the corrected curves of bare coatings in adsorption always above the adsorption curve of the mortars with the application of paint A.

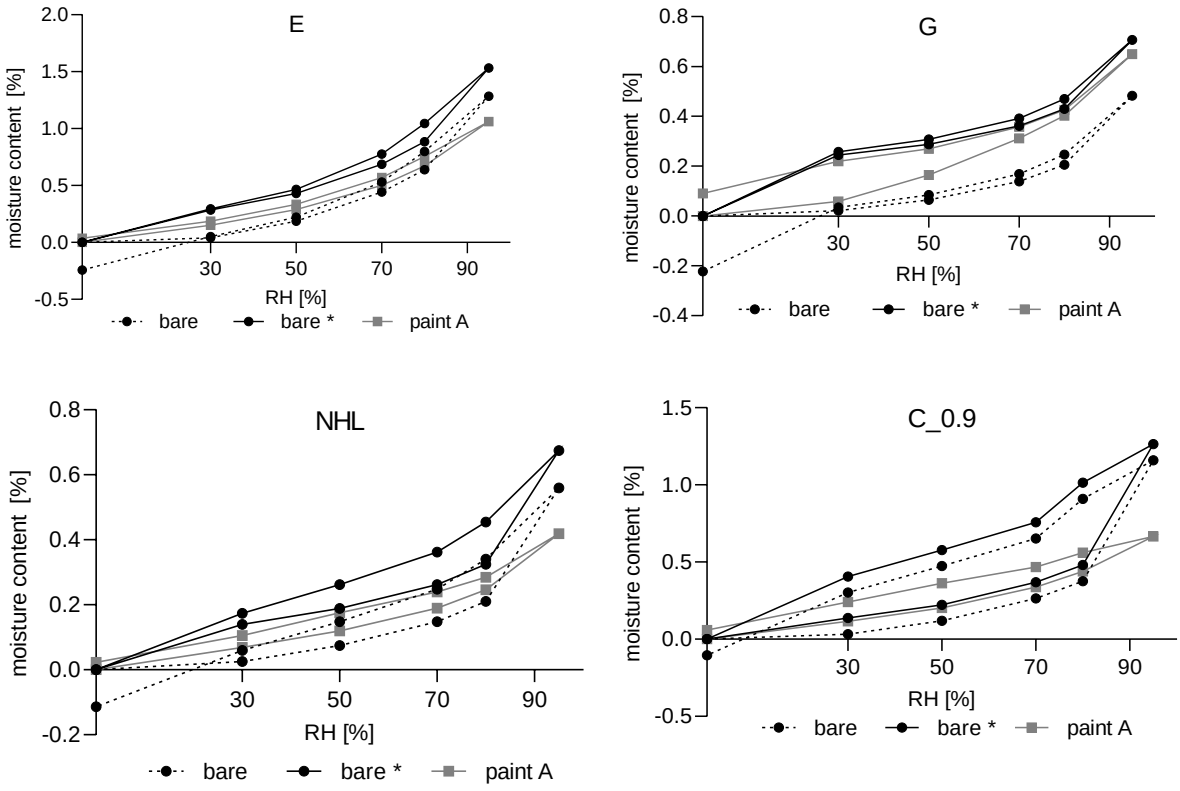


**Figure 3.15.** Correction factor (*) applied on the sorption isotherms for mortars based on: E – earth, G – gypsum, NHL – Natural Hydraulic Lime, C_0.9 – cement.

Nevertheless, the slope of the curves of the painted and unpainted specimens, needed for the calculation of the moisture penetration depth and the theoretical MBV, resulted quite similar.

#### 3.3.4.3 Moisture Penetration Depth

The moisture diffusivity ($D_w$) of the plasters was calculated according to equation (3). The saturation vapor pressure calculated according to equation (4) at the temperature of 23°C was found equal to 2807.81 Pa. The moisture storage capacity ($\xi_u$) was obtained from the sorption

curve although, as evidenced by McGregor et al. (2014) and by Roels and Janssen (2006), the non-linearity of the hygric properties represents a challenge for the determination. The same authors (McGregor et al., 2014; Roeals and Janssen, 2004) suggest considering the middle range of RH, excluding the sharpest segments of the slopes. Thus, the range of RH 50-70% of the adsorption curves, was considered to calculate the moisture storage capacity of each plaster, also consistent with the moisture buffering testing conditions selected with the RH step 50-75%. Results (**Table 3.13**) of moisture penetration depth for the bare clay plaster for $d_{p,1\%}$ and $d_{p,1/e}$ are 37 mm and 8 mm, respectively, for a calculated diffusivity of 2.379 $E^{-9}$ $m^2/s$. A similar result was found by Maskell et al. (2018) for an earthen plaster, with calculated moisture penetration depth at 1% and 1/e, respectively 57 mm and 12 mm. When polyvinyl paint A is applied, the moisture diffusivity decreases together with the water vapor permeability. The diffusivity when the clay plaster is painted, in fact, decreases to 2.0521 $E^{-9}$ $m^2/s$ and the penetration depth, according to one model or the other, is found equal to 35 mm and 8 mm.

**Table 3.13.** Synthesis of results for calculated moisture penetration depth of the bare and with paint A mortars.

| **Plaster** | $d_{real}$ | $D_w$ [$m^2/s$] | | $d_{p,1\%}$ [mm] | | $d_{p,1/e}$ [mm] | |
|---|---|---|---|---|---|---|---|
| | [mm] | Bare | Paint A | Bare | Paint A | Bare | Paint A |
| E | 22 | 2.379E-09 | 2.051 E-09 | 37 | 35 | 8 | 8 |
| AL | 23 | 1.993 E-08 | 2.001 E-08 | 108 | 108 | 23 | 23 |
| NHL | 20 | 8.442 E-09 | 6.625 E-09 | 70 | 62 | 15 | 13 |
| C1.3 | 21 | 3.865 E-09 | 2.425 E-09 | 48 | 38 | 10 | 8 |
| C0.9 | 22 | 1.895 E-09 | 2.108 E-09 | 33 | 35 | 7 | 8 |
| AL70_G20 | 21 | 1.161 E-08 | 7.983 E-09 | 82 | 68 | 18 | 15 |
| AL50_G50 | 22 | 1.331 E-08 | 9.674 E-09 | 88 | 75 | 19 | 16 |
| G | 21 | 2.488 E-08 | 8.170 E-09 | 121 | 69 | 26 | 15 |

Notation: $D_w$ – moisture diffusivity ($m^2/s$); $d_{p,1\%}$ and $d_{p,1/e}$ – moisture penetration depth (mm); binders: E – earth; AL – air lime; NHL – natural hydraulic lime; C – cement; G – gypsum.

It is evident that, according to both models, the decrease in MPD of the mortars with the application of paint A is very small, probably having little or no consequences on their moisture buffering capacity, in case the $d_p$=1% method is followed, and then all the mortars are less thick than their calculated MPD (all the section is involved in the mechanism either with or without paint). In that case, their practical MBV could be an underestimation of the MBV the same mortars would have if their thickness was above the values $d_{p,1\%}$. If the MPD is, instead, lower than the real thickness of the specimens (according to $d_{p,1/e}$ calculations) then the

practical MBV of mortars with application of paint A would be lower than the bare mortars in some cases (like NHL) and greater in others (like C_0.9).

#### 3.3.4.4 Moisture Buffering Value

MBV resulting from the experimental campaign of bare, painted A and painted B plasters are shown in **Figure 3.16** with the limits proposed by NORDTEST (Rode et al., 2005) for buildings materials. The mortars AL, NHL and C_0.9 showed an MBV slightly higher than *limited* both with and without the application of the paint A. The MBVs of C_1.3 and G are very similar and between the *limited* and *moderate* classifications. The application of paint A seems to slightly increase their buffering capacity. The same effect is visible on the gypsum pastes AL70_G20 and AL50_G20, even if for higher values (very close to the *good* class). The *good* moisture buffering of the clay-based plaster (with the highest MBV equal to 1.41 $g \cdot m^{-2}\%RH^{-1}$), instead, is slightly reduced by the paint A application. Overall, paint system A does not seem to have a big impact on the moisture buffering of the mortars. Paint system B developed for outdoors use, instead, reduces the performances in all cases, seeming to equalize all the mortars to *negligible,* in some case *low limited* class.

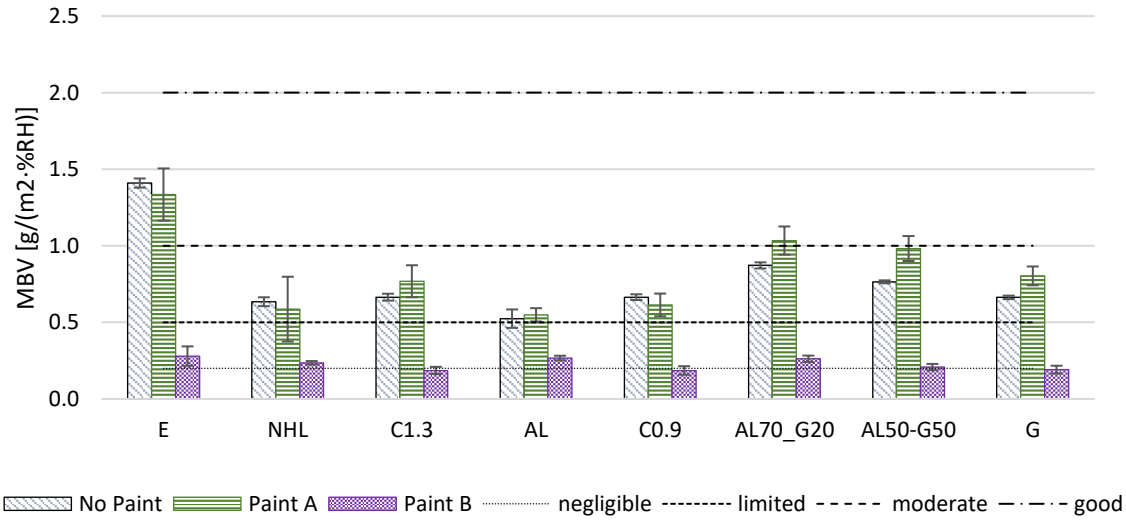


**Figure 3.16.** MBV of the plasters with and without paints (average and standard deviation) compared with limits of classes from NORDTEST (Rode et. Al, 2005).

The ideal MBV for the bare mortars and the system mortars with paint A was calculated according to equation (10). The same parameters described for the calculation of moisture penetration depth (section **3.3.3.3**) were used. Results of practical and ideal MBV (in this case only for plasters with paint A) are resumed in **Table 3.14**.

In both cases, painted A and unpainted plasters, the practical MBV obtained by the test method is lower than the theoretical MBV. This can be related to the assumptions made by the equation (6) for the calculation of the theoretical MBV, as observed by Roels and Janssen (2006), of a moisture behavior related to the square root of time when the surface film resistance is neglected, and the specimen is assumed semi-infinite. Moreover, according to results of MPD with $d_p$=1%, it is possible that the real thickness of the specimens is lower than the ideal thickness involved in the mechanism.

**Table 3.14**. Synthesis of the ideal and practical MBV according to ISO 24353 (2018) of the plasters.

| Plaster | No Paint | | Paint A | | Paint B |
|---|---|---|---|---|---|
| | MBV $_{ideal}$ | MBV $_{practical}$ | MBV $_{ideal}$ | MBV $_{practical}$ | MBV $_{practical}$ |
| **E** | 1.95 | **1.41** | 1.53 | **1.33** | **0.28** |
| **AL** | 0.88 | **0.52** | 0.85 | **0.55** | **0.27** |
| **NHL** | 1.11 | **0.63** | 0.94 | **0.59** | **0.24** |
| **C1.3** | 1.08 | **0.66** | 0.96 | **0.77** | **0.19** |
| **C0.9** | 1.10 | **0.66** | 0.92 | **0.61** | **0.19** |
| **AL70_G20** | 1.72 | **0.87** | 1.27 | **1.03** | **0.26** |
| **AL50_G50** | 1.58 | **0.76** | 1.21 | **0.98** | **0.21** |
| **G** | 1.09 | **0.66** | 1.24 | **0.80** | **0.19** |

The fact that the ideal value is found always to overestimate the real behavior of the material and that probably there are other factors affecting the moisture buffering behavior was concluded also by Maskell et al. (2018). Nevertheless, the differences between the adsorption and desorption curves of the painted A and unpainted specimens are very small, as showed in **Figure 3.17**. Considering that the tests were not run simultaneously, it seems reasonable to conclude that the application of the vinyl paint A did not strongly modify the MBV of the plasters. It seems possible, in some cases like the AL mortar, that the paint system contributed to a quicker stabilization at the quasi-steady state. Instead, the paint system B, developed for outdoors application where this is not a requirement, and just used for comparison, has a very big impact on the moisture buffer capacity of these mortars, lowering very much their response also when tested at quasi-steady states.

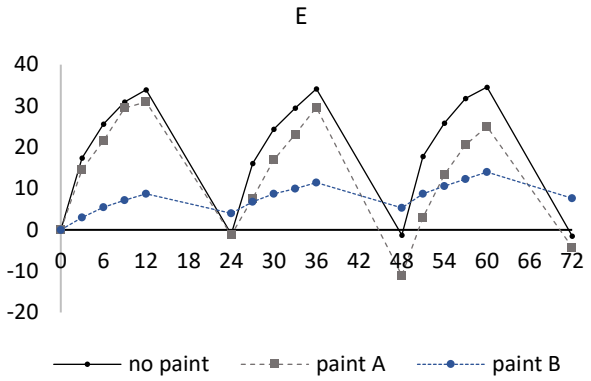
E
40
30
20
10
0
-10
-20
0 6 12 18 24 30 36 42 48 54 60 66 72
no paint
paint A
paint B

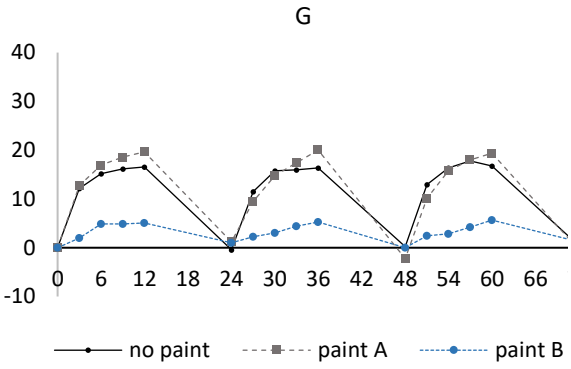
G
40
30
20
10
0
-10
0 6 12 18 24 30 36 42 48 54 60 66
no paint
paint A
paint B

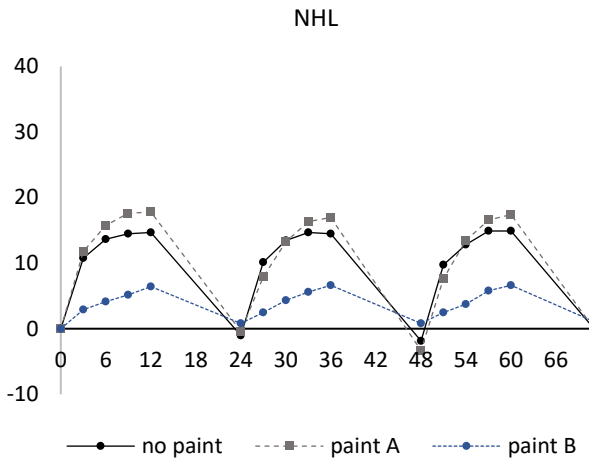
NHL
40
30
20
10
0
-10
0 6 12 18 24 30 36 42 48 54 60 66
no paint
paint A
paint B

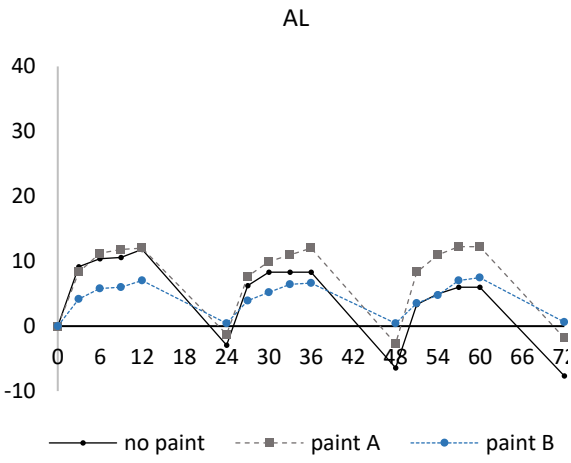
AL
40
30
20
10
0
-10
0 6 12 18 24 30 36 42 48 54 60 66
no paint
paint A
paint B

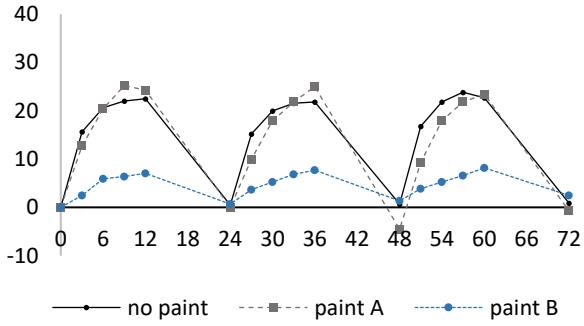
AL70_G20
40
30
20
10
0
-10
0 6 12 18 24 30 36 42 48 54 60 66 72
no paint
paint A
paint B

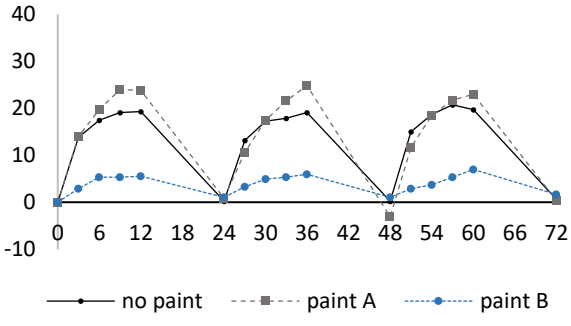
AL50_G50
40
30
20
10
0
-10
0 6 12 18 24 30 36 42 48 54 60 66 72
no paint
paint A
paint B

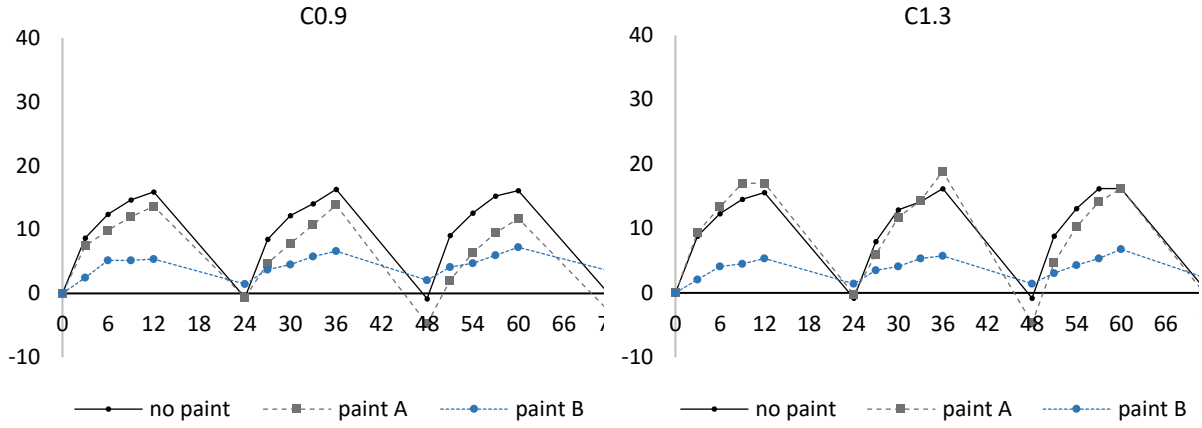


**Figure 3.17.** Adsorption/desorption curves of the last three cycles run in *middle humidity level* according to ISO 24353 (2008) over the time (hours). In blue (dashed) the painted A, in grey (dashes) the painted B and in black (continuous) the unpainted specimens.

### 3.3.5 Conclusions

Overall, the water vapor permeability (WVP) of the tested traditional and modern plastering mortars was decreased by the paint A application. The highest effect was observed for the pastes of gypsum and gypsum plus air lime (G, AL70_G20, AL50_G50) that showed the highest permeability when unpainted and the lowest surface roughness. The WVP of the clay-based plaster, which is commonly applied uncoated too to profit from aesthetics of the natural pigmentation, was also consistently reduced by the paint A application, and similar effect was observed for the NHL mortar. The C_0.9 and C_1.3, cement-based mortars commonly finished by a paint system, did not show a big decrease of WVP when an indoor paint system A was applied. The air lime was the only mortar with WVP almost not affected by the application of paint A.

The sorption isotherms of all the mortars were found very affected by the application of the paint B with a decrease in moisture content at all the RH steps when compared with bare mortars and a flatten response of all the coatings at the range 0-0.5% of moisture content. Recalling that this paint was developed for outdoors application, where hygroscopicity is not a requirement, this could be expected. Instead, the application of paint A overall has no significative effect on the static hygroscopic behavior of the plasters, with equilibrium reached at very similar moisture content than their unpainted versions. The paint A was found to have

itself some moisture capacity and, in some cases, able to smooth the hysteresis of some plasters.

The moisture penetration depth (MPD) was calculated for bare plasters and plasters with the application of the paint A system according to two different methods. The MPDs calculated are quite different, with results from the method defined for Northen European countries always above the real thickness of the specimens, and results from the second method almost always below or equal to them. According to the results from moisture buffering values (MBV), paint A has some effects on the moisture buffering of the plasters, suggesting that the second method is more suitable for the studied coatings. Nevertheless, according to both calculation methods, the MPD of the plasters is only slightly reduced by the paint A application.

The practical MBV results confirm the different effects of the two painting systems, with the very small influence of paint A on the moisture buffering of plasters and the large reduction introduced by paint B. The ideal MBV always overestimated the real moisture buffering of plasters, as already observed by other authors, probably because it is modelled on specimens with thicker penetration depths ($d_{p,1\%}$) or specimens assumed as semi-infinites, for instance.

The present study shows that two different water-based paints and different formulations (A with a polyvinyl acetate binder and B with an acrylic binder) and different in use destinations (A for indoors and B for exterior surfaces) have very different effects on the coatings. The indoor paint lowers the WVP of almost all the mortars (showing more effect on some types than on others) and has very small effects on their hygroscopic behavior both under dynamic and static conditions. The exterior painting system B, instead, significantly reduces the same hygroscopic behavior. Finally, with the present knowledge, it seems difficult to determine in advance if a paint system would significantly affect the moisture buffering of plastering mortars and pastes without testing the specific painting system. But overall, it seems possible that an optimization of indoor paint formulations is being carried out to not jeopardize the potential passive moisture contribution of the system plaster-paint to indoor comfort.

## Acknowledges

This research was supported by Portuguese Foundation for Science and Technology (FCT-Fundação para a Ciência e a Tecnologia): PD/BD/150399/2019 – 1st author Doctoral Training Program EcoCoRe. The authors are also grateful for FCT support through funding UIDB/04625/2020 of the research unit CERIS. The authors would like to thank the National Laboratory for Civil Engineering of Portugal (LNEC) for the laboratory equipment and the support provided through the projects REuSE - Wall coverings for Rehabilitation: Safety and

Sustainability and RevBar – Polymeric based barrier coatings: functionality and sustainability and the Department of Civil Engineering of the NOVA School of Science and Technology of the NOVA University Lisbon.

## References

Arundel AV, Sterling EM, Biggin JH, Sterling TD. Indirect health effects of relative humidity in indoor environments. Environmental Health Perspectives. 1986; 65: 351-61.

Ashour T, Georg H, Wu W. An experimental investigation on equilibrium moisture content of earth plaster with natural reinforcement fibres for straw bale buildings. Applied Thermal Engineering. 2011; 31(2–3): 293-303. https://doi.org/10.1016/j.applthermaleng.2010.09.009.

Cascione V, Maskell D, Shea A, Walker P, Mani M. Comparison of moisture buffering properties of plasters in full scale simulations and laboratory testing. Construction and Building Materials. 2020; 252: 119033. https://doi.org/10.1016/j.conbuildmat.2020.119033.

EN 1062-1:2004. Paints and varnishes - Coating materials and coating systems for exterior masonry and concrete - Part 1: Classification. CEN, Brussels, Belgium.

EN 1936: 2006. Natural stone test methods - Determination of real density and apparent density, and of total and open porosity. CEN, Brussels, Belgium.

Fang L, Clausen G, Fanger P O. Impact of temperature and humidity on the perception of indoor air quality. Indoor Air. 1998; 8: 80-90. DOI: 10.1111/j.1600-0668.1998.t01-2-00003.x.

Ferreira C, de Freitas V P, Delgado J M P Q. The influence of hygroscopic materials on the fluctuation of relative humidity in museums located in historical buildings. Studies in Conservation. 2020; 65(3): 127-141. https://doi.org/10.1080/00393630.2019.1638666.

Frey S E, Destaillats H, Cohn S, Ahrentzen S, Fraser MP. The effects of an energy efficiency retrofit on indoor air quality. Indoor Air. 2015; 25: 210-219. https://doi.org/10.1111/ina.12134.

Guarnieri G, Olivieri B, Senna G, Vianello A. Relative humidity and its impact on the immune system and infections. *International Journal of Molecular Sciences*. 2023; 24(11):9456. https://doi.org/10.3390/ijms24119456.

Hansen K K. Sorption Isotherms: A Catalogue. Technical Report 162/86. Technical University of Denmark (Eds). 1986.

ISO 10456: 2007. Building materials and products Hygrothermal properties — Tabulated design values and procedures for determining declared and design thermal values. ISO, Geneva, Switzerland.

ISO 12571: 2013. Hygrothermal performance of building materials and products — determination of hygroscopic sorption properties. ISO, Geneva, Switzerland.

ISO 12572:2016. Hygrothermal performance of building materials and products — Determination of water vapour transmission properties — Cup method. ISO, Geneva, Switzerland.

ISO 7783: 2018. Paints and varnishes - Determination of water-vapour transmission method – cup method. ISO, Geneva, Switzerland.

ISO 2808: 2019. Paints and varnishes — Determination of film thickness. ISO, Geneva, Switzerland.

ISO 24353: 2008. Hygrothermal performance of building materials and products - Determination of moisture adsorption/desorption properties in response to humidity variation. ISO, Geneva, Switzerland.

Jones AP. Indoor air quality and health. *Atmos. Environ.* 1999; *33*: 4535–4564. https://doi.org/10.1016/S1352-2310(99)00272-1.

Li X, Ran M. Gypsum-based humidity-control material: preparation, performance and its impact on building energy consumption. Materials. 2023; 16:5211. https://doi.org/10.3390/ma16155211.

Liuzzi S, Rubino C, Stefanizzi P, Petrella A, Boghetich A, Casavola C, Pappalettera G. Hygrothermal properties of clayey plasters with olive fibers. Construction and Building Materials.2018; 158: 4-32. https://doi.org/10.1016/j.conbuildmat.2017.10.013.

McGregor F, Heath A, Fodde E, Shea A. Conditions affecting the moisture buffering measurement performed on compressed earth blocks. Building and Environment. 2014; 75: 11-18. DOI: 10.1016/j.buildenv.2014.01.009.

Maskell D, Thomson A, Walker P, Lemke M. Determination of optimal plaster thickness for moisture buffering of indoor air. Building and Environment. 2018; 130: 143–150. DOI: 10.1016/j.buildenv.2017.11.045.

Osanyintola OF, Simonson CJ. Moisture buffering capacity of hygroscopic building materials: Experimental facilities and energy impact. Energy and Buildings. 2006; 38: 1270–1282. DOI: 10.1016/j.enbuild.2006.03.026.

Padfield T. Humidity buffering of the indoor climate by absorbent walls. In 5th Symposium on Building Physics in the Nordic Countries, 2, 637–644. 1999.

Pederneiras C, Veiga R, de Brito J. Rendering mortars reinforced with natural sheep's wool fibers. Materials. 2019; 12: 3648. DOI: 628 10.3390/ma12223648.

Ramos NMM, Delgado JMPQ, de Freitas VP. Influence of finishing coatings on hygroscopic moisture buffering in building elements. Construction and Building Materials. 2010; 24: 2590–2597. DOI: 10.1016/j.conbuildmat.2010.05.017.

Randazzo L, Montana G, Hein A, Castiglia A, Rodonò G, Donato DI. Moisture absorption, thermal conductivity and noise mitigation of clay based plasters: The influence of mineralogical and textural characteristics. Applied Clay Science. 2016; 132–133: 498-507. https://doi.org/10.1016/j.clay.2016.07.021.

Ranesi A, Veiga R, Faria P. Traditional and Modern Plasters for Built Heritage: Suitability and Contribution for Passive Relative Humidity Regulation. Heritage. 2021a; 4: 2337–2355. DOI: 10.3390/heritage4030132.

Ranesi A, Faria P, Veiga R. Laboratory characterization of relative humidity dependant properties for plasters: a systematic review. *Construction and Building Materials.* 2021b; 304: 124595. https://doi.org/10.1016/j.conbuildmat.2021.124595.

Rode C, Peuhkuri RH, Mortensen LH, Hansen KK, Time B, Gustavsen A, Ojanen T, Ahonen J, Svennberg K, Harderup LE, Arfvidsson J. Moisture buffering of building materials. Technical University of Denmark, Department of Civil Engineering. BYG Report, R-127. 2005.

Roels S, Janssen H. A comparison of the Nordtest and Japanese test methods for the moisture buffering performance of building materials. J Build Phys. 2006; 30:137. DOI: 10.1177/174425910606810.

Santos T, Gomes M I, Santos Silva A, Ferraz E, Faria P. Comparison of mineralogical, mechanical and hygroscopic characteristic of earthen, gypsum and cement-based plasters. Construction and Building Materials. 2020; 254: 119222. https://doi.org/10.1016/j.conbuildmat.2020.119222.

Woods J, Winkler J, Christensen D. Evaluation of the effective moisture penetration depth model for estimating moisture buffering in buildings. United States. 2013. Web. https://doi.org/10.2172/1067948.

UNEP-SBCI. Buildings and Climate Change, Summary for Decision-Makers, Sustainable Buildings and Climate Initiative, Paris. 2009.

Wolkoff P. Indoor air humidity, air quality, and health – An overview. International Journal of Hygiene and Environmental Health. 2018; 221: 376-90. DOI: 10.1016/j.ijheh.2018.01.015.

Zhang M, Qin M, Rode C, Chen Z Moisture buffering phenomenon and its impact on building energy consumption. Applied Thermal Engineering. 2017; 124: 337-345. DOI: 10.1016/j.applthermaleng.2017.05.173.

## 3.4 Additional Considerations

The relative humidity dependent properties of traditional and modern binder-based plasters were analyzed and quantified through the study 3.2. A table of synthesis of these with a comparison of ranges based on the literature review (**Table 2.11.** Synthesis of results for mortars RH dependent properties from literature.**Table 2.11**) is presented in **Table 3.15**.

**Table 3.15.** Synthesis of results for adsorption at 95% RH, WVP and MBV from laboratory characterization compared with ranges found in literature (**Table 2.11**).

| Property | | E | E* | AL | AL* | G | G* | G-AL | G-AL* | CE | CE* | NHL |
|---|---|---|---|---|---|---|---|---|---|---|---|---|
| Adsorption [%] at 95% RH | max | 1.29 | 6.30 | 0.40 | 10 | 0.48 | 3.10 | 5.05 | 0.98 | 1.16 | - | 0.56 |
| | min | | 0.10 | | 0.03 | | 0.08 | 2.39 | 0.16 | 0.91 | | |
| MBV [g/(m$^2$·%RH)] | max | 1.49 | 3.3 | 0.42 | 1.64 | 0.61 | 0.95 | 1.27 | 0.47 | 0.84 | 0.30 | 0.80 |
| | min | | 0.93 | | 0.67 | | 0.33 | 1.03 | 0.42 | 0.82 | | |
| WVP E[11] [kg/(m·Pa·s)] | max | 2.15 | 7.60 | 2.63 | 6.50 | 3.55 | 2.92 | 3.77 | 2.89 | 1.35 | 1.40 | 2.09 |
| | min | | 0.8 | | 0.48 | | 2.06 | 3.74 | 1.36 | 0.95 | 0.49 | |

Notation : MBV - moisture buffering value; WVP – water vapour permeability; E – clay; AL – air lime; G – gypsum; CE– cement; NHL – natural hydraulic lime 3.5; * - range found in literature; in green results from the laboratory characterization higher than the range from literature.

It is difficult to compare different plasters, even when based on the same binder, considering the many parameters that could change from a production to another (the binder/aggregate ratio, the binder/water ratio, the type of binder, the shape, size, and mineralogy of the aggregates, etc.). More variables would enter the equation if the plaster was based on more than one binder, e.g., the case of calcium sulfate hemihydrate and calcium hydroxide (G-AL), and it is necessary to take into account also proportions between the two binders than could differ. Indeed, the formulations of the G-AL plasters analyzed in the study 3.2 are 70% of hydrated lime, 20% of gypsum, 10 % of calcitic aggregate (< 45 µm) and 50% of hydrated lime and 50% of gypsum. Both the plasters were obtained with small additions of water-retaining agents (0.1%) and set retarder (0.02%) to assess a required workability (Freire et al., 2021). Results from laboratory characterization point out an important enhancement (with values higher than the ones found in literature) of the hygroscopic behavior of combined gypsum and air lime by comparison to any of the single binders (even if with an important hysteresis). Nevertheless, even if the specimens were aged several years at the time of the tests, their complete carbonation was not checked and verified, and further studies are needed to quantify the effect of completely carbonated air lime on the hygroscopic behavior of gypsum-based plasters. The gypsum plaster has high water vapor permeability; thus, a high moisture

penetration depth (MPD) with a thick portion of the upper layer (closer to the indoor air) interested by the moisture adsorption/desorption mechanism would be expected. Indeed, the MPD of the gypsum paste was calculated in section 3.3 and found the highest among all the plasters. Hence, either under dynamic (MBV) or static (sorption isotherms) conditions, its reactivity to moisture fluctuations was expected to be higher than the one found out. The next chapter (4) will deeply explore the gypsum-based plaster and present solutions for a possible enhancement of its moisture regulation. Moreover, from section 3.3 the effect of the application of paint systems on the same bare mortars on these properties related the most to RH fluctuations (sorption isotherms, water vapor permeability and moisture buffering) was analyzed and discussed. In a realistic scenario of common application, these plasters could be coated with a vinylic paint for indoors and, for comparison, in a less realistic but still possible scenario, with an acrylic paint for outdoors. Consistent differences were found. Paint A formulated for indoors undermines only a little the moisture behavior of the plasters, and after its application a different behavior between different binder-based plasters is still observed. Paint B for external applications, instead, probably formulated and optimized to perform a more protective role to weathering, removes the differences of moisture behavior between plasters and has a sealing effect, bringing the MBV of all of them close to 0.2 $g \cdot m^{-2}\%RH^{-1}$(for the clay-based plaster reduced from 1.41 $g \cdot m^{-2}\%RH^{-1}$ and for the gypsum-air lime pastes from ≈ 0.8 $g \cdot m^{-2}\%RH^{-1}$).

# 4
# GYPSUM-BASED PLASTERS

## 4.1 Preamble

Results from the study on the relative humidity dependent properties (section 3.2) raised some doubts about the hygroscopic behavior of gypsum plastering mortars. At the same time these mortars are very often used to coat indoor walls and ceilings as much in historic, traditional constructions as in new designs. The MBV of building materials, especially when directly exposed to indoor air in large areas, can be a key factor for indoor passive regulation of relative humidity and, consequently, comfort improvement without energy consumption increase. For this reason, the present chapter is focused on the enhancement of hygroscopic behavior of gypsum mortars. The purpose to improve their MBV was combined with the intent of reusing a second-generation biowaste from pharmaceutical and cosmetic industry, without increasing the carbon footprint of the mortar. The *Acacia dealbata* is an invasive plant, native of Australia, very competitive with the local flora (allelopathic capacity) and with a high dispersion capacity in burnt environment. The addition of this biomass slightly increases the volume of plaster produced with the same amount of binder, decreasing the embodied energy of the plaster and, at the same time, reducing the volume of biowaste to manage; overall, turning the industry value-chain and the plasters more eco-efficient.

The biomass by-product (after recovery of extractives) consists in five different fractions of the same plant, the *Acacia dealbata*: Fl - flowers; Le - leaves; Br - branchlets; Wo - wood; Ba - bark. After minimal treatments (milling and sieving) the fractions were added to mortars formulations in two different percentages: 5% and 10% by vol. of a powder premixed gypsum-based plastering mortar product. The use of ashes from *A. dealbata* was discarded due to the doubts raised in literature on its use for energy production. The *Acacia*, in fact, has a high chlorine content (0.04%) (Nunes et al., 2020), low thermal efficiency (seven times lower than

*Pinus*) and its combustion generates high emission of contaminants in gaseous form (CO, $SO_2$ and $NO_x$) and particle matter ($PM_{10}$) (Ferreira et al., 2014; Vicente et al., 2019). That is why alternative uses for this biomass are important to avoid burning.

The fresh state and mechanical properties (section 4.2), capillary water adsorption, drying and hygroscopic behavior (section 4.3) of the gypsum-biomass plasters are presented. The aim of the studies is to evaluate the new plastering mortars formulation, ensure that they meet the requirements for gypsum plasters and quantify - when possible - improvements and drawbacks.

## 4.2 Article C1 - Enhancement of Gypsum Mortar: fresh state and mechanical characterization

(the article has been published in the journal *Buildings* 2022, 12 (3), 339; https://doi.org/10.3390/buildings12030339)

### Gypsum Mortars with *Acacia dealbata* Biomass Waste Additions: Effect of Different Fractions and Contents

### Abstract

In recent decades, interest in the eco-efficiency of building materials has led to numerous research projects focused on the replacement of raw materials with mineral and biomass wastes, and on the production of mortars with low-energy-consuming binders, such as gypsum. In this context, five different fractions (bark, wood, branchlets, leaves, and flowers) of *Acacia dealbata*—an invasive species—were evaluated as fillers for premixed gypsum mortars, at 5% and 10% (vol.) addition levels and fixed water content. Although these biomass fractions had different bulk densities (>50% of variation), all the mortars were workable, although presenting different consistencies. As expected, dry density decreased with biomass addition, but, while mortars with addition at 5% presented a slight shrinkage, a slight expansion occurred with those with 10% addition. Generally, the mechanical properties decreased with the biomass additions even if this was not always proportional to the added content. The wood fraction showed the most positive mechanical results but flexural and compressive strengths of all the tested mortars were found to be higher than the lower standard limit, justifying further studies.

### Keywords

Bio-based mortars; invasive species; biomass additions; bio-composites; by-products; agro-industrial wastes; density; dimensional variation; mechanical properties; pore structure.

#### 4.2.1 Introduction

In recent years many findings have been made on the effects of indoor relative humidity and temperature on human health [1–3]. It is common knowledge that an intermediate range of relative humidity (RH) can prevent airway and ocular irritations in various diseases [4,5] and is often related to thermal comfort in free-running buildings [6] when adaptive models are considered [7].

Plastering mortars usually cover large indoor surfaces and, thus, can contribute to passively equilibrating indoor relative humidity improving occupants' comfort and, in some cases, health.

To provide that contribution, they have to be highly hygroscopic, adsorbing and desorbing moisture from and to the indoor air.

Gypsum plasters are broadly used to coat (plaster) indoor walls and ceilings as they appear to be an appropriate option not only in new construction but also in many restoration interventions [8]. Moreover, hemihydrate gypsum binder is produced at around 120–180 °C, having a much lower firing temperature and milling energy for production than other binders, i.e., cement (around 1500 °C) or air lime (around 900 °C). Thus, the associated low embodied energy makes gypsum plasters a sustainable solution. However, among common plastering mortars, gypsum-based mortars present very low hygroscopicity [9–11]. Although not studied in the present work, it is probable that the moisture buffer capacity of gypsum plasters may be improved with the addition of hygroscopic materials.

Nonetheless, the eco-efficiency of building products can be increased by addition of wastes and the replacement of raw materials [12,13]. Among these wastes, agro-industrial wastes can be used in the production of eco-products for construction [14] with the purpose of enhancing relevant physical and chemical properties, such as bulk density, thermal conductivity, and the hygric and hygroscopic behavior of those products, while creating useful applications for various biomass wastes [15–19]. Actually, as biomass is usually hygroscopic, it is expected that they may improve gypsum plasters hygroscopicity. However, in comparison to cement-based mortars [20–22], studies on the effects of the incorporation of agro-industrial wastes in gypsum-based mortars are rare.

Acacia species mostly originated in Australia but have spread all over the world and have become invasive due to their high capacity for growth, seed production, and seed germination, which can be active for several years. Their selective removal is not economically viable if added-value applications are not found for the collected biomass. The use of biomass collected in forest environments contributes to reducing the danger of forest fires [23,24] and, in the case of invasive species, may constitute a method of propagation control since it disrupts the reproductive cycle, namely by preventing seed formation [25].

Use of Acacia wastes in plaster formulations was not found in literature although applications of Acacia biomass in composite materials have been described by some authors [26,27]. Also, some fractions of the plant have already been used in other sectors, namely bark as a source of tannins for the leather industry [28] or flowers used to produce absolute oils for the perfume industry [29]. Other fractions of Acacia biomass have traditionally been used as a source of bioactive components for folk medicines [30]. After recovery of these functional extractives,

the biomass still retains most of its lignocellulosic components, keeping its potential to be used in energy production or material applications.

The aim of the present study was to assess if the addition of different fractions and contents of *Acacia dealbata* biomass to gypsum plastering mortars jeopardizes the common fresh-state properties of the mortars or their mechanical properties in order to discard formulations which do not meet the requirements for further studies related to hygroscopicity. Hence, five different fractions of the same plant (*Acacia dealbata*) were selected and added to a gypsum premixed mortar (5% and 10% vol.) after the recovery of extractives for other applications. Although the premixed product is based on a low embodied energy binder, such as hemihydrate gypsum, the addition of biomass reduces the consumption of raw materials needed to produce it, reducing the environmental impact of the plasters. Nevertheless, it is important to confirm if the addition require a higher consumption of water to present adequate workability and comply with the mechanical requirements for gypsum-based plastering mortars.

## 4.2.2 Materials and methods

### 4.2.2.1 Materials

A premixed industrial powder product (GP), Sival Reabilita, produced by the company Sival, in Portugal was selected for the study. This product is based on gypsum, mineral fillers, and admixtures and is ready to mix with water for manual application in interior walls and ceilings. It complies with EN 13279-1 [31], type B1/20/2 and can be used to plaster old indoor walls as well as new ones.

Five different *Acacia dealbata* fractions were selected to be incorporated in the mortar formulations: flowers (Fl), leaves (Le), branchlets (Br), wood (Wo), and bark (Ba). The biomasses were collected in the regions of Alcobaça and Caparica (Central Portugal), from at least ten different trees at each location. The fractions were milled, sieved to 2 mm, and macerated in acetone, at 25 °C, to recover extractives that could be valorized in various applications, such as nutraceutical products. The extracted biomasses were air-dried at 25 °C for 48 h and characterized for loose bulk density and color coordinates according to the CIELab color system before use in the mortar preparations. Instrumental color was determined using a colorimeter (CHROMA METER CR-410, Tokyo, Japan), calibrated using a standard white reflector plate. The visual observation of the *A. dealbata* fractions at the time of the mortar production is presented in **Figure 4.1**, and **Table 4.1** presents their loose bulk density and color parameters.

(a) (b) (c) (d) (e)

**Figure 4.1.** *Acacia dealbata* fractions: (**a**) wood, (**b**) branchlets, (**c**) leaves, (**d**) flowers, and (**e**) bark.

**Table 4.1.** Loose bulk density and color coordinates of *Acacia dealbata* fractions.

| *A. dealbata* Fraction | Loose Bulk Density (g/cm$^3$) | Color (CIELB Coordinates) | | |
|---|---|---|---|---|
| | | L* | a* | b* |
| Wood | 0.211 | 65.58 | 0.68 | 18.94 |
| Branchlets | 0.378 | 59.11 | 1.31 | 17.51 |
| Leaves | 0.415 | 34.97 | 0.59 | 11.04 |
| Flowers | 0.217 | 35.33 | 8.50 | 11.39 |
| Bark | 0.435 | 43.19 | 7.58 | 12.85 |

A decrease in the luminosity parameter L* observed for leaves and flowers indicates darker colors. Although fresh Acacia flowers had a light yellow color, the process of solvent extraction and drying, promotes oxidation reactions that result in a brownish darker color. Low values of a* indicate an increase of the green component, an effect that was more evident for leaves and wood. The yellow component was higher for the biomass fraction with higher b* values, namely wood and branchlets. These different colors of the biomasses can influence the color of the mortars and are important if the plasters have no finishing layer. The loose bulk density of the factions varied up to 51% from the denser bark fraction to the lighter wood one.

#### 4.2.2.2 Mix Design

The selected fractions of *A. dealbata* were added to the GP, at 0% (reference mortar), 5%, and 10% by volume, and manually homogenized. Additions of constant volumes of all the different fractions were made so that the physical changes were comparable. The mass for exact incorporation of each fraction (**Table 4.2**) was calculated according to the loose bulk density of each biomass (**Table 4.1**).

The powder mix was added to water for 1 min using the sprinkling method, left to soak for another minute, and then mechanically mixed for 1 min (**Figure 4.2**). A volumetric ratio of 1:3 (water:GP) corresponding to a ratio by mass of 0.45, was kept for all the mortars (**Table 4.2**).

**Table 4.2.** Composition of the mortars and flow table consistence.

| Mortar | *Acacia* Fraction | Addition (vol, %) | Addition (Mass, g) | Flow (mm) |
|---|---|---|---|---|
| REF | – | – | – | 163.0 |
| Fl5 | Flowers | 5 | 32.6 | 163.0 |
| Le5 | Leaves | 5 | 62.2 | 168.5 |
| Br5 | Branchlets | 5 | 56.7 | 171.3 |
| Wo5 | Wood | 5 | 31.7 | 160.3 |
| Ba5 | Bark | 5 | 65.2 | 175.5 |
| Fl10 | Flowers | 10 | 65.3 | 165.5 |
| Le10 | Leaves | 10 | 124.4 | 156.5 |
| Br10 | Branchlets | 10 | 113.5 | 171.0 |
| Wo10 | Wood | 10 | 63.3 | 165.3 |
| Ba10 | Bark | 10 | 130.4 | 165.0 |

(**a**) (**b**) (**c**)

**Figure 4.2.** Mortar preparation: (**a**) sprinkling method, (**b**) soaking, and (**c**) mechanical mix.

#### 4.2.2.3 Specimens and Methods

In **Figure 4.3** a flowchart is presented to resume the experimental steps.

The fresh mortars were tested for consistency using the flow-table method, determined based on EN 13279-2 [32] at a fixed amount of water. The fresh-state density was determined based on EN 1015-6 [33]. For the hardened mortars, a minimum of five standardized prismatic specimens (160 mm × 40 mm × 40 mm) were produced for each formulation and the following properties were determined:

- Volumetric shrinkage—determined using a digital caliper.
- Apparent bulk density—based on EN 1015-10 [34]—geometrically determined using a digital caliper and a balance with 0.001 g resolution.
- Flexural and compressive strengths—based on EN 1015-11 [35]—using an electromechanical testing device from Microtest, model EM1/100/FR. The loading rates were adjusted so that failure occurred within a period of 10–25 s for flexural strength and

30–90 s for compressive strength. Load cells of 2 kN and 200 kN were used, depending on the mechanical strength of the material (**Figure 4.4**).

- Dynamic modulus of elasticity—based on EN 14146 [36]—by resonance frequency using a Zeus ZRM equipment.
- Optical microscope observation—using an Olympus SZH-10 stereo microscope.
- Open porosity—based on EN 1936 [37]—by vacuum and hydrostatic weighing.

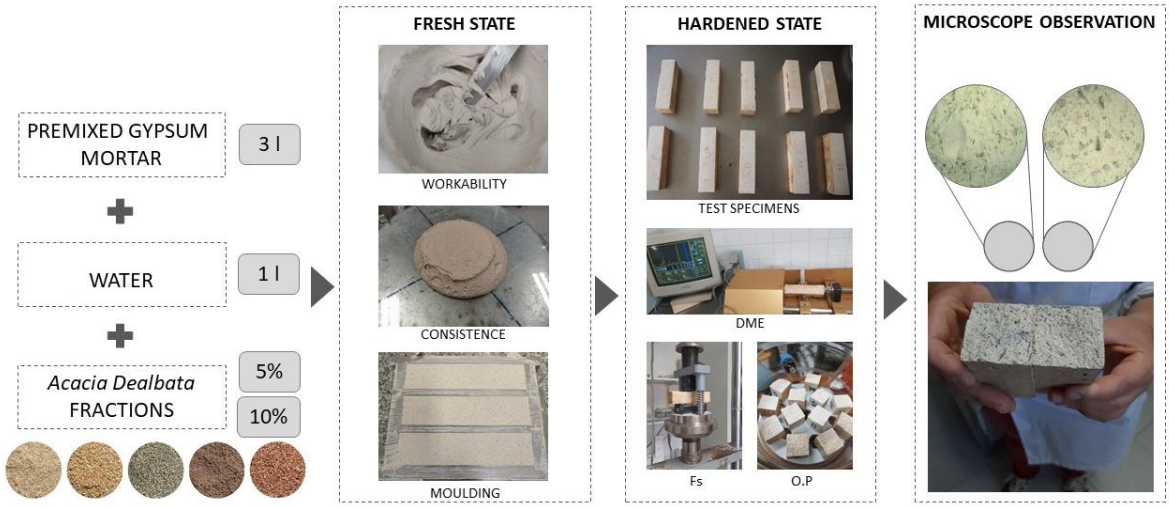


**Figure 4.3.** Experimental flowchart. DME, dynamic modulus of elasticity; Fs, flexural strength test; O.P., open porosity by vacuum and hydrostatic weighing.

- 

(**a**) (**b**) (**c**)

**Figure 4.4.** Flexural (**a**) and compressive (**b**) strength tests, and Wo10 specimens after the flexural tests (**c**).

## 4.2.3 Results and discussion

### 4.2.3.1 Flow-Table Consistency, Density, and Drying Shrinkage

The consistency of the mortars (**Figure 4.5**) was determined using the flow-table method and the results obtained are presented in **Table 4.2**. All the mortars showed adequate spreading

values, coherent with a good workability. Except for wood, the addition of 5% of biomasses slightly improved the flow of the mortars. The same happened for the 10% addition, except for the leaves. Therefore, the influence of the biomasses was in general very positive, as the additions did not require additional water to maintain workability. Moreover, it was expected that, for a fixed amount of water, an increase in the volume of powders would have led to lower values of flow-table consistency. This was not observed in the case of flowers and wood which, on the contrary, showed a flow increase. This may have been related to the combined effects of different particle size distribution, particle shapes, and hygroscopicity of the different biomass fractions. Hygroscopicity of a biomass is typically higher than that of biochar and affects the water available for hydration of other mortar components [38]. Unlike biochar particles or sand particles, biomass particles have irregular shapes that influence the mechanical interactions between themselves and other mortar components, thus affecting the flow behavior of the wet mortars [39]. These observations suggest that further tests using biomass particles of different granulometries may help to elucidate these effects.

(**a**) (**b**)

**Figure 4.5.** Flow-table consistency at the removal of the cone of the reference mortar (**a**) and after jolting the flow table fifteen times (**b**).

Figure 4.6 shows the values of the bulk density of the mortars from the fresh state to the 28th curing day. It can be easily observed that during the first 14 days, the density decreased for all the formulations, and that the drying essentially occurred during that period. The addition of biomasses, in both volumetric percentages (5% and 10%), did not significantly modify the bulk density of the mortars which was around 1.6 kg/dm$^3$ in the fresh state and 1.2 kg/dm$^3$ from the 14th curing day onwards. Only for the plastering mortars with addition of bark did the first 7 days of curing show a higher decrease in bulk density, possibly caused by a faster evaporation of water. The bark particles had some differences in their contents of cellulose, hemicellulose, and lignin, relative to the other biomass fractions [40], which determines the surface groups of these particles and may have influenced their interactions with water molecules. Generally, the

volume reduction was lower for the mortars with 5% biomass addition relative to the reference mortar, while all the formulations with 10% (vol.) biomass addition showed a slight volume increase up to one month of age. No cracks were observed in either the reference or the modified mortar samples. Therefore, the addition of biomass had a positive effect in the prevention of significant volume variation that could cause plaster cracking or lack of adherence to the support.

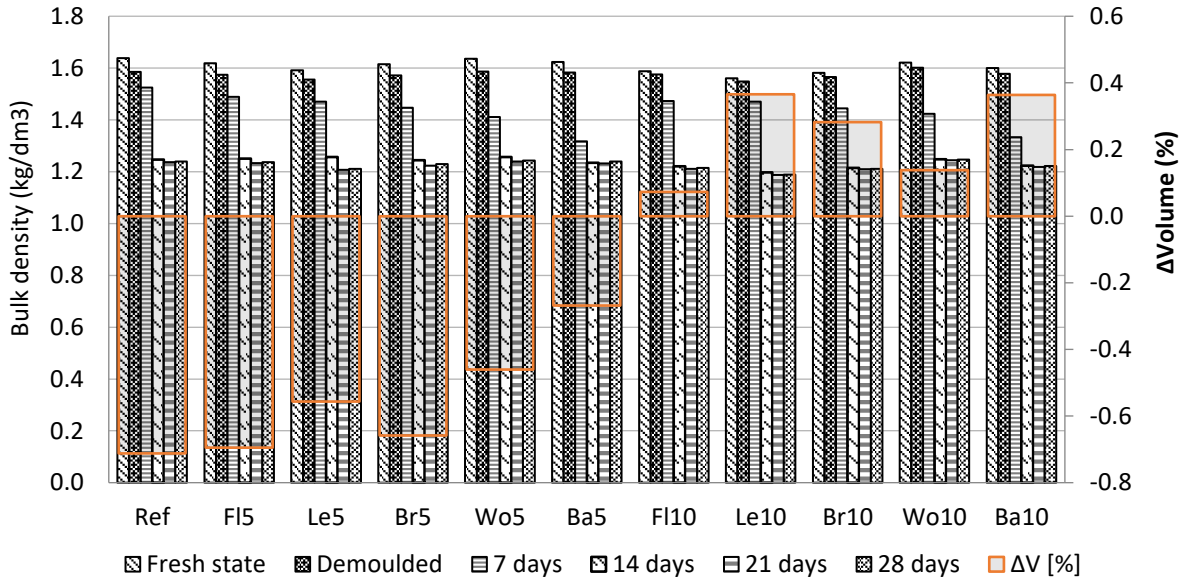


**Figure 4.6.** Bulk density of the tested mortars and, in orange, the volumetric drying shrinkage at 28 days.

#### 4.2.3.2 Flexural and Compressive Strength

Flexural and compressive strength tests were performed after 30 days. All the mortars with added bio-based wastes presented lower flexural and compressive strengths than the reference mortar. This was much less significant for those with the addition of the wood fraction, especially at 5%. Indeed, a general decrease was noticed, namely between 40 and 55%. Moreover, a higher content of the same biomass usually corresponded with a lower flexural strength of the mortar, except for leaves and branchlets where the content presented insignificant differences. Although the latter showed a similar flexural strength at 5% and 10% of biomass addition, the compressive strength increased with an increase in biomass. In addition, bark showed this tendency to a small degree, whereas particles of flowers and wood reduced the compressive strength with increased contents. As mentioned previously, the different fractions of *A. dealbata* biomass have different amounts of cellulose, hemicellulose, and lignin. This affects their surface and their tenacity during milling, resulting in different particle shapes and different particle size distributions [40]. These different characteristics will

also affect chemical and physical interactions with other mortar components, thus influencing mechanical properties. This tendency for a decrease in mechanical properties with the addition of biomass was already observed by other authors [41,42]. Morales-Conde [43] found that not exceeding 5% of sawdust incorporation on gypsum mortars led to an improvement of flexural strength, whereas all the percentages of sawdust additions decreased the compressive strength. The same authors related this phenomenon to a discontinuity introduced by the particles in the gypsum matrix which might have caused a reduction of strength. A lower hydration rate in the composites was also referenced by Chiki et al. [44], Panesar et al. [45] (2012), and Fatma et al. [42]. Nevertheless, all the mortars fulfilled the flexural and compressive strengths requirements of the EN 13279-1 [31] for gypsum plasters, as presented in **Figure 4.7**.

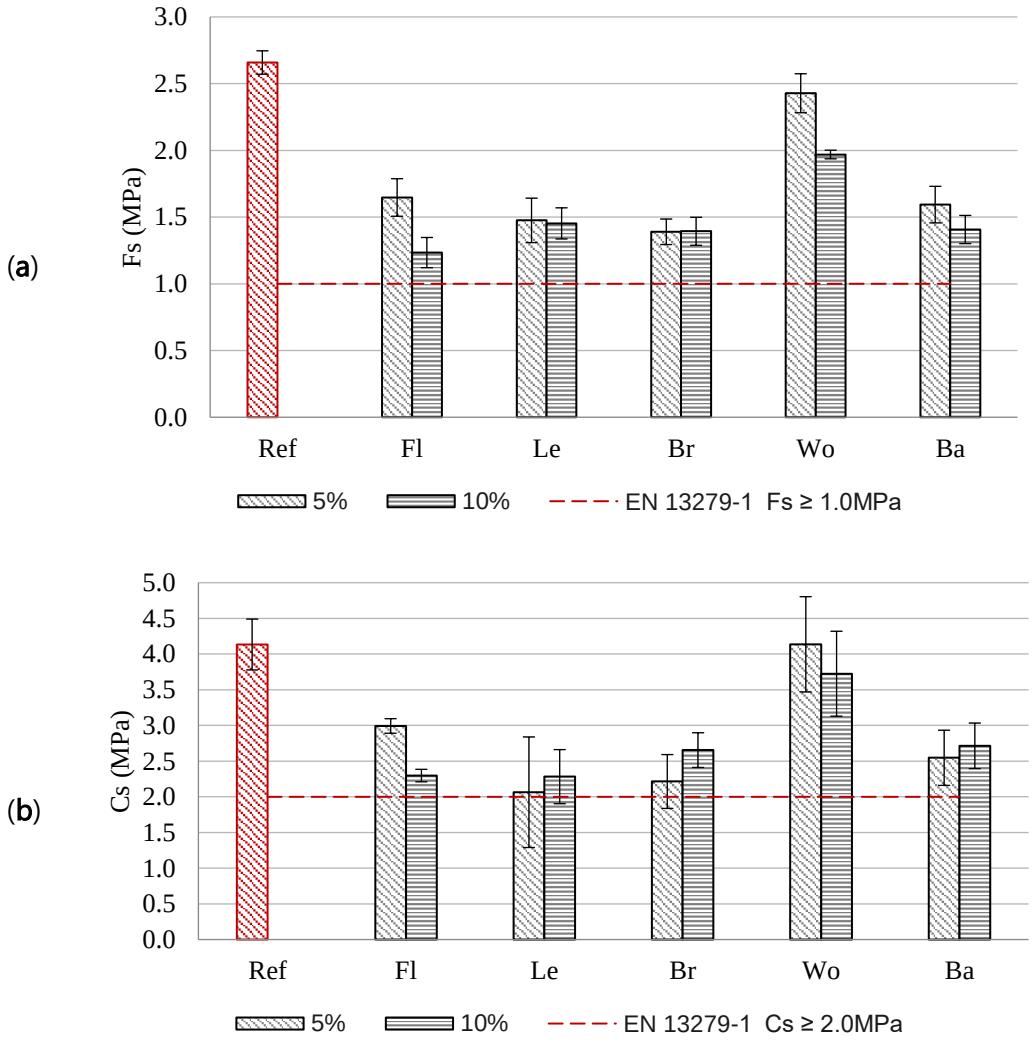


**Figure 4.7.** Flexural (**a**) and compressive (**b**) strengths of the mortars—average values and standard deviation. Dashed red lines represent the lower limits of the EN 13279-1 [31] for gypsum plasters (B1 to B6 class).

#### 4.2.3.3 Dynamic Modulus of Elasticity (DME)

The dynamic modulus of elasticity (DME) generally showed a similar tendency to the flexural and compressive strengths. The incorporation of 5% and 10% (vol.) of different *A. dealbata* fractions introduced a decrease in the DME of the mortars (**Figure 4.8**). Moreover, the higher the volume of biomass added, the lower the modulus, as expected. These results can indicate a higher deformability of the mortars, which can lead to a lower susceptibility to cracking phenomena. Nevertheless, the particles of biomass could be responsible for the DME decrease by triggering new voids in the mortar matrix, as evidenced by the Olympus SZH-10 stereo microscope observation (**Figure 4.9**). A poor interface between the gypsum matrix and the sawdust particles, and a high water absorption of the sawdust were found to be responsible for the poorer mechanical behavior of the gypsum–sawdust composites studied by Dai et al. [46]. Some differences in the hydrophilic nature of the fractions of *A. dealbata* may have led to a high absorption of the mixing water and a consequent increase of volume of the biomass particles during the mixing process. Thus, less water available during the gypsum hydration process could have led to a lower hydration rate (with lower mechanical properties) of the modified mortars when compared to the reference one. Moreover, once dried, the particles of biomass could have lost their gained volume creating the big voids that were found (**Figure 4.9**). The biomass particles could also have physically replaced a corresponding volume of the gypsum paste, therefore, decreasing the mechanical properties of the mortar.

The color of the dry mortars was also assessed by naked eye and optical microscope observation. It could be seen that the differences in color due to the addition of the different biomasses and contents was not relevant when compared with the reference mortar.

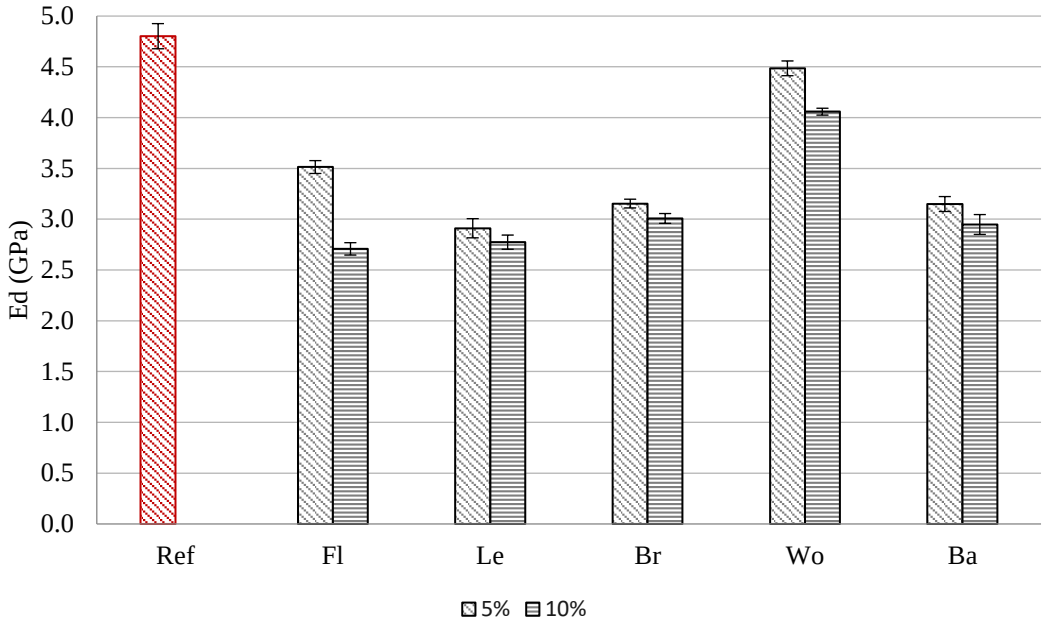


**Figure 4.8.** Dynamic modulus of elasticity of the tested mortars—average values and standard deviation.

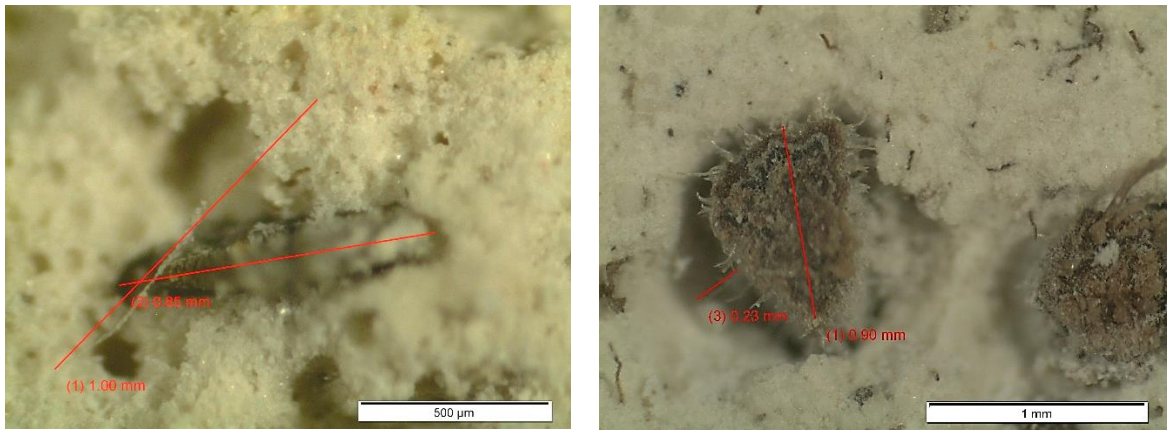


(**a**) (**b**)

**Figure 4.9.** Optical microscope observations showing voids introduced by the biomass in Le5 (**a**) and Fl10 (**b**) mortar.

#### 4.2.3.4 Open Porosity

The values of open porosity of the eleven mortars were quite similar, although a small amount of variation was observed (**Figure 4.10**). All the mortars were highly porous, with values around 40%. The addition of flowers, leaves, and branchlets increased the porosity (the higher the percentage, the higher the effect). The addition of wood and bark, instead, kept the open porosity below the value of the reference mortar. The results agreed with the observed values of DME and flexural and compressive strengths, whereby the mortars with incorporation of *A.*

*dealbata* wood particles showed the lowest open porosity and one of the highest mechanical properties.

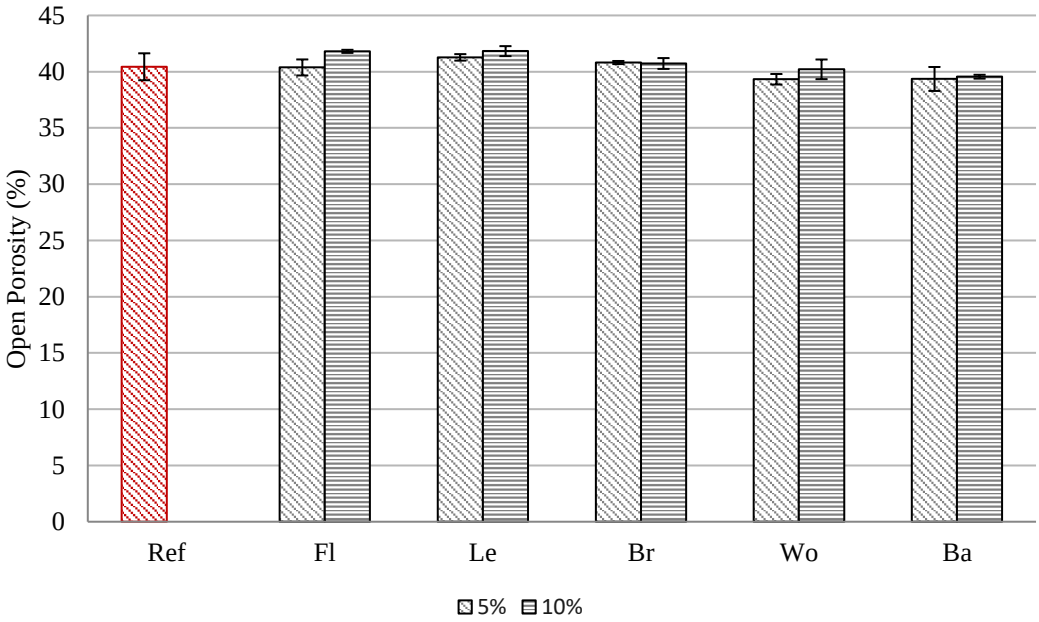


**Figure 4.10.** Open porosity of tested mortars. The average values and the standard deviation were calculated from three specimens.

### 4.2.4 Conclusions

After the removal of extracts that can be used in value-added chemical products, the wastes of five different fractions of *A. dealbata*, an invasive species in many countries, were added to a premixed gypsum plastering mortar in 5% and 10% volumes.

The study showed that the addition of *A. dealbata* biomasses did not significantly affect the workability of the mortars and their water requirements—seven mortars out of ten showed a higher flow-table consistency than the reference mortar despite a fixed amount of water being used for all. In addition, the bulk density, open porosity, and color were not appreciably modified by the additions, but a general decrease in mechanical properties was observed. However, mortars with all the studied fractions and contents presented flexural and compressive values that complied with the requirements of EN 13279-1 [31] for gypsum plasters. *Acacia dealbata* wood showed the closest mechanical properties to the reference mortar, having the best potential to be used as an addition to gypsum mortars, at least up to 10% volume incorporation rate, without causing relevant changes in their workability, density, or flexural or compressive strengths. Thus, this study allows us to conclude that gypsum-based

products with the inclusion of the studied additives are viable as plasters, according to EN 13279-1 [31].

Further studies will assess whether the addition of these biomasses, beyond their advantages in the reduction of incorporated energy, can improve the hygroscopicity of gypsum plasters and, therefore, their passive contribution to comfort and health in indoor environments. Moreover, the biomass fractions which had more negative effects on the mechanical properties of the studied plasters, might still present a high relative humidity passive regulation performance and therefore be promising for this reason.

### Author Contributions

Conceptualization, A.R., P.F., M.T.F., and M.G.; investigation, A.R., R.C., M.T.F., and M.G.; writing—original draft preparation, A.R.; writing—review and editing, P.F., R.C., M.T.F., R.V., and M.G.; supervision, P.F. and R.V. All authors have read and agreed to the published version of the manuscript.

### Funding

This research was funded by Portuguese Foundation For Science and Technology: 1st author Doctoral Training Programme EcoCoRe grant number PD/BD/150399/2019 and Civil Engineering Research And Innovation For Sustainability Unit-CERIS (UIDB/04378/2020).

### Acknowledgments

The authors would like to thank the National Laboratory for Civil Engineering of Portugal (LNEC) for the laboratory equipment and the support provided through the projects PRESERVe and REuSE; the Department of Civil Engineering of the NOVA School of Science and Technology of the University of Lisbon, and the Department of R&D of SIVAL—Gessos Especiais,, Lda.

## References

1. Mäkinen, T.M.; Juvonen, R.; Jokelainen, J.; Harju, T.H.; Peitso, A.; Bloigu, A.; Silvennionen-Kassinen, S.; Leinonen, M.; Hassi, J. Cold temperature and low humidity are associated with increased occurrence of respiratory tract infections. *Respir. Med.* **2009**, *103*, 456–462. https://doi.org/10.1016/j.rmed.2008.09.011.
2. Reinikainen, L.M.; Jaakkola, J.J. Efffects of temperature and humidification in the office environment. *Arch. Environ. Health* **2001**, *56*, 365–368. https://doi.org/10.1080/00039890109604469.

3. Markowicz, P.; Larsson, L. Influence of relative humidity on VOC concentrations in indoor air. *Environ. Sci. Pollut. Res.* **2015**, *22*, 5772–5779. https://doi.org/10.1007/s11356-014-3678-x.
4. Jones, A.P. Indoor air quality and health. *Atmos. Environ.* **1999**, *33*, 4535–4564. https://doi.org/10.1016/S1352-2310(99)00272-1.
5. Walkoff, P. Indoor air humidity, air quality, and health—An overview. *Int. J. Hyg. Environ. Health* **2018**, *221*, 376–390. https://doi.org/10.1016/j.ijheh.2018.01.015.
6. Almeida, R.M.S.F.; Ramon, N.M.M.; Freitas, V.P. Thermal comfort models and pupils' perception in free-running school buildings of a mild climate country. *Energy Build.* **2016**, *11*, 64–75. https://doi.org/10.1016/j.enbuild.2015.09.066.
7. Vellei, M.; Herrera, M.; Fosas, D.; Natarajan, S. The influence of relative humidity on adaptive thermal comfort. *Build. Environ.* **2017**, *124*, 171–185. https://doi.org/10.1016/J.BUILDENV.2017.08.005.
8. Freire, M.T.; Veiga, R.; Santos Silva, A.; de Brito, J. Restoration of ancient gypsum-based plasters: Design of compatible materials. *Cem. Concr. Compos.* **2021**, *120*, 104014. https://doi.org/10.1016/j.cemconcomp.2021.104014.
9. Lima, J.; Faria, P.; Veiga, R. Comparison of an earth mortar and common binder mortars for indoor plastering. In Proceedings of the ICSEFCM2021—2nd International Conference on Sustainable, Environmentally Friendly Construction Materials, Szczecin, Poland, 31 August–2 September 2021*;* Horszczaruk, E.*,* Brzozowski, P., Eds.; pp. 71–76. ISBN: 978-83-7663-324-4.
10. Santos, T.; Gomes, M.I.; Santos Silva, A.; Ferraz, E.; Faria, P. Comparison of mineralogical, mechanical and hygroscopic characteristic of earthen, gypsum and cement-based plasters. *Constr. Build. Mater.* **2020**, *254*, 119222. https://doi.org/10.1016/j.conbuildmat.2020.119222.
11. Ranesi, A.; Faria, P.; Veiga, M.R. Traditional and modern plasters for built heritage: Suitability and contribution for relative humidity passive regulation. *Heritage* **2021**, *4*, 2337–2355. https://doi.org/10.3390/heritage4030132.
12. Santos, T.; Almeida, J.; Silvestre, J.D.; Faria, P. Life cycle assessment of mortars: A review on technical potential and drawbacks. *Constr. Build. Mater.* **2021**, *288*, 123069. https://doi.org/10.1016/j.conbuildmat.2021.123069.
13. Brazão Farinha, C.; Silvestre, J.D.; de Brito, J.; Veiga, R. Life Cycle Assessment of Mortars with Incorporation of Industrial Wastes. *Fibers* **2019**, *7*, 1–19. https://doi.org/10.3390/FIB7070059.

14. Cintura, E.; Nunes, L.; Esteves, B.; Faria, P. Agro-industrial wastes as building insulation materials: A review and challenges for Euro-Mediterranean countries. *Ind. Crops Prod.* **2021**, *171*, 113833. https://doi.org/10.1016/j.indcrop.2021.113833.
15. Mazhoud, B.; Collet, F.; Pretot, S.; Chamoin, J. Hygric and thermal properties of hemp-lime plasters. *Build. Environ.* **2016**, *96*, 206–216. https://doi.org/10.1016/J.BUILDENV.2015.11.013.
16. Liuzzi, S.; Rubino, C.; Stefanizzi, P.; Petrella, A.; Boghetich, A.; Casavola, C.; Pappalettera, G. Hygrothermal properties of clayey plasters with olive fiber. *Constr. Build. Mater. J.* **2018**, *158*, 24–32. https://doi.org/10.1016/J.CONBUILDMAT.2017.10.013.
17. Pavlíková, M.; Zemanová, L.; Pokorný, J.; Záleská, M.; Jankovský, O.; Lojka, M.; Pavlík, Z. Influence of wood-based biomass ash admixing on the structural, mechanical, hygric, and thermal properties of air lime mortars. *Materials* **2019**, *12*, 2227. https://doi.org/10.3390/ma12142227.
18. Maskell, D.; da Silva, C.F.; Mower, K.; Rana, C.; Dengel, A.; Ball, R.J.; Ansell, M.P.; Thomson, A.; Peter, U.; Walker, P.J. Bio-based plasters for improved indoor air quality. In Proceedings of the ICBBM–2nd International Conference on Bio-based Building Materials, Clermont-Ferrand, France, 21–23 June 2017.
19. Romano, A.; Bras, A.; Grammatikos, S.; Shaw, A.; Riley, M. Bio-based and recycled materials: Characterisation and hygrothermal assessment for passive relative humidity management. In Proceedings of the 3rd International Conference on Bio-based Building Materials, Belfast, UK, 26–28 June 2018.
20. Kunchariyakun, K.; Sinyoung, S.; Kajitvichyanukul, P. Comparative microstructures and mechanical properties of mortar incorporating wood fiber waste from various curing conditions. *Case Stud. Constr. Mater.* **2022**, *16*, e00855. https://doi.10.1016/j.cscm.2021.e00855.
21. de Azevedo, A.R.G.; Klyuev, S.; Marvila, M.T.; Vatin, N.; Alfimova, N.; de Lima, T.E.S.; Fediuk, R.; Olisov, A. Investigation of the potential use of Curauá fiber for reinforcing mortars. *Fibers* **2020**, *8*, 69. https://doi.org/10.3390/fib8110069.
22. Maia Pederneira, C.; Veiga, R.; de Brito, J. Physical and Mechanical Performance of Coir Fiber-Reinforced Rendering Mortars. *Materials* **2020**, *14*, 823. https://doi.org/10.3390/ma14040823.
23. Nunes, L.J.R.; Rodrigues, A.M.; Loureiro, L.M.E.F.; Sá, L.C.R.; Matias, J.C.O. Energy recovery from invasive species: Creation of value chains to promote control and eradication. *Recycling* **2021**, *6,* 21. https://doi.org/10.3390/recycling6010021.

24. Raposo, M.A.M.; Pinto-Gomes, C.J.; Nunes, L.J.R. Selective shrub management to preserve Mediterranean forests and reduce the risk of fire: The case of mainland Portugal. *Fire* **2020**, *3*, 65. https://doi.org/10.3390/fire3040065.
25. Lorenzo, P.; González, L.; Reigosa, M.J. The Genus Acacia as Invader: The characteristic case of acacia dealbata link in Europe. *Ann. For. Sci.* **2010**, 67, 101.
26. Dawit, J.B.; Lemu, H.G.; Regassa, Y.; Akessa, A.D. Investigation of the mechanical properties of Acacia tortilis fiber reinforced natural composite. *Mater. Today Proc.* **2021**, *38*, 2953–2958. https://doi.org/10.1016/j.matpr.2020.09.308.
27. Sakthi Vadivel, K.; Govindasamy, P. Mechanical and water absorption properties of Acacia Arabica bark fiber/polyester composites: Effect of alkali treatment and fiber volume fraction. *Mater. Today Proc.* **2021**, *46*, 2281–2287. https://doi.org/10.1016/j.matpr.2021.04.057.
28. Ogawa, S.; Yazaki, Y. Tannins from Acacia mearnsii De Wild. Bark: Tannin determination and biological activities. *Molecules* **2018**, *23*, 1–18. https://doi.org/10.3390/molecules23040837.
29. Perriot, R.; Breme, K.; Uwe, J.M.; Carenini, E.; Ferrando, G.; Baldovini, N. Chemical composition of french mimosa absolute oil. *J. Agric. Food Chem.* **2010**, *58*, 1844–1849. https://doi.org/10.1021/jf903264n.
30. Sowndhararajan, K.; Joseph, J.M.; Manian, S. Antioxidant and Free Radical Scavenging Activities of Indian Acacias: Acacia Leucophloea (Roxb.) Willd., Acacia Ferruginea Dc., Acacia Dealbata Link. and Acacia Pennata (l.) Willd. *Int. J. Food Prop.* **2013**, *16*, 1717–1729. https://doi.org/10.1080/10942912.2011.604895.
31. EN 13279-1. *Gypsum Binders and Gypsum Plasters—Part 1: Definitions and Requirements*; European Committee for Standardization (CEN): Brussels, Belgium, 2008.
32. EN 13279-2. *Gypsum Binders and Gypsum Plasters—Part 2: Test methods*; European Committee for Standardization (CEN): Brussels, Belgium, 2014.
33. EN 1015-6. *Methods of Test for Mortar for Masonry—Part 6: Determination of Bulk Density of Fresh Mortar;* European Committee for Standardization (CEN): Brussels, Belgium, 1999.
34. EN 1015-10. *Methods of Test for Mortar for Masonry—Part 10: Determination of Dry Bulk Density of Hardened Mortar;* European Committee for Standardization (CEN): Brussels, Belgium, 1999.
35. EN 1015-11. *Methods of Test for Mortar for Masonry—Part 11: Determination of Flexural and Compressive Strength of Hardened Mortar*; European Committee for Standardization (CEN): Brussels, Belgium, 1999.

36. EN 14146. *Natural Stone Test Methods. Determination of the Dynamic Modulus of Elasticity (by Measuring the Fundamental Resonance Frequency)*; European Committee for Standardization (CEN): Brussels, Belgium, 2004.
37. EN 1936. *Determination of Real Density and Apparent Density and Total and Partial Open Porosity;* European Committee for Standardization (CEN): Brussels, Belgium, 2007.
38. Tan, K.; Qin, Y.; Du, T.; Li, L.; Zhang, L.; Wang, J. Biochar from waste biomass as hygroscopic filler for pervious concrete to improve evaporative cooling performance. *Constr. Build. Mater.* **2021**, *287*, 123078. https://doi.org/10.1016/j.conbuildmat.2021.123078.
39. Pachón-Morales, J.; Colin, J.; Pierre, F.; Puel, F.; Perré, P. Effect of torrefaction intensity on the flow properties of lignocellulosic biomass powders. *Biomass Bioenergy* **2019**, *120*, 301–312. https://doi.org/10.1016/j.biombioe.2018.11.017.
40. López-Hortas, L.; Rodríguez-González, I.; Díaz-Reinoso, B.; Torres, M.D.; Moure, A.; Domínguez, H. Tools for a multiproduct biorefinery of *Acacia dealbata* biomass. *Ind. Crops Prod.* **2021**, *169*, 113655. https://doi.org/10.1016/j.indcrop.2021.113655.
41. Pedreño-Rojas, M.A.; Morales-Condes, M.J.; Rubio-de-Hita, P.; Pérez-Gálvez, F. Impact of wetting–drying cycles on the mechanical properties and microstructure of wood waste–gypsum composites. *Materials* **2019**, *12*, 1829. https://doi.org/10.3390/ma12111829.
42. Fatma, N.; Allègue, L.; Salem, M.; Zitoune, R.; Zidi, M. The effect of doum palm fibers on the mechanical and thermal properties of gypsum mortar. *J. Compos. Mater.* ***2019***, 1–19. https://doi.org/10.1177/0021998319838319.
43. Morales-Conde, M.J.; Rodríguez-Liñán, C.; Pedreño-Rojas, M.A. Physical and mechanical properties of wood-gypsum composites from demolition material in rehabilitation works. *Constr. Build. Mater.* **2016**, *114*, 6–14. https://doi.org/10.1016/j.conbuildmat.2016.03.137.
44. Chicki, M.; Agoudjil, B.; Boudenne, A.; Gherabli, A. Experimental investigation of new biocomposite with low cost forthermal insulation. *Energy Build.* **2013**, *66*, 267–273. https://doi.org/10.1016/j.enbuild.2013.07.019.
45. Panesar, D.K.; Shindman, B. The mechanical, transport and thermal properties of mortar and concrete containing waste cork. *Cem. Concr. Compos.* **2012**, *34*, 982–992. https://doi.org/10.1016/j.cemconcomp.2012.06.003.
46. Dai, D.; Fan, M. Preparation of bio-composite from wood sawdust and gypsum. *Ind. Crops And Products* **2015**, *74*, 417–424. https://doi.org/10.1016/j.indcrop.2015.05.036.

## 4.3 Article C2 - Enhancement of Gypsum Mortar: characterization of liquid water and moisture transport

(the article has been published in the journal *Construction and Building Materials* 2023, 404, 133283; https://doi.org/10.1016/j.conbuildmat.2023.133283)

### Gypsum plastering mortars with *Acacia dealbata* biowaste additions: effect of different fractions and contents on the relative humidity dependent properties


### Abstract

Hemihydrate gypsum is a very eco-efficient binder. Gypsum plasters were commonly used in the past and should be still chosen nowadays for being an eco-efficient choice. However, their hygroscopicity and contribution to act as moisture buffer are not very high. The present study analyses the hygrothermal behaviour of mortars based on gypsum and modified with the addition of residual biomass of A. dealbata, an invasive species in Portugal. Five different fractions of the plant were tested as additions for mortars, at incorporation levels of 5% and 10% by volume, with the purpose of enhancing the moisture buffering of the plasters without jeopardizing other properties. The study found that the addition of A. dealbata increases their hygroscopic behaviour. In some cases (bark fraction) the Moisture Buffering Value of the reference mortar is triplicated, and the behaviour is comparable with high hygroscopic plasters as clay-based ones. However, biological colonization must be controlled.



### Keywords

Bio-based plasters, invasive species, agro-industrial wastes, moisture adsorption, moisture buffering, physical characterization.


#### 4.3.1 Introduction

Gypsum plasters were commonly used in traditional construction and, thus, are often highly compatible with built heritage [1, 2]. In fact, due to its prevalent application in old European palaces and churches [3, 4], gypsum still represents the most compatible option in many restoration projects [5, 6].

Hemihydrate gypsum is a very eco-efficient binder, presenting a low calcination temperature (120-180 ˚C) and an embodied energy five to six times lower than other common binders like cement [7]. Gypsum plasters are also well-known for their high durability over the centuries

[3]. The choice of hemihydrate gypsum as binder has been often related to its malleability when in fresh state and its fast-setting time, properties that make this binder a suitable and valuable choice for artistic decoration. Due to all the previous reasons, gypsum went on being applied and is still a common binder also for indoor coatings of walls and ceilings of contemporary buildings.

Despite having high permeability to water vapour, gypsum plasters usually present a limited capacity of interacting with environmental moisture, namely to uptake or release it in moist or dry environments [8 - 11]. This property is considered essential for the passive contribution to moisture regulation, an efficient tool to enhance indoor comfort without additional energy consumption.

The introduction of more sustainable practices in the building sector is nowadays an imperative to reduce its high carbon footprint and preserve natural resources. Mortar production, as a relevant part of the building sector, is also involved in this green transition tendency. In this context, several studies targeting a reduction of mortars carbon footprint and improvement of mortars performance have been published in recent years. Some of these studies analyse the possibility to add compatible wastes from industries, i.e., textile industry wastes [12] or sanitary ware wastes [13], to reduce the amount of raw material used to produce mortars. The construction industry itself produces construction and demolition waste (CDW) that can be added to mortars [14] as a partial or total replacement of natural aggregates. The addition of different by-products and biowaste from agriculture and food industry has also been explored in recent years in mortars [15, 16]. As biomass residues are commonly highly hygroscopic [17], they can probably increase mortars hygroscopicity and improve their contribution for indoor air quality when used in plasters.

The *Acacia dealbata* is an invasive species presently spread in many regions of the world including the Mediterranean Countries (Portugal, Spain, France, Italy) [18]. The first naturalization of Acacia dealbata in Portugal (Continental) dates back to 1968 according to Domingues de Almeida and Freitas [19] and its growth has exponentially increased over 90% in the last decades [20]. The invasive nature of this species is related to its high dispersion capacity in burnt areas [21] and capacity to germinate and proliferate in a wide range of environments [22, 23]. Moreover, Acacia populations compete with native plants due to their allelopathic capacity, what raises concerns on ecosystems biodiversity [24, 25]. The control and eradication of invasive plants represent a high cost therefore becomes more sustainable when the collected biomass is valorized for energy production or material applications [26]. Pellets produced from A. dealbata biomass showed similar properties to the conventional pellets

produced with Pinus pinaster or Eucalyptus globulus biomass [27], although its high chlorine content may affect this use. Some fractions of the A. dealbata can also be a source of extracts, with antimicrobial and antioxidant activities [28]. Material applications of A. dealbata biomass have been reviewed by Correia et al. [29] who concluded there are various other potential applications that can involve a great variety of markets like: clothes industry (tannins for leather); polymer and composite industry (nanomaterials); water filters industry (adsorbent materials); iron and steel industry (corrosion and degradation protection). A multiproduct biorefinery approach can be pursued to optimize the number of extractives obtained from different fractions with different methods, and the spent biomass could be also converted into biofuel, for energy production, according to a zero-waste perspective [30]. The spent biomass can also be used in the formulation of different biomaterials, avoiding the production of second-generation wastes.

The present study analyses the hygrothermal behaviour of mortars based on gypsum and modified with the addition of residual wastes of A. dealbata. Five different fractions of the plant were previously extracted with polar and nonpolar solvents to isolate aromatic and antioxidant extracts and the spent biomasses were selected to be tested as mortar addition. Incorporation rates of 5% and 10% by volume of biomass were used in mortars formulation with the purpose of enhancing the moisture buffering of the plasters without jeopardizing other properties.

## 4.3.2 Materials and methods

### 4.3.2.1 Materials

The gypsum-based product used was an industrial pre-dosed gypsum filling plaster from Sival - Gessos Especiais, Lda, based on calcium sulphate hemi-hydrate, calcium carbonate aggregates and small quantities of organic additives (set retarder, water-retention agent., etc.), classified as B1/50/2 according to EN 13279-1. The loose bulk density of the product from the batch selected for this study is 733 kg/m$^3$.

Five fractions of *Acacia dealbata* waste were used: flowers, leaves, branchlets, wood and bark. The biomass fractions were collected from *Acacia* trees in the regions of Alcobaça and Caparica. After solvent extraction with petroleum ether and 70% acetone, each biomass fraction was air-dried during 1 week with periodic turning over, to eliminate solvent residues. When dried and free of solvent residues the biomass fractions were grinded and sieved at 2 mm. The extractives obtained can be used by the pharmaceutical and cosmetic industries and the spent biomass

needs to be valorised. An alternative to energy production is its use in building materials hereafter.

A synthesis of the chemical composition of raw biomass fractions is shown in **Figure 4.11** [31]. It should be highlighted that the suberin, which is a poly (acylglycerol) macromolecule [32], was detected only in the bark fraction. According to Koch *et al.* [33], the suberized tissue of a plant is composed by cells whose external walls are covered by non-polymeric waxes turning into a hydrophobic or super-hydrophobic structure.

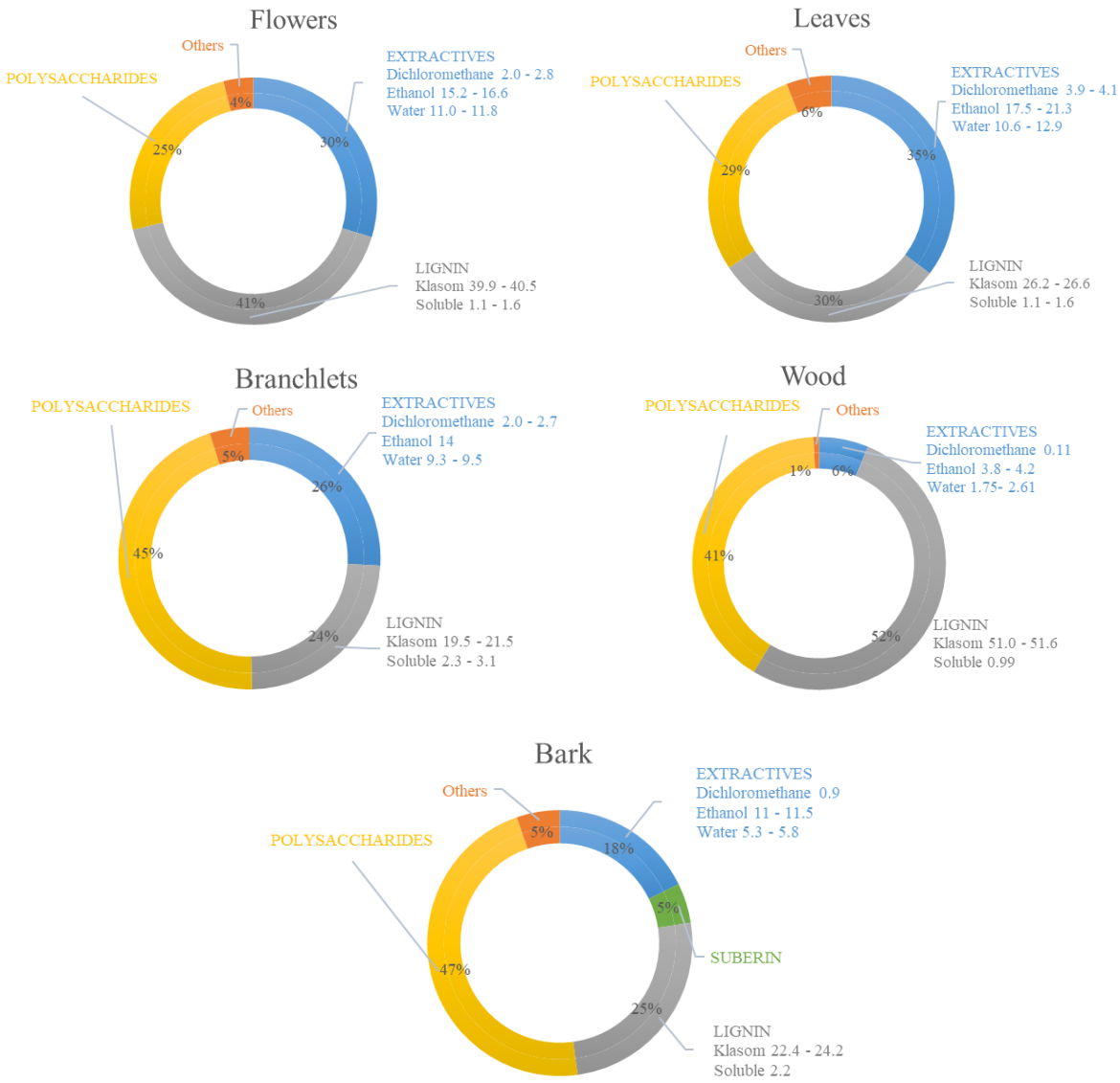


**Figure 4.11**. Chemical composition of the five fractions of *A. dealbata* [adapted from 31].

These spent materials were used for the mortars formulations and their compositions are similar to those described in **Figure 4.11**, without the extractives. To better discuss the effect of the fractions' addition on the mortars, in **Table 4.3** are reported the main physical properties

of those fractions. The methods for the biomass characterization are extensively described in Correia [31], but a short overview is presented. The loose bulk density was obtained dropping each fraction from a high of 10 cm approx. up to fill a container of 251 $cm^3$ without applying any compaction and weighting the known volume of biomass. The water vapour and water holding capacity were determined by exposing each fraction either to water vapour (for five days) and liquid water (5 min exposure to ultrasound and kept in distilled water for 24 h). Once saturated, the biomass samples were weighed and then dried for 12 h at 40°C. The dry mass was obtained after cooling the fractions to room temperature and water vapour and water holding capacity were calculated. The particle shape was obtained by the Morphologi G3 (Malvern) analyzer, performed in duplicate with at least two different dispersions with 30000 particles counted.

**Table 4.3.** Synthesis from the characterization of the *A. dealbata* fractions with, where possible, values of standard deviation [31]

| Biomass | Flowers | Leaves | Branchlets | Wood | Bark |
|---|---|---|---|---|---|
| LBD [g/$dm^3$] | 217.5±4.4 | 414.7±7.8 | 378.3±9.2 | 211.1±1.3 | 434.8±7.2 |
| Vol. 10% [g] | 65.3 | 124 | 114 | 63.3 | 130 |
| Water Vapor Holding Capacity [wt.%] | 22.7±1.5 | 20.1±0.6 | 20.4±0.9 | 21.6±0.5 | 23.1±0.3 |
| Water Holding Capacity [wt.%] | 590.2±31.9 | 478.4±28.5 | 423.5±18.2 | 494.3±24.0 | 330.5±6.9 |
| CE diameter [µm] | 4.75±0.28 | 5.29±0.21 | 4.42±0.04 | 7.62±0.04 | 4.53±0.10 |
| Circularity [-] | 0.59±0.02 | 0.77±0.04 | 0.82±0.00 | 0.63±0.02 | 0.80±0.02 |

Notation: LBD –loose bulk density; CE diameter – circle equivalent diameter.

#### 4.3.2.2 The mortars and basic characterization

Eleven mortars based on a powder premixed gypsum-based mortar product for plastering were produced: a reference mortar and mortars with two different contents (5% and 10% vol. premixed gypsum product) of the five different fractions of *Acacia dealbata* (flowers, leaves, branchlet, wood and bark). The content of biomass added was calculated as a percentage of the premixed gypsum product volume due to the large differences of apparent bulk density observed between different fractions. Each fraction was previously manually homogenized with the gypsum premixed product. Then, the powders (gypsum premixed product for the reference mortar and gypsum premixed product with addition of biomass for the other mortars) were sprinkled into the water for one minute and left one minute soaking, to be finally mechanically mixed for one minute. A fixed amount of water was used for all mortars (water:premixed gypsum product ratio 1:3 by volume). All the mixes resulted in workable plastering mortars. They were previously characterized for basic properties in the fresh (flow table consistence and fresh density) [34, 35] and hardened state (bulk density, open porosity, dynamic modulus of

elasticity, flexural and compressive strength) [36-40]. A synthesis of the results obtained is shown in **Table 4.4**.

**Table 4.4.** Synthesis of the plastering mortars fresh and hardened state basic properties from Ranesi et al. [40].

| Mortar | *A. dealbata* fraction | Addition | | Flow | FBD | BD | OP | Ed | Fs | Cs |
|---|---|---|---|---|---|---|---|---|---|---|
| | | [vol., %] | [wt., %] | [mm] | [kg/dm$^3$] | [kg/dm$^3$] | [%] | [GPa] | [MPa] | [MPa] |
| **REF** | – | – | – | 163.0 | 1.639 | 1.24 | 40.44 | 4.80 | 2.72 | 4.22 |
| **Fl_5** | Flowers | 5 | 1.48 | 163.0 | 1.619 | 1.24 | 40.38 | 3.51 | 1.69 | 3.05 |
| **Fl_10** | Flowers | 10 | 2.97 | 165.5 | 1.592 | 1.22 | 41.81 | 2.71 | 1.26 | 2.34 |
| **Le_5** | Leaves | 5 | 2.83 | 168.5 | 1.615 | 1.21 | 41.27 | 2.91 | 1.50 | 2.11 |
| **Le_10** | Leaves | 10 | 5.66 | 156.5 | 1.636 | 1.19 | 41.83 | 2.77 | 1.48 | 2.33 |
| **Br_5** | Branchlet | 5 | 2.58 | 171.3 | 1.624 | 1.23 | 40.81 | 3.15 | 1.42 | 2.26 |
| **Br_10** | Branchlet | 10 | 5.16 | 171.0 | 1.588 | 1.21 | 40.73 | 3.01 | 1.42 | 2.71 |
| **Wo_5** | Wood | 5 | 1.44 | 160.3 | 1.561 | 1.24 | 39.33 | 4.49 | 2.48 | 3.93 |
| **Wo_10** | Wood | 10 | 2.88 | 165.3 | 1.582 | 1.21 | 40.21 | 4.06 | 2.01 | 4.02 |
| **Ba_5** | Bark | 5 | 2.96 | 175.5 | 1.621 | 1.24 | 39.35 | 3.15 | 1.63 | 2.60 |
| **Ba_10** | Bark | 10 | 5.93 | 165.0 | 1.600 | 1.22 | 39.55 | 2.95 | 1.44 | 2.77 |

Notation: Flow – flow table consistence; FBD – fresh bulk density; BD – bulk density at 28 days; OP – open porosity; Ed – dynamic modulus of elasticity by resonance frequency at 30 days; Fs – flexural strength at 30 days; Cs – compressive strength at 30 days.

The biomass addition, as expected, modified some REF properties, i.e., consistence, density, and mechanical strengths, but all the mixes met the requirements defined by EN 13279, parts 1 and 2 [41, 42] and, for this reason, were considered acceptable solutions. Nevertheless, a deeper analysis of the effect of the biomass addition on the fresh state was needed for a better understanding of the plasters behaviour and was performed through a second batch production of some of the mortars, tested for setting time and shrinkage. Complementary properties of the mortars were tested: thermal conductivity, capillarity and drying, hygroscopicity and susceptibility for biological colonization.

## 4.3.3 Test methods and specimens

### 4.3.3.1 Workability, setting time and shrinkage: mortars from the second set of mixes

A complementary set of mixes was done, including only mortars with the highest addition (10% vol. addition – these mortars are distinguished by *), that affected the most their workability, setting time and shrinkage. The new production followed the same protocol of the previous one; only a different batch of premixed gypsum plaster product was used. The workability was

empirically evaluated, relying on the expertise of a technician, according to two parameters: heaviness and stickiness. The heaviness has to do with the perception of the effort it has to be made by the person who is working with the plaster during its application. For example, a plaster with incorporation of lightweight aggregates is lighter and easier to spread on a surface, meaning that the worker does not need to spend so much energy. The stickiness is related to the interaction of the fresh plaster with the tools: if it sticks to the trowel, it is more difficult to apply, needing a longer processing time to obtain a satisfactory result than a plaster that does not stick.

The setting time was determined according to the knife method described in EN13279-2 [42], defining the initial (IST) and final (FST) setting times. To evaluate the shrinkage, the fresh mortars were applied on the surface of a hollow perforated brick with an area of 456 $cm^2$ and a thickness of 15 mm, simulating the application of a filling plaster, and visually observed.

#### 4.3.3.2 The specimens for hardened state characterization

In the present study the eleven plastering mortars are characterized at hygrothermal behaviour. Three cylindrical specimens for each mortar formulation, with 85 mm diameter and 22 mm thickness, were cast into 22 mm slices of PVC pipes and tested at colour, biological colonization, thermal conductivity, sorption isotherms and moisture buffering. To characterize water absorption by capillarity and drying three specimens (40 mm x 40 mm x 40 mm) per mortar were used. They were obtained by mechanical cut from standard mortar prismatic specimens. All specimens were let dry under non-ventilated laboratory conditions. The prismatic specimens were demolded after 2 days while the cylindrical ones were left in their plastic molds.

#### 4.3.3.3 Thermal conductivity

The thermal conductivity of the mortars was evaluated in dry conditions. For each mortar, three cylindrical specimens (d=85mm, s=20mm) were placed in an oven at 60 °C until constant mass and their thermal conductivity was measured by the ISOMET 2104 equipment. An API 210412 contact probe with 60 mm diameter was used, and the conductivity range was set 0.3 – 3 W/(m·K) based on literature values for gypsum plasters. The method followed here was similar to the one described by Cintura *et al.* [43] with the difference that the contact probe was applied only once on each specimen due to the small size of these and three specimens for each mortar were measured to get an average value and a standard deviation. After dried in the oven, the specimens were put into a desiccator, for cooling, and then moved on a support

of expanded polystyrene and covered by a plastic box. The measurement was conducted at constant power (lasting around 15/20 minutes each).

#### 4.3.3.4 Water absorption by capillarity and drying

The water absorption by capillarity test was run according to EN 15801 [44] on three cubic specimens of 40 mm x 40 mm x 40 mm (**Figure 4.12**) for each mortar. The lower and upper surface of the cubes were gently polished and brushed and their four lateral sides were sealed by paraffin to avoid any additional lateral drying. Once the specimens were dried at 60±2 °C and the initial dry mass ($m_0$) determined using a balance of 0.01 g precision, the specimens were placed on glass poles trying to minimize the contact surface (to have the entire bottom face of the cube in contact with water). The water absorption by capillarity test was run for 5 days, weighing at different time intervals, gradually increasing the period between weighing from minutes to hours during the first 8 h and, after the first day, weighing every 24 h. The room conditions were kept at 23±5 °C and 60±5% relative humidity (RH). The capillarity coefficient (CC) was calculated as the slope of at least five successive aligned points on the capillary curve displaying the absorbed water per area against the square root of time, with a linear regression factor above 0.99. Thus, the time basis for the calculation of CC varies from mortar to mortar, calculated as the slope of the linear regression line between the starting time (0 minutes) and ending point at 20 to 90 minutes of absorption.

**Figure 4.12.** Specimens during water absorption by capillarity test: 1 – reference mortar; 2 – flowers at 5%; 3 – leaves at 5%.

After saturation by the capillarity test, the specimens underwent the unidirectional drying test, according to EN16322 [45]. The cubes were kept in the same room at the same hygrothermal conditions, and placed on a hydrophobic surface, to ensure a monodirectional drying. The weight loss was monitored every 10 minutes during the first hour. After, the time interval was

widened until constant mass. The mortars resistance to evaporation of water can be quantified by the drying index (ID) [–] calculated by the drying curve with the weight variation in the Y axis and the time in the X axis, as [45]:

$$ID = \int_0^{t_f} \frac{m_i d_t}{m_{max} t_f} \quad (1)$$

with $m_i$ as the i-mass [g] of the specimen (corresponding to successive weighing), $m_{max}$ the mass [g] at the beginning of the test and $t_f$ the entire period of testing [h]. For comparison, $t_f$ was the same for all specimens.

To better describe the drying mechanism, the drying rate of first ($D_1$) [g/(m$^2$h)] and second ($D_2$) [g/(m$^2$min$^{0.5}$)] phases were calculated. The first phase of drying, $D_1$, is characterized by liquid transport to the surface and corresponds to the negative slope of initial linear section of the drying curve with time on the X axis; in this study it was always calculated with at least five successive measurements and a regression factor above 0.97 (often above 0.99). The second phase, $D_2$, is mainly characterized by vapour transport and corresponds to the negative slope of the intermediate linear segment of the drying curve with square root of time on the X axis, always with a regression factor above 0.99. The drying rates were calculated according to EN 16322 [45] on an average of three specimens as:

$$D_1 = \frac{m_i - m_f}{A \cdot t_f}; \quad D_2 = \frac{m_i - m_f}{A \cdot \sqrt{t_f}} \quad (2)$$

with $m_i$ [g] being the mass at the beginning of the phase, $m_f$ [g] the mass at the end of the phase, $A$ the surface of evaporation [m$^2$] and $t_f$ the time duration [h] or [h$^{0.5}$].

#### 4.3.3.5 Hygroscopic behaviour

The hygroscopic behaviour of the mortars was tested on the cylindrical specimens with a diameter of 85 mm and a thickness of 20 mm. The bottom of the cylinders was sealed by aluminium tape; the PVC mold sealed the lateral surface. The specimens were tested following the ISO 12571 [46] to assess their sorption isotherms. They were dried until constant mass in oven at 60°C, and after that placed in a climatic chamber Aralab Fitoclima 700EDTU at the fixed temperature of 23±0.5 °C and at increasing RH levels (30%, 50%, 70%, 80%, 95%), each kept until the equilibrium was reached (change in mass, observed by three consecutive weighing at 24 h apart, was less than 0.1% of the total mass). The desorption curve was obtained performing the same steps backwards. Moreover, a cyclic test for hygroscopic dynamic

response was performed following prescriptions of the ISO 24353 [47] for the "middle humidity level" conditions. The test was run at a fixed temperature of 23±0.5 °C. The specimens were preconditioned at 63% RH in the climatic chamber and exposed during 12 h to 75% RH followed by 12 h at 50% RH. The daily cycle was repeated five times and the last three were considered a quasi-steady state to quantify the moisture adsorption and desorption content. The specimens were weighed at 3, 6, 9 and 12 h during adsorption and after 12 h of desorption. Moreover, the data obtained were processed to calculate the Moisture Buffering Value (MBV) of the plastering mortars, according to NORDTEST [48].

#### 4.3.3.6 Biological susceptibility

The addition of the biomass fractions introduced a yellow/ light brownish shade in the mortar circular specimens. The colour alteration was more evident in the case of bark and leaves, less for branchlets and flowers and almost null for wood. 10% by vol. of addition introduced a higher chromatic change than 5%, but all the specimens fall into variations of beige. During the first 28 days of curing, the gypsum mortars were kept in a controlled environment at 23±5 °C and 60±10% RH with no ventilation. At the end of 14 days the mortars were observed visually and by Olympus SZH10 stereo zoom microscope, to assess biological colonization. The contamination was visually classified according to the ranking 0 (no growth) to 4 (>60% of the surface contaminated) adapted from ASTM D5590-17 [49, 43]. The drying in oven was run for all the tests at the temperature of 60 °C that, even if slightly above the heating temperature of 45°C recommended for calcium sulphate dihydrate, was selected as the most adequate to obtain a thermal inactivation of the Aspergillus niger spores according to Fujikawa and Itoh, 1996 [50]. The identification of the biological colonies on the specimens wasn't run, but the Aspergillus/Penicillium group are the commonest for indoor airborne according to Andersen et al., 2021 [51].

### 4.3.4 Results and discussion

#### 4.3.4.1 Assessment of fresh state performance of the second production of mortars

Results from the second production show that the addition of 10% of biomass modified the workability and the setting times of the mortars, with visible effects (cracks) on brick applications (**Table 4.5**). The plastering mortar with addition of wood (Wo_10*) had the best workability, even better than the reference mortar, and similar setting time than the reference.

The addition of all the other fractions, instead, resulted in a worse workability and an increase of the setting times. The mortar with addition of 10% vol. leaves (Le_10*) was the heaviest to work even if a bit less sticky than the reference mortar and showed the highest retarding effect on final setting time. The addition of flowers also increased the heaviness of the mortar introducing a little retard in both first and second setting times. The mortar with addition of bark was found as dense as the reference mortar but slightly stickier. The bark introduced a delay in setting times very similar to the one introduced by flowers, almost doubling the REF times. The mortar Br_10* with addition of acacia branchlets, was less heavy than the REF but stickier, with an important retarding effect. The bulk density and consistency by flow table of the mortars were slightly lower than the REF., except for mortars with addition of flowers and wood (Fl_10* and Wo_10*).

**Table 4.5.** Results of fresh state characterization of a second production.

| Mortar | REF | Fl_10* | Le_10* | Br_10* | Wo_10* | Ba_10* |
|---|---|---|---|---|---|---|
| FBD [kg/dm$^3$] | 1.656 | 1.664 | 1.654 | 1.653 | 1.666 | 1.643 |
| Flow [mm] | 155.0 | 143.0 | 139.0 | 145.5 | 139.8 | 147.3 |
| Heavy | REF | + | ++ | – | – | REF |
| Sticky | REF | REF | – | + | – | + |
| IST | 48′ | 1h11′ | 1h16′ | 2h03′ | 48′ | 1h20′ |
| FST | 1h20′ | 2h24′ | 6h35′ | 4h53′ | 1h23′ | 2h43′ |
| Crack | 0 | 1 | 2 | 2 | 0 | 0 |

Notation: FBD – fresh bulk density; Flow – Flow table consistence; IST – initial setting time; FST – final setting time; REF – control mortar; + slightly higher than REF; + + higher than REF; – slightly lower than REF; 0 – no cracks; 1 – small cracks; 2 – cracks.

It is possible that the higher fresh bulk density of the two mortars depends on the higher amount of water retained by these fraction particles (high water holding capacity from **Table 4.3**) and on the capability of the biomass grains to find space in the voids of the gypsum matrix, with the consequent result of compacting the mortar instead of expanding it (low circularity index). The amount of fraction (mass) added in each formulation differs according to their bulk density. For the fixed volume of 10%, the bark fraction is the heaviest addition and the wood fraction the lightest. It is expected, for this reason, that for the fixed amount of gypsum and water, the fresh bulk density of Ba_10* and Wo_10*, still lower than the REF, are respectively the highest and the lowest. Nevertheless, this hypothesis is not verified due to the combined effect of other properties deeper investigated in this section.

To investigate if there is any (linear) correlation between the physical properties of the biomass fractions and the fresh bulk density of the plastering mortars and quantify it, a statistical

analysis was run. The Pearson's correlation coefficient ($r_P$) was calculated as the covariance of the two compared properties divided by the product of their variance. The analysis was applied to quantify if there is a positive (+1), negative (-1) or weak (0) linear relation. The correlation matrix for the mortars from the 2nd production is presented in **Table 4.6**.

**Table 4.6.** Pearson's correlation matrix for fresh bulk densities of mortars with 10% biomass from the 2nd production.

| | FBD_10* | LBD | WVHC | WHC | CE | Ci |
|---|---|---|---|---|---|---|
| **FDB_10*** | 1.00 | -0.93 | -0.07 | 0.88 | 0.64 | -0.87 |
| **LBD** | -0.93 | 1.00 | -0.27 | -0.78 | -0.59 | 0.94 |
| **WVHC** | -0.07 | -0.27 | 1.00 | -0.07 | -0.08 | -0.40 |
| **WHC** | 0.88 | -0.78 | -0.07 | 1.00 | 0.27 | -0.83 |
| **CE** | 0.64 | -0.59 | -0.08 | 0.27 | 1.00 | -0.52 |
| **Ci** | -0.87 | 0.94 | -0.40 | -0.83 | -0.52 | 1.00 |

Notation: FBD_10* – Fresh bulk density of the mortars with 10% biomass addition from the 2nd production; LBD – biomass loose bulk density; WVHC – biomass water vapor holding capacity; WHC – biomass water holding capacity; CE – circle equivalent diameter; Ci – circularity index.

In green the strong correlations ($r_P$ > ±0.70) between the fresh bulk densities of the mortars and the bulk densities of the fractions (negative), their water holding capacity (positive) and circularity index (negative): the addition of the biomass fractions increases the fresh bulk density as much as the loose bulk density of the biomass decreases; to higher water holding capacity of the fractions corresponds a higher fresh bulk density of the mortars; the rounder the grains the lower the fresh bulk density.

The mortars of the 1st production (**Table 4.4**) have lower fresh bulk density for higher amount of biomass addition and all the FBD are lower than the reference, as expected (REF>FBD_5>FBD_10). The Pearson's correlation coefficient evidences a weaker relation of the FBD (5% and 10%) with the properties of the biomass fractions. The difference is probably due to the different batch of premixed gypsum product and eventually to hygrothermal conditions of the production environment. Nevertheless, a strong correlation was found between the fresh bulk densities of the mortars produced with 5% and 10% by volume of biomass addition (**Table 4.7**) belonging to the same production.

**Table 4.7.** Pearson's correlation coefficient for fresh bulk densities of mortars from 1st and 2nd productions.

| | FBD5 | FBD_10 | FBD_10* | LBD | WVHC | WHC | CE | Ci |
|---|---|---|---|---|---|---|---|---|
| **FDB_5** | 1.00 | 0.97 | 0.29 | -0.57 | 0.62 | -0.06 | 0.46 | -0.43 |
| **FBD_10** | 0.97 | 1.00 | 0.30 | -0.54 | 0.57 | -0.09 | 0.62 | -0.43 |
| **FBD_10*** | 0.29 | 0.30 | 1.00 | -0.93 | -0.07 | 0.88 | 0.64 | -0.87 |

For both mortars with 5% and 10% addition there is a weak correlation with the loose bulk density of the biomasses and their water vapor permeability, circular equivalent diameter, and circularity. The correlation of the fresh bulk densities with the water holding capacity of the fraction is almost null.

#### 4.3.4.2 Thermal conductivity

The bulk density [40] and thermal conductivity, displayed in **Table 4.8**, of the reference mortar are 1.24 kg/dm$^3$ and 0.34 W/(m·K), respectively. The design value of thermal conductivity according to the EN 13279-1 [41] for gypsum plasters with density of 1.2 kg/dm$^3$ tested at 23°C and 50% RH is 0.43 W/(m·K) and according to the EN 1745 [52] (Table A.12 – P=50%) for other mineral binder plastering mortars [53] of the same density, tested at 10°C and dry conditions, is 0.33 W/(m·K). Thus, the result of 0.34 W/(m·K) at dry condition and temperature of 23°C is consistent with the values referred in the standards. Generally, the thermal conductivity is slightly decreased by the biomass addition, as the fractions have lower densities, although reductions are not very significant due to the small percentage by volume of biomass added on the studied mortars. The lowest thermal conductivity is observed with leaves addition, followed by branchlets and bark.

**Table 4.8.** Thermal conductivity of the analysed mortars and density at 28 days (mean value ± standard deviation).

| | REF | Fl_5 | Fl_10 | Le_5 | Le_10 | Br_5 | Br_10 | Wo_5 | Wo_10 | Ba_5 | Ba_10 |
|---|---|---|---|---|---|---|---|---|---|---|---|
| $\lambda_{DRY}$ [W/(mK)] | 0.342 ± 0.013 | 0.323 ± 0.015 | 0.285 ± 0.016 | 0.276 ± 0.005 | 0.269 ± 0.019 | 0.287 ± 0.015 | 0.298 ± 0.002 | 0.309 ± 0.035 | 0.315 ± 0.019 | 0.297 ± 0.006 | 0.300 ± 0.012 |
| $\rho_{DRY}$ [kg/dm$^3$] | 1.239 ± 0.003 | 1.237 ± 0.006 | 1.215 ± 0.005 | 1.211 ± 0.005 | 1.189 ± 0.004 | 1.229 ± 0.005 | 1.211 ± 0.003 | 1.243 ± 0.004 | 1.246 ± 0.005 | 1.239 ± 0.008 | 1.222 ± 0.004 |

The thermal conductivity of the mortars decreases ($r_P$= -0.83) at higher loose bulk densities of the fractions added at the 5% and increases for higher bulk densities of the hardened mortars ($r_P$=0.82), as expected. For the additions at 10% such a strong linear relation was not found. The tendency is the same with lower Pearson's coefficients (respectively -0.37 and 0.55), probably due to the higher amount of biomass introduced. The interaction between the gypsum matrix and the acacia grains possibly changes at higher volumes of addition. Nevertheless, the negative correlation of the mortars conductivity with their open porosity is stronger for the addition at 10% ($r_P$=-0.79) than at 5% by vol ($r_P$=-0.54).

#### 4.3.4.3 Water absorption by capillarity and drying

In **Figure 4.13** are displayed the first 24 h of mortars capillary absorption against the square root of time, after which all the curves were found horizontal. All the eleven mortars were produced with the same water–powder (premixed product) ratio and cured the same way. Thus, the capillary absorption differences found are caused by the biomass additions. It is evident that the mortars with higher addition (10%), especially bark and flowers, diverge from the reference behaviour more than mortars with only 5%. Fractions of flowers are responsible to speed up the capillary absorption and bark to slow it down. This result is consistent with the water holding capacity of the biomasses, being the flowers and the bark the highest and the lowest, respectively. The additions of *A. dealbata* fractions generally decrease the absorption velocity, not modifying or only slightly increasing the final amount of absorbed water (FWS). Only the mortars with wood additions (Wo_5 and Wo_10) show a value of FWS lower than the reference. The capillarity coefficient (CC) of the mortars was calculated according to their saturation time: faster saturations are seen in shorter time and present higher CC (**Table 4.9**).The correlation between the capillary coefficient of the mortars and water holding capacity of the fractions is stronger when 10% by volume is added ($r_P$= 0.92) and only for branchlet (both %) the same tendency is not observed.

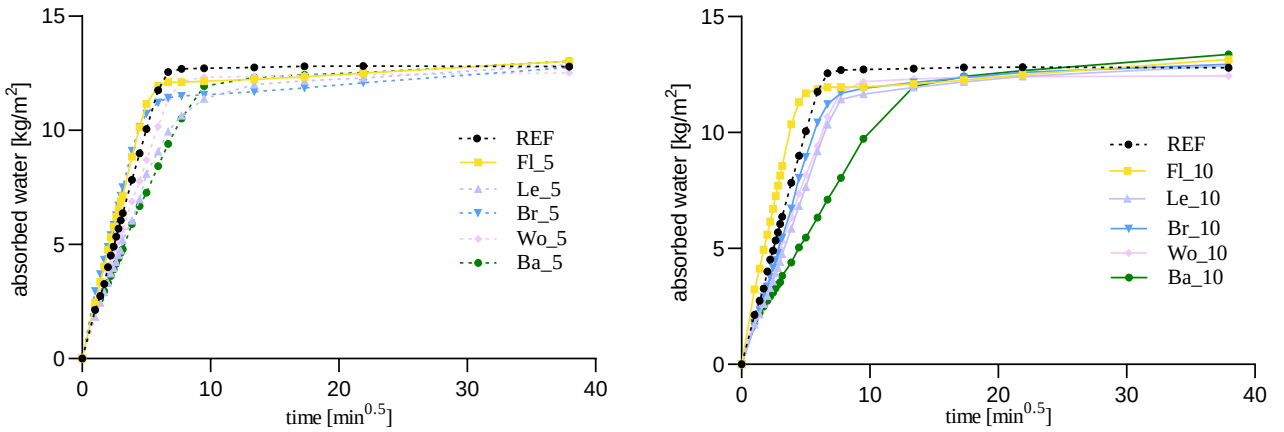


**Figure 4.13.** Water absorption by capillarity of reference mortar and mortars with 5% **(a)** and 10% **(b)** biomass addition.

The pores responsible for the capillary water absorption of mortars are the interconnected capillary pores, in the range of 0.1 – 10 μm, which form the open porosity together with the interconnected pores of sorption and coarse pores [54]. All the studied mortars have a very similar open porosity (**Table 4.4**), but their pore size distribution is probably different due to

the diversity of biomass fractions. Indeed, the fractions show different grain size distribution, i.e., bark with 56% wt. grains between 500 and 1000 μm and leaves with finer grains (48% in the range 200-500 μm), and shapes (the circularity index varying from 0.52 of flowers to 0.82 of branchlets). The shape of the particles can have an impact on the water absorption even if added in low quantities. Also, the different chemical composition of the fractions, showed in **Figure 4.11**, can have influenced the water behaviour of the plastering mortars. For example, bark is the only fraction with suberin which, even if detected in small quantities, can be responsible for the higher hydrophobicity showed by the bark plasters. In fact, the suberin percentage of the bark oven-dry-mass is around 5%, quite low if compared, for instance, with the average 40% present in cork from *Q. suber* [55, 56], but maybe still enough to reduce the capillary absorption of the plasters.

After capillary water absorption, the drying test started and took 17 days to reach constant mass. The final mass in some cases was found lower than the starting dry mass (negative values at the end of the drying curves in **Figure 4.14**). Due to the five days' capillary water absorption testing, a partial dissolution of gypsum occurred with loss of final weight. Generally, results from drying are consistent with results of capillary water absorption. The first phase of drying was defined for all the mortars during the first 480 min of drying and the second phase withing 5 days. The mortar FL_10 shows the highest slope of the second drying phase, that for this mortar only lasts 3 days.

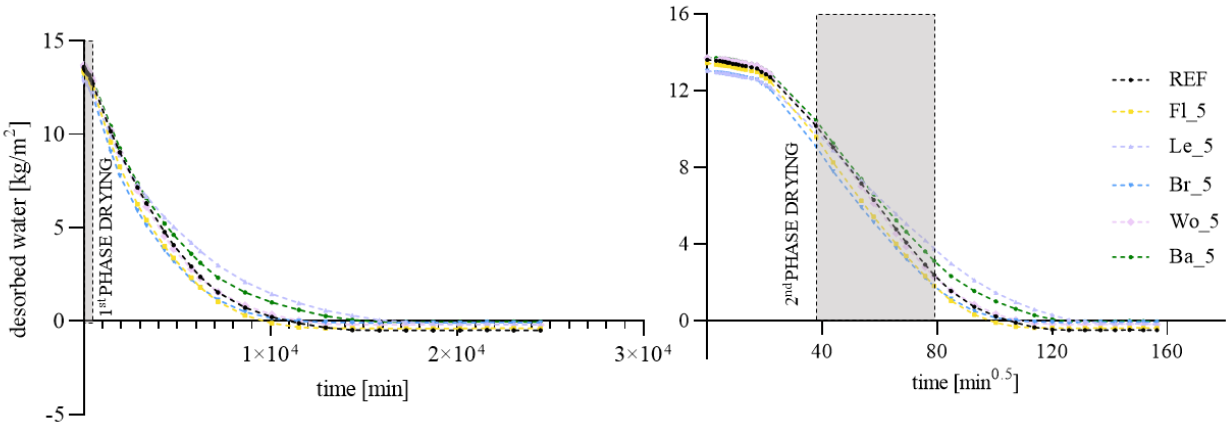


(a)

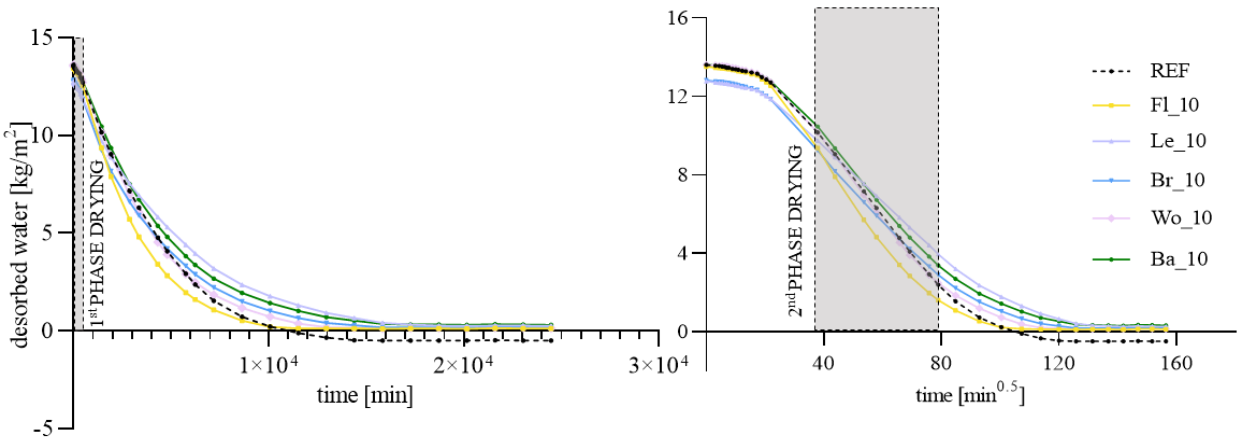


(b)

**Figure 4.14.** Drying curves of reference mortar and mortars with 5% **(a)** and 10% **(b)** biomass addition.

Generally, it was observed (**Table 4.9**) that to a slower/faster absorption (lower/higher CC) corresponds a slower/faster first drying phase, with rates $D_1$, not varying much when the addition is 5% or 10%. The second drying phase, with rates $D_2$, results more affected by the biomass introduction with a slower drying for higher additions (except for flowers). The slope of the reference mortar in the second phase of drying was the highest (excluding Fl_10), probably due to the greater speed of vapour transport in the empty voids.

**Table 4.9.** Capillarity coefficient (CC), free water saturation (FSW), drying index (DI), first (D1) and second (D2) drying rates: mean values (MV) and standard deviation (SD) on 3 specimens.

| Mortar | CC [g/(m²min$^{0.5}$)] | | $FWS_{(24\ h)}$ [kg/m²] | | DI [-] | | 1st drying rate $D_1$ [g/(m²h)] | | 2nd drying rate $D_2$ [g/(m²h$^{0.5}$)] | |
|---|---|---|---|---|---|---|---|---|---|---|
| | MV | SD | MV | SD | MV | SD | MV | SD | MV | SD |
| REF | 1.99 | ±0.05 | 12.79 | ±0.46 | 0.12 | ±0.03 | 0.114 | ±0.011 | 1.467 | ±0.032 |
| Fl_5 | 2.02 | ±0.04 | 13.03 | ±0.04 | 0.11 | ±0.01 | 0.120 | ±0.008 | 1.466 | ±0.043 |
| Fl_10 | 2.53 | ±0.15 | 13.16 | ±0.33 | 0.12 | ±0.00 | 0.120 | ±0.003 | 1.588 | ±0.075 |
| Le_5 | 1.48 | ±0.32 | 12.88 | ±0.33 | 0.18 | ±0.04 | 0.108 | ±0.010 | 1.139 | ±0.143 |
| Le_10 | 1.54 | ±0.02 | 12.88 | ±0.41 | 0.20 | ±0.02 | 0.111 | ±0.006 | 1.080 | ±0.016 |
| Br_5 | 2.15 | ±0.21 | 12.75 | ±0.19 | 0.12 | ±0.02 | 0.120 | ±0.003 | 1.373 | ±0.099 |
| Br_10 | 1.79 | ±0.17 | 12.95 | ±0.51 | 0.16 | ±0.02 | 0.121 | ±0.005 | 1.185 | ±0.087 |
| Wo_5 | 1.69 | ±0.06 | 12.52 | ±0.20 | 0.12 | ±0.01 | 0.100 | ±0.005 | 1.431 | ±0.086 |
| Wo_10 | 1.59 | ±0.03 | 12.45 | ±0.36 | 0.15 | ±0.01 | 0.108 | ±0.002 | 1.387 | ±0.035 |
| Ba_5 | 1.40 | ±0.11 | 13.03 | ±0.72 | 0.16 | ±0.00 | 0.103 | ±0.005 | 1.380 | ±0.123 |
| Ba_10 | 1.03 | ±0.03 | 13.37 | ±0.39 | 0.18 | ±0.02 | 0.106 | ±0.001 | 1.242 | ±0.029 |

#### 4.3.4.4 Hygroscopic behaviour

##### 4.3.4.4.1 Sorption Isotherms

The sorption isotherms of the eleven plastering mortars are displayed in **Figure 4.15**. The addition of the different fractions of *A. dealbata* influences the hygroscopic behaviour of the mortars proportionally when added at 5% and 10%. The biomass waste that introduces the highest adsorption capacity is the bark, followed by leaves, branchlets, flowers and wood in decreasing order. As expected, the reference mortar is found the least hygroscopic with a maximum moisture content, at 95% RH, equal to 0.42% wt. This result agrees with results from a previous study [8], where a finishing paste of only gypsum adsorbed 0.48% wt at 95% RH. At the same RH exposure, the mortar Ba_10 shows a moisture content of 1.85% wt, four times higher than the REF. At lower RH values, like 70% or 80% RH, the gap between the mortars Ba_10 and REF is already notable and means that the modified plaster would ensure a better performance than the reference one at steady state also in a mild environment. Nevertheless, the addition of all the fractions introduces an enhancement of the hygroscopic behaviour at steady state considering that the lowest percentage of addition of the less hygroscopic fraction (wood) still adsorbs 1.5 times more than the reference mortar.

Considering results from **Table 4.3**, the bark has the highest water vapour holding capacity, followed by flowers, wood, branchlets and leaves. Thus, no direct correlation between the hygroscopic behaviour of the mortars and the water holding capacity of the respective added fractions is found, except for bark. For this reason, the Pearson's correlation matrix for the adsorbed moisture content of the plasters exposed at 50%, 70%, 80% and 95% RH, the water holding capacity and water vapor holding capacity of the biomass fractions were calculated and displayed in **Table 4.10**. The correlation is very strong between the moisture contents at different RH exposure and results also strong between the moisture contents and the water holding capacity of the biomass fractions. It is supposed, then, a condensation phenomenon inside the gypsum-based porous matrix that brings liquid water in contact with the biomass. Generally, the highest the RH of exposure, the highest the correlation and, as expected, mortars with higher amounts of biomass (10%) have higher correlation factors between the moisture uptaken and the water holding capacity of the fractions.

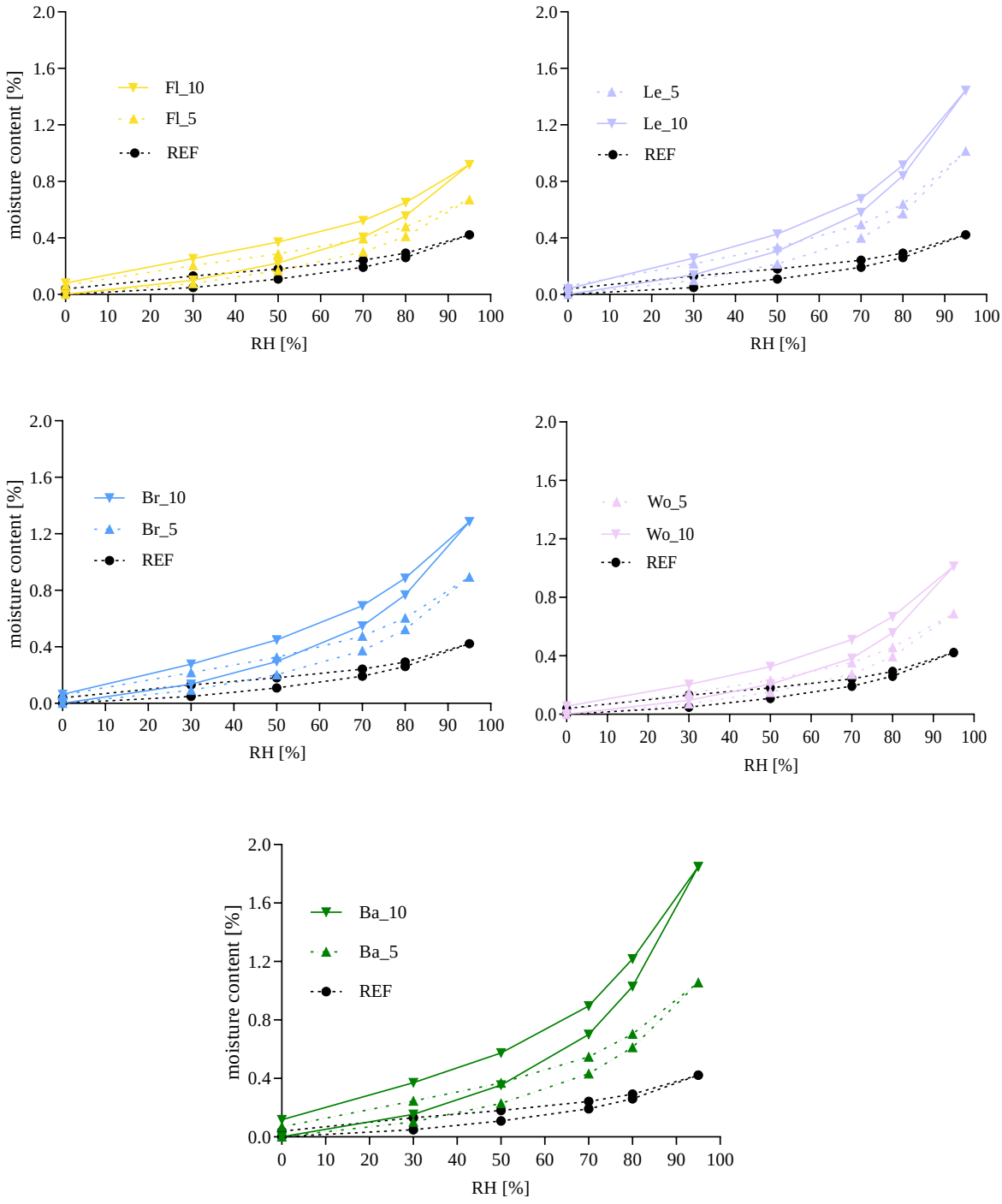


**Figure 4.15**. Sorption isotherms of the plastering mortars: REF, flowers (Fl), leaves (Le), branchlets (Br), wood (Wo) and bark (Ba).

**Table 4.10.** Pearson's correlation matrix of plasters moisture content for different RH exposures and biomass water and water vapor holding capacities.

| | | $M_{50\%}$ | $M_{70\%}$ | $M_{80\%}$ | $M_{95\%}$ | WHC | WVHC |
|---|---|---|---|---|---|---|---|
| 5% | $M_{50\%}$ | 1.00 | 1.00 | 0.99 | 0.97 | -0.74 | -0.12 |
| | $M_{70\%}$ | 1.00 | 1.00 | 1.00 | 0.98 | -0.77 | -0.10 |
| | $M_{80\%}$ | 0.99 | 1.00 | 1.00 | 0.99 | -0.80 | -0.14 |
| | $M_{95\%}$ | 0.97 | 0.98 | 0.99 | 1.00 | -0.79 | -0.21 |
| | WHC | -0.74 | -0.77 | -0.80 | -0.79 | 1.00 | -0.07 |
| | WVHC | -0.12 | -0.10 | -0.14 | -0.21 | -0.07 | 1.00 |
| 10% | $M_{50\%}$ | 1.00 | 1.00 | 0.99 | 0.96 | -0.84 | -0.04 |
| | $M_{70\%}$ | 1.00 | 1.00 | 1.00 | 0.98 | -0.85 | 0.02 |
| | $M_{80\%}$ | 0.99 | 1.00 | 1.00 | 0.99 | -0.87 | 0.03 |
| | $M_{95\%}$ | 0.96 | 0.98 | 0.99 | 1.00 | -0.90 | 0.09 |
| | WHC | -0.84 | -0.85 | -0.87 | -0.90 | 1.00 | -0.07 |
| | WVHC | -0.04 | 0.02 | 0.03 | 0.09 | -0.07 | 1.00 |

Notation: $M_{x\%}$ – mass variation (%) in equilibrium with X% RH; WHC – biomass water holding capacity; WVHC – biomass water vapor holding capacity.

#### 4.3.4.4.2 Moisture buffering

The mass variation from the last three cycles of 75%-50% RH exposures [47] is shown in **Figure 4.16**. Results are consistent with the sorption curves, with approx. 40 g/m$^2$ of moisture gained at the end of every cycle from the mortars Ba_10 and Le_10, about three times the reference mortar. After 9 h of adsorption the moisture capacity of the REF is saturated whereas all the other formulations can keep adsorbing. A better hygroscopic response of the plasters with the biomass addition is confirmed. The negative values at the end of the desorbing phase of the second cycle can depend on: the experimental conditions (i.e. the climatic chamber getting to lower RH than set); the plasters themselves which could not have completely reached the quasi steady state; a combination of these factors. However, the negative variation observed represents an unfavourable starting point for the next adsorbing phase, which registered the same behaviour and peak values of the previous cycle.

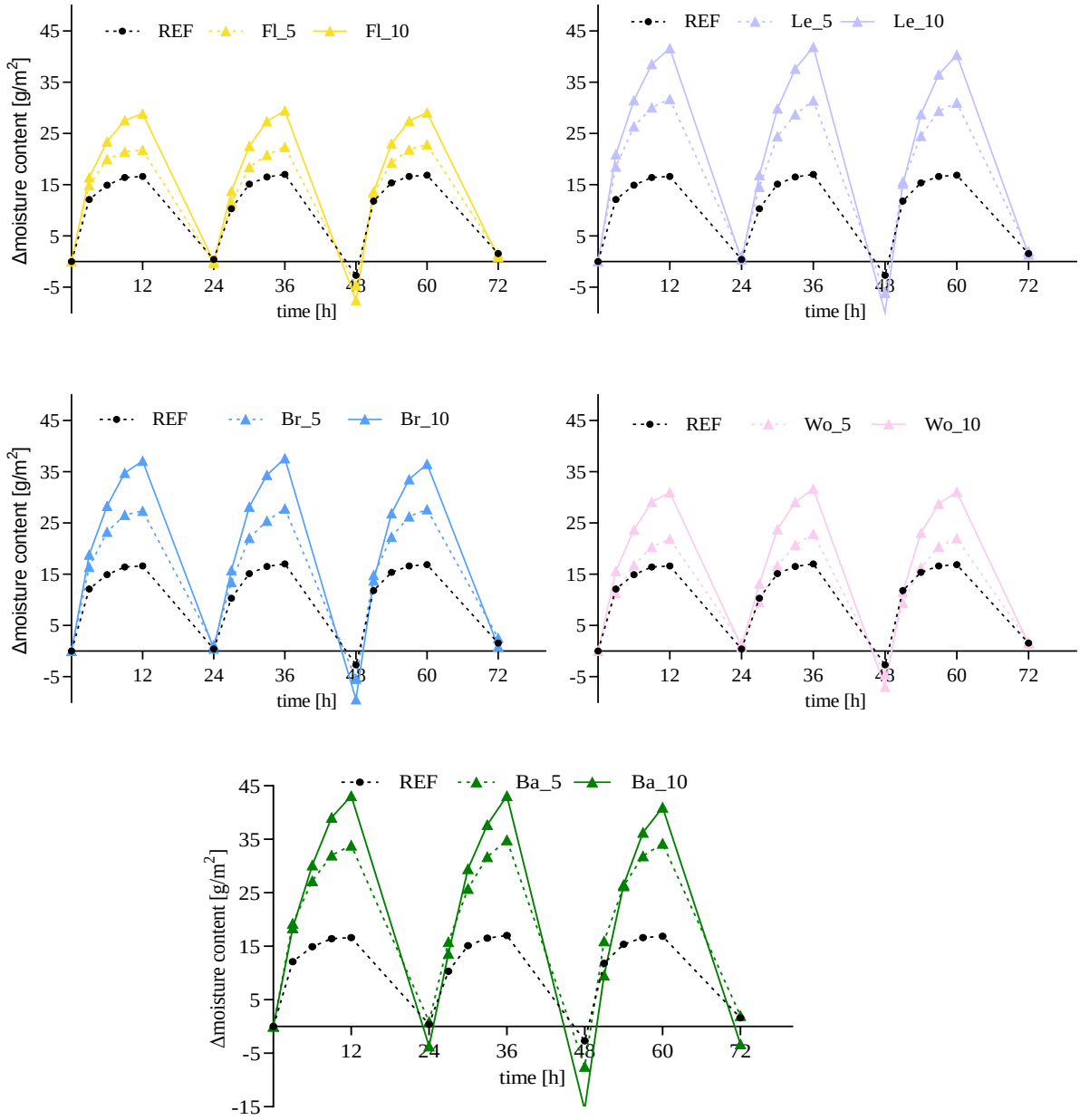


**Figure 4.16.** Mass variation for unit surface during the last three cycles of moisture adsorption/desorption of plastering mortars: REF and with flowers (Fl), leaves (Le), branchlets (Br), wood (Wo) and bark (Ba).

The moisture buffering value was calculated on the average value of the last three adsorption and desorption cycles (the same showed in **Figure 4.16**) referred to the RH step (25% RH) applied. In **Figure 4.17**, MBV results are displayed together with limits from NORDTEST [48] from *moderate* MBV in the range of 0.5 and 1.0 kg/(m$^2$%RH) to *good* classification, 1.0 < MBV < 2.0 kg/(m$^2$%RH). *Excellent* class is not observed because no MBV are found to exceed 2.0 kg/(m$^2$%RH). The MBV in some cases almost triplicates with the addition of 10% of biomass. The higher percentage of addition corresponds to higher moisture buffer capacity and the

enhancement is greater for some fractions than others. Testing daily cyclic adsorption/desorption at quasi steady state confirms results from sorption isotherms: the biomass from *A. dealbata* that improves the most the hygroscopic behaviour of the mortar is bark, followed by leaves and branchlets. The addition of this fractions at 10% by volume turns the gypsum plaster competitive in terms of MBV with earth-based plasters (from some references [56] their range is reported also in **Figure 4.17** for comparison) which are referred as the most hygroscopic plasters.

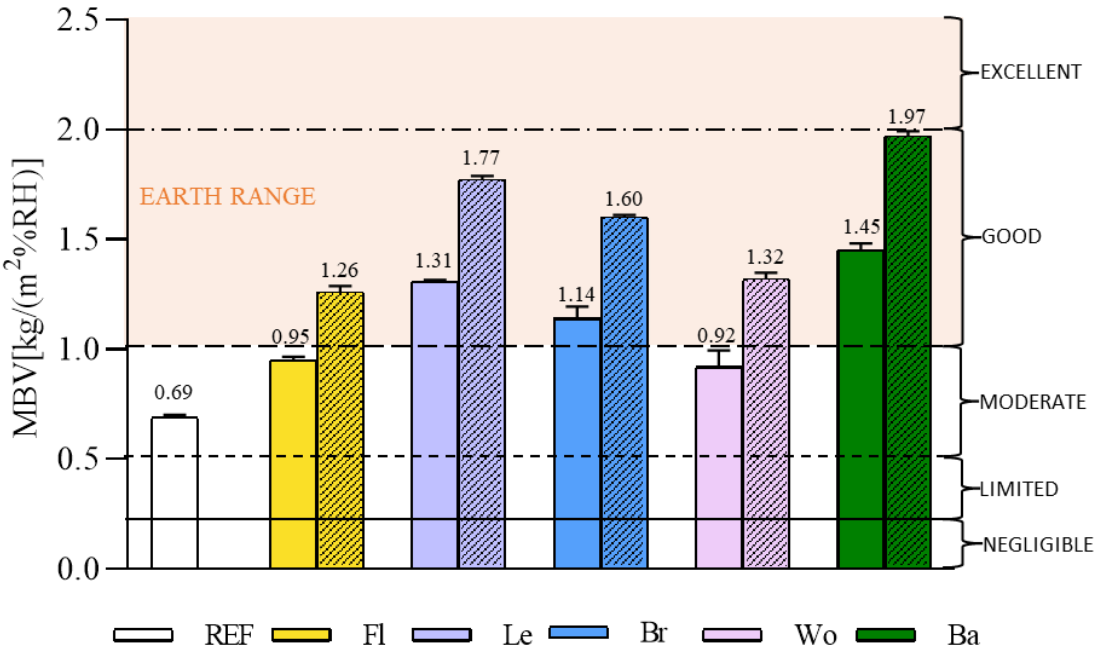


**Figure 4.17.** Moisture Buffering Value of the REF and mortars with 5% (solid) and 10% (dashed) biomass, limits from NORDTEST [48] and range for earth plasters [56].

#### 4.3.4.5 Biological susceptibility

Although the good results obtained in terms of hygroscopic behaviour, an important drawback was found regarding the mortars' biological colonization. The extractives previously removed from the biomass are phenolic compounds that could indeed contribute to the inhibition of biological growth, but their previous removal is the first step of biomass valorisation in a circular economy perspective. The resulting waste biomass contains lignocellulosic polymers that can be a substrate for fungal development, namely for the fungi existing in atmospheric air and in the environment in general. Also, the exposure of the biomass to moisture during mortar preparation can create the conditions for the development of spores existing in the biomass itself. It is important to remember that contrary to what is recommended whenever

bio-sourced wastes are used in plastering mortars (oral information from producers and professionals, and commonly implemented *in situ* and when testing in laboratory), the specimens were dried in a non-ventilated laboratory. Nevertheless, the different parts of the plant *Acacia dealbata* did not introduce the same rate of mould growth in the mortars. Pictures of the circular specimens and their optical microscope observations are displayed in **Figure 4.18**. The only mortars without moulds growth on their surface, apart from the reference one, are the mortars with wood fraction, Wo_5 and Wo_10 (for this reason not listed in **Figure 4.18**). Moreover, to higher content of biomass corresponds a higher mould development in most cases (only the addition of bark does not show this tendence) quantified according to ASTM [49] in **Table 4.11**. Thus, the biomass can be considered, in almost all its fractions, a good substrate for microorganisms. The different development is probably related with a specific component, present in higher quantities in leaves, branchlets and flowers, less observed in bark and almost absent in wood. Referring to chemical composition of the different parts of *A. dealbata*, according to López-Hortas *et al.* [30] the tannin contents are very low in the wood and sapwood of this species, and this could have inhibited the biological growth for plasters with the additions (5% and 10%) of the wooden fraction.

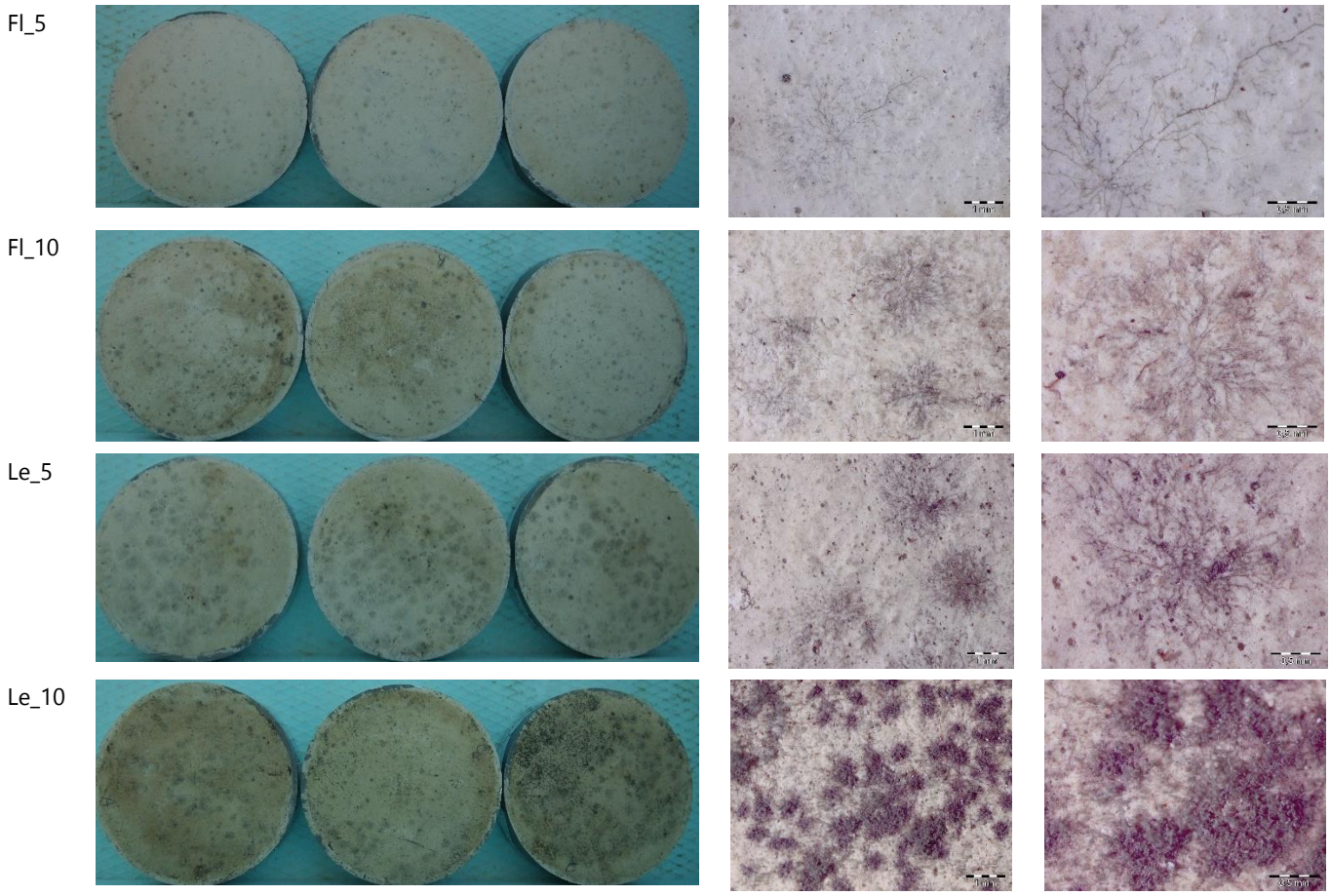

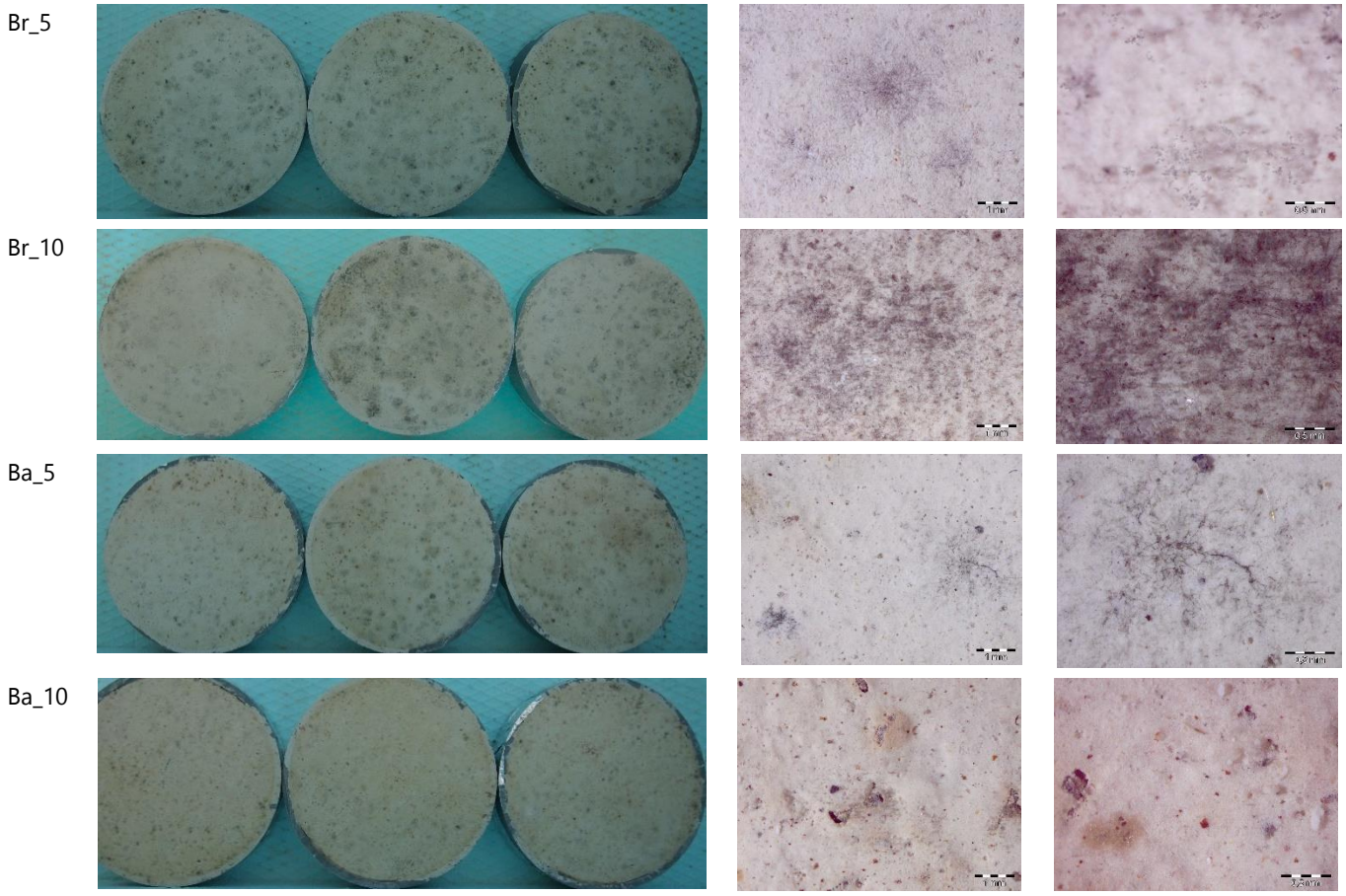


**Figure 4.18.** Pictures of the biological development on mortars surfaces and optical microscope observation of the same.

**Table 4.11.** Classification of mould growth based on ASTM D5590-17 [49].

| ASTM | REF | Fl_5 | Fl_10 | Le_5 | Le_10 | Br_5 | Br_10 | Wo_5 | Wo_10 | Ba_5 | Ba_10 |
|---|---|---|---|---|---|---|---|---|---|---|---|
| Class | 0 | 2 | 3 | 3 | 4 | 3 | 4 | 0 | 0 | 1 | 1 |

Notation: 0 – None; 1 – Traces of growth (<10 %); 2 – Light growth (10–30 %); 3 – Moderate growth (30–60 %); 4 – Heavy growth (60 % to complete coverage).

The biological growth appears after the first 14 curing days, when the specimens were left curing in a low ventilated and relatively high moisturized environment. After that no further development of moulds/fungi was observed but to ensure the process would not evolve, all the specimens were kept 24 hours in oven, at 60˚C, before being tested to hygroscopic behavior. After the tests in the climatic chamber exposed to high RH values like 95%, no sign of further biological development was observed on the surfaces. Either the thermal treatment works on the specific species present on the surface (no analysis was run yet for the identification), or the growth is only related with the drying of kneading water. To address this problem, the recommendation of ensuring a ventilated conditioning of the plaster specimens

may be fundamental; furthermore, a thermal treatment of the biomass can be considered to turn it a poorer substrate or any action targeting the pH of the mortar, like for example some lime addition to increase it.

### 4.3.5 Statistical analysis

Even if only three specimens (and relative results) were available for each formulation, a MANOVA (multivariate analyses of variance) has been carried out (software: IBM-SPSS Statistics) to test the statistical significance between the analysed properties of mortars. The independent variable considered are the mortars (REF, Ba5, Ba10, Br10, Br5, Fl10, Fl5, Le10, Le5, Wo10, Wo5) and the dependent variables are the properties, namely: open porosity (OP), moisture buffering value (MBV), capillarity coefficient (CC), drying index (DI), thermal conductivity in dry condition (λ) and dry density (ρ). The significance (*p-value*) was set at $p < 0.05$ and the multiple comparisons have been calculated with Bonferroni adjustment. **Table 4.12** reports the mean differences and *p-values* of the comparisons between the reference mortar (REF) and all the other formulations. Positive mean differences point out that, for the analysed property, the reference mortar has higher result than the compared modified one; negative mean differences indicate the opposite.

**Table 4.12.** MANOVA results of mean differences and *p-values* for the comparison of the reference mortar vs modified formulations.

| | | Ba10 | Ba5 | Br10 | Br5 | Fl10 | Fl5 | Le10 | Le5 | Wo10 | Wo5 |
|---|---|---|---|---|---|---|---|---|---|---|---|
| OP [%] | mean difference | .882 | 1.083 | -.292 | -.378 | -1.372 | .059 | -1.393 | -.837 | .226 | 1.108 |
| | p-value | 1.000 | 1.000 | 1.000 | 1.000 | .920 | 1.000 | .844 | 1.000 | 1.000 | 1.000 |
| MBV | mean difference | -1.282* | -.753* | -.904* | -.451* | -.568* | -.255* | -1.078* | -.616* | -.629* | -.226* |
| [kg/(m²%RH)] | p-value | .000 | .000 | .000 | .000 | .000 | .000 | .000 | .000 | .000 | .000 |
| CC | mean difference | .961* | .585* | .198 | -.159 | -.542* | -.032 | .446* | .504* | .395 | .292 |
| [g/(m²min$^{0.5}$)] | p-value | .000 | .002 | 1.000 | 1.000 | .006 | 1.000 | .046 | .013 | .134 | 1.000 |
| DI [-] | mean difference | -.063 | -.038 | -.043 | .001 | -.001 | .014 | -.083* | -.058 | -.029 | -.003 |
| | p-value | .067 | 1.000 | .961 | 1.000 | 1.000 | 1.000 | .003 | .128 | 1.000 | 1.000 |
| $\lambda_{DRY}$ [W/(mK)] | mean difference | .041 | .045 | .044 | .055* | .056* | .018 | .073* | .065* | .027 | .032 |
| | p-value | .317 | .170 | .218 | .030 | .022 | 1.000 | .001 | .005 | 1.000 | 1.000 |
| $\rho_{DRY}$ [kg/dm³] | mean difference | .0145 | -.0199 | .0256 | .0015 | .0010 | -.0100 | .0499* | .0114 | -.0071 | -.0115 |
| | p-value | 1.000 | 1.000 | .551 | 1.000 | 1.000 | 1.000 | .001 | 1.000 | 1.000 | 1.000 |

Notation: * - values statistically significant.

No significant (statistically) difference is found for the open porosity (and the dry density) of the mortars, with a *p-value* often equal to 1 and never below 0.05. The water absorption by capillarity of the mortars differs significantly from the reference mortar with the addition of bark (5% and 10%), leaves (5% and 10%) and flowers (only 10%) with the general effect of

increasing the capillarity coefficient (apart from flowers at 10%). The drying index, instead, does not report any significant variation except for the formulation with leaves at 10%, the only one showing a significative difference from the reference with a higher drying index. For what concerns the thermal conductivity, according to the statistical analysis, a significant decrease of the property is introduced with the addition of leaves (both at 5% and 10%), of branchlets at 5% and flower at 10%. The moisture buffering of all the modified mortars is found significantly different from the reference one, with a general increase of the property due to the additions.

Moreover, a MANOVA has been run to test if the variation on percentage of addition (5% and 10%) influences the analysed properties (OP, MBV, CC, DI, λ and ρ). The statistical model has been built considering the mortars (Fl, Le, Wo, Br, Ba) and the percentage of addition (5% vs 10%) as the independent variables. Due to research purposes, the model tested only the interaction effect of the two independent variables on the considered properties. **Table 4.13** reports the mean differences and *p-values* of the pairwise comparisons between the different percentages for each fraction (5% vs 10%).

**Table 4.13.** Mean differences and *p-values* for results of mortars with the same fraction addition at 5% vs 10%.

| | | Fl | Le | Br | Wo | Ba |
|---|---|---|---|---|---|---|
| **OP [%]** | mean difference (5% vs 10%) | -1.430* | -.555 | .086 | -.882 | -.201 |
| | p-value | .006 | .243 | .854 | .070 | .667 |
| **MBV** | mean difference (5% vs 10%) | -.313* | -.461* | -.453* | -.402* | -.529* |
| **[kg/(m²%RH)]** | p-value | .000 | .000 | .000 | .000 | .000 |
| **CC** | mean difference (5% vs 10%) | -.510* | -.059 | .357* | .102 | .376* |
| **[g/(m²min$^{0.5}$)]** | p-value | .000 | .631 | .008 | .405 | .005 |
| **DI [-]** | mean difference (5% vs 10%) | -.015 | -.025 | -.044* | -.027 | -.024 |
| | p-value | .343 | .121 | .010 | .104 | .133 |
| **$\lambda_{DRY}$ [W/(mK)]** | mean difference (5% vs 10%) | .038* | .008 | -.011 | -.005 | -.004 |
| | p-value | .012 | .586 | .431 | .712 | .799 |
| **$\rho_{DRY}$ [kg/dm³]** | mean difference (5% vs 10%) | 0.011 | 0.039* | 0.024* | 0.004 | 0.034* |
| | p-value | .261 | .001 | .019 | .652 | .002 |

Notation: * - values statistically significant.

Overall, the most affected property from the addition of 10% by volume of a fraction instead of the 5% is found to be the MBV, always significative with positive effect (increase in MVB) of higher additions. The dry density of the mortars decreases when 10% of leaves, branchlet and bark are added instead of 5% but the increase in addition for the other fractions is not significantly affecting the property. The thermal conductivity decreases when flowers are added at 10% instead of 5%, and the drying index increases when branchlet are added at 10%. The

percentage variation for all the other fractions is not found statistically significant for these two properties. The coefficient of capillarity statistically differs for flowers, branchlet and bark added at 5% or 10%. The open porosity is higher for the addition of flowers at 10% vs 5%, but the % variation has no significative effect on open porosity for all the other additions.

### 4.3.6 Conclusions

So far, gypsum plastering mortars seem to have a low moisture buffering value (MBV) when compared with other plasters and other building materials used for coatings. At the same time these mortars are very often used to coat indoor walls and ceilings as much in historic, traditional constructions as in new designs. The MBV of building materials, especially when directly exposed to indoor air in large areas, can be a key factor for indoor passive regulation of relative humidity and, consequently, comfort enhancement without energy consumption increase. The purpose to improve the MBV of gypsum plasters was combined, in the present work, with the intent of reusing a second-generation biowaste from pharmaceutical and cosmetic industry. The by-product consists in five different fractions of the same plant, the *Acacia Dealbata* that, after minimal treatment (milling and sieving), were added to mortars formulation in two different percentages: 5% and 10% by vol. of a powder premixed gypsum-based plastering mortar product.

The results of the study evidence that a major enhancement of the hygroscopic behaviour both in static and dynamic conditions is found for all the modified mortars (compared with the reference one). Generally, the addition at 10% by vol. introduces a greater change in the mortars' MBV (according to the statistical analysis). Above all the fractions, the bark is the most hygroscopic, introducing an increase in the gypsum mortar up to four and three times the reference when tested respectively at steady state or quasi steady state. The thermal conductivity of the plasters is only slightly modified by the fractions, as already expected for the low amount of biomass added. For what concerns the response to liquid water: the biomass addition slows down the capillary absorption of the mortars (not significant for wood and branchlet addition) but also their drying capacity (statistically significant only for leaves at 10%), and the final amount of absorbed water is almost not modified. The main drawback observed was the biological growth during the first 14 curing days. The causes for the growth can be environmental factors, for instance the kneading water and low ventilation of the curing room, and biological factors related with the chemical composition of the biomasses or a combination of both.

To conclude, among all the eleven mortars here analysed, the one resulting from bark addition at 10% by vol. shows a great hygroscopic behaviour (MBV in the range of earth-based plasters), a slightly higher thermal insulation capacity and the slowest absorption by capillarity, although also of drying capacity (1st phase). It is given to further studies to better investigate how to prevent the risk of biological attack, which is found the main drawback of the modified mortars. It is recommended to continue the study ensuring a ventilated hardening period and modifying the formulation of the mortars to obtain a less favourable substrate for the mould growth (i.e., with a more alkaline pH) or modifying the biomass itself before adding it to the mortars (i.e., applying a thermal treatment). It is not excluded that the combination of more measures will be more effective for the purpose, thus, further studies will be intended to find the best solution.

### Funding

This research was supported by Portuguese Foundation for Science and Technology: PD/BD/150399/2019 – 1st author Doctoral Training Programme EcoCoRe, UIDB/04378/2020 - Civil Engineering Research and Innovation for Sustainability Unit-CERIS, UIDB/04077/2020 – Mechanical Engineering and Research Sustainability Center – METRICS and UIDB/05064/2020 - Research Centre for Endogenous Resource Valorization – VALORIZA.

### Acknowledgments

The authors would like to thank the National Laboratory for Civil Engineering of Portugal (LNEC) for the laboratory equipment and the support provided through the projects REuSE - Wall coverings for Rehabilitation: Safety and Sustainability; the Departments of Civil Engineering and Chemistry of the NOVA School of Science and Technology of the NOVA University of Lisbon, and the Department of R&D of SIVAL-Gessos Especiais, Lda.

## References

1. M.T. Freire, M.R. Veiga, A. Santos Silva, J. de Brito, Restoration of ancient gypsum-based plasters: Design of compatible materials, Cement and Concrete Composites, 120 (2021), 104014. https://doi.org/10.1016/j.cemconcomp.2021.104014.
2. P. Malta da Silveira, M.R. Veiga, J. de Brito, Gypsum coatings in ancient buildings, Construction and Building Materials, 21-1 (2007) 126-131, ISSN 0950-0618, https://doi.org/10.1016/j.conbuildmat.2005.06.035.

3. M. T. Freire, M.R. Veiga, A. Santos Silva, J. de Brito, Studies in ancient gypsum based plasters towards their repair: Physical and mechanical properties, Construction and Building Materials, 202 (2019) 319-331. https://doi.org/10.1016/j.conbuildmat.2018.12.214.
4. M. Caroselli, G. Cavallo, A. Felici, S. Luppichini, G. Nicoli, L. Aliverti, G. Jean, Gypsum in Ticinese stucco artworks of the 16–17th century: Use, characterization, provenance and induced decay phenomena, Journal of Archaeological Science: Reports, 24 (2019) 208-219, ISSN 2352-409X, https://doi.org/10.1016/j.jasrep.2019.01.009.
5. H. Cotrim, M.R. Veiga, J. de Brito, Freixo palace: Rehabilitation of decorative gypsum plasters, Construction and Building Materials, 22-1 (2008) 41-49, ISSN 0950-0618, https://doi.org/10.1016/j.conbuildmat.2006.05.060.
6. M.P. Sáez-Pérez, J.A. Durán-Suárez, A. Verdú-Vázquez, T. Gil-López, Study and characterization of special gypsum-based pastes for their use as a replacement material in architectural restoration and construction. *Materials*. 15(17) (2022), 5877. https://doi.org/10.3390/ma15175877.
7. J. Fořt, R. Černý, Carbon footprint analysis of calcined gypsum production in the Czech Republic, Journal of Cleaner Production, 177 (2018) 795-802, ISSN 0959-6526, https://doi.org/10.1016/j.jclepro.2018.01.002.
8. A. Ranesi, P. Faria, M.R. Veiga, Traditional and Modern Plasters for Built Heritage: Suitability and Contribution for Passive Relative Humidity Regulation. Heritage, 4 (2021) 2337-2355. https://doi.org/10.3390/heritage4030132.
9. J. Lima, P. Faria, R. Veiga, Comparison of an earth mortar and common binder mortars for indoor plastering. In: Horszczaruk, E.m Brzozowski, P. (eds.), Proceedings of the 2nd International Conference on Sustainable, Environmentally Friendly Construction Materials – ICSEFCM 2021 (2021), 71–76.
10. T. Santos, P. Faria, M.I. Gomes, 2021. Earth, Gypsum and Cement-Based Plasters Contribution to Indoor Comfort and Health. In: Pereira, E.B., Barros, J.A.O., Figueiredo, F.P. (eds.). Proceedings of the 3rd RILEM Spring Convention and Conference - RSCC2020. RILEM Bookseries, vol 32. Springer, Cham. https://doi.org/10.1007/978-3-030-76547-7_10
11. T. Santos, M.I. Gomes, A. Santos Silva, E. Ferraz, P. Faria, Comparison of mineralogical, mechanical and hygroscopic characteristic of earthen, gypsum and cement-based plasters, Construction and Building Materials, 254 (2020), 119222, ISSN 0950-0618, https://doi.org/10.1016/j.conbuildmat.2020.119222.

12. C. Maia Pederneiras, M.R. Veiga, J. de Brito, Impact resistance of rendering mortars with natural and textile-acrylic waste fibres. *Fibers*. 10-5 (2022) 44. https://doi.org/10.3390/fib10050044.
13. C. Brazão Farinha, J. de Brito, R. Veiga, Rendering Mortars with Low Sand and Cement Content. Incorporation of Sanitary Ware Waste and Forest Biomass Ashes. *Applied Sciences*. 10(9) (2020) 3146. https://doi.org/10.3390/app10093146.
14. M. del Río-Merino, A. Vidales-Barriguete, C. Piña-Ramírez, V. Vitiello, J. S. Cruz-Astorqui, R. Castelluccio, A review of the research about gypsum mortars with waste aggregates, Journal of Building Engineering, 45 (2022), 103338, ISSN 2352-7102, https://doi.org/10.1016/j.jobe.2021.103338.
15. M. Saeli, M.N. Capela, C. Piccirillo, D.M. Tobaldi, M.P. Seabra, F. Scalera, R. Striani, C. Esposito Corcione, T. Campisi, Development of energy-saving innovative hydraulic mortars reusing spent coffee ground for applications in construction, Journal of Cleaner Production, 399 (2023) 136664, https://doi.org/10.1016/j.jclepro.2023.136664.
16. S. Liuzzi, C. Rubino, P. Stefanizzi, F. Martellotta, The Agro-Waste Production in Selected EUSAIR Regions and Its Potential Use for Building Applications: A Review. *Sustainability*. 14(2) (2022) 670. https://doi.org/10.3390/su14020670.
17. M. Wang, Z. Lu, Study on the hygroscopic performances of poplar wood fiber biomass brick, International Communications in Heat and Mass Transfer. 135 (2022) 106063, ISSN 0735-1933, https://doi.org/10.1016/j.icheatmasstransfer.2022.106063.
18. P. Lorenzo, L. González, M.J. Reigosa, The genus Acacia as invader: the characteristic case of Acacia dealbata Link in Europe. Ann. For. Sci. 67 (2010) 101. https://doi.org/10.1051/forest/2009082.
19. J. Domingues de Almeida, H. Freitas, Exotic naturalized flora of continental Portugal – A reassessment. Botanica Complutensis 30 (2006) 117-130.
20. M.M. Fernandes, N. Devy-Vareta, H. Rangan (In Portuguese) Invasive exotic plants and territorial management tools. The paradigmatic case of the genus Acacia in Portugal. GOT, nr. 4 – Geography and Spatial Planning Journal (December 2013). Center for Studies in Geography and Spatial Planning, (2013) 83-107.
21. L.J.R. Nunes, M.A.M. Raposo, C.I.R. Meireles, C.J.P. Gomes, N.M.C.A. Ribeiro, the impact of rural fires on the development of invasive species: analysis of a case study with Acacia dealbata Link. in Casal do Rei (Seia, Portugal). Environments 8 (2021) 44. https://doi.org/10.3390/environments8050044.

22. L. Dessì, L. Podda, G. Brundu, V. Lozano, A. Carrouée, E. Marchante, H. Marchante, Y. Petit, M. Porceddu, G. Bacchetta, Seed germination ecophysiology of acacia dealbata link and acacia mearnsii de wild.: two invasive species in the mediterranean basin. Sustainability 13 (2021), 11588. https://doi.org/10.3390/su132111588.
23. O. Cruz, S.F. Riveiro, D. Arán, J. Bernal, M. Casal, O. Reyes, Germinative behaviour of Acacia dealbata Link, Ailanthus altissima (Mill.) Swingle and Robinia pseudoacacia L. in relation to fire and exploration of the regenerative niche of native species for the control of invaders, Global Ecology and Conservation, 31 (2021). https://doi.org/10.1016/j.gecco.2021.e01811.
24. P. Lorenzo, J. Rodríguez, L. González, S. Rodríguez-Echeverría, Changes in microhabitat, but not allelopathy, affect plant establishment after *Acacia dealbata* invasion. Journal of Plant Ecology, 10(4) (2017) 610–617. doi: 10.1093/jpe/rtw061.
25. L. Minuto, G. Casazza, D. Dagnino, M. Guerrina, C. Macrì, E. Zappa, M.G. Mariotti, Reproductive traits of the invasive species *Acacia dealbata* LINK. in the Northern Mediterranean basin. *Ann. Bot.,* 10 (2020) 13–20. doi: 10.13133/2239-3129/15642.
26. L.J.R. Nunes, C.I.R. Meireles, C.J.P. Gomes, N.M.C.A. Ribeiro, Acacia dealbata Link. Aboveground Biomass Assessment: Sustainability of Control and Eradication Actions to Reduce Rural Fires Risk. Fire, 5 (2022) 7. https://doi.org/10.3390/fire5010007.
27. L.J.R. Nunes, M.A.M. Raposo, C.I.R. Meireles, C.J. Pinto Gomes, N.M.C.A. Ribeiro. Control of Invasive Forest Species through the Creation of a Value Chain: Acacia dealbata Biomass Recovery. Environments, 7(5) (2020) 39. https://doi.org/10.3390/environments7050039.
28. A. Borges, H. José, V. Homem, M. Simões, Comparison of techniques and solvents on the antimicrobial and antioxidant potential of extracts from Acacia dealbata and Olea europaea. Antibiotics (Basel), 9(2) (2020) 48. doi:10.3390/antibiotics9020048.
29. R. Correia, J.C. Quintela, M.P. Duarte, M. Gonçalves, Insights for the valorization of biomass from Portuguese invasive *Acacia* spp. in a biorefinery perspective. *Forests,* 11(12) (2020) 1342. https://doi.org/10.3390/f11121342.
30. [30] L. López-Hortas, I. Rodríguez-González, B. Díaz-Reinoso, M.D. Torres, A. Moure, H. Domínguez, Tools for a multiproduct biorefinery of *Acacia dealbata* biomass, Industrial Crops and Products, 169 (2021) 113655, ISSN 0926-6690. https://doi.org/10.1016/j.indcrop.2021.113655.
31. R. Correia, Development of an Acacia-based biorefinery – an advanced system for biomass valorization and environmental sustainability. PhD thesis, NOVA University Lisbon (2023).
32. J. Graça, J. Suberin: the biopolyester at the frontier of plants. Frontiers of Chemistry, 3 (2015) 62. DOI: 10.3389/fchem.2015.00062.

33. K. Koch, B. Bhushan, W. Barthlott, Diversity of structure, morphology and wetting of plant surface. Soft Matter, 4 (2008) 1943-1963. DOI: 10.1039/b804854a.
34. EN 1015-3; Methods of Test for Mortar for Masonry—Part 3: Determination of Consistence of Fresh Mortar (by Flow Table). European Committee for Standardization (CEN): Brussels, Belgium, 1999.
35. EN 1015-6; Methods of Test for Mortar for Masonry—Part 6: Determination of Bulk Density of Fresh Mortar. European Committee for Standardization (CEN): Brussels, Belgium, 1999.
36. EN 1015-10; Methods of Test for Mortar for Masonry—Part 10: Determination of Dry Bulk Density of Hardened Mortar. European Committee for Standardization (CEN): Brussels, Belgium,1999.
37. EN 1936; Determination of Real Density and Apparent Density and Total and Partial Open Porosity. European Committee for Standardization (CEN): Brussels, Belgium, 2007.
38. EN 14146; Natural Stone Test Methods. Determination of the Dynamic Modulus of Elasticity (by Measuring the Fundamental Resonance Frequency). European Committee for Standardization (CEN): Brussels, Belgium, 2004.
39. EN 1015-11; Methods of Test for Mortar for Masonry—Part 11: Determination of Flexural and Compressive Strength of Hardened Mortar. European Committee for Standardization (CEN): Brussels, Belgium, 1999.
40. A. Ranesi, P. Faria, R. Correia, M.T. Freire, R. Veiga, M. Gonçalves, Gypsum mortars with Acacia dealbata biomass waste additions: effect of different fractions and contents. Buildings, 12(3) (2022) 339. https://doi.org/10.3390/buildings12030339.
41. EN 13279-1; Gypsum Binders and Gypsum Plasters—Part 1: Definitions and Requirements. European Committee for Standardization (CEN): Brussels, Belgium, 2008.
42. EN 13279-2; Gypsum Binders and Gypsum Plasters—Part 2: Test methods. European Committee for Standardization (CEN): Brussels, Belgium, 2014.
43. E. Cintura, P. Faria, M. Duarte, L. Nunes, Bio-wastes as aggregates for eco-efficient boards and panels: screening tests of physical properties and bio-susceptibility. Infrastructures, 7 (2022) 26. https://doi.org/10.3390/infrastructures7030026.
44. EN 15801; Conservation of Cultural Property—Test Methods— Determination of Water Absorption by Capillarity. European Committee for Standardization (CEN): Brussels, Belgium, 2009.
45. Conservation of Cultural Heritage—Test Methods— Determination of Drying Properties. European Committee for Standardization (CEN): Brussels, Belgium, 2013.

46. ISO (International Standards Organization), ISO 12571: Hygrothermal performance of building materials and products - Determination of hygroscopic sorption properties. ISO, Geneva, Switzerland, 2013.
47. ISO (International Standards Organization), ISO 24353: Hygrothermal performance of building materials and products - Determination of moisture adsorption/desorption properties in response to humidity variation. ISO, Geneva, Switzerland, 2008.
48. C. Rode, R.H. Peuhkuri, L.H. Mortensen, K.K. Hansen, B. Time, A. Gustavsen, T. Ojanen, J. Ahonen, K. Svennberg, L.E. Harderup, J. Arfvidsson, (2005) Moisture buffering of building materials. Technical University of Denmark, Department of Civil Engineering. BYG Report, R-127.
49. ASTM D5590-17; Determining the Resistance of Paint Films and Related Coatings to Fungal Defacement by Accelerated Four-Week Agar Plate Assay. ASTM International: Pennsylvania, PA, USA, 2021.
50. A.H. Fujikawa, A.T. Itoh, Tailing of thermal inactivation curve of Aspergillus niger spores, Applied and Environmental Microbiology, 62(1)0 (1996) 3745-3749, doi:10.1128/aem.62.10.3745-3749.1996.
51. B. Andersen, J.C. Frisvad, R.R. Dunn, U. Thrane, A pilot study on baseline fungi and moisture indicator fungi in danish homes. J Fungi (Basel), 7(2) (2021) 71. https://doi.org/10.3390/jof7020071.
52. EN 1745; Masonry and masonry products - Methods for determining thermal properties. European Committee for Standardization (CEN): Brussels, Belgium, 2020.
53. EN 998-1; Specification for mortar for masonry - Part 1: Rendering and plastering mor-tar. CEN, Brussels, Belgium, 2016.
54. M. Thomson, J-E Lindqvist, J. Elsen, C.J.W.P. Groot, Chapter 2.5: Porosity of mortars. In: RILEM TC167-COM (eds.), Characterization of old mortars with respect to their repair, State-of-the-Art Report, November 2004.
55. A.L. Fonseca, C. Brazinha, H. Pereira, J.G. Crespo, O.M. Teodoro, Permeability of cork for water and ethanol. J Agric Food Chem., 61(40) (2013) 9672-9. DOI: 10.1021/jf4015729.
56. A. Ranesi, M. R. Veiga, P. Faria, Laboratory characterization of relative humidity dependent properties for plasters: A systematic review, Construction and Building Materials, 304 (2021) 124595, ISSN 0950-0618, https://doi.org/10.1016/j.conbuildmat.2021.124595.

## 4.4 Additional Considerations

Results from sections 4.2 and 4.3 evidence that all the additions increase the hygroscopic response of the gypsum reference mortar (both in static and dynamic conditions) without jeopardizing mechanical properties. In fact, the compressive and flexural strengths of all the modified plastering mortars are still complying with the requirements of EN 13279-1 (2008). Moreover, the addition of the different biomass fractions at 10% by vol. increases the moisture reactivity by more than 5%. Above all the fractions the greater enhancement is obtained by the addition of bark and an overall effect of slight hydrophobisation of the mortars is given by almost all the fractions. **Table 4.14** presents a synthesis of results of the properties related with water in liquid and vapor phase.

**Table 4.14.** Synthesis of results from hygroscopic and hygric behavior of plasters.

| Property | Unit | REF | Fl5 | Fl10 | Le5 | Le10 | Br5 | Br10 | Wo5 | Wo10 | Ba5 | Ba10 |
|---|---|---|---|---|---|---|---|---|---|---|---|---|
| Ads.* | [%] | 0.42 | 0.67 | 0.91 | 1.01 | 1.44 | 0.89 | 1.28 | 0.68 | 1.01 | 1.05 | 1.85 |
| MBV | [g/(m$^2$·%RH)] | 0.60 | 0.95 | 1.26 | 1.31 | 1.77 | 1.14 | 1.60 | 0.92 | 1.32 | 1.45 | 1.97 |
| CC | [g/(m$^2$min$^{0.5}$)] | 1.99 | 2.02 | 2.53 | 1.48 | 1.54 | 2.15 | 1.79 | 1.69 | 1.59 | 1.40 | 1.03 |
| $D_1$ | [g/(m$^2$h)] | 0.114 | 0.120 | 0.120 | 0.108 | 0.111 | 0.120 | 0.121 | 0.100 | 0.108 | 0.103 | 0.106 |
| $D_2$ | [g/(m$^2$h$^{0.5}$)] | 1.467 | 1.466 | 1.588 | 1.139 | 1.080 | 1.373 | 1.185 | 1.431 | 1.387 | 1.380 | 1.242 |

Notation: * - adsorption at 95% RH; MBV - moisture buffering value; CC - capillary coefficient; $D_1$ - first drying phase rate, $D_2$ - second drying phase rate. Mortars: REF - reference; Fl - flowers; Le - leaves; Br - branchlets; Wo - wood; Ba - bark; 5 or 10 - addition of the fraction at 5% or 10% by vol.

Nevertheless, biological colonization was found as a main drawback for the biomass addition. It was not possible to identify the source of it, as it can depend on environmental factors, biological factors or a combination of both. To stop the biological development, the mortar specimens underwent a thermal treatment (60ºC for 24 h). The colonization of the specimens was constantly controlled during the tests and no further growth was detected. The next chapter presents and discusses the final formulations of modified gypsum mortars, obtained as a result of a preliminary study, briefly referred in section 5.1, and their comparison to two premixed clay-based plasters.

# 5

# INNOVATIVE GYPSUM-BASED PLASTERS FOR PASSIVE MOISTURE REGULATION AND POLLUTANT REMOVAL

## 5.1 Preamble

The study on gypsum plastering mortars enhanced with the addition of 10% and 5% by volume of different fraction of the invasive plant *Acacia dealbata* (chapter 4) showed overall good results. The main drawback, the biological growth during the first 14 curing days of the mortars, was addressed in a preliminary study to define the final formulations then tested at moisture and pollutant removal together with the clay-based ones.

The preliminary study

The bark was selected as the best fraction to be added at 10% by volume to improve the passive moisture regulation of the plasters and different solutions were tested to prevent biological attack:

- Thermal treatments of the biomass:
  - The bark was heated up to 120˚C for 4 hours (pasteurization temperature).
  - The bark was heated up to 200˚C for 1 hour (starting to turn into charcoal).
  - The bark was heated up to 250 ˚C for 1 hour (partially turned into charcoal).
- Alteration of the pH of the mortar:
  - Addition of 4.4% by wt. of air lime.

The plastering mortars were prepared combining the additions as reported in **Table 5.1**, plus water. The designed formulations were:

- REF: premixed gypsum product (no additions);
- BA: premixed gypsum product + 10% by vol. bark;
- BA_AL: premixed gypsum product + 10% by vol. bark + 4.4 % by wt. air lime;
- BATT: premixed gypsum product + 10% by vol. bark heated at 120˚C (from here designated as thermally threated bark);
- BATT_AL: premixed gypsum product + 10% by vol. thermally treated bark + 4.4 % by wt. lime;
- BA200: premixed gypsum product + 10% by vol. bark heated at 200˚C;
- BA250: premixed gypsum product + 10% by vol. bark heated at 250˚C.

The mortars production and fresh state characterization followed the same procedures that will be described in sections **5.2.2.2.1** and **5.2.2.2.3**. The fixed amount of water was 48% by wt. of the gypsum premixed product, and only increased for BATT_AL (accounting in the mass to consider also the 4.4% of the air lime). The decision was taken during the preparation of the mortar, because the workability of the previous mix with air lime, BA_AL, was found to be not so adequate (3 in a scale from 1 to 5 - **Table 5.1**). It turns out that additional water is required when the addition of air lime and/or thermally treated biomass (from BATT preparation) are done.

**Table 5.1.** Production and fresh state characterization.

| Mortar | Gypsum premixed product | | Air lime (4.4% by wt.) | | $H_2O$ | Biomass | Tot Vol. | w/dry (wt) | Flow | FBD | Workability 1 to 5 |
|---|---|---|---|---|---|---|---|---|---|---|---|
| | Vol. [$cm^3$] | Mass [g] | Vol. [%] | Mass [g] | [ml] | [g] | [$cm^3$] | [%] | [mm] | [$kg/dm^3$] | [-] |
| **REF** | 3000 | 2442 | - | - | 1172 | - | 3300 | 0.48 | 161.5 | 1.629 | 5 |
| **BA** | 3000 | 2442 | - | - | 1172 | 143.79 | 3300 | 0.45 | 155.3 | 1.603 | 4.8 |
| **BA_AL** | 3000 | 2442 | 272.9 | 107.4 | 1172 | 143.79 | 3573 | 0.44 | 130.5 | 1.623 | 3 |
| **BATT** | 3000 | 2442 | - | - | 1172 | 134.94 | 3300 | 0.45 | 153.0 | 1.625 | 4.5 |
| **BATT_AL** | 3000 | 2442 | 272.9 | 107.4 | 1224 | 134.94 | 3573 | 0.46 | 136.5 | 1.627 | 3.5 |
| **BA200** | 3000 | 2442 | - | - | 1172 | 137.31 | 3300 | 0.45 | 152.8 | 1.625 | 4.2 |
| **BA250** | 3000 | 2442 | - | - | 1172 | 119.46 | 3300 | 0.46 | 152.0 | 1.616 | 4 |

The mortars were characterized at shrinkage and hardened state according to test methods described in section **5.2.2.2.4** while keeping track of the biological development. Results are referred in **Table 5.2** and volumetric variations in **Figure 5.1**.

**Table 5.2.** Hardened state characterization (average values, AV, and standard deviations, SD): modulus of elasticity (Ed), flexural strength (Fs), compressive strength (Cs), surface hardness (Hs) adhesive strength (Ads), apparent bulk density (BD) and open porosity (OP).

| Mortar | Ed [GPa] | | Fs [MPa] | | Cs [MPa] | | Hs [Shore C] | | Ads [MPa] | | BD [kg/dm³] | | OP [%] | |
|---|---|---|---|---|---|---|---|---|---|---|---|---|---|---|
| | Av | S.D. | Av. | S.D. | Av. | SD | Av. | S.D. | Av. | S.D. | Av. | S.D. | Av. | S.D. |
| REF | 3.7 | 0.04 | 2.0 | 0.14 | 3.7 | 0.26 | 70.7 | 3.15 | 0.65 | 0.09 | 1.203 | 0.00 | 45.1 | 0.11 |
| BA | 3.2 | 0.00 | 1.8 | 0.03 | 3.5 | 0.12 | 68.1 | 2.19 | 0.47 | 0.16 | 1.201 | 0.00 | 44.6 | 0.23 |
| BA_AL | 3.6 | 0.02 | 1.7 | 0.27 | 3.7 | 0.18 | 74.3 | 2.51 | 0.52 | 0.06 | 1.227 | 0.01 | 44.6 | 0.12 |
| BATT | 3.4 | 0.07 | 1.7 | 0.08 | 3.8 | 0.33 | 70.1 | 2.19 | 0.60 | 0.03 | 1.210 | 0.00 | 45.1 | 0.13 |
| BATT_AL | 3.4 | 0.07 | 1.8 | 0.07 | 3.5 | 0.10 | 72.4 | 1.27 | 0.45 | 0.02 | 1.208 | 0.01 | 45.6 | 0.30 |
| BA200 | 3.5 | 0.02 | 1.7 | 0.12 | 3.9 | 0.50 | 72.3 | 1.70 | 0.59 | 0.08 | 1.216 | 0.00 | 44.8 | 0.11 |
| BA250 | 3.3 | 0.02 | 1.7 | 0.20 | 3.3 | 0.27 | 73.4 | 1.27 | 0.50 | 0.05 | 1.214 | 0.00 | 45.1 | 0.21 |

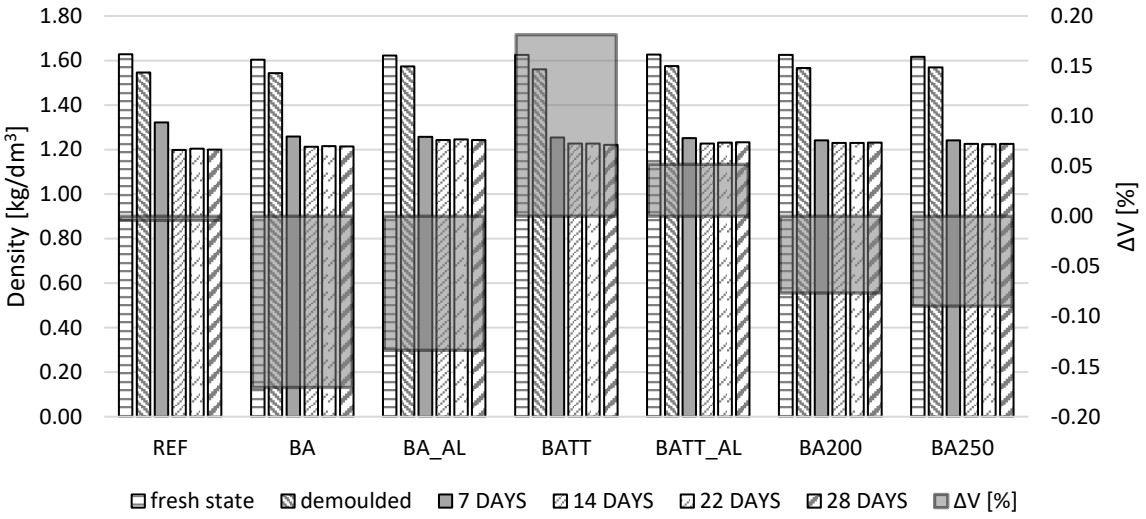


**Figure 5.1.** Volumetric variation at fresh state and after 2, 7, 14, 21 and 28 days.

Overall, the compressive and flexural strength were found complying with the requirements from EN 13279-1 (2014) for gypsum plasters, there is an increase of the surface hardness when air lime is added and, with the heating of the biomass, the adhesive strength decrease a little with the additions. With the fixed amount of kneading water, the results from open porosity, bulk density and shrinkage are consistent and indicate that the total volume of open porosity was not very much affected by the additions. This does not exclude the possibility of a different pore size distribution caused by the biomass and air lime additions. The study found that, at the end of the 28 days, only the prismatic specimens with the addition of air lime (and the reference one), did not show any trace of biological growth (**Table 5.3**).

**Table 5.3.** Biological growth of the produced mortars (prisms), evaluation based on ASTM D5590-17 (2021).

| Mortar | BA250 | BA200 | BATT_AL | BATT | BA_AL | BA | REF |
|---|---|---|---|---|---|---|---|
| BioCol. [1-5] | 1 | 1 | 0 | 1 | 0 | 1 | 0 |

The mortars' application on bricks had no visible (by eye) traces of biological growth. To further investigate the difference between prismatic specimens and application on the bricks, three samples from each plaster applied on brick were manually collected and underwent the open porosity test by vacuum and hydrostatic weighing (**Figure 5.2**), based on EN 1936 (2007) and the apparent bulk density was calculated too (**Table 5.4**), together with samples from the prismatic specimens.

**(a)** **(b)**

**Figure 5.2**. Samples collected from plasters applied on bricks **(a)** and from prismatic specimens **(b)** that underwent vacuum and hydrostatic weighing open porosity test.

**Table 5.4.** Results of apparent bulk density (BD) of samples collected from bricks application and prisms - average values (Av) and standard deviation (SD).

| BD [kg/dm3] | | REF | BA | BA_AL | BATT | BATT_AL | BA200 | BA250 |
|---|---|---|---|---|---|---|---|---|
| Brick | Av | 1.330 | 1.298 | 1.281 | 1.297 | 1.295 | 1.216 | 1.214 |
| | SD | 0.01 | 0.01 | 0.00 | 0.00 | 0.01 | 0.00 | 0.00 |
| Prism | Av | 1.203 | 1.201 | 1.227 | 1.210 | 1.208 | 1.216 | 1.214 |
| | SD | 0.00 | 0.00 | 0.01 | 0.00 | 0.01 | 0.00 | 0.00 |

Results show that the application of the plaster in contact with the brick substrate slightly increases its bulk density (lowering porosity, probably due to water absorbed by the substrate while the plaster is still fresh), except for the mortars with bark thermally treated at higher

temperatures that show no difference. The faster drying of the mortars applied on the bricks is eventually related to the lower biological growth there observed and suggests less susceptibility in real applications.

For the exposed reasons, to prevent the biological growth, the addition of air lime was considered mandatory, and the final mortars were produced with:

- Bark of *A. dealbata* with addition of 5% by vol. of air lime.
- Bark of *A. dealbata* heated during 1 hour at 250 ˚C with addition of 5% by vol. of lime.

In this section of the study, the bark fraction was not obtained after extractives recovery (to be used for pharmaceutical or cosmetic industry) but just milled and sieved.

The so optimized plastering mortars were characterized at fresh state and hardened state and their relative humidity dependent properties are presented (section 5.2) and compared with premixed clay-based plastering mortars. Moreover, all these plastering were tested to ozone reaction and primary and secondary VOCs emissions (section 5.3). Coating materials can be responsible for primary emissions and, when exposed to certain pollutants, e.g., ozone ($O_3$), also for secondary emissions. The latter are commonly reaction products (carbonyl compounds) of the pollutant exposure. The experiment aimed at identifying and quantifying the primary and secondary emissions of the different coating products together with their deposition velocities. The coatings selected for the study are the three gypsum-based plastering mortars (reference, with bark and air lime, with thermally treated bark for 1 h at 250 ˚C and air lime) and two clay plasters applied as a base coat (to be described in section 5.2); as a topcoat on drywall; the drywall (a very common building material in USA and Europe).

# 5.2 Article D1 - Enhancement of the Hygroscopic Behavior of Innovative Plastering Mortars based on Gypsum

(the article was submitted on 17/10/2023 to the journal *Construction and Building Materials*; reviews from the thesis advisory committee were applied)

## Eco-efficient plastering mortars for improved indoor comfort - The influence of *A. dealbata* bark addition

Alessandra Ranesi[1,2*], Paulina Faria[1], Maria Teresa Freire[3], Margarida Gonçalves[4], M. Rosário Veiga[2]
[1] CERIS, Department of Civil Engineering, NOVA School of Science and Technology, NOVA University of Lisbon, Quinta da Torre, 2829-516 Caparica, Portugal
2 National Laboratory for Civil Engineering, Avenida do Brasil 101, 1700-066 Lisbon, Portugal
3 CERIS and SIVAL-Gessos Especiais Lda, Rua Emídio Oliveira Faria, 2425-879 Souto da Carpalhosa, Portugal
4 METRICs, Department of Chemistry, NOVA School of Science and Technology, NOVA University of Lisbon, Quinta da Torre, 2829-516 Caparica, Portugal and VALORIZA, Polythechnic Institute of Portalegre, Campus Politécnico, 7300-555 Portalegre, Portugal
* corresponding author: a.ranesi@campus.fct.unl.pt

## Abstract

The passive contribution of indoor coatings to improve interior comfort is an eco-efficient challenge nowadays. Gypsum is one of the more eco-efficient binders available to produce plasters. *Acacia dealbata* is an invasive species in many countries, and the management of its wood waste for fires prevention is imperative. This study intends to evaluate the effect of using *Acacia dealbata* bark waste, directly after milling (raw) or with additional thermal treatment (1 h at 250 ºC), as an addition to an industrial gypsum-based plastering mortar to passively improve indoor comfort. To prevent the biological colonization, air lime is also added. Two clay-based plasters are used for comparison, together with a reference gypsum plaster. Results show that both the gypsum-bark mortars fulfill the standard requirements and do not show biological vulnerability. They doubled the moisture buffering of the reference gypsum plaster and got closer to the hygroscopic performance of the clay plasters. The very similar results between the two gypsum-bark mortars suggest that the thermal treatment of bark is not an eco-effective choice. So, the raw bark-added gypsum mortar is selected as a promising coating material to passively contribute for indoor comfort in an innovative, eco-efficient, way.

## Keywords

Calcium sulfate hemihydrate gypsum; air lime; clay; biomass; moisture buffering; passive moisture indoors regulation.

### 5.2.1 Introduction

The passive moisture regulation of coating materials and products for the improvement of indoor comfort (Xiong et al., 2015; Arundel, 1986), of the perceived indoor air quality (Fang, 1998) and for the design of healthier environment (Guarnieri et al., 2023) with lower energy demand (Rode et al., 2008; Zhang et al., 2017) is nowadays a very investigated topic. The aim of regulating indoor relative humidity (RH) through the passive (no energy demand) activity of coating materials and products is being pursued either by studying the enhancement of traditional (Lima and Faria 2016; McGregor et al., 2016; Pawełkowicz et al., 2022; Gentile et al., 2023; Li et al., 2023) and modern ( Yang et al., 2022; Gbekou et al., 2022) plastering mortars than by designing new ones (Zu et al., 2022, Magda et al., 2023).

Calcium sulphate hemihydrate (gypsum) has been used for several decades to coat and decorate indoor walls and ceilings (Malta da Silveira et al., 2007; Gariani et al., 2018; Kamel et al., 2015; Mahmoud and Papadopoulou, 2013; Válek et al., 2020; Caroselli et al., 2021) in huge parts of the world and, for this reason, is a suitable material for restoration in ancient buildings (Freire et al., 2021; Sáez-Pérez et al., 2022; Torres-González et al., 2023). Furthermore, gypsum-based mortars are a suitable product for plastering indoors of new buildings. Nevertheless, even if traditional gypsum plasters have a high-water vapor permeability (Záleská et al., 2021; Ranesi et al., 2021a) that makes them compatible with many substrates, their hygroscopic behavior is poor when compared with other coatings, such as clay-based plasters (Ranesi et al., 2021a; Santos et al., 2020). However, the production of hemihydrate gypsum requires calcination temperatures (120-180 ˚ C) lower than other common binders used for mortar's production, and easy milling, with all the positive consequences in terms of environmental impact (Meireles et al., 2019). Therefore, gypsum plaster is considered an eco-efficient building product (Ranesi et al., 2021b).

The *Acacia dealbata* is an invasive species original from Australia and very spread in Southern European countries (Raposo et al., 2020) due to its germination rate (above 70%), rapid growth, allelopathic capacity, dispersion capacity in burnt environments and high resistance to chemical attack Lorenzo et al., 2010). The recovery of the plant, besides reducing the risk of forest fires (Nunes et al., 2021a) and contribution to a greener circular economy (Nunes et al., 2020; Nunes et al., 2021b), can be used for extractives with antioxidant and antimicrobial activity (Sowndhararajan et al., 2013; Borges et al., 2020). The biowaste of the extraction can be re-used for different purposes in a more multiproduct biorefinery approach (Correia et al., 2020; López-Hortas et al., 2021). The production of energy from the biomass has also been

investigated in literature, but there are some issues not solved yet like the high chlorine content (0.04%) (from resinous species <0.02%)(Nunes et al., 2020), the low thermal efficiency (seven times lower than *Pine*) and the emission of environmentally relevant contaminants generated by the combustion both in gaseous form (CO, $SO_2$ and $NO_x$) and particle matter ($PM_{10}$) (Ferreira et al., 2014; Vicente et al., 2019).

This study intends to evaluate the effect of the reuse of *Acacia dealbata* bark waste, directly or after thermal treatment, as an addition to gypsum-based plastering mortars. The complete characterization of a new eco-efficient gypsum-bio-based plaster is presented, its potential to passively improve indoor comfort is evaluated and compared with two clay-based plasters considered a benchmark for hygroscopic behavior. Clay plasters, in fact, are recognized for being highly hygroscopic (Ranesi et al., 2021a) and their embodied energy appears to be very low (Marcelino-Sadaba et al., 2017; Santos et al., 2021).

## 5.2.2 Materials and methods

### 5.2.2.1 Materials

#### 5.2.2.1.1 The biomass characterization

The biomass selected for the study is a fraction of the plant *Acacia dealbata* collected in the region of Caparica, in Portugal. In a previous study (Ranesi et al., 2022; Ranesi et al., 2023) five different fractions of the same plant were added to gypsum mortar formulations and their effect was evaluated: bark, branchlets, flowers, leaves, wood. The bark was selected among the five different fractions to enhance the hygroscopic behavior of the plastering mortars because its addition was found of highest impact on the moisture buffering of the mortar (Ranesi et al., 2023). The biomass, once collected, was cut in 5 cm pieces, milled (cutting mill, Retsch) and sieved at 1 mm using a vibrating sieve (Retsch), BA. A fraction of this bark sample was thermally treated, by heating at 250 ˚ C for 1 hour, stored in glass Petri Dishes and cooled down in a desiccator before being used as an alternative addition (BA250).

The proximate composition of the biomass fractions BA and BA250 were determined using European standards EN 14774-2 (2009) for moisture content (MC), EN 14775 (2009) for ash content (Ash), and EN 15148 (2009) for volatile matter (VM). Fixed carbon was determined by difference. The ultimate analysis of the biomass samples was performed using an elemental analyzer (Thermo Finnigan – CE Instruments Model Flash EA 112 CHNS series). Oxygen (O) was determined by difference, in a dry basis. Loose bulk density was determined by measuring the volume occupied by 5 g of material, using a calibrated glass beaker. Determinations were

performed in triplicate and results are expressed as the corresponding averages and standard deviations. Particle size distribution was determined on a vibrating sieve (Retsch, AS200 digit) equipped with sieves with mesh openings of 2000, 1000, 500, 200, 100 and 50 μm; a known amount of each sample (100g) was sieved at an amplitude of 50, for 10 min. After this period, the sample mass collected in each sieve and the fraction less than 50 μm were determined gravimetrically.

The water holding capacity of samples BA and BA250 was determined by mixing 1 g of biomass sample to 100 ml of distilled water, stir the mixture in an ultrasonic bath for 5 minutes, and leave it in contact for 24 h. After this period, the samples were filtered and left in the funnel for 2 h to drain the water retained between the biomass particles. The wet biomass samples were transferred to pre-weighed Petri dishes, and weighed, before and after oven drying for 12 h at 40°C. Water holding capacity was calculated as the ratio between the mass of adsorbed water divided by the mass of dried sample and expressed as percentage.

The water vapor holding capacity was determined by exposing 10 g of biomass kept in open beakers to water vapor for 5 days. The beakers with biomass were placed inside a metal container filled with warm water and covered with a plastic lid. The samples were kept for 5 days to equilibrate water vapor in the headspace and water adsorbed by the biomasses. After this period, the biomass samples were transferred to pre-weighed Petri dishes, weighed, and then oven dried for 12 h at 40°C. The water vapor holding capacity was calculated as the ratio between the adsorbed water mass and the dried sample mass and expressed as percentage.

The thermally treated (heated at 250˚ C for 1 h) bark has a brownish colour, darker than the raw, untreated, bark (**Figure 5.3**). The composition of the BA and BA250 according to ultimate analysis, did not show big differences (**Figure 5.4**), with the percentage of carbon slightly higher after the thermal treatment and, consequently, all the other elements a bit less detected. The same can be said for the grain size distribution (**Figure 5.5**) with the particle of BA250 slightly shrank by the treatment.

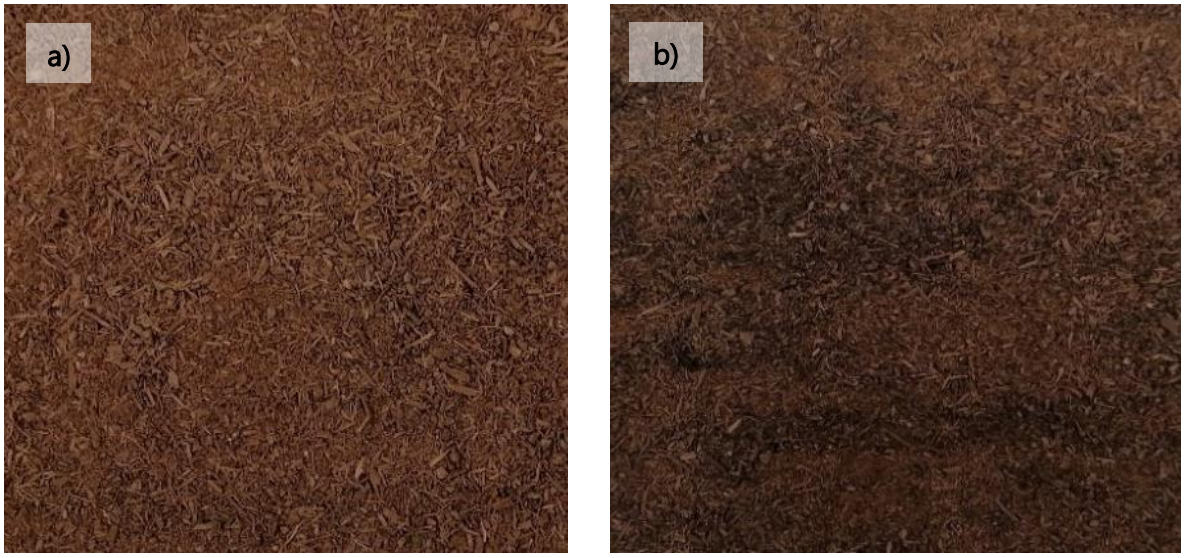


**Figure 5.3.** Appearance of bark samples before and after the thermal treatment **(a)** raw bark and **(b)** heated bark (250 ˚ C for 1 h).

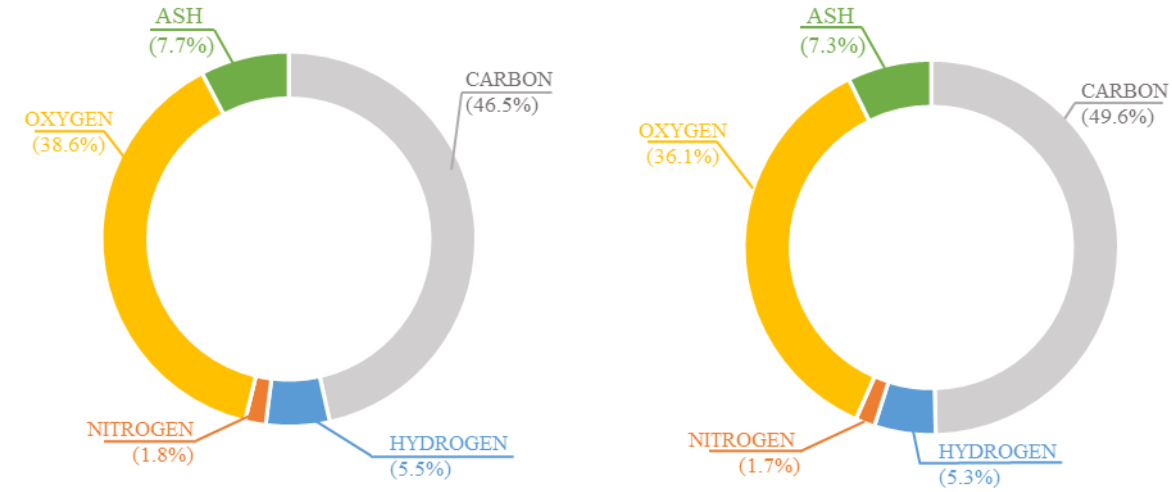


(a) (b)

**Figure 5.4.** Ultimate analysis composition for **(a)** bark and **(b)** bark heated at 250˚ C for 1 hour.

The loose bulk density, water holding capacity and water vapor holding capacity are presented in **Table 5.5** for BA and BA250. The heating process seems to decrease the hygric and hygroscopic properties of the biomass. As expected, the thermal treatment decreased the volatile components of biomass (moisture content, MC, and volatile matter, VM) and increased fixed carbon, FC (**Table 5.5**). The loss of moisture and volatiles also explains the decrease of the loose bulk density of BA250 compared to BA. The thermal treatment also decreased the relative concentration of oxygen in the BA250 sample compared to the BA, which corresponds to a lower availability of -OH and -COOH groups in the surface of the biomass particles. These polar

groups are strongly involved in the interaction with water molecules; therefore their reduction in the BA250 sample also justifies its lower holding capacities for water and water vapor.

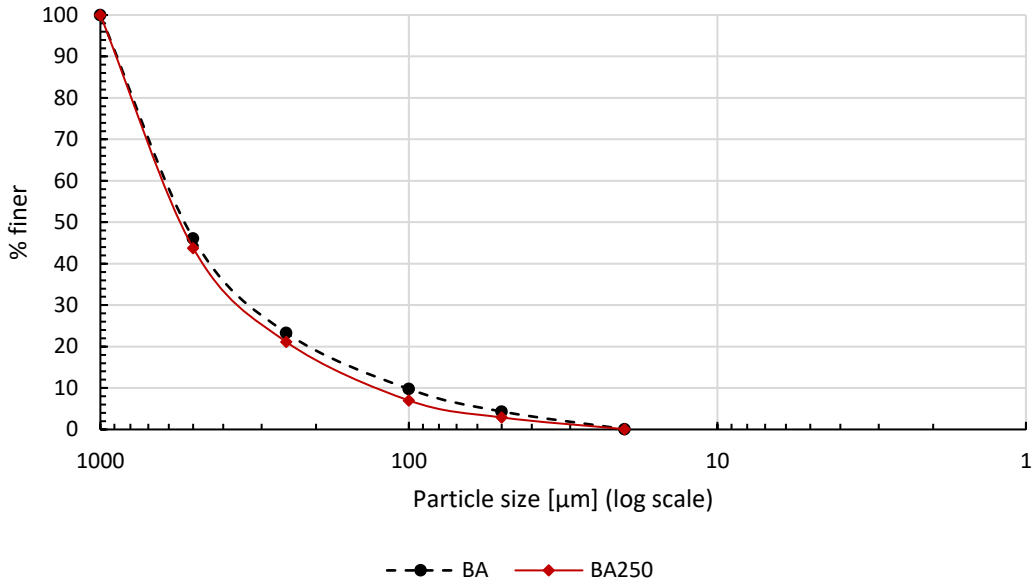


**Figure 5.5.** Grain size distribution of bark (BA) and heated bark (BA250).

**Table 5.5.** Results from biomass characterization.

| | LBD [kg/m$^3$] | WHC [%] | WVHC [%] | MC [%] | Ash [%] | VM [%] | FC [%] |
|---|---|---|---|---|---|---|---|
| **BA** | 479 | 265.5 | 13.1 | 10.83 | 7.67 | 74.39 | 17.95 |
| **BA250** | 398 | 171.2 | 11.3 | 1.71 | 7.26 | 71.45 | 21.29 |

Notation: LBD – loose bulk density; WHC – water holding capacity; WVHC – water vapor holding capacity; MC – moisture content; Ash – ash content; VM – volatile matter; FC – fixed carbon.

#### 5.2.2.1.2 The plastering mortar characterization

A gypsum powder premixed product from SIVAL - Gessos Especiais, Lda, Portugal, was used for plastering mortars production. The loose bulk density of the powder was 755 kg/m$^3$. The product contains calcium sulphate hemihydrate and calcium carbonate aggregates. The producer also declares small quantities of organic additives, not defined. The product is classified according to EN 13279-1 (2008) as B1/50/2: gypsum building plaster with an initial setting time > 50 min and a compressive strength ≥ 1 N/mm$^2$. An additional small amount of hydrated air lime CL90-S (classified by EN 459-1 (2015)) was added to the modified mortars for biological growth control, with a loose bulk density of 388 kg/m$^3$. The loose bulk densities of the gypsum-based product and the air lime were assessed based on EN 1015-2 (1999).

Due to the well-known high hygroscopic behavior of clay-based plasters, two premixed clay-based plasters (Enjarre (CL) and Maritimo (CL_M) from American Clay Enterprises LLC (American Clay technical sheet)) were prepared for comparison. The difference between them is that crushed seashells are incorporated in the CL_M formulation. The clay-based premixed products, CL and CL_M, had a loose bulk density of 1.21 and 1.08 kg/dm$^3$ respectively.

#### 5.2.2.2 Methods

##### 5.2.2.2.1 Mortars formulation and specimens' production

The volume of the gypsum premixed product was fixed at 3000 cm$^3$ per batch and the mortars with addition of BA and BA250 were produced with the respective biomass at 10% by volume of the gypsum product. Moreover, to prevent any biological development related to the addition of biomass (Ranesi et al., 2023; Cintura et al., 2023), 4% by mass (on the gypsum product) of hydrated air lime (AL) was added to the modified mortars. All the mortars were produced with the addition of 36% by total volume of water. The dry materials were homogenized (mixed in a plastic bag). The water was added to the mixer bowl and then the dry product was sprinkled in water for 1 minute. After 1 additional minute soaking, the mixing started, also for 1 minute, with a mortar mixer (CONTROLS-65-LS 140 rpm). Then, the mortar was additionally mixed manually (for 1 min) and mechanically (10 sec), and the fresh state characterization started. The mortars formulation is synthesized in **Table 5.6**.

**Table 5.6.** Mortars formulation by volume and mass.

| Mortar | Gypsum premixed product | | Lime addition | | Tot Vol.* [cm3] | H2O [ml] | w/dry(wt) [%] | Biomass [g] |
|---|---|---|---|---|---|---|---|---|
| | Vol. [cm3] | Mass [g] | Vol. [cm3] | Mass [g] | | | | 10% by vol |
| **REF** | 3000 | 2264 | - | - | 3000 | 1080 | 48 | - |
| **BA_AL** | 3000 | 2264 | 233.44 | 90.6 | 3233 | 1164 | 51 | 143.79 |
| **BA250_AL** | 3000 | 2264 | 233.44 | 90.6 | 3233 | 1164 | 51 | 119.46 |

Notation: w/dry – water/dry material excluding the biomass; * – biomass excluded.

The plastering mortars were cast in metallic prismatic molds (160 mm x 40 mm x 40 mm) to be characterized at compressive and flexural strengths after 28-curing days. The prismatic specimens were demolded two days after production. To test adhesion and hardness of the mortars, they were applied on hollow bricks with a 30 cm x 20 cm surface. Two-centimeter-thick plasters were applied on wet bricks (brushed with water) to reproduce plastering application in common practice. Five disks of about 100 mm diameter and 20 mm thickness of

each plastering mortar were produced for testing the hygroscopic behavior. The mortars were cast into round molds obtained as slices of a PVC pipe (leave-in-place) with the lower surface placed on plastic foil and the upper surface exposed to laboratory environment (for drying).
The preparation of the clay-based plasters, CL and CL_M, was run with a water/dry ratio fixed according to producer recommendations and workability criteria at 30% and 31% by weight, respectively (the Maritimo product required a little bit more water). Five rounded specimens with about 80 mm diameter and 20 mm thickness were prepared for each mortar to be tested for hygroscopic behavior. The methodology followed for casting the specimens was the same as for the gypsum-based mortars. No prismatic samples were prepared due to a shortage of premixed products. Anyway, being the premixed product already on the market, it was considered dispensable to run a mechanical characterization and, due to the solubility in water of not stabilized clay-based product, the water absorption by capillarity was dispensed too.

##### 5.2.2.2.2 Fresh state characterization and shrinkage

The fresh state was assessed by flow table consistence based on EN 13279-2 (2014) and EN 1015-3 (1999), fresh density according to EN 1015-6 (1999) and workability was empirically evaluated. The volumetric shrinkage was also assessed. The consistence by flow table of each mortar batch was calculated as the average of four measured directions. The fresh density was calculated by the mass of the mortar filling a container with a known mass and volume, divided by that volume. The workability was evaluated relying on the experience of a skilled technician, using the scale 1–not workable to 5–very workable. The volumetric shrinkage was determined at the end of 2, 7, 14, 21 and 28 days from production, using a digital caliper and calculating the volume from the average on three measurements of each surface of each prism of the gypsum mortars.

##### 5.2.2.2.3 Pore size distribution of the gypsum mortars

The pore size distribution of the gypsum mortars was obtained by mercury intrusion porosimetry (MIP). Two samples (about 2 g each, 11 months aged) of each mortar were analyzed. The test was performed in an *AutoPore IV 9500 V1.09* with a penetrometer *0444-(09) 5 Bulb, 1.131 Stem, Solid* with mercury in (low) filling pressure at 0.54 psi. The contact angle and the surface tension of the mercury were 130° and $485 \cdot 10^3$ N/mm, respectively.

##### 5.2.2.2.4 Density and mechanical tests of the gypsum mortars

The apparent bulk density, based on EN 1015-10 (1999), was geometrically obtained on six prismatic specimens per mortar at the end of 28 curing days using a digital caliper and a balance with 0.001 g resolution. The dynamic modulus of elasticity by resonance frequency

was obtained using a ZEUS ZRM equipment. The test followed the prescriptions of EN 14146 (2004) and each result was calculated on average of six prismatic specimens. The flexural and compressive strengths, tested by a universal force equipment PROETI ETI-HM-S/CPT, were calculated out of three results for each mortar, using three specimens. The testing methods followed the EN1015-11 (1999), with a 2 kN and 200 kN loading cells and 20N/s and 100 N/s loading speeds, respectively for flexural and compressive tests. Due to the addition of air lime in the mortars, an evaluation of carbonation depth was run dropping of a solution of 1% phenolphthalein diluted in water (30%) and ethanol (70%) on the freshly broken surfaces resulting from the flexural test. The applications on bricks were used for evaluating the surface hardness (average of seven measures per mortar) using a Hildebrand durometer HD3000, and adhesive strength (three coring made with a drill HILTI DD 100-RA), based on EN 1015-12 (2016).

5.2.2.2.5 Water absorption by capillarity and drying tests of the gypsum mortars

One half of each specimen resulting from the flexural strength test was used for the determination of water absorption by capillarity and unidirectional drying. The partial leftovers of each prism were mechanically cut into cubes with 4 cm; the cut surface and its opposite surface (bottom and top) were gently polished and brushed according to the EN 15801 (2009) prescriptions and the four lateral sides sealed with paraffin and wax. The specimens were dried at 45˚ C and once the dry mass was determined, using a 0.01 g precision balance, the capillary test started. The specimens were placed in a laboratory tray on top of glass poles trying to maximize the contact of their bottom surface with the water. The level of the water in the tray was kept, by manual control, 5 mm high, and each cubic specimen (three of each mortar) weighed at fixed time. For the first 8 h the interval between weighing changed from very short (1 min during the first 10 minutes) to a bit longer (1.5 h after 4 h). Then, the weighing was performed every 24 h for the last days of the experiment. The test was kept ongoing for 5 days with the main objective of understanding if the addition of air lime and biomass would reduce the solubility of gypsum. As in a previous article also testing mortars (Ranesi et al., 2023), "the capillarity coefficient (CC) was calculated as the slope of at least five successive aligned points on the first part of the capillary curve displaying the absorbed water per area against the square root of time, with a linear regression factor above 0.99".

The unidirectional drying started at the end of the capillary water absorption test with the saturated specimens. The specimens were kept in the same room at the same climatic conditions (26±0.5˚ C T, 55±5% RH) and placed on a hydrophobic surface with their upper face

(upside-down as compared to capillary absorption), to ensure the drying would only happen through their top area. Their weight was controlled each 5 minutes during the first 20 minutes, then at longer time frames (10, 30, 60 minutes) during the first 8 h and each 24 h until constant mass. The drying index (DI) [-], first (D1) [g/(m$^2$h)] and second (D2) [g/(m$^2$min$^{0.5}$)] drying phase rates were calculated according to the standard prescriptions (EN 16322:2013).

5.2.2.2.6 Hygroscopic behavior

The sorption isotherms, according to ISO 12571 (2013), were run on the specimens with circular shape. The specimens were dried at 45˚ C to avoid any risk of dehydration of calcium sulfate dihydrate until constant mass. According to the standard, constant mass was reached when three consecutive weighing, with a period of at least 24 h, gave a mass variation < 0.1% of the total mass (ISO 12571:2013). The temperature in a climatic chamber Aralab Fitoclima 700EDTU was fixed at 23±0.5 °C and the RH levels were set on successive steps at 30%, 50%, 70%, 80%, 95% forward and back. Each step was kept until constant mass. During the experiment the climatic chamber could not keep the 90% RH for the period needed to stabilize the samples. After three days it cut out and it was decided to return to 80% RH and start the desorption curve. Nevertheless, for a better understanding of the different responses a nonlinear regression analysis was applied on the experimental data already collected to fit the curve and be able to assess the prediction of moisture value at 90% RH. The model used to describe and predict the hygroscopic behavior of the plasters was selected by Ferreira el al., 2020 (Ferreira et al., 2020) among many models as a good fit for hygroscopic materials. The equation was first proposed by Hansen in 1986 (Hansen, 1986) for building materials and is reported in Equation 1 with u the moisture content [kg/kg], φ the relative humidity [-] and a, b, c the parameters to be calculated to fit the prediction curve to the experimental data (**Table 5.7**):

$$u = a \cdot (1 - \frac{\ln \varphi}{b})^{-\frac{1}{c}} \quad (1)$$

To obtain a better fit, it was decided to write two equations (one for adsorption and one for desorption) and the predicted moisture content corresponding to 90% RH exposure was taken as the highest value between adsorption and desorption prediction curves.

The same specimens were tested at moisture buffering according to the middle humidity level of ISO 24353 (2008). The same temperature of 23±0.5 °C was set in the climatic chamber and the specimens were firstly preconditioned at 63% RH and, once the equilibrium was reached, underwent the cycles. Seven cycles were run to ensure the quasi-steady state was reached. The last three cycles were used to calculate the moisture buffering value (MBV) of the mortars.

**Table 5.7.** Values of the parameters a, b, c (and R-squared) fitting the Hansen equation (Hansen, 1986) for adsorption and desorption curves of the plasters, at 23° C, according to the nonlinear regression analysis.

| Mortar | Adsorption | | | $R^2$ | Desorption | | | $R^2$ |
|---|---|---|---|---|---|---|---|---|
| | a | b | c | | a | b | c | |
| REF | 0.00356 | 0.43084 | 0.57624 | 0.96 | 0.00326 | 0.59031 | 0.68752 | 0.97 |
| BA_AL | 0.00832 | 17.41139 | 0.02924 | 0.99 | 0.00765 | 234.20535 | 0.00567 | 0.98 |
| BA250_AL | 0.00763 | 19.53797 | 0.02624 | 0.99 | 0.00702 | 572.51432 | 0.00239 | 0.98 |
| CL | 0.01171 | 21.40625 | 0.02431 | 1.00 | 0.01234 | 0.67829 | 0.60823 | 0.99 |
| CL_M | 0.01504 | 21.16248 | 0.02396 | 1.00 | 0.01553 | 0.69487 | 0.63191 | 0.99 |

As prescribed by the standard, the daily cycle was split into 12 h of relative humidity at 50% and 12 h at 75%. During the last three cycles the specimens were weighed at 3, 6, 9, 12 h and 24 h from the beginning of each cycle. During the previous cycles the weighing was fixed each 24 h to keep track of the initial and final mass.

## 5.2.3 Results and discussion

### 5.2.3.1 Fresh state properties and shrinkage

Two mortar batches were prepared for each gypsum-based mortar and characterized by flow table, fresh bulk density, and workability (**Table 5.8**). Only one batch for each clay-based plaster was prepared. The reference mortar shows the highest flow table consistency and fresh bulk density even if the lowest ratio water/dry product (by wt., excluding the biomass) was used for the mixing. Between the two mortars with addition of biomass and air lime, obtained with the same w/dry (by wt., excluding the biomass), there is a slight difference of flow and fresh bulk density that seems consistent with the lower water holding capacity of the biomass BA250, presented in section **5.2.2.1.1.** Nevertheless, even if the flow table was found to be a little bit low (should be 165±5 mm according to EN13279-2 (2014)), the workability was evaluated by a skilled plasterer as great (5) for the reference mortar and very good (4.5) for both mortars with additions.

**Table 5.8.** Results from fresh state characterization.

| Mortar | Flow table consistency [mm] | Fresh bulk density [kg/dm$^3$] | Workability [1:5] |
|---|---|---|---|
| REF | 153.9 ± 0.5 | 1.65 | 5 |
| BA_AL | 139.8 ± 3.2 | 1.61 | 4.5 |
| BA250_AL | 148.3 ± 1.4 | 1.62 | 4.5 |
| CL | - | 1.98 | 5 |
| CL_M | - | 1.75 | 4.5 |

The addition of raw bark, heated bark (250˚ C) and air lime did not affect the dimensional variation of the mortars (prismatic specimens) during the first 28 curing days (**Figure 5.6**): the highest variation, in the range of 0.001 $dm^3$ for the mortar BA250_AL (between 2 and 7 curing days), is still as small as standard deviation.

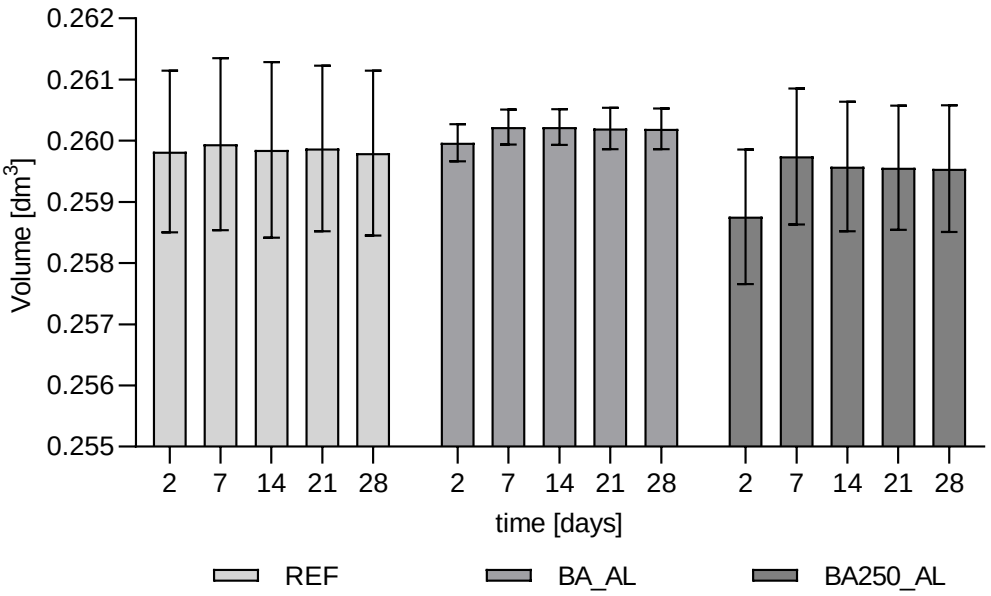


**Figure 5.6.** Volumetric variation during the first 28 curing days - average and standard deviation of the reference mortar and mortars with raw bark (BA_AL) and with thermal treated bark (BA250_AL)

Overall, at fresh state the three mortars showed very similar characteristics, with the modified formulations only a little stickier probably due to higher consistency but still with good workability and slightly lower density. However, the dispersion of the mortars volumetric variation is much lower for the mortars with raw bark and air lime up to 28 days.

#### 5.2.3.2 Pore size distribution of the gypsum mortars

Results from the mercury intrusion porosimetry (MIP) are referred in **Table 5.9** and **Figure 5.7**. Generally, a decrease of the volume of pores corresponding to the median (diameter ≈ 6 μm) is evident for mortars with addition of biomass and air lime. It is possible that the missing volume of voids corresponds to a volume occupied or blocked by the grains of *A. dealbata* and/or by the portlandite/calcite formation - for this reason not detected as pores. All the mortars show an almost unimodal curve (as expected from gypsum) with most of the pores ranging between 1-10 μm in agreement with literature (in a previous study on gypsum plasters, the main pore radius was found to be above the maximum detection limit of 4 μm, i.e., diameter of 8 μm (Freire et al., 2021). The small pores (in the range of 0.1 μm) that are also significant in

air lime mortars [66] are found in a small amount (0.02 mL/g) and can depend on the addition of air lime and the higher amount of kneading water. Nevertheless, to observe the eventual introduction of smaller (nano) porosity, a nitrogen adsorption test should be run in future studies.

**Table 5.9.** Microstructure parameters obtained by MIP.

| Mortar | Total porosity [%] | | Median pore diam. (Vol.) [µm] | |
|---|---|---|---|---|
| | MV | SD | MV | SD |
| REF | 50.2 | 1.9 | 6.52 | 0.15 |
| BA_AL | 41.4 | 0.6 | 5.48 | 0.07 |
| BA250_AL | 45.7 | 2.2 | 6.41 | 0.06 |

Overall, when displaying the mercury incremental intrusion vs pore size diameter (**Figure 5.7**) seems that the heating at 250 ˚ C of the biomass did not particularly affect the porosity of the mortars, and the additions of both barks (raw and heated) and air lime mainly reduced the content of pores between 5-8 µm.

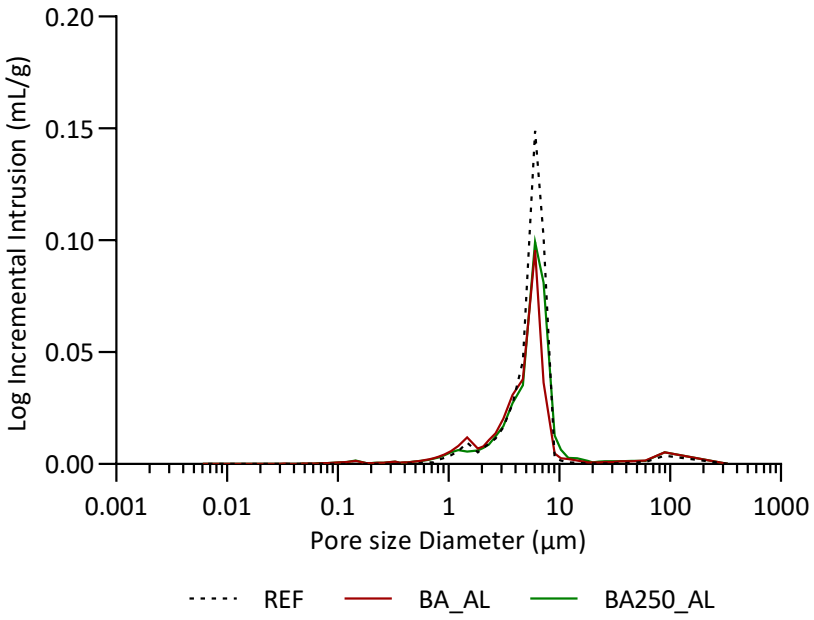


**Figure 5.7.** Incremental intrusion vs pore size diameter of the reference mortar and the two modified mortars.

### 5.2.3.3 Mechanical and pore structure properties of the gypsum mortars

In **Table 5.10** is displayed a synthesis of results from mechanical characterization. All the tests reported were performed after 28 days from production, apart from the open porosity and the bulk density, performed after 9 months. The open porosity shows a very low variation with the addition of bark and air lime, with values a little higher than the reference mortar. However,

the results registered for OP are in the range for gypsum and gypsum with small amount of air lime plasters (Freire et al., 2021; Elert et al., 2023).

**Table 5.10.** Average and standard deviation values resulting from mechanical and porous characterization of the mortars.

| Mortar | Ed [GPa] | | Fs [MPa] | | Cs [MPa] | | Hs [Shore C] | | Ads [MPa] | | BD [kg/m³] | | OP [%] | |
|---|---|---|---|---|---|---|---|---|---|---|---|---|---|---|
| | **Av** | **S.D.** | **Av.** | **S.D.** | **Av.** | SD | **Av.** | S.D. | **Av.** | S.D. | **Av.** | S.D. | **Av.** | S.D. |
| REF | **4.1** | 0.05 | **2.25** | 0.05 | **4.06** | 1.224 | **69.57** | 2.15 | **0.533** | 0.12 | **1.224** | 0.005 | **44.1** | 0.2 |
| BA_AL | **3.4** | 0.09 | **1.79** | 0.06 | **3.23** | 1.216 | **70.86** | 2.67 | **0.527** | 0.01 | **1.216** | 0.006 | **44.9** | 0.3 |
| BA250_AL | **3.0** | 0.08 | **1.54** | 0.22 | **2.72** | 1.214 | 74.86 | 1.07 | **0.531** | 0.04 | **1.214** | 0.004 | **44.8** | 0.5 |

Notation: $F_s$ – Flexural strength; $C_s$ – Compressive strength; $E_d$ – Dynamic modulus of elasticity; $H_s$ – Surface hardness; $Ad_s$ – Adhesive strength; BD - Bulk density; OP – Open porosity.

Flexural and compressive strengths, as well as dynamic modulus of elasticity, present a decrease when air lime and bark are added, mainly heated bark (in agreement with results of bulk density). However, the differences in bulk densities are so small that is difficult that they can account for the loss of mechanical strength. More likely, the addition of air lime introduced breaks over the continuous gypsum matrix, with the consequent loss in strength at this curing stage. Anyway, even if the addition of bark and heated bark reduces the mechanical properties of the mortars, they still complied with the standard requirements for gypsum plasters (Fs ≥ 1,0 and Cs≥ 2,0 MPa) (EN 13279-1:2008).

When assessing the surface hardness of the plaster specimens, the tendency was the inverse: the greater surface hardness was shown (**Table 5.10**) by the mortar BA250_AL, followed by BA_AL and the reference mortar. That may show a positive influence of the heated bark on surface hardness. An insignificant variation is registered for the adhesive strength with almost 100% cohesive fracture (in the mortar itself) showed by all the mortars. This result points out a good adhesion to the substrate (not too weak as to show an adhesive fracture and neither too strong as causing a fracture in the substrate).

To evaluate the contribution of the air lime to the mechanical response, some phenolphthalein solution was dropped on the section of rupture just after the flexural test. Carbonation depth was around 5-8 mm (**Figure 5.8**) on the three sides cast in contact with the metallic mold and 0 mm on the free side. The not homogeneous distribution of carbonated air lime at this stage (28 days), as previously discussed, can be responsible for gaps in the gypsum matrix with the consequent decrease of mechanical response. According to some authors (Freire et al., 2021; Elert et al., 2023) it is expected that after a longer curing period (i.e., 56 days for the authors) the carbonation degree would increase, with consequent increase of compressive strength.

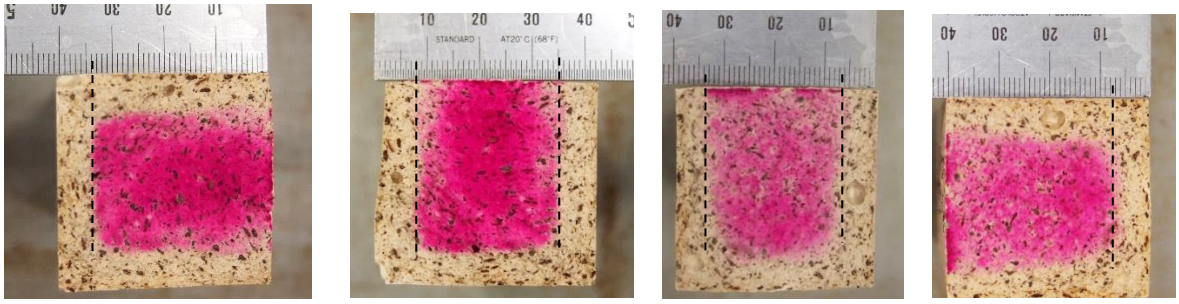

(a) (b)

**Figure 5.8.** Carbonation of the specimens BA_AL (a) and BA250_AL (b) after mechanical rupture at 28 days.

Indeed, after 9 months the carbonation depth was found to be around 8-10 mm and still 0 mm on the fourth side. The different carbonation on the free sides of the prisms and on the surface of application can most probably be justified by a higher compaction (less $CO_2$ entering) happening while smoothing out the surface for casting the prisms with the formation of a water layer on the top. The water probably dragged the thinnest particles to the surface, creating a less porous layer on the top after evaporation, as observed by Freire et al. (2021). Other authors (Elert et al., 2023) also refer to the possibility of bleeding in mortars made of 95% gypsum and 5% air lime. Moreover, the same authors, found the low addition (5 %wt) of lime responsible for a "size reduction of the needle-shaped gypsum crystals" that passes from 20-30 µm in pure gypsum paste to "10–20 µm in length and appeared together with nano or micrometer sized partially carbonated aggregated lime particles" with the partial loss of the typical gypsum crystals interlocked structure, coherent with results of the present study for mechanical strength.

#### 5.2.3.4 Water absorption by capillarity and drying capacity of the gypsum mortars

The curves of absorption displayed in **Figure 5.9** show that the mortars have similar behavior to liquid water. The introduction of the bark did not affect the slope of the first part of the curve, hence the speed of the absorption. In fact, the capillary coefficient at 15 minutes (**Table 5.11**), always ensuring $R^2 > 0.99$, was found similar for the three mortars, with REF>BA_AL>BA250_AL. Thus, the water absorption is slightly delayed by the biomass addition, more by the more hydrophobic BA250. The inversion of the slope for the mortars REF, BA_AL and BA250_AL happens at the same time, namely after 15 minutes (3.87 $min^{0.5}$) of absorption, but after that the reference is overall saturated while the other two mortars keep absorbing (slower) water probably due to the absorption capacity of the bark.

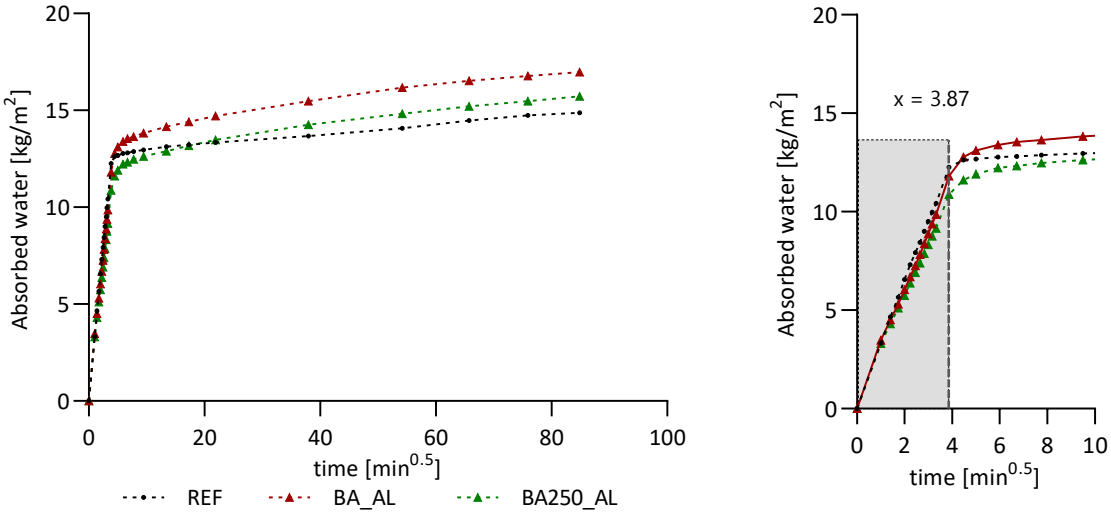


**Figure 5.9.** Water absorption by capillarity, average on three specimens of the reference mortar (REF) and the mortars with bark addition (BA_AL and BA250_AL).

**Table 5.11.** Capillarity coefficient (CC), drying index (DI), first (D1) and second (D2) drying rates: mean values (MV) and standard deviation (SD) on 3 specimens.

| Mortar | CC [kg/(m²min^0.5)] | | DI [-] | | 1st drying rate $D_1$ [kg/(m²h)] | | 2nd drying rate $D_2$ [kg/(m²h^0.5)] | |
|---|---|---|---|---|---|---|---|---|
| | MV | SD | MV | SD | MV | SD | MV | SD |
| REF | 2.95 | 0.04 | 0.37 | 0.002 | 0.116 | 0.001 | 1.529 | 0.027 |
| BA_AL | 2.92 | 0.06 | 0.47 | 0.016 | 0.104 | 0.003 | 1.502 | 0.036 |
| BA250_AL | 2.67 | 0.04 | 0.46 | 0.012 | 0.093 | 0.004 | 1.476 | 0.063 |

The drying index (DI) was calculated at 192 h (8 days). After that time, the mass of the reference mortar was found to be lower than the starting mass, due to the little dissolution in water of the gypsum, and results were excluded from calculation. The mortars with addition of bark (either dried or heated) and air lime showed a lower solubility in water: the average (on three) weight loss for the gypsum mortar is 0.50 kg/m$^2$ where the modified mortars, namely BA_AL and BA250_AL, lost 0.08 kg/m$^2$ and 0.03 kg/m$^2$. The highest drying index was found for the mortar BA_AL, consistent with the highest absorption observed. To better compare the drying behavior of the mortars, the first and second drying phase were calculated respectively for the period of drying 0 - 32 h and 48 - 144 h, with the regression lines always ensuring $R^2 > 0.99$. Results (**Table 5.11** and **Figure 5.10**) show that the introduction of biomass and air lime slightly slowed down the drying of water both in liquid and vapor phase and that the thermal treatment of the bark turned it more hydrophobic. Overall, the addition of biomass and air lime did not significantly affect the water absorption by capillarity and the drying of the mortars but reduced their solubility, which is a very positive effect.

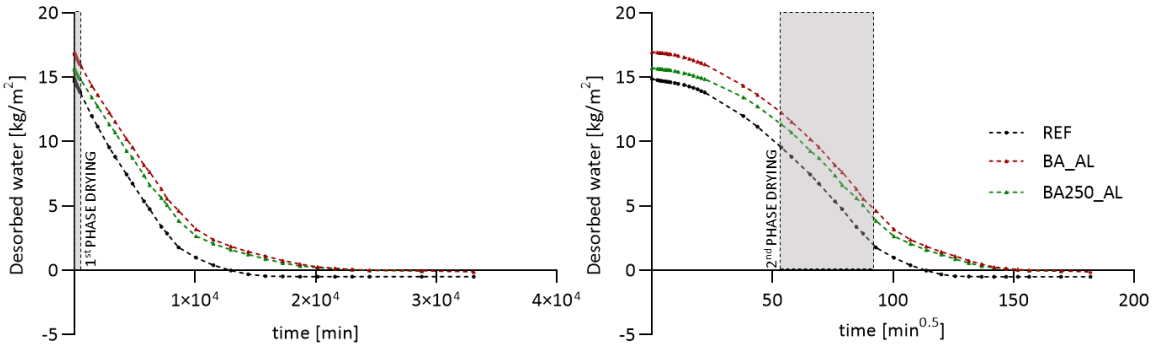


**Figure 5.10.** Drying curves of the reference mortar and mortars with bark additions.

#### 5.2.3.5 Hygroscopic behaviour

##### 5.2.3.5.1 Sorption isotherms

Overall, it was possible to obtain a good match between the experimental and the modelled hygroscopic behavior of the mortars, confirmed by the high $R^2$ values reported in **Table 5.7** and by the curves and points displayed in **Figure 5.11**. The reference mortar fits a little bit less the equation than the other two mortars, probably for being the least hygroscopic.

Both the clay-based plasters CL and CL_M show higher moisture adsorption than the gypsum-based mortars. Also, their desorption curve is better matching the adsorption one, suggesting a higher capacity of releasing moisture when RH decreases. The gypsum hygroscopic curve has a similar shape, but the amount of moisture adsorbed/desorbed is less. It is evident that the modified mortars are more hygroscopic than the reference one with the "natural" bark showing a bit higher moisture content at each RH step (adsorption and desorption). Possibly the addition of air lime, bark and the higher amount of kneading water led to a different porosity in the modified mortars, responsible for their higher moisture content. Moreover, bio-based materials present, apart from the intra-binder porosity and the porosity at the binder-aggregate interface, also an intra-particle porosity. The bio-aggregates are mainly composed of lignin, cellulose and hemicellulose. Cellulose presents often crystalline and amorphous regions. It has been demonstrated that the amorphous cellulose is a nanoporous media that has high water adsorption (hydrogen bonds) and causes macroscopic hysteresis (Rosa Latapie et al., 2023).

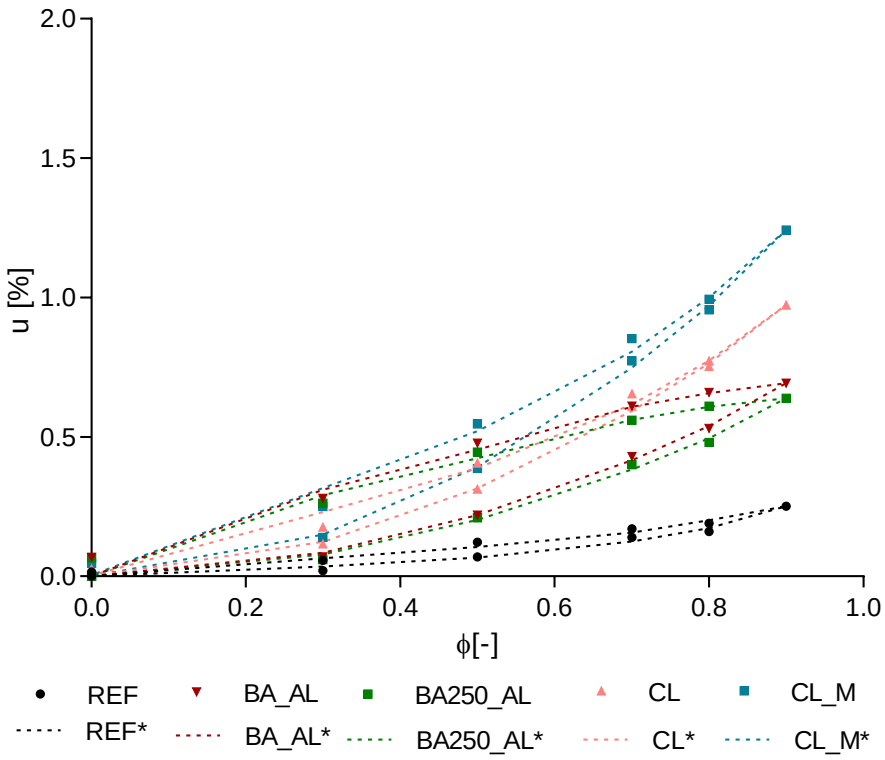


**Figure 5.11.** Sorption isotherms of the mortars. Experimental data (only symbols) average on five specimens and predicted curves (*) (dashed lines).

The small differences between them can be ascribed to the thermal treatment of the bark and its hydrophobic effect on the grains (both in vapor and liquid state). Results are consistent with those of a previous study (Ranesi et al., 2021a) where the addition of air lime to gypsum plasters was found to increase the moisture adsorption and residual content of the mortars. Nevertheless, due to the higher ratio gypsum/air lime and to the addition of the bio-aggregate in the present study, the hysteresis is reduced.

#### 5.2.3.5.2 Moisture buffering

The moisture buffering according to the middle humidity conditions of ISO24353 (2008) is obtained with the exposure of the specimens to a RH step 50-75%. The addition of biomass and air lime enhances the hygroscopic behavior of the gypsum mortar: the adsorption increases about two times and, the desorption is still complete (**Figure 5.12**). Compared with the mortars CL and CL_M based on clay, the maximum variation in moisture content after 12 h is about half of the value (the clay-based mortars show an adsorption at 12 h that is more than four times higher than the reference). The curves show a little retention of moisture for the plaster CL_M at the end of the desorption phases, but it was however considered at quasi steady state since the residual moisture content did not increase in successive cycles.

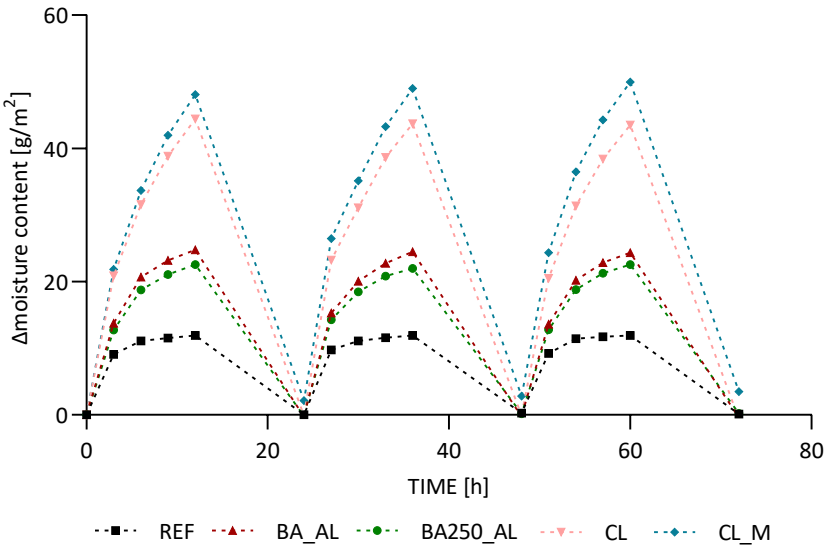


**Figure 5.12.** Variation of moisture content vs time, from ISO 24353 [65], last 3 cycles (out of 7) for REF, BA_AL and BA250_AL.

Results from the curves are consistent with moisture buffering value for REF, BA_AL and BA250_AL, found 0.47±0.004, 0.99±0.006 and 0.89±0.012 $g \cdot m^{-2}\%RH^{-1}$, respectively (**Figure 5.13**). There is a slight decrease of the hygroscopicity of the modified mortar when the bark is thermally treated, as observed already for the sorption isotherms. The values of moisture buffering of the clay-based plasters are confirmed to be higher, almost twice the values of the enhanced gypsum plasters, and in the range observed in literature for clay (Ranesi et al., 2021c).

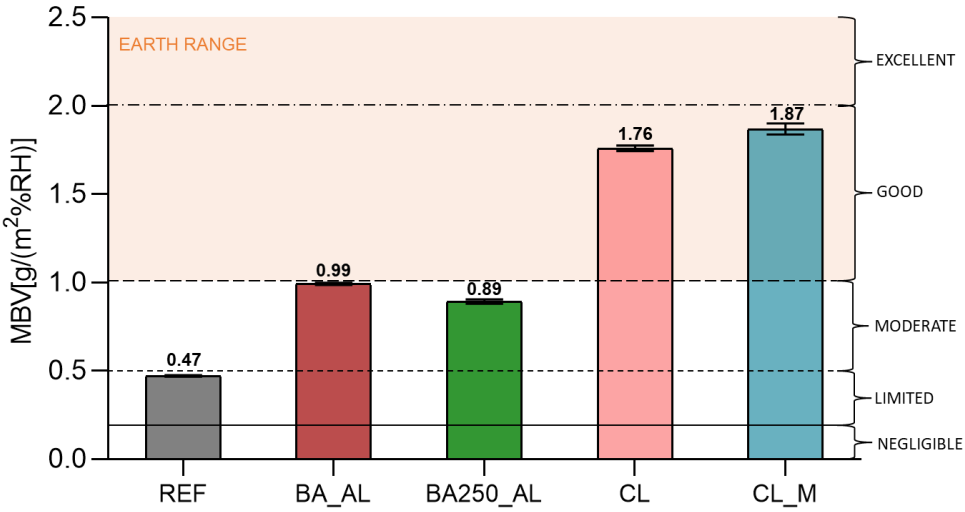


**Figure 5.13.** MBV (with standard deviation) of the tested plasters, limits proposed by Rode et al. (2005) and clay-based plasters range of values in orange (Ranesi et al., 2021c).

#### 5.2.3.5.3 Model of application

According to the middle humidity condition of ISO 24353 (2008) the daily variation of RH is 25% ($\Delta RH_{in}$). In a bedroom of 30 $m^3$ with a minimum natural ventilation (0.5 $h^{-1}$), occupied by two sleeping people, the moisture load is assumed to be 60 $g \cdot h^{-1}$ (according to NORDTEST theory (Rode et al., 2005)). If an occupation of 12 hours is assumed (as the previously applied conditions of the moisture buffering test (ISO 24353: 2008) the amount of additional moisture load would be 60 $g \cdot h^{-1}$ x 12 h= 720 g. Considering that the room configuration (**Figure 5.14**) includes a door (2x0.8 $m^2$) and a window (1.2x1.5 $m^2$), with all the walls and the ceiling coated with a plaster, the total reactive surface has 43.6 $m^2$. In this scenario, the moisture buffering requirement per coated area would be 16.5 $g \cdot m^{-2}$, calculated as 720g/43.6$m^2$. For the RH variation of 25%, the MBV required will be 16.5 $g \cdot m^{-2}$/25%RH, 0.66 $g \cdot m^{-2} \cdot$%RH. In this case, thus, among the materials tested, only the gypsum reference would not meet the requirement. Nevertheless, the passive moisture removal of the five plastering mortars at the end of 12 hours, can be easily quantified as their MBV x ΔRH x A (with A the plastered area) and is reported in **Table 5.12**.

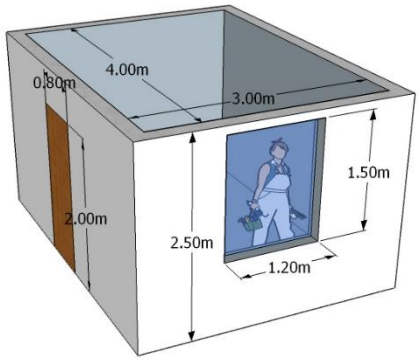


**Figure 5.14.** Model of the room configuration.

**Table 5.12.** Uptaken moisture from each plastering mortar at the end of 12 hours of exposure to a ΔRH of 25% if applied to the indoor surface of 43.6 $m^2$.

| Mortar | REF | BA_AL | BA250_AL | CL | CL_M |
|---|---|---|---|---|---|
| Uptaken moisture [g] | 512.3 | 1079.1 | 970.1 | 1918.4 | 2038.3 |

As expected, the different MBV of plastering mortars can have a huge impact on their passive moisture removal due to the usually large surface areas of application of these coatings. In the observed case of a common bedroom (12 $m^2$ area) the potential amount of moisture uptaken from a clay plaster would be around 2 kg and 0.5 kg for reference gypsum. Through the

addition of the bark from *A. dealbata* with no thermal treatment (and a small quantity of air lime) the latter would double to 1 kg.

### 5.2.4 Conclusions

The addition of bark from *Acacia dealbata*, a biowaste generated from the reuse of an invasive species, and low contents of air lime slightly decreases the workability of the premixed gypsum mortars, increasing the requirement of kneading water. When the bark is thermally treated (250 °C for 1 h) it is more hydrophobic and the same amount of water used for the mortar with addition of raw (untreated) bark, with the fixed amount of air lime, lead to a more fluid consistence. However, bark-added mortars workability is good even with low flow. The drying shrinkage is not significantly affected by the addition of the biomass, with a volumetric variation during the first 28 curing days very similar for the reference gypsum mortar and the two modified formulations analyzed. The mechanical performance of the reference mortar is the highest, followed by the mortars BA_AL and BA250_AL. This result is consistent with the fresh state characterization: the mortar BA_AL showed lower flow table consistence, so it is expected to be more compact and mechanically resistant. This is not in agreement with MIP results (the reference mortar showed the highest volume of pores) most probably because the bigger porosity, that is commonly related with mechanical resistance of the mortars, is not detected by MIP. When applied on the brick, all the mortars showed a good and similar hardness and adhesive strength, with almost 100% cohesive fracture, very good for restoration mortars.

The MIP analysis confirms that the higher volume of pores falls in the diameter range of 1-10 μm. Probably the missing volume of these pores is partially occupied by the biomass (when added). Nonetheless, the intra-particle nanoporosity of the bark can be responsible for the enhanced hygroscopic behavior of mortars and their slight hysteresis.

The addition of bark and thermally treated bark with a small air lime content (4% by wt.) to the gypsum mortar did not significantly modify its water absorption by capillarity and drying capacity. Anyway, the tested additions decreased the solubility in water of the gypsum mortar and retarded the absorption, which is an interesting result that can be further investigated. The possibility of a bio-stabilization of gypsum, with a reduction of its susceptibility to liquid water, can lead to an improvement of mortar durability.

Results from sorption isotherms and moisture buffering show that the hygroscopicity of the gypsum mortar, both in static and dynamic tests, was greatly enhanced by the addition of bark

and air lime. Overall, it does not seem that the thermal treatment of the biomass (at 250 °C) improved this property significatively, introducing only a slightly higher adsorption capacity. Nevertheless, all the mortars undergoing daily cycles of RH present a good capacity of desorption and the modified ones show MBV almost two times higher than the reference mortar. Thus, in environments where the RH is fluctuating during the day (like in the case of a bedroom analyzed from NORDTEST project) the mortars BA_AL and BA250_AL would better contribute to passive moisture control in comparison to the reference. As expected, the clay-based plasters tested at sorption isotherms and moisture buffering confirm that they are very hygroscopic. Both mortars, with low differences between them, showed a very high adsorption/desorption capacity at steady state and were performing at very high (good but almost excellent) levels of moisture buffering. Although their contribution was found still lower than the highly hygroscopic clay plasters, the modified gypsum plastering mortars doubled the MBV of the reference one, passing from limited (almost moderate) to moderate (almost good). The different behavior of the reference gypsum, the modified gypsum and the clay plasters, result in a very different amount of moisture uptaken when simulating the application of these plasters in a common bedroom.

It is concluded, in fact, that the addition of the bark from *A. dealbata* and a low amount of air lime to the industrial gypsum-based dry product, significantly enhances the passive moisture control ability of the gypsum plaster, without jeopardizing other requirements. Finally, the thermal treatment of the biomass is not advised, considering the results here obtained and the increase in embodied energy the biowaste would suffer.

## Acknowledgments

This research was supported by Portuguese Foundation for Science and Technology (FCT-Fundação para a Ciência e a Tecnologia): PD/BD/150399/2019 – 1st author Doctoral Training Program EcoCoRe. The authors are also grateful for FCT support through funding UIDB/04625/2020 of the research unit CERIS and UIDB/04077/2020 – Mechanical Engineering and Research Sustainability Center – METRICS and UIDB/05064/2020 - Research Centre for Endogenous Resource Valorization – VALORIZA and for the support of the projects Back2Future (2020-1-PT01-KA203-078406) and BIO-FIBRE (2022-1-DK01-KA220-HED-000086641) funded by the Erasmus+ Programme of the European Union. The authors would like to thank the National Laboratory for Civil Engineering of Portugal (LNEC) for the laboratory equipment and the support provided through the projects REuSE - Wall coverings for Rehabilitation: Safety and Sustainability; the Departments of Civil Engineering and Chemistry

of the School of Science and Technology of the NOVA University of Lisbon, the Department of R&D of SIVAL-Gessos Especiais, Lda and the Healthy Building Research Laboratory of the Portland State University.

## References

American Clay: https://www.americanclay.com/original-plasters (accessed on September 15, 2023).

Arundel A V, Sterling E M, Biggin J H, Sterling T D. Indirect health effects of relative humidity in indoor environments. *Environmental Health Perspectives*. 1986; 65:351, https://doi.org/10.1289/ehp.8665351.

Borges A, José H, Homem V, Simões M. Comparison of techniques and solvents on the antimicrobial and antioxidant potential of extracts from Acacia dealbata and Olea europaea. *Antibiotics* (Basel). 2020; 9(2):48. https://doi.org/10.3390/antibiotics9020048.

Caroselli M, Válek J, Zapletalová J, Felici A, Frankeová D, Kozlovcev P, Nicoli G, Jean G. Study of materials and technique of late baroque stucco decorations: Baldassarre Fontana from Ticino to Czechia. *Heritage*. 2021; 4(3):1737-1753. https://doi.org/10.3390/heritage4030097.

Cintura E, Faria P, Duarte M, Nunes L. Eco-efficient boards with agro-industrial wastes – Assessment of different adhesives. *Construction and Building Materials.* 2023; 404:132665. ISSN 0950-0618. https://doi.org/10.1016/j.conbuildmat.2023.132665.

Correia R, Quintela J C, Duarte M P, Gonçalves M. Insights for the valorization of biomass from portuguese invasive Acacia spp. in a biorefinery perspective. *Forests.* 2020; 11(12):1342. https://doi.org/10.3390/f11121342.

Elert K, Alabarce Alaminos R, Benavides-Reyes C, Burgos-Ruiz M. The effect of lime addition on weathering resistance and mechanical strength of gypsum plasters and renders. *Cement and Concrete Composites.* 2023; 139:105012. ISSN 0958-9465. https://doi.org/10.1016/j.cemconcomp.2023.105012.

EN 459-1; Building lime - Part 1: definitions, specifications and conformity criteria. European Committee for Standardization (CEN): Brussels, Belgium, 2015.

EN 1015-2; Methods of test for mortar for masonry—Part 2: Bulk sampling of mortars and preparation of test mortars. European Committee for Standardization (CEN): Brussels, Belgium, 1999.

EN 1015-3; Methods of test for mortar for masonry—Part 3: determination of consistence of fresh mortar (by flow table). European Committee for Standardization (CEN): Brussels, Belgium, 1999.

EN 1015-6; Methods of test for mortar for masonry—Part 6: determination of bulk density of fresh mortar. European Committee for Standardization (CEN): Brussels, Belgium, 1999.

EN 1015-10; Methods of test for mortar for masonry—Part 10: determination of dry bulk density of hardened mortar. European Committee for Standardization (CEN): Brussels, Belgium,1999.

EN 1015-11; Methods of test for mortar for masonry—Part 11: determination of flexural and compressive strength of hardened mortar. European Committee for Standardization (CEN): Brussels, Belgium, 1999.

EN 1015-12; Methods of test for mortar for masonry - Part 12: determination of adhesive strength of hardened rendering and plastering mortars on substrates. European Committee for Standardization (CEN): Brussels, Belgium, 2016.

EN 13279-1; Gypsum binders and gypsum plasters—Part 1: definitions and requirements. European Committee for Standardization (CEN): Brussels, Belgium, 2008.

EN 13279-2; Gypsum binders and gypsum plasters—Part 2: Test methods. European Committee for Standardization (CEN): Brussels, Belgium, 2014.

EN 14146; Natural stone test methods. determination of the dynamic modulus of elasticity (by measuring the fundamental resonance frequency). European Committee for Standardization (CEN): Brussels, Belgium, 2004.

EN 14774-2; Solid biofuels - determination of moisture content - oven dry method - Part 2: total moisture - simplified method. European Committee for Standardization (CEN): Brussels, Belgium, 2009.

EN 14775; Solid biofuels - Determination of ash content. European Committee for Standardization (CEN): Brussels, Belgium, 2009.

EN 15148; Solid biofuels - Determination of the content of volatile matter. European Committee for Standardization (CEN): Brussels, Belgium, 2009.

EN 15801; Conservation of cultural property—test methods— determination of water absorption by capillarity. European Committee for Standardization (CEN): Brussels, Belgium, 2009.

EN 16322; Conservation of cultural heritage—test methods— determination of drying properties. European Committee for Standardization (CEN): Brussels, Belgium, 2013.

Fang L, Clausen G, Fanger P O. Impact of temperature and humidity on the perception of indoor air quality. Indoor Air. 1998; 8: 80-90. https://doi.org/10.1111/j.1600-0668.1998.t01-2-00003.x

Ferreira T, Monney Paiva J, Pinho C. performance assessment of invasive Acacia dealbata as a fuel for a domestic pellet boiler. Chemical Engineering Transactions. 2014; 42. ISSN 2283-9216. http://dx.doi.org/10.3303/CET1442013.

Ferreira C, de Freitas V P, Delgado J M P Q. The influence of hygroscopic materials on the fluctuation of relative humidity in museums located in historical buildings. Studies in Conservation. 2020; 65(3): 127-141. https://doi.org/10.1080/00393630.2019.1638666.

Freire M T, Veiga M R, Santos Silva A, de Brito J. Restoration of ancient gypsum-based plasters: Design of compatible materials. Cement and Concrete Composites. 2021; 120:104014, ISSN 0958-9465. https://doi.org/10.1016/j.cemconcomp.2021.104014.

Gariani G, Lehuédé P, Leroux L, Wallez G, Goubard F, Bouquillon A, Bormand M. First insights on the mineral composition of "stucco" devotional reliefs from Italian Renaissance Masters: investigating technological practices and raw material sourcing. Journal of Cultural Heritage. 2018; 34:23-32, ISSN 1296-2074. https://doi.org/10.1016/j.culher.2018.05.003.

Gbekou F K, Boudenne A, Eddhahak A, Benzarti K. Mechanical and hygrothermal properties of cement mortars including both phase change materials and miscanthus fibers. Bio-Based Building Materials. ICBBM 2023. Amziane S, Merta I, Page J. (Eds) Springer, RILEM Bookseries; 2023. 45:804–816. https://doi.org/10.1007/978-3-031-33465-8_62.

Gentile V, Libralato M, Fantucci S, Shtrepi L, Autretto G. Enhancement of the hygroscopic and acoustic properties of indoor plasters with a super adsorbent calcium alginate biopolymer. Journal of Building Engineering. 2023; 76:107147, ISSN 2352-7102, https://doi.org/10.1016/j.jobe.2023.107147.

Guarnieri G, Olivieri B, Senna G, Vianello A. Relative Humidity and Its Impact on the Immune System and Infections. International Journal of Molecular Sciences. 2023; 24(11):9456. https://doi.org/10.3390/ijms24119456.

Hansen K K. Sorption Isotherms: A Catalogue. Technical Report 162/86. Technical University of Denmark (Eds). 1986.

ISO 12571 (International Standards Organization): Hygrothermal performance of building materials and products - determination of hygroscopic sorption properties. ISO, Geneva, Switzerland, 2013.

ISO 24353 (International Standards Organization): Hygrothermal performance of building materials and products - determination of moisture adsorption/desorption properties in response to humidity variation. ISO, Geneva, Switzerland, 2008.

Kamel A M A, Marie H A H, Mahmoud H A, Ali M F. Mineralogical characterization of Islamic stucco: Minaret of Shams El-Deen El-Wasty, Bulaq, Egypt. Construction and Building Materials. 2015; 101(1):692-701, ISSN 0950-0618. https://doi.org/10.1016/j.conbuildmat.2015.10.059.

Li X, Ran M. Gypsum-based humidity-control material: preparation, performance and its impact on building energy consumption. Materials. 2023; 16:5211. https://doi.org/10.3390/ma16155211.

Lima J, Faria P. Eco-efficient earthen plasters. The influence of the addition of natural fibers. Natural Fibres: Advances in Science and Technology Towards Industrial Applications. From Science to Markets, Fangueiro, Raul, Rana, Sohel (Eds.). Springer, RILEM Book Series; 2016. 12: 315-327. Doi:10.1007/978-94-017-7515-1_24.

López-Hortas L, Rodríguez-González I, Díaz-Reinoso B, Torres M D, Moure A, Domínguez H. Tools for a multiproduct biorefinery of Acacia dealbata biomass. Industrial Crops and Products. 2021; 169:113655, ISSN 0926-6690. https://doi.org/10.1016/j.indcrop.2021.113655.

Lorenzo P, González L, Reigosa M J. The Genus Acacia as Invader: The characteristic case of acacia dealbata link in Europe. Annals of Forest Science. 2010; 67:101. https://doi.org/10.1051/forest/2009082.

Mahmoud H M, Papadopoulou L. archaeometric analysis of pigments from the tomb of Nakht-Djehuty (TT189), El-Qurna Necropolis, Upper Egypt. ArcheoSciences. 2013; 37:19-33. https://doi.org/10.4000/archeosciences.3967.

Marcelino-Sadaba S, Kinuthia J, Oti J, Seco Meneses A. Challenges in Life Cycle Assessment (LCA) of stabilised clay-based construction materials. Applied Clay Science. 2017; 144: 121-130. ISSN 0169-1317. https://doi.org/10.1016/j.clay.2017.05.012.

McGregor F, Heath A, Maskell D, Fabbri A, Morel J-C. A review on the buffering capacity of earth building materials. Proc. of the Institution of Civil Engineers: Construction Materials. 2016; 169(5), 241-251. https://doi.org/10.1680/jcoma.15.00035.

Meireles P D S, Pereira D S S, Melo M A F, Braga R M, Freitas J C O, Melo D M A, Silvestre F R S. Technical evaluation of calcium sulphate α-hemihydrate in oilwell application: An alternative to reduce the environmental impacts of Portland cement. Journal of Cleaner Production. 2019; 220: 1215-1221. https://doi.org/10.1016/j.jclepro.2019.02.120.

Nunes L J R, Raposo M A M, Meireles C I R, Gomes C J P, Ribeiro N M C A. Control of invasive forest species through the creation of a value chain: acacia dealbata biomass recovery. Environments. 2020; 7(5):39. https://doi.org/10.3390/environments7050039.

Nunes L J R, Raposo M A M, Meireles C I R, Gomes C J P, Ribeiro N M C A. The impact of rural fires on the development of invasive species: analysis of a case study with Acacia dealbata Link. in Casal do Rei (Seia, Portugal). Environments. 2021a; 8:44. https://doi.org/10.3390/environments8050044.

Nunes L J R, Rodrigues A M, Loureiro L M E F, Sá L C R, Matias J C O. Energy recovery from invasive species: Creation of value chains to promote control and eradication. Recycling. 2021b; 6:21. https://doi.org/10.3390/recycling6010021.

Paulo M S, Veiga M R, de Brito J. Gypsum coatings in ancient buildings. Construction and Building Materials. 2007; 21(1):126-131, ISSN 0950-0618. https://doi.org/10.1016/j.conbuildmat.2005.06.035.

Pawełkowicz S S, Svora P, Prošek Z, Keppert M, Vejmelková E, Murafa N, Sawoszczuk T, Syguła–Cholewińska J, Bíbová H. Laboratory assessment of a photoactive gypsum-based repair plaster. Construction and Building Materials. 2022; 346:128426, ISSN 0950-0618, https://doi.org/10.1016/j.conbuildmat.2022.128426.

Posani M, Voney V, Odaglia P, Eschbach D, Habert G. High-Tech, Low-Carbon Material Fabrication: 3D-printed geopolymers for optimized indoor comfort. Proceedings of the 2nd International Conference on Construction, Energy, Environment and Sustainability (CEES 2023). Funchal, Portugal 27-30 June 2023. Itecons (Eds.), ISBN: 978-989-54499-3-4.

Ranesi A, Faria P, Veiga M R. Traditional and modern plasters for built heritage: suitability and contribution for passive relative humidity regulation. Heritage. 2021a; 4(3):2337-2355. https://doi.org/10.3390/heritage4030132.

Ranesi A, Faria P, Veiga M R. Eco-efficiency of plasters for rehabilitation and new buildings. Proc. of 2nd International Conference on Sustainable, Environmentally Friendly Construction Materials. Horszczaruk E, Brzozowski P (Eds). 2021b; 91–96.

Ranesi A, Veiga M R, Faria P. Laboratory characterization of relative humidity dependent properties for plasters: A systematic review. Construction and Building Materials. 2021c; 304. https://doi.org/10.1016/j.conbuildmat.2021.124595.

Ranesi A, Faria P, Correia R, Freire MT, Veiga R, Gonçalves M. Gypsum mortars with Acacia dealbata biomass waste additions: effect of different fractions and contents. Buildings. 2022; 12(3):339. https://doi.org/10.3390/buildings12030339.

Ranesi A, Faria P, Freire M T, Gonçalves M, Veiga R. Gypsum plastering mortars with acacia dealbata biowaste additions: Effect of different fractions and contents on the relative humidity dependent properties. Construction and Building Materials. 2023; 404:133283. ISSN 0950-0618. https://doi.org/10.1016/j.conbuildmat.2023.133283.

Raposo M A M, Pinto-Gomes C J, Nunes L J R. Selective shrub management to preserve Mediterranean forests and reduce the risk of fire: The case of mainland Portugal. Fire. 2020; 3:65. https://doi.org/10.3390/fire3040065.

Rode C, Peuhkuri RH, Mortensen LH, Hansen KK, Time B, Gustavsen A, Ojanen T, Ahonen J, Svennberg K, Arfvidsson J, Harderup LE. Moisture buffering of building materials. Technical University of Denmark, Department of Civil Engineering (Eds.). 2005.

Rode C, Grau K. Moisture Buffering and its Consequence in Whole Building Hygrothermal Modeling. Journal of Building Physics. 2008; 31(4):333-360. https://doi.org/10.1177/1744259108088960.

Rosa Latapie S, Abou-Chakra A, Sabathier V. Microstructure of bio-based building materials: new insights into the hysteresis phenomenon and its consequences. Buildings. 2023; 13: 1650. https://doi.org/10.3390/buildings13071650.

Sáez-Pérez M P, Durán-Suárez J A, Verdú-Vázquez A, Gil-López T. Study and characterization of special gypsum-based pastes for their use as a replacement material in architectural restoration and construction. Materials. 2022; 15:5877. https://doi.org/10.3390/ma15175877.

Santos A R, Veiga M R, Santos Silva A, de Brito J, Álvarez J I. Evolution of the microstructure of lime based mortars and influence on the mechanical behaviour: the role of the aggregates. Construction and Building Materials. 2018; 187:907-922. ISSN 0950-0618. https://doi.org/10.1016/j.conbuildmat.2018.07.223.

Santos T, Gomes M I, Santos Silva A, Ferraz E, Faria P. Comparison of mineralogical, mechanical and hygroscopic characteristic of earthen, gypsum and cement-based plasters. Construction and Building Materials. 2020; 254:119222, ISSN 0950-0618. https://doi.org/10.1016/j.conbuildmat.2020.119222.

Santos T, Almeida J, Silvestre JD, Faria P. Life cycle assessment of mortars: A review on technical potential and drawbacks. Construction and Building Materials. 2021; 288:123069. ISSN 0950-0618. https://doi.org/10.1016/j.conbuildmat.2021.123069.

Sowndhararajan K, Joseph J M, Manian S. Antioxidant and free radical scavenging activities of indian Acacias: Acacia Leucophloea (Roxb.) Willd., Acacia Ferruginea Dc., Acacia Dealbata Link. and Acacia Pennata (l.) Willd. International Journal of Food Properties. 2013; 16(8):1717-1729. https://doi.org/10.1080/10942912.2011.604895.

Torres-González M, Jesús Martín-Del-Rio J, Alejandre-Sánchez F J, León Muñoz M, Bienvenido-Huertas D, Macías Bernal J M. guidelines for conservation and restoration of historic polychrome plasterwork: the church of St María la Blanca in Seville, Spain. Studies in Conservation. 2023; 68(5): 529-547, DOI: 10.1080/00393630.2022.2072096.

Válek J, Skružná O, Kozlovcev P, Frankeová D, Mácová P, Viani A, Kumpová I. Composition and technology of the 17th century stucco decorations at Červená Lhota Castle in Southern Bohemia. International Journal of Architectural Heritage. 2020; 14(7): 1042-1057 DOI: 10.1080/15583058.2020.1731627.

Vicente E D, Vicente A M, Evtyugina M, Carvalho R, Tarelho L A C, Paniagua S, Nunes T, Otero M, Calvo L F, Alves C. Emissions from residential pellet combustion of an invasive acacia species. Renewable Energy. 2019; 140:319-329. https://doi.org/10.1016/j.renene.2019.03.057.

Xiong J, Lian Z, Zhou X, You J, Lin Y. Effects of temperature steps on human health and thermal comfort. Building and Environment. 2015; 94:144-154. https://doi.org/10.1016/j.buildenv.2015.07.032.

Yang Y, Shen Z, Wu W, Zhang H, Ren Y, Yang Q. Preparation of a novel diatomite-based PCM gypsum board for temperature-humidity control of buildings. Building and Environment. 2022; 226: 109732, ISSN 0360-1323. https://doi.org/10.1016/j.buildenv.2022.109732.

Záleská M, Pavlíková M, Pivák A, Lauermannová AM, Jankovský O, Pavlík Z. Lightweight vapor-permeable plasters for building repair detailed experimental analysis of the functional properties. Materials (Basel). 2021; 14(10):2613. https://doi.org/10.3390/ma14102613.

Zhang M, Qin M, Chen Z. Moisture Buffer Effect and its Impact on Indoor Environment. Procedia Engineering. 2017; 205:1123-1129, https://doi.org/10.1016/j.proeng.2017.10.417.

Zu K, Qin M. (2022). Energy-saving potential of using metal-organic frameworks (MOFs) for indoor moisture control: a passive approach. In Proc. of Indoor Air 2022. International Society of Indoor Air Quality and Climate (Pub.). 12-16 June 2022. 1832.

# 5.3 Article D2 - Primary Emissions, Deposition Velocities and Secondary Emissions

(the article was submitted on 27/10/2023 to the journal *Building and Environment;* reviews from the thesis advisory committee were applied)

## Eco-efficient coatings for healthy indoors: ozone deposition velocities, primary and secondary emissions

Alessandra Ranesi[1,2*], Paulina Faria[1], M. Rosário Veiga[2], Elliott T. Gall[3]
1. CERIS, Department of Civil Engineering, NOVA School of Science and Technology, NOVA University Lisbon, Quinta da Torre, 2829-516 Caparica, Portugal
2. National Laboratory for Civil Engineering, Avenida do Brasil 101, 1700-066 Lisbon, Portugal
3. Department of Mechanical and Materials Engineering, Portland State University, 1930 SW 4th Ave, 97201 Portland, OR, United States
* corresponding author: a.ranesi@campus.fct.unl.pt

## Abstract

Volatile organic compounds (VOCs) and ozone (O3) are harmful pollutants present in indoor air. Indoor concentrations of VOCs are typically higher than outdoors, due to the presence of indoor sources like building materials and reactions of surfaces with ozone. Indoor coatings can also be responsible for primary emissions of VOCs. The study aims to identify and quantify the ozone reactivity and primary and secondary emissions of different indoor coatings. The coatings selected for the study were three gypsum-based plastering mortar, without or with addition of Acacia dealbata bark as bio-waste (raw, BA, and after being heated at 250 °C, BA250), two clay plasters (one with sand and the other with seashells as additional aggregate), applied both as basecoat and topcoat (on drywall), and one un-coated drywall. All the products tested had ozone deposition velocities that would reduce the indoor ozone concentration meaningfully if implemented in a real indoor space, contributing to the improvement of indoor air quality. The addition of bark to the formulation of the gypsum-based plasters, either raw or heated at 250 °C, increased by 50% the ozone deposition velocity of the coating. The gypsum-based plaster shows the lowest ozone deposition velocity, but also the lowest primary and secondary emissions. However, the addition of BA and BA250 increased by 80% and 200%, respectively, both primary and secondary emissions, with methanol (m/z 33.030) accounting for about 60% of the increase. The addition of crushed seashells to the formulation of the clay-based plasters lowered the secondary emission yields (102% and 120% respectively, when applied as base and topcoat). Moreover, the addition of BA250 to the gypsum plaster decreased by 640% the total molar yield of VOCs.

**Keywords:** Clay plaster, gypsum mortars, biomass, drywall, removal mechanisms, volatile organic compounds.

### 5.3.1 Introduction

Human exposure to volatile organic compounds (VOC) indoors is a problem of increasing interest (Kotzias 2023). There are many possible indoor sources of VOCs, including human occupancy (Weschler, 2016; Wang et al., 2022; Tang et al., 2016); building materials (Chin et al., 2019; Harčárová et al., 2020; Zhou, 2022; Braish et al., 2023); ozone surface reactivity (Nicolas et al., 2007; Poppendieck et al., 2007); and the combination of the previous factors (Weschler and Nazaroff, 2023a). Indoor exposure to specific concentration levels of VOCs (WHO, 2010) can have detrimental effects on human health and has been shown to increase the risk of diseases like leukemia and asthma and increase likelihood of low birth weight (Liu et al., 2022; Maung et al., 2022). The concentration of VOCs is modified by chemical reactions with other pollutants, e.g., ozone, which is an important driver of indoor chemistry. Weschler (Weschler, 2000) in his review paper clearly presented the main factors involved in indoor air chemistry as "thermodynamics, kinetics, reactant concentration and air exchange rates". Typically, the stable byproducts of oxidations are aldehydes, organic acids, and ketones. In this case the author states that "the concentration of the sum of the products is at least twice the initial concentration of the precursor" (Weschler, 2000). According to the previous considerations, the consideration of the indoor ozone concentration levels is a priority issue not only due to direct exposure to this pollutant, but also the impact it may have on indoor chemistry.

Ozone is a harmful secondary pollutant, associated with occurrence of airway diseases (Kim et al., 2020) and increase of mortality (Mousavinezhad et al., 2023). This pollutant is generated outdoors by reactions between VOCs, NOx, and CO in the presence of sunlight and is normally found in higher concentration in the suburban areas. In the Lisbon region, Portugal, ozone was found to exceed the threshold of 180 µg·m3 (Directive 2002/3/CE) in 86% of instances between 1 pm to 5 pm in summer (Ferreira et al., 2004). Nevertheless, when the attention is moved from outdoor ozone to the indoors, there are many additional parameters to be considered. It is commonly expected that most of the ozone indoor is coming from the outdoor, but higher concentration indoors may result from indoor sources (Huang et al., 2019). The building outdoor air exchange rates, ozone removal by filtering systems (activated carbon in mechanical ventilation supply air or in portable air cleaners), and by indoor surfaces are building related factors (Nazaroff and Weschler, 2022) that can contribute to the control of the indoor ozone.

Chemical reactions on indoor surfaces of increasing research interest (Ault et al, 2020) due to their complexity and the important role they can play on indoor air quality. Indeed, one of the mitigation strategies for elevated ozone indoors is passive removal of ozone by building

materials selected to help purify the indoor air without energy consumption. The mechanism for an assumed smooth surface is described in two main phases: the transport of the pollutant to the surface and the uptake onto the surface (Reiss et al., 1994). The capability of a material to remove ozone is often parameterized by the deposition velocity (vd), which characterizes the projected area-normalized rate of ozone uptake due to transport to, and reactions with, a surface. Deposition velocity theory combines the fluid mechanics of the space (transport from a well-mixed indoor core zone through a boundary layer to the surface) and the chemistry (via a reaction probability ( $\gamma$ ), which is the fraction of ozone-surface collisions resulting in a chemical reaction) into a single parameter. It is highly recommended to monitor the reaction products when quantifying the rate of ozone uptake on a specific building material (Weschler and Nazaroff, 2023b).

Building materials and products with different composition and porosity (from glass to clay plasters) showed different reactivity to ozone and byproduct generation (Shen and Gao, 2018; Chin et al., 2019). Ozone passive removal materials may help controlling indoor ozone concentrations while reducing energy consumptions (Darling et al., 2016). The coating materials and products already studied are: gypsum drywall (Kunkel et al., 2010; Rim et al., 2016; Kleno et al., 2001; Lamble et al., 2011; Cros et al., 2012; Poppendieck et al., 2007), activated carbon filters (Gall et al., 2014), carpets (Nicolas et al., 2007, Morrison and Nazaroff, 2002) clay-based plasters and paints (Lamble et al., 2011, Darling and Corsi, 2016, Darling et al., 2012), concrete tiles (Grøntoft, 2002; Grøntoft, 2004) and wooden flooring (Lin and Hsu, 2015).

Clay-based materials have potential to be employed in the current building sector thanks to their many positive properties (hygroscopic behavior, thermal inertia, aesthetic value) and high eco-efficiency. For example, unstabilized clay-based mortars produced with local earths have a very positive life cycle analysis in comparison to other plasters (Santos et al.,2021) and high reusability (Pelicaen et al., 2021). Their high hygroscopicity makes them very good candidates for passive survivability (Ben-Alon and Rempel, 2023) and carbon dioxide removal (Arris-Roucan et al., 2023). However, as clay is a very heterogeneous family of binders, and not standardized, broader research is needed to gather results from a larger number of used clay-based plasters.

Gypsum-based plastering mortars (with small addition of air lime) were commonly used in several countries as traditional coatings and decorations (Alejandre et al., 2021; Gariani et al., 2018; Kamel et al., 2015; Mahmoud and Papadopoulou, 2013; Válek et al., 2020; Caroselli at al., 2021). Thus, they commonly represent a viable option for restoration projects (Freire et al.,

2021; Sáez-Pérez et al., 2022, Torres-González et al., 2023). The gypsum plasters are considered a green choice because their main binder, calcium sulphate hemihydrate, has low embodied energy (calcination temperature of 120-180 ºC) and is highly recyclable (up to 5 times according to Rodrigo et al., 2017) still using low temperatures (130 °C for 4 h according to Brumanis et al., 2022). These plasters are highly performative under several aspects, for instance high mechanical strength and water vapor permeability, and less under other aspects, e.g. their moisture reactivity that some studies present as lower than other traditional plasters like clay-based ones (Santos et al., 2020; Ranesi et al., 2021).

The addition of biomass to clay-based materials may improve some aspects of material performance. Acacia dealbata is an invasive species spread in many countries, that has a high germination rate in burnt environments and contributes to fires propagation. The biowastes generated from the plant-control-actions must be recycled, to turn the mechanical removal more sustainable (Sowndhararajan et al., 2013; Borges et al., 2020; Nunes et al, 2021; López-Hortas et al., 2021). The addition of the A. dealbata biomass to building materials is one of these recycling strategies.

Based on the previous considerations, the present study analyses the ozone reactivity and primary and secondary emission rates (VOCs) of eight indoor building coatings with a specific focus on coatings based on gypsum and clay. Two formulations of clay-based plasters applied both as top and base coats and three formulations of gypsum-based plasters with the addition of A. dealbata biowaste, were selected for the study together with the gypsum drywall. The aim of the study is to assess the potential for these coatings to be used as passive ozone removal products, ideally while contributing minimally to indoor VOCs concentrations.

## 5.3.2 Materials and methods

### 5.3.2.1 Materials and products

The building coatings included in the study were two different formulated clay-based plasters, one drywall (plasterboard) and three gypsum-based formulations. Drywall is a very common building product, widely used in modern practice. It was selected for the study as "control material" since some literature on its effect on passive ozone removal and associated VOCs level already existed (Lamble et al., 2011; Darling et al., 2017).

The gypsum plastering mortars are based on a dry powder pre-mixed restoration product for integration and/or substitution of traditional plasters that can also be applied to new construction. It is produced by Sival, Gessos Especiais, Lda, Portugal. The product is based on

calcium sulphate hemihydrate with the addition of calcium carbonate aggregates and proprietary additives. The bark of *Acacia dealbata* was added to the gypsum-based plaster. The raw bark (BA) was obtained by drying, crushing, and sieving the biowaste at 1 mm. A thermally threated version was obtained by heating a fraction of material at 250 °C for one hour (this material is named BA250 in this study). A low content of hydrated air lime CL-90S (EN 459-1, 2015) was used to formulate the pre-dosed gypsum-biomass mortars as it is recognized for its antibacterial behavior and increase in hygroscopicity (Ranesi et al., 2024).

For the clay plasters the commercial premixed products *Enjarre* (CL) and *Maritimo* (CL-M), from American Clay Enterprises LLC, were used. The two premixed products have very similar formulations with the addition of recycled, crushed seashells from the U.S. Gulf Coast to the CL-M, designated as maritime clay plaster. According to the producer the addition should improve the hygroscopic behavior of the plaster.

An uncoated drywall with a thickness of 12.7 mm was used as a control coating, for validation of results and calibration of the protocol. It was also used as substrate for the plasters' topcoat application.

#### 5.3.2.2 Mortars and plaster specimens

Five specimens of the reference gypsum-based plastering mortar (G) were prepared mixing the product with water (water/dry ratio of 48%). Two additional mortars were obtained from the same gypsum pre-dosed product with the addition of biomass. Each bark addition (BA and BA250) was done at 10% by volume of the gypsum powdered product, first mixing with the dry product and then adding water. Both the modified gypsum-based plastering mortars BA_AL and BA250_AL were obtained with the addition of a small amount of the hydrated lime (AL) to prevent biological attack (increasing the neutral pH of gypsum). All the specimens of G, BA_AL and BA250_AL were cast into 20 mm-slices cut from a plastic pipe with an external diameter of 110 mm and a wall thickness of 2 mm.

The clay-based plasters were obtained by mixing the two commercial premixed products (CL and CL-M*)* with water, according to workability requirements. Both the products were applied as base and topcoats, the latter with the drywall as substrate as advised by the producer. The basecoat specimens (CL, CL-M) were obtained with a cylindrical shape mold, 20 mm high and with a diameter of about 80 mm. The topcoat specimens were obtained by application on disks of drywall, cut with about 90 mm diameter and coated by a water-based commercial primer (Zinsser) enhanced with sand addition (mixed with it). To ensure low shrinkage and good adhesion, the finishing clay-based topcoat plasters (DW_CL, DW_CL-M) were applied in three

successive layers, spaced 24 hours apart, with a final thickness of about 5 mm. The specimens of drywall were obtained by cutting in squares (60 mm sides) the drywall panel. All the samples were kept preconditioned (RH 30±5%, T 23±3˚C) in the controlled environment of the laboratory and cured for a minimum of 28 days before being tested.

The coatings (**Figure 5.15**) used in this study are presented in **Table 5.13**, along with descriptions of number of specimens tested and specimens' dimensions (diameter or side of the square and thickness). The loose bulk density of the dried industrial gypsum-based and clay-based products, the water/dry product ratio of the mortars and their fresh density are also presented.

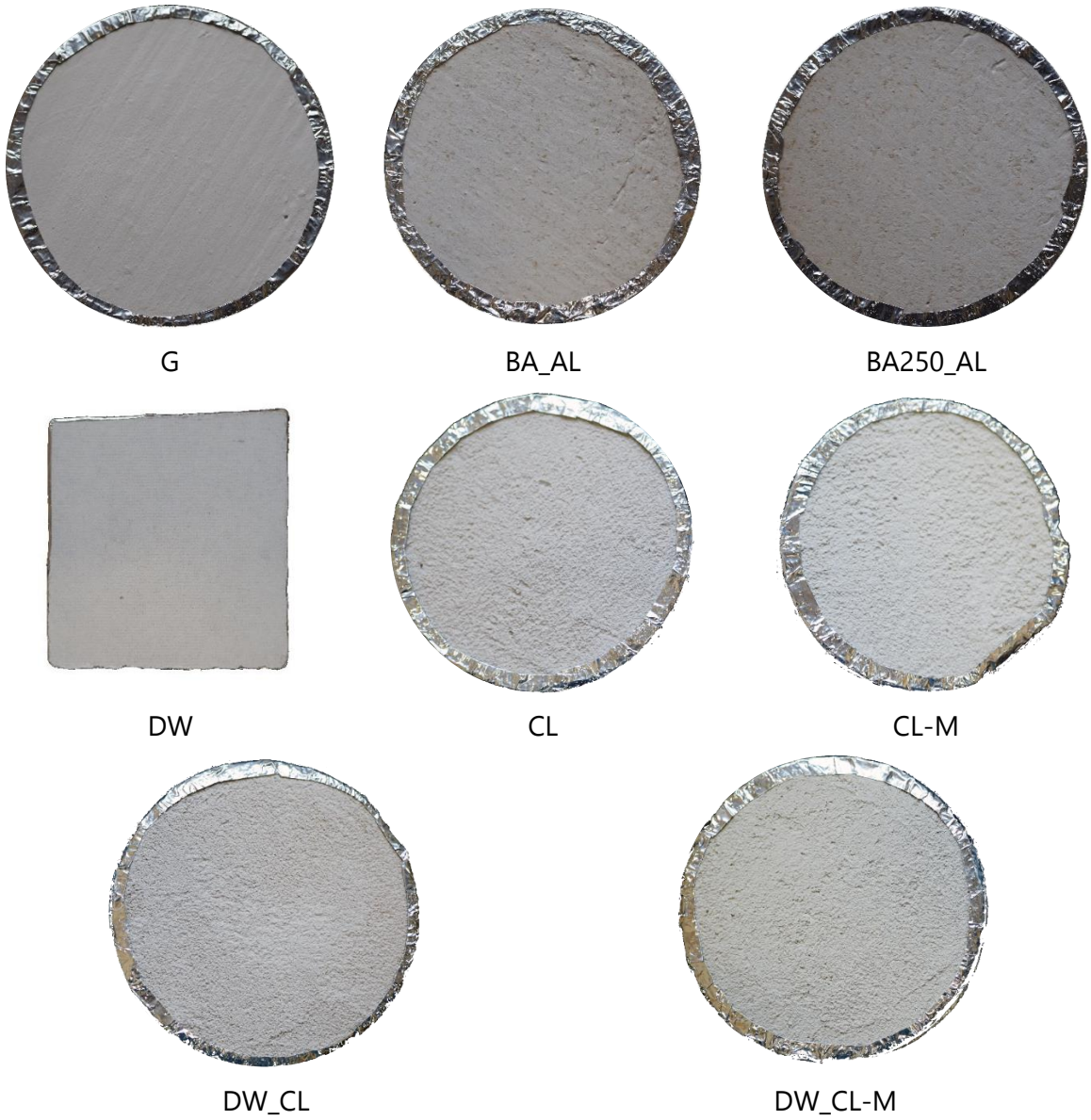


**Figure 5.15.** Specimens of the plastering mortars and drywall tested.

The plasters coatings used in this study are enumerated in **Table 5.13**, along with descriptions of number of specimens prepared for the study and specimens' dimensions (diameter or side of the square). The loose bulk density of the dried industrial gypsum-based and clay-based products, the water/dry product ratio of the mortars and their fresh density are also presented.

**Table 5.13.** Synthesis of tested coatings, fresh mortars and specimens' characterization.

| | nº | d/s [mm] | t [mm] | LBD [kg/dm³] | w/dry [%] | FBD [kg/dm³] |
|---|---|---|---|---|---|---|
| **G** | 5 | 101 ± 2 | 20 ± 2 | 0.75 | 48 | 1.65 |
| **BA_AL** | 5 | 98 ± 2 | 20 ± 2 | | 51 | 1.61 |
| **BA250_AL** | 5 | 99 ± 2 | 20 ± 2 | | 51 | 1.62 |
| **CL** | 5 | 85 ± 2 | 20 ± 2 | 1.21 | 30 | 1.98 |
| **DW_CL** | 5 | 90 ± 2 | 18 ± 2 | | 25 | - |
| **CL-M** | 5 | 80 ± 3 | 20 ± 2 | 1.08 | 31 | 1.75 |
| **DW_CL-M** | 5 | 87 ± 3 | 18 ± 2 | | 25 | - |
| **DW** | 3 | 60 ± 2 | 12.7 | - | - | - |

Notation: nº - number of specimens prepared; d/s – diameter or side, according to the geometry; ; t – total thickness; LBD – loose bulk density of the dry products; w/dry – water/dry product ratio; FBD – fresh bulk density; * - only of the topcoat.

#### 5.3.2.3 Test methods

##### 5.3.2.3.1 Experimental layout and timing

The experiments described here are designed to identify and quantify the primary and secondary emissions together with the ozone deposition velocities for each tested building coating. **Figure 5.16** shows a scheme of the experimental apparatus used to enable these experiments.

Dry air at positive pressure passed through a high efficiency particulate air (HEPA) filter and an activated carbon (AC) filter with a reduction valve (0.3 MPa). Then, the flow mass controller (FMC from GFC, Aalborg) was set at 3.6 L/min to ensure the sufficient stream of flow to the chambers (about 1.3 L/min each, inlet) for the ozone monitor. The air flow in each line was frequently checked by a calibrator (Model Gilibrator 2, Gilian, Sensidyne, LP). Although the exchange rate of 12 $h^{-1}$ can be considered high for actual indoor spaces, it is similar to other experimental setups using similar small-scale chambers (Lamble et al., 2011; Grøntoft et al., 2004a, 2004b; Grøntoft, 2004; Grøntoft, 2002; Gall et al., 2014; Rim et al., 2016). A UV lamp produced ozone (on: ≈ 100 ppb; off: 0 ppb) and then the flow passed through a humidifier (manually controlling the moisture of the air flow to be around 50±10% RH). The apparatus included two borosilicate glass chambers, each with volume 6.5 L. Sensors (HOBO, S-THB-

M008) were placed and sealed in each chamber to continuously measure temperature and relative humidity. A bypass was set on the inlet line of the sample chamber to allow measurement of the inlet concentration of ozone ($C_{O3,in}$). The two ozone monitors were positioned at the end of the setup line, one model 1003 AH, DAISIBI, and one model 106-L, 2B Technologies, both with resolution of 0.1 ppb and accuracy greater than 1.5 ppb or 2% of the measurement. The monitors were calibrated at the beginning of the experiment, with both the chambers empty, using a five-point regression line with $R^2 > 0.99$. Note that without activating the bypass both monitors read the ozone concentration at the exhaust of the respective chambers ($C_{O3,e}$). The proton transfer reaction – time of flight – mass spectrometer (PTR-ToF-MS, Ionicon, PTR-ToF 1000) reports the concentration of the emitted volatile organic compounds (VOCs) (further on indicated by the subscript b of byproduct) present in: inlet air (#1), outlet air from the sample chamber (#2) and from the control chamber (#3).

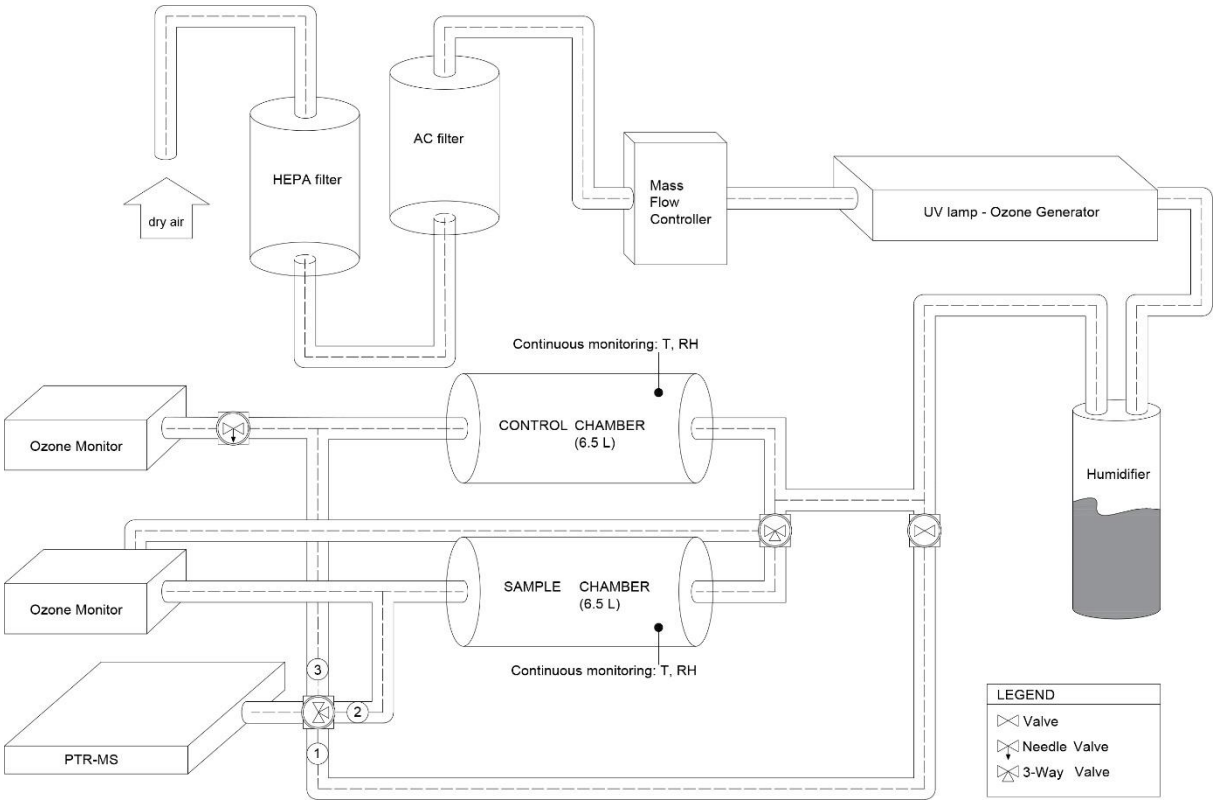


**Figure 5.16.** Experimental system layout. Acronyms in the diagram: HEPA – high efficiency particulate air, AC – activate carbon, UV – ultraviolet, T – temperature, RH – relative humidity, PTR-MS – proton transfer reaction mass spectrometer.

Prior to testing and after material changeout a passivation protocol was developed to ensure the non-reactivity of the glazed surfaces of the chambers (i.e., the protocol was run with empty chambers). The sample chamber was cleaned with lint-free wipes (Kimwipes, KIMTECH). Then

the chambers, both empty, were exposed to high $O_3$ concentration (>300 ppb) for a minimum of 12 hours. After the ozone passivation, clean air was flushed through the chambers for a minimum of 12 hours.

The test procedure lasted around 5.5 hours, with three main steps, schematized in **Figure 5.17** and briefly described.

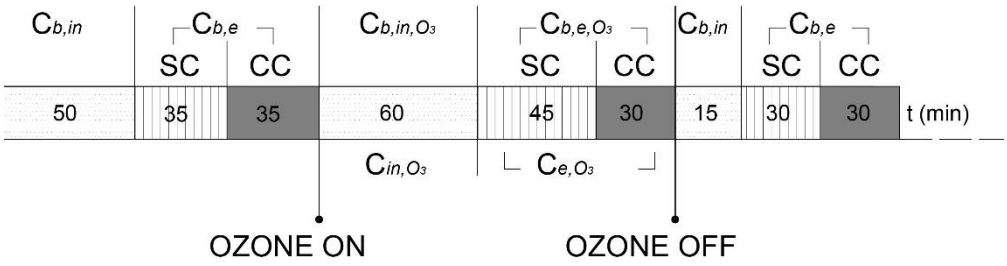


**Figure 5.17.** Sample timing of the experiment in the sample chamber (SC) and control chamber (CC). The experiment aims to quantify the concentration (C) of byproducts (b), ozone ($O_3$) and byproducts in presence of ozone (b,$O_3$) of the airflow inlet (in) or at the exhaust (e).

First, VOC and ozone concentrations prior to ozone exposure (2 hours) were collected: the air flow was flushed into the chambers and the valve of the PTR_MS was on position #1 for 50 minutes (inlet reading); #2 for 35 minutes (exhaust of the sample chamber) and #3 for additional 35 minutes (exhaust of the control chamber).

Next, VOC and ozone concentrations during ozone exposure (2 hours and 15 minutes) were collected. The ozone generator was switched on with the bypass of the sample chamber on; 60 minutes of measurements were made of the ozone and VOCs concentration at the inlet of the chambers. Then the bypass was turned off and the ozonated air was directed to the sample chamber and control chambers. For the next 45 minutes, the PTR-MS valve was switched to position #2 and both the reading of ozone and VOCs concentration at the exhaust of the sample chamber were run. After, the PTR-MS valve was moved to position #3, for 30 minutes, to monitor VOCs concentration at the exhaust of the control chamber. The ozone concentration in the outlet of the control chamber was continuously monitored.

The experiment continued after the ozone exposure for a total of 1 hour and 15 minutes to characterize post-ozonation VOCs emissions. During this period, the ozone was switched off and the first step was run again, with shorter intervals of time. The valve was switched to position #1 for 15 minutes, to read the VOCs concentration of the inlet clean air, and switched to position #2 and #3, each for 30 minutes, with the air flow flushed through the chambers.

The sampling timeline of the protocol was followed until the near-steady state of each step was reached, as described in section 5.3.2.3.1.

#### 5.3.2.3.2 Analytical instrumentation

The ozone inlet concentration was fixed around 100 ppb that corresponds to the lower limit of "unhealthy for sensitive groups" classification of air quality index (AQI) according to U.S. Environmental Protection Agency (USPEA, 2015) and exceed the currently established standard limit of 70 ppb (EPA, 2023). Note that our goal is to measure the deposition velocity, which normalizes the concentration of ozone in the test chamber; prior studies show deposition velocities are relatively insensitive to ozone concentration at the range of concentration used here (~100) to that more typical of indoor spaces (~10 ppb) (Lamble et al., 2011). The measurement of ozone concentration was done on the average of 30 datapoints, at steady state, with a standard deviation below 1%. The primary and secondary (during $O_3$ exposure) VOC emissions were monitored using a proton transfer reaction – time of flight - mass spectrometer (PTR-ToF-MS, Ionicon, PTR-ToF 1000). The principle of the PTR-ToF-MS has been well described in the literature (Hansel et al., 1995; Lindinger and Jordan, 1988). Specifics of operation of the instrument are similar to a prior study of building materials (Chin et al., 2019) The mass spectrum acquisition was set to 10 s and then the traces of the targeted compounds (for the study) were analyzed to define the end of each experimental phase. From that point the previous 30 datapoint would be considered to calculate the average value of concentration of the specific compound, to ensure the steady state of the system.

#### 5.3.2.3.3 Deposition velocities

The deposition velocity is a coefficient that parameterizes a pollutant loss rate to surfaces. The material's surface deposition velocity (cm $s^{-1}$) is quantified by using the deposition velocity observed in the control chamber ($v_{dg}$) and in the sample chamber ($v_{ds}$) through a steady-state mass balance on the well-mixed 6.5 L chambers using equations (1) and (2):

$$v_{dg} = \lambda\left(\frac{V}{A_g}\right) \times \left(\frac{C_{in,O3,g}}{C_{e,O3,g}} - 1\right) \quad (1)$$

$$v_{ds} = \lambda\left(\frac{V}{A_s}\right) \times \left(\frac{C_{in,O3,s}}{C_{e,O3,s}} - 1\right) - v_{dg}\left(\frac{A_g - A_s}{A_s}\right) \quad (2)$$

where: $\lambda = Q/V$ is the air exchange rate ($s^{-1}$); Q the airflow rate ($cm^3\ s^{-1}$); V the volume of the chamber ($cm^3$); A the area of the glass exposed $A_g$ or of the sample $A_s$ ($cm^2$); $C_{in,O3}$ is the ozone concentration inlet (ppb) either in the control (subscript g) or in the sample (subscript s)

chamber; $C_{e,O3}$ the ozone concentration at the exhaust (ppb) either in the control (subscript g) or in the sample (subscript s) chamber.

5.3.2.3.4 Primary and secondary emission rates

Primary and secondary emission rates quantify, respectively, the rate of carbonyl compounds emitted from coatings in absence and in presence of ozone. Primary emissions from the sample chamber ($\varepsilon_{1,b}$) and the control chamber ($\varepsilon_g$) (µg/h) are calculated from steady state mass balance on the chambers, as shown in equations (3) and (4):

$$\varepsilon_{1,b} = QC_{b,e,s} - QC_{b,in,s} - \varepsilon_g \quad (3)$$

$$\varepsilon_g = QC_{b,e,g} - QC_{b,in,g} \quad (4)$$

with Q the airflow rate ($cm^3\ s^{-1}$); $C_{b,e,s}$ the byproduct concentration at the exhaust of the sample chamber (ppb); $C_{b,in,s}$ the byproduct concentration at the inlet of the sample chamber (ppb); $C_{b,e,g}$ the byproduct concentration at the exhaust of the control chamber (ppb); $C_{b,in,g}$ the byproduct concentration at the inlet of the control chamber (ppb). Assuming to have the same concentration inlet for the sample and the control chamber since the flow is split directly upstream the two chamber ($C_{b,in,s} = C_{b,in,g}$) we have equation (5):

$$\varepsilon_{1,b} = Q(C_{b,e,s} - C_{b,e,g}) \quad (5)$$

Primary emissions of the material $\varepsilon_s$ depend on the airflow rate (Q) and on the concentration of pollutant at the exhaust from the sample chamber ($C_{b,e,s}$) and from the control chamber ($C_{b,e,g}$).

The same mass balance (5) in presence of ozone gives the equation (6) for calculating the secondary byproduct ($\varepsilon_{2,b}$):

$$\varepsilon_{2,b} = Q(C_{b,e,s,O3} - C_{b,e,g,O3}) \quad (6)$$

5.3.2.3.5 Secondary emissions molar yields

The secondary emission molar yields quantify the molar emission rate of carbonyl compounds produced by reaction between coatings and ozone. To quantify the rate of VOCs generated as product of the interaction of ozone with the coatings' surface, the byproducts yields were calculated.

Appling the equation (7) developed by Reiss *et al.*, 1995 (Reiss et al., 1995):

$$Y = \frac{\varepsilon_{2,b} - \varepsilon_{1,b}}{v_d \cdot A \cdot C} \quad (7)$$

the denominator of Y can be calculated from ozone mass balance as shown in equation (8):

$$v_d \cdot A \cdot C_{O3,in} = Q(C_{O3,e} - C_{O3,in}) \quad (8)$$

The same airflow rate (Q) could be assumed during the experiment and the final equation (9) to calculate the byproduct yield is written as:

$$Y = \frac{C_{b,e,s,O3} - C_{b,e,g,O3} - C_{b,e,s} + C_{b,e,g}}{(C_{O3,e,g} - C_{O3,e,s})} \quad (9)$$

The building ozonation byproducts most expected are presented in **Table 5.14** and informed the list of target compounds for analysis in the PTR-MS mass spectra, of the present study. Darling and Corsi (2017) while testing a clay paint and a clay-based plaster decided to address only C5-C10 *n*-aldehydes (+ BA-benzaldehyde and TA- tolualdehyde) because they were considered of bigger impact on the perceived air quality. The emissions of $C_4$ and lower aldehydes (and acetone) were found, also in other studies (Lamble et al., 2011; Cros et al., 2012) according to Darling and Corsi (2017), "negligible to comparative very low" both for clay-based coatings than not clay-based ones.

**Table 5.14.** Synthesis of the carbonyl compounds selected in literature.

| Compounds | $C_1$:$C_4$ | $C_5$:$C_{10}$ | benzaldehyde | o-tolualdheyde | acetone | Sampling method |
|---|---|---|---|---|---|---|
| **Study** | | | | | | |
| **Poppendieck et al. (2007)** | YES | YES | YES | YES | YES | DNPH, Tenax-TA tubes |
| **Darling and Corsi (2017)** | NO | YES | YES | YES | NO | Tenax-TA tubes |
| **Lamble et al. (2011)** | YES | YES | NO | NO | YES | DNPH, Tenax-TA tubes |
| **Cros et al. (2011)** | YES | YES | YES | YES | YES | DNPH, Tenax-TA tubes |

Notation: DNPH – 2.4-dinitrophenylhydrazine cartridge, C3 – propanal, C4 – butanal, C5 – pentanal, C6 – hexanal, C7 – heptanal, C8 – octanal, C9 – nonanal, C10 – decanal.

The mentioned studies are very consistent in sampling method: all the authors sampled the lighter compounds on DNPH (2.4-dinitrophenylhydrazine) tubes and heavier ones using Tenax-TA tubes. The present study, instead, used the PTR-MS equipment, that relies on the proton transfer reaction with $H_3O^+$. The compound identification is more limited due to assignment based on m/z ratio with the possibility of possibility of fragmentation of the aldehydes (Ernle et al., 2023) with consequent identification issues. For this reason, the VOCs targeted will be identified with their m/z ratio (**Table 5.15**).

**Table 5.15.** List of compounds identified for the m/z ratio and respective putative identifications.

| **m/z** | **31.018** | **33.030** | **45.026** | **47.017** | **47.057** | **59.046** | **69.054** | **71.066** | **73.070** |
|---|---|---|---|---|---|---|---|---|---|
| putative identification | Form-Aldehyde H+ | Methanol H+ | Acet-Aldehyde H+ | Formic Acid H+ | Ethanol H+ | Acetone H+ | Isoprene H+ | Croton-Aldehyde H+ | Butyr-Aldehyde H+ |
| **m/z** | **73.064** | **79.050** | **89.084** | **93.078** | **101.054** | **107.095** | **61.017; 43.011** | **61.064; 43.047** | **137.086; 81.044** |
| putative identification | MEK H+, tetrahydrofuran H+ | Benzene H+ | Ethyl Acetate H+ | Toluene H+ | 4-OPA | Xylene H+ | Acetic Acid H+; fragment | IPA H+; fragment | Terpenes H+; fragment |

## 5.3.3 Results and discussion

### 5.3.3.1 Deposition velocities

The average (over three samples) deposition velocities for the studied building coatings are displayed in **Figure 5.18**. The highest deposition velocities found among the tested coatings are observed for the clay-based plasters applied as a topcoat on the drywall (0.19±0.042 $cm \cdot s^{-1}$ for DW_CL and 0.16±0.002 $cm \cdot s^{-1}$ for DW_CL-M) followed by the bare drywall. The deposition velocity of drywall was found 0.15 ± 0.002 $cm \cdot s^{-1}$, consistent with values from literature for small-scale chamber experiments (0.18 $cm \cdot s^{-1}$ determined by Lamble et al., 2011 with ozone challenge concentration 150-200 ppb) or 0.15-0.18 $cm \cdot s^{-1}$ for painted drywall (varying according to the time of exposure and the relative humidity) at 60 ppb ozone exposure (Rim et al., 2016). Also, higher results were found such as 0.8 ± 0.4 $cm \cdot s^{-1}$ (Kleno et al., 2001) when drywall samples were tested through the FLEC (field and laboratory emission cell) and exposed to 50 ppm or somewhat lower, as 0.069 $cm \cdot s^{-1}$ (Nicolas et al.; 2007) or 0.06±0.02 $cm \cdot s^{-1}$ (Kunkel et al., 2010) tested in a larger chamber (respectively 17 L and 14.3 $m^3$) with a more similar ozone exposure (100 to 120 ppb and 150-200 ppb).

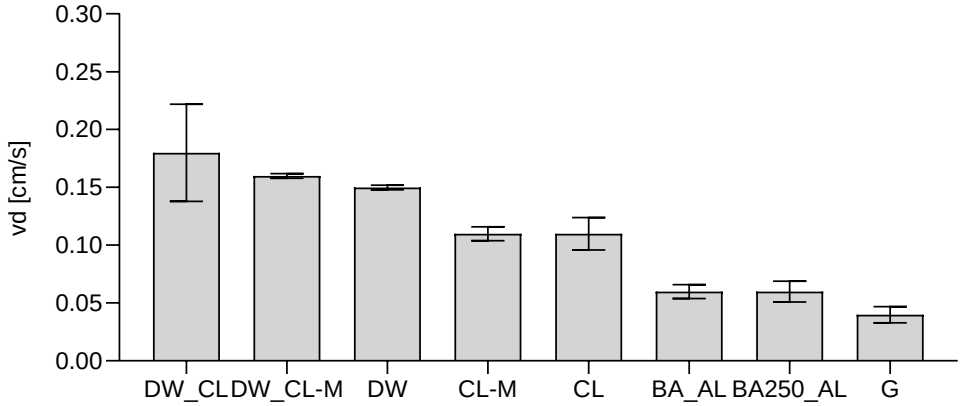


Notation: DW – drywall; CL – clay-based plaster, CL-M – maritime clay-based plaster: DW_CL – clay-based plaster applied on drywall; DW_CL-M – maritime clay-based plaster applied on drywall; G – gypsum-based plaster, BA_AL – gypsum plaster with addition of bark and air lime; BA250_AL – gypsum plaster with addition of bark heated at 250 ºC and air lime.

**Figure 5.18.** Deposition velocities vd for the tested coatings: average values with standard deviation.

The lowest $v_d$ are observed for the gypsum reference mortar G and the addition of *A.dealbata* bark slightly increase it (from 0.04±0.007 $cm \cdot s^{-1}$ to 0.06±0.009 and 0.06±0.006 $cm \cdot s^{-1}$, namely for BA250_AL and BA_AL). Only one reference was found in literature for gypsum plaster, calculated as the mean values for the deposition velocities on ''softer less dense alkaline stone materials'' and ''fine concrete'' (Grøntoft and Raychaudhuri, 2004). The value calculated from the authors, at 50% and 70% RH is 0.044 $cm \cdot s^{-1}$, very consistent with the value experimentally obtained in the present work. The addition of bark and low content of air lime in the gypsum plaster introduces an increase of ozone deposition velocities possibly related to the enhancement of their moisture buffering ability (Ranesi et al., 2023).

#### 5.3.3.1.1 The ozone removal mechanism of clay and the RH influence

Similar results of ozone removal activity were found by Lamble et al. (Lamble et al., 2011). The authors related the high ozone reactivity of these coatings, both drywall and clay plasters, to their mineral content, responsible for the "iron or aluminum catalyzed decomposition of ozone" (Lamble et al., 2011). It is true that the smectites (clay) for example contain different amount of iron (hydr)oxides $Fe^{2+}$ and $Fe^{3+}$ (Stucki et al., 2013) that can be used to design products for ozone catalytic decomposition (Wang et al., 2018). Moreover, both clay plasters when applied as a base coat (CL and CL-M) showed less reactivity to ozone. Thus, there might be a relation between the ozone deposition velocity and the plasters' application. The topcoat was applied in three layers, each one very thin, while the base coat was applied in one thicker layer, in the 2cm thick mold (with no constraints to avoid the shrinkage from creating cracking

in the material). The difference in thickness of the two applications and the effect of different substrates (drywall instead of mold) could have led to a topcoat with higher bulk density (more compact) and, thus, a lower porosity, than the one of the basecoats with the same mortar. Moreover, the addition of crushed seashells of the CL-M formulation decreases a bit the reactivity to ozone (while an increase of hygroscopicity was found in a parallel study (Ranesi et al., 2024)). It is possible that a higher moisture content in the maritime clay plaster (when exposed to the same RH levels) affects its reactivity to ozone.

Few studies were found on the effect of RH on deposition velocities in building coatings. One study from Gall et al. (Gall et al., 2013) concluded that the influence of RH is not large for the building materials and products tested: stainless steel background, nylon loop pile carpet, perlite-based ceiling tiles and acrylic painted drywall. Nevertheless, the materials included in the study were not characterized by their hygroscopic behavior and, among them, the drywall is likely to be the most reactive to RH conditions. Other studies pointed out an increase in ozone deposition velocities for gypsum drywall exposed to higher RH. For example, Grøntoft and Raychaudhuri (2004) found for this building material an increase in deposition velocities from 0.12 $cm \cdot s^{-1}$ at 50% RH to 0.15 $cm \cdot s^{-1}$ at 90% RH. Also, Rim et al. (Rim et al., 2016) for painted drywall reported an increase of $v_d$ when RH test condition is increased from 50% to 75%. The moisture content of a hygroscopic material is higher when the material is exposed to higher levels of RH. If a positive correlation between ozone deposition velocities and equilibrium moisture content of coating materials is verified, the maritime clay should have higher deposition velocity than the clay with no addition, unlike what is observed. It is possible that the maritime plaster product has a lower content of clay (note that the formulation is unknown) and, for this reason, is found less reactive to ozone. Otherwise, what is true for hygroscopic coatings in general may not apply for highly hygroscopic clay-based coatings if their removal mechanism is based on iron catalyzed decomposition of ozone and ozone could compete with water (from moisture adsorption) (Yan et al., 2019). Still, the influence of RH on ozone deposition velocities of highly hygroscopic coatings, and among them the clay-based ones, should be further investigated.

#### 5.3.3.2 Primary and secondary emission rates

In **Figure 5.19** are shown the results for primary and secondary emissions. The addition of crushed seashell (CL-M) seems to prevent the increase of secondary emission of the clay plaster (during the ozone exposure the total VOCs amount is the same that without ozone) with a small decrease in acetic acid (m/z 61.017) and a slight increase in acetone (m/z 59.046). When

the same plaster is applied as topcoat on drywall (DW_CL-M), the emissions of methanol (m/z 33.030) increased from 20 to 90 μg $h^{-1}m^{-2}$, probably related to the reaction of clay with the cellulose layer present on the substrate, and acetaldehyde (m/z 45.026) was no longer detected. The total amount of VOCs detected is very similar in primary and secondary emissions for both DW_CL-M and CL-M plasters and the biggest difference between them is the methanol emission (m/z 33.030). The clay plaster with no maritime shells (CL) is more reactive with ozone and the secondary emission rate is overall higher, above all for acetone (m/z 59.046), IPA (m/z 61.064 + 43.047 fragment) and acetaldehyde (m/z 45.026). When the clay plaster is applied on drywall (DW_CL), again, the levels of methanol (m/z 33.030) in primary and secondary emissions rise sharply (from 15 to 80 ($\varepsilon_1$) and from 20 to 140 ($\varepsilon_2$) μg $h^{-1}m^{-2}$). Both DW_CL and CL plaster show high total secondary emissions. In both cases of clay application on drywall, DW_CL and DW_CL-M, the VOCs primary emissions increase above all in methanol.

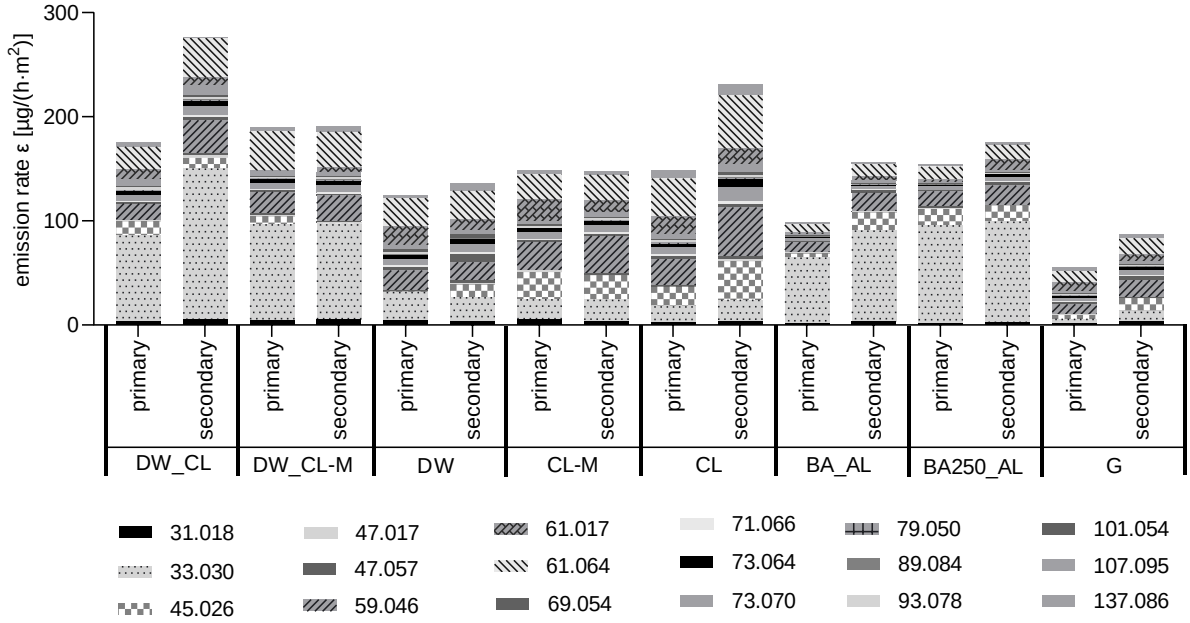


Notation: DW – drywall; CL – clay-based plaster, CL-M – maritime clay-based plaster: DW_CL – clay-based plaster applied on drywall; DW_CL-M – maritime clay-based plaster applied on drywall; G – gypsum plaster, BA_AL – gypsum plaster with addition of bark and air lime; BA250_AL – gypsum plaster with addition of bark heated at 250 ºC and air lime.

**Figure 5.19.** Primary and secondary emission rates for the analyzed building coatings

The drywall tested showed overall low production of VOCs, with some higher values in primary emission of methanol (m/z 33.030), IPA (m/z 61.064 + 43.047 fragment), acetone (m/z 59.046) and acetic acid (m/z 61.017 + 43.011 fragment). The latter appears to decrease due to ozone

exposure, but a small production of acetaldehyde (m/z 45.026) was observed. The decrease in secondary emissions of methanol (m/z 33.030) was unexpected. Also, the amount of methanol (m/z 33.030) in primary emission for DW is lower than for DW_CL and DW_CL-M. The possibility that the high amount of methanol (m/z 33.030) for DW_CL and DW_CL-M is related to the water-based primer should be the subject of further study.

Gypsum plaster (G) showed the lowest emissions, both primary and secondary. The primary emissions are mainly IPA (m/z 61.064 + 43.047 fragment), acetone (m/z 59.046) and acetic acid (m/z 61.017 + 43.011 fragment) with very low values (≤ 4 μg $h^{-1}m^{-2}$) of other compounds quantified in this work. Secondary emissions are higher than primary emissions, with the greatest relative increase of acetaldehyde (m/z 45.026) from 3.7 to 12.8 μg $h^{-1}m^{-2}$, but also in acetone (m/z 59.046) and IPA (m/z 61.064 + 43.047 fragment) and methanol (m/z 33.030) with a decrease in acetic acid (m/z 61.017 + 43.011 fragments) and the tendency of low variation or low decrease in the other VOCs. Overall, the addition of a small amount of air lime and bark, either only dried or also heated (BA_AL and BA250_AL), to the gypsum plaster did not modify the behavior, apart from the higher amount of methanol (m/z 33.030) observed in primary (from 4.4 to about 65 and 95 μg $h^{-1}m^{-2}$) and secondary (from 10 to about 88 and 97 μg $h^{-1}m^{-2}$) emissions. The methanol (m/z 33.030) accounts for about 60% of the higher primary and secondary emissions of the modified gypsum plasters.

#### 5.3.3.3 Secondary emissions molar yields

Average specific-compounds yields are given in **Figure 5.20** providing a more accurate quantification of the effect of ozone on the coatings in terms of byproduct, as it also considers the ozone concentration at the inlet and exhaust, during the experiment.

Overall, all the coatings tested present a low total average yield (**Figure 5.20**) if compared, for instance, with other building coatings as the finished hardwood floor (0.4), the fabric acoustical wall panel (0.5), the bio-based resilient tiles (>0.3) or the porcelain tiles (≈0.2) analysed by Lamble et al. (2011). The same authors found the average total yield for a recycled drywall a little bit lower than the one tested here (slightly below 0.1). The total average yields for the clay-based plasters are consistent with what observed by Lamble et al. (2011) (total molar yield after 2 h and 24 h exposure below 0.05 for the clay plaster applied as topcoat) and by Darling and Corsi (2017) (0.06 referred as the average total yield at Month 0). The lowest yield is exhibited by the maritime clay plaster when applied on drywall (DW_CL-M), and when used as a basecoat (CL-M).

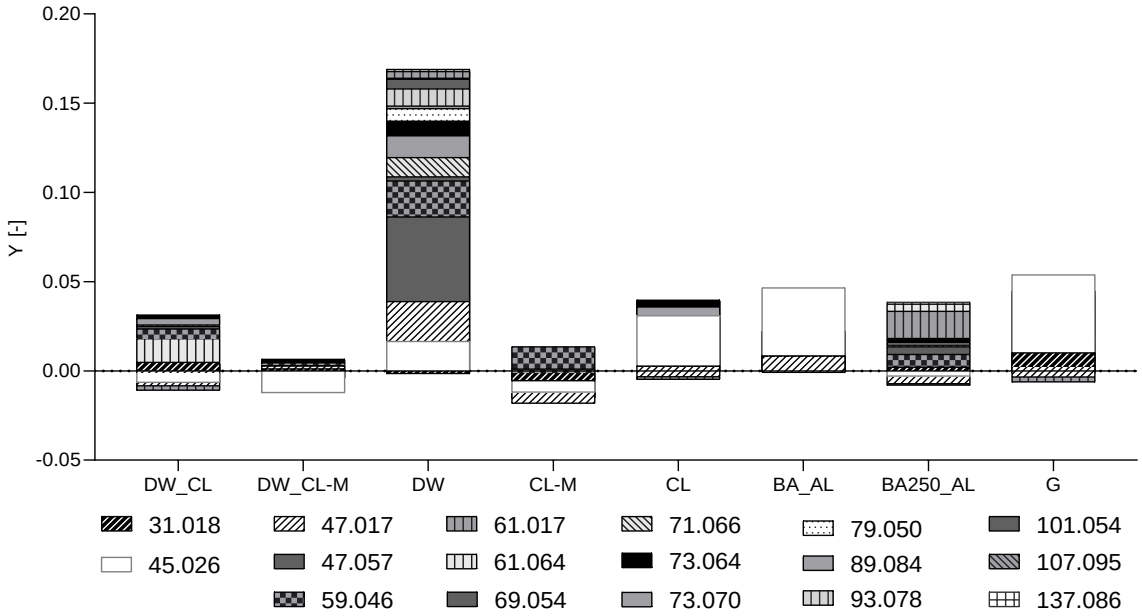


Notation: DW – drywall; CL – clay-based plaster, CL-M – maritime clay-based plaster: DW_CL – clay-based plaster applied on drywall; DW_CL-M – maritime clay-based plaster applied on drywall; G – gypsum plaster, BA_AL – gypsum plaster with addition of bark and air lime; BA250_AL – gypsum plaster with addition of bark heated at 250 ºC and air lime.

**Figure 5.20.** Average specific compounds yields for the eight tested coatings.

The latter shows some removed compounds like formaldehyde (m/z 31.018), acetaldehyde and formic acid (m/z 45.026 and 47.017, respectively) and acetic acid (61.017). DW_CL-M has a negative yield of acetaldehyde (m/z 45.026). The clay plaster (CL) shows a production of acetaldehyde (m/z 45.026) in secondary emissions, like the gypsum reference plaster (G) and the modified version with raw bark added (BA_AL). The same plaster, applied on drywall (DW_CL), has a negative yield of acetaldehyde but some other byproducts are released, all in very small quantities. All the clay-based products showed a removal activity and two plasters based on gypsum (G and BA250_AL) did too. The positive yield of gypsum modified with heated bark (BA250_AL) is very heterogeneous, with some higher presence of acetic acid (m/z 61.017) and acetone (m/z 59.046).

### 5.3.4 Conclusions

The eight coatings selected for the study would reduce the indoor ozone concentration if applied on indoor walls and ceilings. The highest ozone removal activity was found for the clay-based plasters applied in thin layer on drywall. A positive effect on the ozone removal activity (+50% ozone deposition velocity) was obtained with *Acacia dealbata* bark additions to

the reference gypsum mortars. It is an interesting outcome that the small addition (10% by vol.) of the bark to the mortars' formulation had a positive effect on passive ozone removal activity, as it shows an interesting way of dealing with this waste when the invasive species is cut. Moreover, the thermal treatment of the bark (250°C for 1 h) has no impact on this property, avoiding the need for extra energy consumption. The primary and secondary emissions of the gypsum reference mortar are the lowest among the tested coatings. The addition of bark and heated bark, together with air lime, increased namely 80% and 200% both primary and secondary emissions, with methanol (m/z 33.030) accounting for about 60% of the increase. Methanol is observed in high quantities in indoor air and thought to potentially be a decomposition product of cellulose and other wood materials. Future work is necessary to identify the source of methanol on the coatings studied here. The lowest byproducts of oxidation were found for the clay plasters with crushed seashells both as base and topcoats (-102% and -120%, respectively). Finally, the yield rates confirm that the clay-based plaster with seashells is promising as a passive removal coating, showing negative yields of some compounds both applied as a base or a topcoat. The gypsum-biomass-air lime plasters have slightly lower yield than the reference one when raw bark is added and -60% total yields, with some removal activity, when the thermally threated bark is added. Very low yields are observed for all the plastering mortars; indeed, there is an important difference of the total average yield between the mortars and the drywall.

According to the test conditions and results interpretation, both the clay-based plasters and the gypsum-based ones appear to be promising passive removal coatings. These traditional plasters, widely used for coating indoor masonry walls and ceilings with reinforced concrete slabs, showed their potential contribution to indoor air quality. Moreover, their formulations with both types of biowastes (crushed seashells for clay-based and bark from *A. dealbata* for the gypsum-based plasters), can further enhance their contribution for healthier indoors while lowering the plasters environmental impact. Nevertheless, further investigations are needed to better justify the high presence of methanol as a byproduct and the humidity dependence of the ozone deposition velocities for highly hygroscopic coatings. The surface chemistry of clay- and gypsum-based plasters needs an in-depth study to better understand the mechanisms behind the ozone removal and to answer questions about the decay of the ozone removal activity and the relation between primary and secondary emissions and aging.

## Acknowledgements

This research was supported by Portuguese Foundation for Science and Technology (FCT-Fundação para a Ciência e a Tecnologia): PD/BD/150399/2019 – 1st author Doctoral Training Program EcoCoRe. The authors are also grateful for FCT support through funding UIDB/04625/2020 of the research unit CERIS. The authors would like to thank the National Laboratory for Civil Engineering of Portugal (LNEC) for the laboratory equipment and the support provided through the projects REuSE - Wall coverings for Rehabilitation: Safety and Sustainability and the Healthy Building Research Laboratory of the Portland State University. A special thanks goes to the research analyst Aurélie Laguerre for the help given with the PTR-MS analysis.

## References

Alejandre FJ, Blasco-López FJ, Flores-Alés V, Villegas R, Freire MT. Study of the influence of limewash on the conservation of Islamic plasterworks through weathering tests. International Journal of Architectural Heritage. 2021; 15(4): 580-592. https://doi.org/10.1080/15583058.2019.1632393.

Arris-Roucan S, McGregor F, Fabbri A, Perlot C. Towards the determination of carbon dioxide retention in earthen materials. Building and Environment. 2023; 239:110415. https://doi.org/10.1016/j.buildenv.2023.110415.

Ault AP, Grassian VH, Carslaw N, Collins DB, Destaillats H, Donaldson DJ, Farmer DK, Jimenez JL, McNeill VF, Morrison GC, O'Brien RE, Shiraiwa M, Vance ME, Wells JR, Xiong W. Indoor surface chemistry: developing a molecular picture of reactions on indoor interfaces. Chem. 2020; 6(12): 3203-3218. https://doi.org/10.1016/j.chempr.2020.08.023.

Ben-Alon L and Rempel AR. Thermal comfort and passive survivability in earthen buildings. Building and Environment. 2023; 238:110339. https://doi.org/10.1016/j.buildenv.2023.110339.

Borges A, José H, Homem V, Simões M. Comparison of techniques and solvents on the antimicrobial and antioxidant potential of extracts from Acacia dealbata and Olea europaea. Antibiotics (Basel). 2020; 9(2):48. https://doi.org/10.3390/antibiotics9020048.

Braish T et al. Evaluation of the seasonal variation of VOC surface emissions and indoor air concentrations in a public building with bio-based insulation. Building and Environment. 2023; 238: 110312. https://doi.org/10.1016/j.buildenv.2023.110312.

Brown SK. Volatile organic pollutants in new and established buildings in Melbourne, Australia. Indoor Air. 2002; 12(1): 55-63. https://doi.org/10.1034/j.1600-0668.2002.120107.x.

Bumanis G, Zorica J, Korjakins A, Bajare D. Processing of Gypsum Construction and Demolition Waste and Properties of Secondary Gypsum Binder. Recycling. 2022; 7(3):30. https://doi.org/10.3390/recycling7030030.

Caroselli M, Válek J, Zapletalová J, Felici A, Frankeová D, Kozlovcev P, Nicoli G, Jean G. Study of materials and technique of late baroque stucco decorations: Baldassarre Fontana from Ticino to Czechia. Heritage. 2021; 4(3):1737-1753. https://doi.org/10.3390/heritage4030097.

Chin K, Laguerre A, Ramasubramanian P, Pleshakov D, Stephens B, Gall ET. Emerging investigator series: primary emissions, ozone reactivity, and byproduct emissions from building insulation materials. Environmental Science: Processes & Impacts. 2019; 21: 1255. https://doi.org/10.1039/C9EM00024K.

Cros CJ, Morrison GC, Siegel JA, Corsi RL. Long-term performance of passive materials for removal of ozone from indoor air. Indoor Air. 2012; 22(1): 43–53. https://doi.org/10.1111/j.1600-0668.2011.00734.x.

Directive 2002/3/EC of the European Parliament and of the Council of 12 February 2002 relating to ozone in ambient air. Official Journal of the European Communities. 2002; L67/14. http://eur-lex.europa.eu/LexUriServ/LexUriServ.do?uri=OJ:L:2002:067:0014:0030:EN:PDF.

Darling EK, Cros CJ, Wargocki P, Kolarik J, Morrison GC, Corsi RL. Impacts of a clay plaster on indoor air quality assessed using chemical and sensory measurements. Building and Environment. 2012; 57: 370-376. . https://doi.org/10.1016/j.buildenv.2012.06.004.

Darling EK, Morrison GC, Corsi RL. Passive removal materials for indoor ozone control. Building and Environment. 2016; 106: 33-44. https://doi.org/10.1016/j.buildenv.2016.06.018.

Darling E, Corsi RL. Field-to-laboratory analysis of clay wall coatings as passive removal materials for ozone in buildings. Indoor Air. 2017; 27(3): 658-669. https://doi.org/10.1111/ina.12345.

EN 459-1; Building lime – Part 1: definitions, specifications and conformity criteria. European Committee for Standardization (CEN): Brussels, Belgium, 2015.

Ernle L, Wang N, Bekö G, Morrison G, Wargocki P, Weschler CJ, Williams J. Assessment of aldehyde contributions to PTR-MS m/z 69.07 in indoor air measurements. Environmental Science: Atmosphere. 2023; 3: 1286-1295. https://doi.org/10.1039/D3EA00055A.

Ferreira FC, Torres PM, Tente HS, Neto JB. Ozone levels in Portugal: The Lisbon region assessment. In Proceedings of the Air and Waste Management Association's Annual Conference and Exhibition, AWMA, Indianapolis, IN, USA. 22–25 June 2004.

Freire MT, Veiga MR, Santos Silva A, de Brito J. Restoration of ancient gypsum-based plasters: design of compatible materials. Cement and Concrete Composites. 2021; 120:104014. https://doi.org/10.1016/j.cemconcomp.2021.104014.

Gall E, Darling E, Siegel JA, Morrison GC, Corsi RL. Evaluation of three common green building materials for ozone removal, and primary and secondary emissions of aldehydes. Atmospheric Environment. 2013; 77: 910-918. https://doi.org/10.1016/j.atmosenv.2013.06.014.

Gall ET, Corsi RL, Siegel JA. Impact of physical properties on ozone removal by several porous materials. Environmental Science & Technology. 2014; 48 (7): 3682-3690. https://doi.org/10.1021/es4051956.

Gariani G, Lehuédé P, Leroux L, Wallez G, Goubard F, Bouquillon A, Bormand M. First insights on the mineral composition of "stucco" devotional reliefs from Italian Renaissance Masters: investigating technological practices and raw material sourcing. Journal of Cultural Heritage. 2018; 34: 23-32. https://doi.org/10.1016/j.culher.2018.05.003.

Geraldo RH, Pinheiro SMM, Silva JS, Andrade HMC, Dweck J, Gonçalves JP, Camarini G. Gypsum plaster waste recycling: a potential environmental and industrial solution. Journal of Cleaner Production. 2017; 164: 288-300. https://doi.org/10.1016/j.jclepro.2017.06.188.

Grøntoft T. Dry deposition of ozone on building materials. Chamber measurements and modelling of the time-dependent deposition, Atmospheric Environment. 2002; 36(36–37): 5661-5670. ISSN 1352-2310. https://doi.org/10.1016/S1352-2310(02)00701-X.

Grøntoft T, Raychaudhuri MR. Compilation of tables of surface deposition velocities for $O_3$, $NO_2$ and $SO_2$ to a range of indoor surfaces. Atmospheric Environment. 2004; 38(4): 533-544.. https://doi.org/10.1016/j.atmosenv.2003.10.010.

Grøntoft T, Henriksen JF, Seip HM. The humidity dependence of ozone deposition onto a variety of building surfaces. Atmospheric Environment. 2004(a); 38 (1): 59-68. https://doi.org/10.1016/j.atmosenv.2003.09.043.

Grøntoft T, Raychaudhuri MR. Compilation of tables of surface deposition velocities for $O_3$, $NO_2$ and $SO_2$ to a range of indoor surfaces. Atmospheric Environment. 2004(b); 38(4): 533-544. https://doi.org/10.1016/j.atmosenv.2003.10.010.

Grøntoft T. Measurements and modelling of the ozone deposition velocity to concrete tiles, including the effect of diffusion, Atmospheric Environment. 2004(c); 38(1): 49-58. https://doi.org/10.1016/j.atmosenv.2003.09.044.

Hansel A, Jordan A, Holzinger R, Prazeller P, Vogel W, Lindinger W. Proton transfer reaction mass spectrometry: on-line trace gas analysis at the ppb level. International Journal of Mass Spectrometry and Ion Processes. 1995; 149–150: 609–619. https://doi.org/10.1016/0168-1176(95)04294-U.

Harčárová K, Vilčeková S, Bálintová M. Building materials as potential emission sources of VOC in the indoor environment of buildings. Key Engineering Materials. 2020; 838: 74-80. https://doi.org/10.4028/www.scientific.net/KEM.838.74.

Huang Y, Yang Z, Gao Z. Contributions of indoor and outdoor sources to ozone in residential buildings in Nanjing. International Journal of Environmental Research and Public Health. 2019; 16: 2587. https://doi.org/10.3390/ijerph16142587.

Kamel A M A, Marie H A H, Mahmoud H A, Ali M F. Mineralogical characterization of Islamic stucco: Minaret of Shams El-Deen El-Wasty, Bulaq, Egypt. Construction and Building Materials. 2015; 101(1):692-701. https://doi.org/10.1016/j.conbuildmat.2015.10.059.

Kim SY, Kim E, Kim WJ. Health effects of ozone on respiratory diseases. Tuberculosis and Respiratory Diseases. 2020; 83(1): S6-S11. https://doi.org/10.4046%2Ftrd.2020.0154.

Kleno JG, Clausen PA, Weschler CJ, Wolkoff P. Determination of ozone removal rates by selected building products using the FLEC emission cell. Environ. Sci. Technol. 2001; 35: 2548–2553. https://doi.org/10.1021/es000284n.

Kotzas D. Exposure to volatile organic compounds in indoor/outdoor environments and methodological approaches for exposure estimates -the European paradigm. Journal of Hazardous Materials Advances. 2023; 8: 100197. https://doi.org/10.1016/j.hazadv.2022.100197.

Kunkel DA, Gall ET, Siegel JA, Novoselac A, Morrison GC, Corsi RL. Passive reduction of human exposure to indoor ozone. Building and Environment. 2010: 45(2): 445-452. https://doi.org/10.1016/j.buildenv.2009.06.024.

Lamble SP, Corsi RL, Morrison GC. Ozone deposition velocities, reaction probabilities and product yields for green building materials. Atmospheric Environment. 2011; 45(38): 6965-6972. https://doi.org/10.1016/j.atmosenv.2011.09.025.

Lin C, Hsu S. Deposition velocities and impact of physical properties on ozone removal for building materials. Atmos. Environ. 2015; 101: 194–199. https://doi.org/10.1016/j.atmosenv.2014.11.029.

Lindinger W, Jordan A. Proton-transfer-reaction mass spectrometry (PTR–MS): on-line monitoring of volatile organic compounds at pptv levels. Chemical Society Reviews. 1998; 27: 347–375. https://doi.org/10.1039/A827347Z.

Liu N, Bu Z, Liu W, Kan H, Zhao Z, Deng F, Huang C, Zhao B, Zeng X, Sun Y, Qian H, Mo J, Sun C, Guo J, Zheng X, Weschler LB, Zhang Y. Health effects of exposure to indoor volatile organic compounds from 1980 to 2017: A systematic review and meta-analysis. Indoor Air. 2022; 32: e13038. DOI: 10.1111/ina.13038.

López-Hortas L, Rodríguez-González I, Díaz-Reinoso B, Torres MD, Moure A, Domínguez H. Tools for a multiproduct biorefinery of Acacia dealbata biomass. Industrial Crops and Products. 2021; 169:113655. https://doi.org/10.1016/j.indcrop.2021.113655.

Mahmoud HM, Papadopoulou L. Archaeometric analysis of pigments from the tomb of Nakht-Djehuty (TT189), El-Qurna Necropolis, Upper Egypt. ArcheoSciences. 2013; 37: 19-33. https://doi.org/10.4000/archeosciences.3967.

Maung, TZ, Bishop, JE, Holt, E, Turner, AM, Pfrang, C. indoor air pollution and the health of vulnerable groups: a systematic review focused on Particulate Matter (PM), Volatile Organic Compounds (VOCs) and their effects on children and people with pre-existing lung disease.

International Journal of Environmental Research and Public Health. 2022; 19: 8752. https://doi.org/10.3390/ijerph19148752.

Morrison GC, Nazaroff WW. Ozone interactions with carpet: secondary emissions of aldehydes. Environmental Science & Technology. 2002; 36 (10): 2185-2192. https://doi.org/10.1021/es0113089.

Mousavinezhad S, Ghahremanloo M, Choi Y, Pouyaei A, Khorshidian N, Sadeghi B. Surface ozone trends and related mortality across the climate regions of the contiguous United States during the most recent climate period, 1991–2020. Atmospheric Environment. 2023; 300: 119693. https://doi.org/10.1016/j.atmosenv.2023.119693.

Nazaroff WW, Weschler CJ. Indoor ozone: Concentrations and influencing factors. Indoor Air. 2022; 32(1): e12942. https://doi.org/10.1111/ina.12942.

Nicolas M, Ramalho O, Maupetit F. Reactions between ozone and building products: impact on primary and secondary emissions. Atmospheric Environment. 2007; 41(15): 3129–3138. https://doi.org/10.1016/j.atmosenv.2006.06.062.

Nunes LJR, Rodrigues AM, Loureiro LMEF, Sá LCR, Matias JCO. Energy recovery from invasive species: creation of value chains to promote control and eradication. Recycling. 2021(b); 6:21. https://doi.org/10.3390/recycling6010021.

Pelicaen E, Janssens B, Knapen E. Circular building with raw earth: a qualitative assessment of two cases in Belgium. IOP Conference Series: Earth and Environmental Science. 2021; 855: 012002. DOI: 10.1088/1755-1315/855/1/012002.

Poppendieck DG, Hubbard HF, Weschler CJ, Corsi RL. Formation and emissions of carbonyls during and following gas-phase ozonation of indoor materials. Atmospheric Environment. 2007; 41(35): 7614-7626. https://doi.org/10.1016/j.atmosenv.2007.05.049.

Ranesi A, Faria P, Veiga MR. Traditional and modern plasters for built heritage: suitability and contribution for passive relative humidity regulation. Heritage. 2021; 4(3):2337-2355. https://doi.org/10.3390/heritage4030132.

Ranesi A, Faria P, Freire MT, Gonçalves M, Veiga MR. Gypsum plastering mortars with *Acacia dealbata* biowaste additions: effect of different fractions and contents on the relative humidity dependent properties. Construction and Building Materials. 2023; 404:133283. https://doi.org/10.1016/j.conbuildmat.2023.133283.

Ranesi A, Faria P, Freire MT, Gonçalves M, Veiga MR. Eco-efficient plastering mortars for improved indoor comfort - The influence of *A. dealbata* bark addition. Construction and Building Materials. 2024. *under review*.

Reiss R, Ryan PB, Koutrakis P. Modelling ozone deposition onto indoor residential surfaces. Environmental science Technology. 1994; 28(3): 504-513. https://doi.org/10.1021/es00052a025.

Reiss R, Ryan PB, Koutrakis P, Tibbetts SJ. Ozone reactive chemistry on interior latex paint. Environmental Science Technology. 1995; 29(8):1906-12. https://doi.org/10.1021/es00008a007.

Rim D, Gall ET, Maddalena RL, Nazaroff WW. Ozone reaction with interior building materials: influence of diurnal ozone variation, temperature and humidity. Atmospheric Environment. 2016; 125: 15–23. http://dx.doi.org/10.1016/j.atmosenv.2015.10.093.

Rodrigo H. Geraldo, Sayonara M.M. Pinheiro, Jefferson S. Silva, Heloysa M.C. Andrade, Jo Dweck, Jardel P. Gonçalves, Gladis Camarini. Gypsum plaster waste recycling: a potential environmental and industrial solution. Journal of Cleaner Production. 2017; 164:288-300. https://doi.org/10.1016/j.jclepro.2017.06.188.

Sáez-Pérez MP, Durán-Suárez JA, Verdú-Vázquez A, Gil-López T. Study and characterization of special gypsum-based pastes for their use as a replacement material in architectural restoration and construction. Materials. 2022; 15:5877. https://doi.org/10.3390/ma15175877.

Santos T, Almeida J, Silvestre JD, Faria P. Life cycle assessment of mortars: a review on technical potential and drawbacks. Construction and Building Materials 2021; 288:123069. https://doi.org/10.1016/j.conbuildmat.2021.123069

Santos T, Gomes MI, Santos Silva A, Ferraz E, Faria P. Comparison of mineralogical, mechanical and hygroscopic characteristic of earthen, gypsum and cement-based plasters. Construction and Building Materials. 2020; 254:119222. https://doi.org/10.1016/j.conbuildmat.2020.119222.

Shen J, Gao Z. Ozone removal on building material surface: A literature review. Building and Environment. 2018; 134: 205-217. https://doi.org/10.1016/j.buildenv.2018.02.046.

Sowndhararajan K, Joseph JM, Manian S. Antioxidant and free radical scavenging activities of indian Acacias: Acacia Leucophloea (Roxb.) Willd., Acacia Ferruginea Dc., Acacia Dealbata Link. and Acacia Pennata (l.) Willd. International Journal of Food Properties. 2013; 16(8):1717-1729. https://doi.org/10.1080/10942912.2011.604895.

Stucki JW. Chapter 11 - Properties and behaviour of iron in clay minerals. Developments in Clay Science, Elsevier. Bergaya F, Lagaly G (Eds). 2013; 5: 559-611. https://doi.org/10.1016/B978-0-08-098258-8.00018-3.

Tang X, Misztal PK, Nazaroff WW, Goldstein AH. Volatile organic compound emissions from humans indoors. Environmental Science Technology. 2016; 50: 12686−12694. https://doi.org/10.1021/acs.est.6b04415.

Torres-González M, Martín-Del-Rio J, Alejandre-Sánchez FJ, León Muñoz M, Bienvenido-Huertas D, Macías Bernal JM. Guidelines for conservation and restoration of historic polychrome plasterwork: the church of St María la Blanca in Seville, Spain. Studies in Conservation. 2023; 68(5): 529-547, https://doi.org/10.1080/00393630.2022.2072096.

United States Environmental Protection Agency (EPA). Updates to the air quality index (AQI) for ozone and ozone monitoring requirements. The National Ambient Air Quality Standards. 2015: 1-6.

United States Environmental Protection Agency (EPA). NAAQS Table. Last updated on March 15, 2023. Available at: https://www.epa.gov/criteria-air-pollutants/naaqs-table. (Accessed on September, 07, 2023)

Válek J, Skružná O, Kozlovcev P, Frankeová D, Mácová P, Viani A, Kumpová I. Composition and technology of the 17th century stucco decorations at Červená Lhota Castle in Southern Bohemia. International Journal of Architectural Heritage. 2020; 14(7): 1042-1057. DOI: 10.1080/15583058.2020.1731627.

Wang H, Rassu P, Wang X, Li H, Wang X, Wang X, Feng X, Yin A, Li P, Jin X, Chen S-L, Ma X, Wang B. An iron-containing metal–organic framework as a highly efficient catalyst for ozone decomposition. Angewandte Chemie International Edition. 2018; 57(50): 16416-16420. https://doi.org/10.1002/anie.201810268.

Wang N, Ernle L, Bekö G, Wargocki P, Williams J. Emission Rates of Volatile Organic Compounds from Humans. Environmental Science Technology. 2022; 56: 4838–4848. https://doi.org/10.1021/acs.est.1c08764.

Weschler CJ. Ozone in Indoor Environments: Concentration and Chemistry. Indoor Air. 2000; 10(4): 269-288. https://doi.org/10.1034/j.1600-0668.2000.010004269.x.

Weschler CJ. Roles of the human occupant in indoor chemistry. Indoor Air. 2016; 26: 6–24. DOI: 10.1111/ina.12185.

Weschler CJ and Nazaroff WW. Human skin oil: a major ozone reactant indoors. Environmental Science: Atmosphere. 2023a; 3(4): 640–661. https://doi.org/10.1039/D3EA00008G.

Weschler CJ and Nazaroff WW. Ozone Loss: A Surrogate for the Indoor Concentration of Ozone-Derived Products. Environmental Science & Technology. 2023b; 57(36): 13569-13578. https://doi.org/10.1021/acs.est.3c03968.

World Health Organization. WHO guidelines for indoor air quality: selected pollutants. World Health Organization. Regional Office for Europe, 2010. https://iris.who.int/handle/10665/260127.

Yan L, Bing J, Wu H. The behavior of ozone on different iron oxides surface sites in water. Scientific Reports. 2019; 9: 14752. https://doi.org/10.1038/s41598-019-50910-w.

Zhou X. Volatile organic compound emissions in building materials. In Woodhead Publishing Series in Civil and Structural Engineering, Advances in the Toxicity of Construction and Building Materials, Woodhead Publishing. Pacheco-Torgal F, Falkinham JO, Gałaj JÁ (Eds). 2022; 55-77. https://doi.org/10.1016/B978-0-12-824533-0.00009-8.

## 5.4 Additional Considerations

The two studies presented in this chapter (sections 5.2 and 5.3) analyzed the effect on hygroscopic behavior and pollutant reaction of the enhanced gypsum-based plasters obtained with the addition of *A. dealbata* bark and a small quantity of air lime, all along compared with clay-based plasters. Results point out that the overall characterization of the gypsum mortars is not significantly modified by the addition of the biomass but a higher hygroscopicity is observed (**Table 5.16**). The sorption isotherms and the moisture buffering tests show an increase in the ability of the products to adsorb moisture and a slight hysteresis effect in desorption, probably introduced by the biomass. Nevertheless, the two modified gypsum-based mortars (BA_AL and BA250_AL) show a higher moisture buffering value (that includes the evaluation of desorption too) than the reference gypsum mortar. The mortars BA_AL and BA250_AL were both produced with the addition of air lime at 4% by wt. of the premixed gypsum product (found effective to prevent biological growth) and differ for the treatment applied on the biomass that was firstly crushed, milled and sieved raw (BA) and then heated at 250°C for 1 h (BA250). Their MBVs are almost double the MBV of the reference gypsum mortar and very similar between them. Indeed, not different enough to justify the thermal treatment of the raw bark (BA250) and the consequent increase in the embodied energy of the product. Moreover, among all the plaster tested, the clay-based ones were still showing the highest hygroscopicity both under static and dynamic conditions.

**Table 5.16.** Synthesis of results from studies 5.2 and 5.3.

| Property | REF | BA_AL | BA250_AL | CL | CL_M |
|---|---|---|---|---|---|
| Adsorption [%] at 80%RH | 0.16 | 0.53 | 0.48 | 0.75 | 0.96 |
| MBV [g/(m$^2$%RH)] | 0.47 | 0.99 | 0.89 | 1.76 | 1.87 |
| $v_d$ [cm/s] | 0.04 | 0.06 | 0.06 | 0.11 | 0.10 |
| $\varepsilon_{1,b}$ * [µg/(m$^2$h)] | 51 | 33 | 59 | 133 | 137 |
| $\varepsilon_{1,b}$ [µg/(m$^2$h)] | 55 | 96 | 153 | 149 | 157 |
| $\varepsilon_{2,b}$ *[µg/(m$^2$h)] | 77 | 66 | 79 | 206 | 126 |
| $\varepsilon_{2,b}$ [µg/(m$^2$h)] | 87 | 154 | 175 | 228 | 147 |
| Y [-] | 0.107 | 0.083 | 0.032 | 0.082 | -0.021 |

Notation: REF - reference gypsum-based plaster; BA_AL - gypsum-based plaster with addition at 10% of raw bark and 4% of air lime (by wt.); BA250_AL - gypsum-based plaster with addition at 10% of heated bark and 4% of air lime (by wt.); CL - clay based plaster; CL_M - clay based plaster with addition of crushed seashells; MBV - moisture buffering value; vd - deposition velocity; $\varepsilon_{1,b}$ - total primary emissions; $\varepsilon_{2,b}$ - secondary emissions; Y - molar yields ; * - without methanol (m/z 33.030).

All the plasters were reactive to ozone and considered promising coatings for passive ozone removal. Deposition velocity shows that the addition of bark (raw and thermally treated) has a positive effect on the property. Moreover, without accounting the methanol that can be somehow linked to the biomass addition and needs further investigations (at these fluxes anyway would likely only introduce a small change in concentration indoors), the total average primary and secondary emissions of the gypsum plasters are the lowest, with very interesting results obtained by the addition of raw bark (33 and 66 $\mu g \cdot m^{-2} h^{-1}$, respectively). Finally, the lowest total average molar yield rate, calculated as the average on three specimens of the sum of positive and negative yields (for all the targeted byproducts), is observed for the clay-based plaster with addition of crushed seashells (-0.021) followed by the very low yield of BA250_AL (0.032). The clay mortar and the mortar BA_AL have similar molar yields (0.082 and 0.083) and the gypsum mortar has the highest total average yield of 0.107, meaning it has the highest emission rate of carbonyl compounds produced by reaction with ozone. Nevertheless, all the yields here found are still very low if compared with other coatings like finished hardwood floor (0.4), bio-based resilient tiles (>0.3) or porcelain tiles (≈0.2) tested by other authors (Lamble et al., 2011).

# 6

# CONCLUSIONS

## 6.1 Final Remarks

The present work investigates the potential of eco-efficient plastering mortars to be used for the passive contribution to indoor comfort and air quality.

Through the brief analysis on the context of the study of the 1st chapter, the guiding principles of the thesis work were exposed: the effect that indoor relative humidity and high concentrations of harmful pollutants, like ozone and volatile organic compounds, can have on human health; the importance of the compatibility and the sustainability of new designed coatings. The purpose, thus, was to better understand the contribution modern and traditional plasters can give to indoor comfort and air quality and, eventually, how to enhance a plaster for the purpose, observing compatibility and sustainability criteria.

The 2nd chapter presents the study on the monitored hygrothermal conditions in residential buildings located in the temperate climate of Lisbon. The study started with a research question about the representativeness under real conditions of widespread methods and protocols to test plasters hygroscopic response. Indoor RH fluctuations were found closer to the middle humidity conditions (ΔRH 50%-75%) of ISO 24353 (2021) than other testing methods and, thus, the use of this method was advised for designing products to be applied in unheated or intermittently heated residential buildings in temperate climates. In terms of indoor comfort, study cases were found over 50% of wintertime out of the comfort area (higher relative humidity and lower temperature). Moreover, hygroscopic behavior of plasters based on clay, air lime, natural hydraulic lime, and cement was modeled (calibrated using results from mortar's

laboratory characterization) and used for simulations under real microclimatic conditions. The moisture content variations were qualitatively in agreement with the MBVs determined by both the NORDTEST (2005) and ISO 24353 (2008) and the clay-based plaster was found to be the most promising coating showing the widest fluctuations, i.e., moisture reactivity. Once the preliminary study settled the most suitable testing conditions and collected results of moisture reactivity for different binder-based plasters (traditional and modern), a research work on their state-of-the-art was run. Test methods and results were collected in a systematic review which principal outcomes was the establishment of ranges of adsorption, MBV and WVP for several binder-based plasters and the ranking of most applied methods for each of these properties. Nevertheless, a huge heterogeneity of test methods and testing conditions was found, turning the comparison of results from different studies more challenging. Also, the review pointed at the clay-based plasters as the most hygroscopic ones.

The 3rd chapter presents the study on the hygroscopic behavior of traditional and modern plasters based on binder presented in the previous chapter. The characterization applies the most popular testing methods according to the previous literature review (section **1.1**) and, through some simplification, permits the comparison of experimental results with ranges from literature. Overall, results are found consistent with the ranges; only in the case of plasters obtained through the combination of gypsum and air lime seems that the bibliographic range underestimate their moisture response. Nevertheless, this was found a very particular case, where the combination of the two binders has a very positive effect on the adsorption, remarkably higher than for any plaster based on only one of the single binders. But it came with drawbacks on desorption capacity, with hysteresis observed in both pastes. Nonetheless, the event of a still ongoing carbonation of the plastering pastes was not discarded and more tests need to be run on plasters based on gypsum and air lime with an assured total carbonation rate. The clay-based plasters were confirmed by this study very hygroscopic and the hydraulic binder-based mortars, such as cements and natural hydraulic lime, showed a behavior in the middle between the clay plaster and gypsum-lime pastes (very good) and the poorest one of only gypsum and only air lime. In the same chapter, the effect of two paint systems (A - vinylic, and B -acrylic) on the same properties was evaluated. It was found out that the effects were very different. Paint A modified the properties very little, increasing the thickness of the equivalent air layer of the systems (plasters + paint A) with different effect on different plasters, and the hygroscopic behavior (which in some case was overall enhanced due to the stabilizing effect of the paint that reduced the hysteresis). On the contrary, the

application of paint system B substantially reduced the water vapor adsorption and the dynamic response to RH fluctuations. Results are consistent with what expected for a paint commercialized for external application and, so, probably designed with a different scope from passive indoor moisture regulation, which, more likely, the paint A has been.

The 4th chapter presents the study on the enhancement of gypsum-based plasters with the addition of the biomass from *Acacia dealbata*. The plant is an invasive species that is very much spread all over the world (in Portugal too) representing a threat for the local ecosystem and for people safety due to its high fire propagation. Furthermore, it is not suited for burning to generate heat. Therefore, all the fractions of the plant were introduced in the study, after extractive recovery, to evaluate their contribution to mortars properties; namely flowers, leaves, branchlets, bark and wood were added at 5% and 10% by vol. to a chosen premixed gypsum-based product and a fixed amount of water. From there, mortars were produced, cured, and characterized. The fresh, hardened, and mechanical properties were found overall adequate (complying with the standard), with the best effect introduced by wood fraction but with all the additions (fractions and quantities) found viable. After that, a study more specifically oriented to the hygroscopic behavior of the mortars found that: all the biomass additions increased the adsorption/desorption of the gypsum-based plasters (static and dynamic conditions); the highest addition (10% by vol.) introduced highest changes in properties; the 10% by vol. of bark was the most promising addition, among all the combinations. In fact, with this addition the hygroscopic behavior of the mortars was found four times enhanced, with a MBV reaching the range of clay-based plasters. Nevertheless, biological growth was observed in all the gypsum-based mortars with biomass addition (apart from wood) during the first curing days, maybe due to environmental factors, biological factors, or a combination of both. Thus, a preliminary study for the final formulations was run to evaluate the possible solutions to avoid biological growth on plasters, either through pH control, thermal treatment of the biomass or a combination of both.

The 5th chapter presents the final formulations for innovative gypsum-based plastering mortars, done with the addition of raw bark and heated bark at 250 °C (for 1 h) at 10% by vol. and air lime at 4% by wt. to the premixed gypsum product. The raw biowaste used for the campaign had never been used for extraction. The mortars were tested among the chapter in comparison with the reference gypsum mortar and with two premixed clay plasters (one with the addition of crushed seashells in formulation). An extended mechanical and physical characterization is presented with a special interest in the hygroscopic response of the plasters.

The enhancement of adsorption capacity through the addition of the biomass (both raw and thermally treated) was confirmed by results of sorption isotherms and moisture buffering test. Nevertheless, the desorption of the mortars showed a minor hysteresis probably introduced by the biomass. Overall, their adsorption/desorption ability, quantified by the calculation of MBV, was found to be double than the gypsum mortar, but still half of the clay ones. All the plasters were found good at ozone removal. The addition of bark (raw and thermally treated) can have a positive effect on this property, increasing deposition velocity for gypsum plasters. Gypsum coatings showed the lowest total average of primary and secondary emissions if methanol emissions are not counted. Finally, the clay-based plaster with the addition of crushed seashells had the lowest total average molar yield rate.

To conclude, the use of clay-based plasters is advised for intervention both on ancient and new constructions, representing a good eco-efficient choice for its low embodied energy and reactivity to indoor moisture variations (adsorbing from the indoor air when the RH is increasing and releasing the moisture back to the air when the RH is decreasing) for moisture passive regulation. Moreover, they have a good ozone removal activity and generally low primary and secondary emissions of VOCs. It seems that some formulations can be better than others for the scope.

Calcium sulfate hemihydrate is a very suitable binder too, for plastering any type of indoors, with good compatibility with heritage (and new buildings) and is produced with low calcination temperature and easy milling. The eco-efficiency and hygroscopic behavior of gypsum-based plastering mortars can be increased with the addition of a biomass, bark from *A. dealbata* selected for this work, better if biowastes from other industry value-chain. The addition of air lime in these cases is advised to prevent biological growth but, anyway, the new plasters show an important increase in their moisture reactivity even with small additions (10% by vol.). The gypsum VOCs primary and secondary emissions are low, and so they are with the bark addition. The ozone removal capacity of the gypsum plasters is improved by bark additions.

As plasters can coat a significative area of indoor walls and ceilings, the impact that eco-efficient clay or gypsum-based plasters can have to passively contribute to indoor comfort and air quality, reducing energy consumption, improving indoor air quality and contributing to inhabitants' health is, therefore, extremely important.

## 6.2 Further Studies/Perspectives

The present work aims to be a starting point for a more environmentally friendly management of indoors, through the implementation of passive solutions to eventually integrate mechanical systems for ensuring good air quality and comfort. Nevertheless, further investigations are needed to better understand:

- The properties that better can describe the plasters moisture regulation.
- If there are other mechanisms involved in the enhancement of indoor hygroscopic comfort.
- The reactivity of traditional and modern plasters to other common indoor pollutants, like carbon dioxide.
- The effect that finishings like different painting systems can have on the passive regulation of moisture and pollutant removal.
- The effect of using bark as byproduct after extractives removal (as the one used in chapter 3) on the optimized bio-gypsum-air lime plaster formulation.
- The reason for high emissions of methanol when the biomass is added to the plasters formulations and what this implies.
- The humidity dependence of the ozone deposition velocities for high hygroscopic coatings.
- The surface chemistry and the mechanisms behind the ozone removal and with them the decay of the ozone removal activity
- The relation between all the considered properties and the aging of the coatings.
- The possibility of obtaining higher enhancements, not increasing drawbacks, with higher additions of biomass.
- Assessing the effect of additions to clay-based plasters on ozone capture.
- The quantification of the environmental impact of different binder-based plasters and the ones here developed, through a life cycle assessment.

# THESIS REFERENCES


Abbass, O.A., Sailor, D.J., Gall, E.T., 2017. "Effectiveness of indoor plants for passive removal of indoor ozone". Building and Environment 119, 62-70. https://doi.org/10.1016/j.buildenv.2017.04.007.

Abbass, O.A., Sailor, D.J., Gall, E.T., 2018. "Ozone removal efficiency and surface analysis of green and white roof HVAC filters", Building and Environment 136, 118-127. https://doi.org/10.1016/j.buildenv.2018.03.042.

Antepara, I., Papada, L., Gouveia, J.P., Katsoulakos, N., Kaliampakos, D., 2020, "Improving Energy Poverty Measurement in Southern European Regions through Equivalization of Modeled Energy Costs", Sustainability 12*,* 5721. https://doi.org/10.3390/su12145721.

Apte, M.G., Buchanan, I.S.H., Mendell, M.J., 2008. "Outdoor ozone and building-related symptoms in the BASE study", Indoor Air 18, 156-170. https://doi.org/10.1111/j.1600-0668.2008.00521.x.

Arriazu-Ramos, A., Bes-Rastrollo, M., Sánchez-Ostiz Gutiérrez, A., Monge-Barrio, A., 2023. "Building parameters that influence overheating of apartment buildings in a temperate climate in Southern Europe", Building and Environment 228, 109899. ISSN 0360-1323. https://doi.org/10.1016/j.buildenv.2022.109899.

Arundel, A. V.; Sterling, E. M.; Biggin, J. H.; Sterling, T. D. 1986. "Indirect health effects of relative humidity in indoor environments", Environmental health perspectives 65, 351-61.

ASTM D5590-17; Determining the Resistance of Paint Films and Related Coatings to Fungal Defacement by Accelerated Four-Week Agar Plate Assay. ASTM International: Pennsylvania, PA, USA, 2021.

Balksten, K. and Klasén, K., 2005. "The Influence of craftsmanship on the Inner Structures of Lime Plasters", in: RILEM Workshop.

Barbosa F.C.; de Freitas V.P.; Almeida M. 2020. "School building experimental characterization in Mediterranean climate regarding comfort, indoor air quality and energy consumption", Energy and Buildings 212, 109782. DOI: 10.1016/j.enbuild.2020.109782.

Bell, M.L., McDermott, A., Zeger, S.L., Samet, J.M., Dominici, F., 2004. "Ozone and short-term mortality in 95 US urban communities", JAMA 292:19, 2372–2378. https://doi.org/10.1001/jama.292.19.2372.

Bell, M.L., Peng, R.D., Dominici, F., 2006. "The exposure–response curve for ozone and risk of mortality and the adequacy of current ozone regulations", Environmental Health Perspectives 114:4. https://doi.org/10.1289/ehp.8816

Berardi, U., Ghaffarian Hoseini, A.H., Ghaffarian Hoseini, A., 2014. "State-of-the-art analysis of the environmental benefits of green roofs", Applied Energy 115, 411-428. https://doi.org/10.1016/j.apenergy.2013.10.047.

Brazão Farinha, C., Silvestre, J.D., de Brito, J., Veiga, M.d.R., 2019. "Life cycle assessment of mortars with incorporation of industrial wastes", Fibers 7, 59. https://doi.org/10.3390/fib7070059

Bumanis, G., Vitola, L., Pundiene, I., Sinka, M., Bajare, D., 2020. "Gypsum, geopolymers, and starch-alternative binders for bio-based building materials: a review and life-cycle assessment", Sustainability, 12:14, 5666. https://doi.org/10.3390/su12145666.

Bumanis, G., Korjakins, A., Bajare, D., 2022. "Environmental benefit of alternative binders in construction industry: life cycle assessment", Environments, 9, 6. https://doi.org/10.3390/environments9010006.

Candeias, A. E., Nogueira, P., Mirão, J., Santos Silva, A., Veiga, R., Casal, M. G., ... Seruya, A. I., 2006. "Characterization of ancient mortars: present methodology and future perspectives", Proc. Workshop on Chemistry in the Conservation of Cultural Heritage: Present and Future Perspectives, Perugia.

Damas, A. L., Veiga, R., & Faria, P., 2016. "Caraterização de argamassas antigas de Portugal – contributo para a sua correta conservação", Congresso Ibero-Americano "Património, Suas Matérias e Imatérias," ISBN: 978-972-49-2288-1.

Diaz-Basteriz, J., Sacramento Rivero, J.C., Menéndez, B. 2022. "Life cycle assessment of restoration mortars and binders", Construction and Building Materials, 326, 126863. https://doi.org/10.1016/j.conbuildmat.2022.126863.

Diffey, B. L., 2011. "An overview analysis of the time people spend outdoors", British journal of dermatology 164, 848-54. DOI : 10.1111/j.1365-2133.2010.10165.x.

Elsen, J., Van Balen, K., Mertens, G. "Hydraulicity in historic lime mortars: a review", Proceeding of the 2nd Historic Mortars Conference (HMC2010) and RILEM TC 203-RHM Final Workshop, 22-24 September 2010, Prague, Czech Republic.

EN 459-1: 2015. Building lime - Part 1: Definitions, specifications and conformity criteria. CEN, Brussels, Belgium.

EN 998-1: 2003. Specification for mortar for masonry - Part 1: Rendering and plastering mortar. CEN, Brussels, Belgium.

EN 1015-10: 2008. Methods of test for mortar for masonry - Part 10: Determination of dry bulk density of hardened mortar. CEN, Brussels, Belgium.

EN 1015-11: 2020. Methods of test for mortar for masonry - Part 11: Determination of flexural and compressive strength of hardened mortar. CEN, Brussels, Belgium.

EN 1015-12: 2016. Methods of test for mortar for masonry - Part 12: Determination of adhesive strength of hardened rendering and plastering mortars on substrates. CEN, Brussels, Belgium.

EN 1015-19: 1998. Methods of test for mortar for masonry - Part 19: Determination of water vapour permeability of hardened rendering and plastering mortars. CEN, Brussels, Belgium.

EN 13279-1: 2008. Gypsum binders and gypsum plasters - Part 1: Definitions and requirements. CEN, Brussels, Belgium.

EN 13279-2: 2014. Gypsum binders and gypsum plasters—Part 2: Test methods. CEN, Brussels, Belgium.

EN 14146: 2004. Natural stone test methods - Determination of the dynamic modulus of elasticity (by measuring the fundamental resonance frequency). CEN, Brussels, Belgium.

EN 1936: 2007. Natural stone test methods - Determination of real density and apparent density, and of total and open porosity. CEN, Brussels, Belgium.

Fang, L., Clausen, G., Fanger, P. O., 1998. "Impact of temperature and humidity on the perception of indoor air quality", Indoor air 8, 80-90. DOI: 10.1111/j.1600-0668.1998.t01-2-00003.x.

Fanger, P. O., 1967. "Calculation of thermal comfort: introduction of a basic comfort equation", Building Engineering 73 (2), III.4.1 and III.4.20.

Faria, P., Henriques, F. and Rato, V., 2008. "Comparative evaluation of lime mortar for architectural conservation," J. Cult. Herit., vol. 9, no. 3, pp. 338–346.

Fernandes, M., 2008. "Earth mortars and earth-lime renders", Conservar Património, 8, 21–27.

Ferreira, F.C., Torres, P.M., Tente, H.S., Neto, J.B., 2004. "Ozone levels in Portugal: The Lisbon region assessment", In Proceedings of the Air and Waste Management Association's Annual Conference and Exhibition, AWMA, Indianapolis, IN, USA, 22–25 June 2004.

Ferreira, C., de Freitas, V. P., Delgado, J.M.P.Q., 2020. "The influence of hygroscopic materials on the fluctuation of relative humidity in museums located in historical buildings", Studies in Conservation 65, 3, 127-41.

Freire, M. T., Santos Silva, A., Veiga, M. R., de Brito, J. 2015. "The history of Portuguese interior plaster coatings: a mineralogical survey using XRD," Archaeometry, vol. 57, Supplement S1, 147-165.

Freire, M. T., Veiga, M. R., Santos Silva, A., de Brito, J., 2021. " Restoration of ancient gypsum-based plasters: Design of compatible materials", Cement and Concrete Composites 120, 104014. https://doi.org/10.1016/j.cemconcomp.2021.104014.

Frontczak, M., Wargocki, P., 2011. "Literature survey on how different factors influence human comfort in indoor environments", Building and Environment, 46, 922-37. DOI: 10.1016/J.BUILDENV.2010.10.021.

Gbekou, F. K., Boudenne, A., Eddhahak, A., Benzarti, K., 2023. "Mechanical and hygrothermal properties of cement mortars including both phase change materials and miscanthus fibers", Bio-Based Building Materials. ICBBM 2023. Amziane S, Merta I, Page J. (Eds) Springer, RILEM Bookseries; 45, 804–816. https://doi.org/10.1007/978-3-031-33465-8_62.

Gentile, V., Libralato, M., Fantucci, S., Shtrepi, L., Autretto, G. 2023. "Enhancement of the hygroscopic and acoustic properties of indoor plasters with a super adsorbent calcium alginate biopolymer", Journal of Building Engineering, 76, 107147, ISSN 2352-7102, https://doi.org/10.1016/j.jobe.2023.107147.

Gryparis, A., Forsberg, B., Katsouyanni, K., Analitis, A., Touloumi, G., Schwartz, J., Samoli, E., Medina, S., Anderson, H.R., Niciu, E.M., Wichmann, H.-E., Kriz, B., Kosnik, M., Skorkovsky, J., Vonk, J.M., Dörtbudak. Z., 2004. "Acute effects of ozone on mortality from the "air pollution and health: a European approach" project", American Journal of Respiratory and Critical Care Medicine, 170:10, 1080-1087. https://www.atsjournals.org/doi/abs/10.1164/rccm.200403-333OC.

Hyttinen, M., Pasanen, P., Kalliokoski, P., 2006. "Removal of ozone on clean, dusty and sooty supply air filters", Atmospheric Environment, 40:2, 315-325. https://doi.org/10.1016/j.atmosenv.2005.09.040.

Huang, Y., Yang, Z., Gao, Z., 2019. "Contributions of indoor and outdoor sources to ozone in residential buildings in Nanjing", Int J Environ Res Public Health, 16:14, 2587. doi: 10.3390/ijerph16142587.

Humphreys, M.A., Nicol, F.J., 1998. "Understanding the adaptive approach to thermal comfort", ASHRAE transactions.

IPMA (Instituto Português do Mar e da Atmosfera) page "climate normals" accessed on October 2023. https://www.ipma.pt/en/oclima/normais.clima/.

ISO (International Standards Organization), ISO 12571: Hygrothermal performance of building materials and products - Determination of hygroscopic sorption properties. ISO, Geneva, Switzerland, 2013.

ISO (International Standards Organization), ISO 12572: Hygrothermal performance of building materials and products - Determination of water vapour transmission properties - Cup method., ISO, Geneva, Switzerland, 2016.

ISO (International Standards Organization), ISO 24353: Hygrothermal performance of building materials and products - Determination of moisture adsorption/desorption properties in response to humidity variation. ISO, Geneva, Switzerland, 2008.

Jing, L., Wang, J., 2022. "Study on indoor ozone removal by PRM under the influence of typical factor". Proceedings of the 16th ROOMVENT Conference. September 16-19, Xi'an, China. A. Li, T. Olofsson and R. Kosonen (Eds.). https://doi.org/10.1051/e3sconf/202235.

Kelly, F.J., Fussell, J.C., 2011. "Air pollution and airway disease", Clinical & Experimental Allergy 41, 1059-1071. https://doi.org/10.1111/j.1365-2222.2011.03776.x.

Lamble, S.P., Corsi, R.L., Morrison, G.C., 2011. "Ozone deposition velocities, reaction probabilities and product yields for green building materials", Atmospheric Environment 45: 38, 6965-6972. https://doi.org/10.1016/j.atmosenv.2011.09.025.

Lee, P., Davidson, J., 1999. "Evaluation of activated carbon filters for removal of ozone at the PPB level", American Industrial Hygiene Association Journal 60:5, 589-600. https://doi.org/10.1080/00028899908984478.

Li, X., Ran, M. 2023. "Gypsum-based humidity-control material: preparation, performance and its impact on building energy consumption", Materials. 16, 5211. https://doi.org/10.3390/ma16155211.

Li, Y., Cheng, M., Guo, Z., He, Y., Zhang, X., Cui, X. and Chen, S. 2020. "Increase in Surface Ozone over Beijing-Tianjin-Hebei and the Surrounding Areas of China Inferred from Satellite Retrievals, 2005-2018", Aerosol and Air Quality Research 20, 2170–2184. https://doi.org/10.4209/aaqr.2019.11.0603.

Lima, J., Faria, P. 2016, "Eco-efficient earthen plasters. The influence of the addition of natural fibers. Natural Fibres: Advances in Science and Technology Towards Industrial Applications", From Science to Markets, Fangueiro, Raul, Rana, Sohel (Eds.). Springer, RILEM Book Series; 12: 315-327. Doi:10.1007/978-94-017-7515-1_24.

Liu, N., Bu, Z., Liu, W., Kan, H., Zhao, Z., Deng, F., Huang, C., Zhao, B., Zeng, X., Sun, Y., Qian, H., Mo, J., Sun, C., Guo, J., Zheng, X., Weschler, L. B., Zhang, Y., 2022 "Health effects of exposure to indoor volatile organic compounds from 1980 to 2017: A systematic review and meta-analysis", Indoor Air, 32, e13038. DOI: 10.1111/ina.13038.

Liuzzi, S., Stefanizzi, P., 2016. "Experimental study on hygrothermal performances of indoor covering materials", International Journal of Heat and Technology 34, 2, S365-70. DOI: 10.18280/ijht.34S225.

Malta da Silveira, P., Veiga, M.R., de Brito, J., 2007. "Gypsum coatings in ancient buildings", Construction and Building Materials, 21(1), 126–131.

Marcelino-Sadaba, S., Kinuthia, J., Oti, J., Seco Meneses, A. 2017. "Challenges in Life Cycle Assessment (LCA) of stabilised clay-based construction materials", Applied Clay Science, 144, 121-130. https://doi.org/10.1016/j.clay.2017.05.012.

Matias, G., Faria, P., Torres, I., 2014. "Lime mortars with heat treated clays and ceramic waste: A review", Constr. Build. Mater., vol. 73, pp. 125–136.

McGregor, F., Heath, A., Maskell, D., Fabbri, A., Morel, J-C. 2016, "A review on the buffering capacity of earth building materials", Proc. of the Institution of Civil Engineers: Construction Materials. 169(5), 241-251. https://doi.org/10.1680/jcoma.15.00035 .

Melià, P., Ruggieri, G., Sabbadini, S., Dotelli, G., 2014. "Environmental impacts of natural and conventional building materials: a case study on earth plasters," J. Clean. Prod., vol. 80, pp. 179–186.

Mestre, V., 2007. "La construcción tradicional en el espacio mediterráneo portugués", (in Portuguese) Apuntes: Revista de Estudios sobre Patrimonio Cultural, vol. 20, no. 2, pp. 278–285.

Moropoulou, A., Koroneos, C., Karoglou, M., Aggelakopoulou, E., Bakolas, A., Dompros, A., 2011. "Life cycle analysis of mortars and its environmental impact", Proc. Mater. Res. Soc. Symp., vol. 895, pp. 145–150.

Nazaroff, W.W., Weschler, C.J., 2022. "Indoor ozone: concentrations and influencing factors", Indoor Air 32, 1. https://doi.org/10.1111/ina.12942.

Padfield, P., 1999. "Humidity buffering of the indoor climate by absorbent walls", Proceeding of the 5th Symposium on Building Physics in the Nordic Countries 2, 637-44.

Pawełkowicz, S. S.; Svora, P., Prošek, Z., Keppert, M., Vejmelková, E., Murafa, N., Sawoszczuk, T., Syguła–Cholewińska, J., Bíbová, H., 2022. "Laboratory assessment of a photoactive gypsum-based repair plaster", Construction and Building Materials 346, 128426. ISSN 0950-0618, https://doi.org/10.1016/j.conbuildmat.2022.128426.

Pedreño-Rojas, M. A., Fořt, J., Černý, R., Rubio-de-Hita, P., 2020. "Life cycle assessment of natural and recycled gypsum production in the Spanish context", Journal of Cleaner Production 253, 120056.

Posani, M., Veiga, M.R., de Freitas, V.P., 2021. "Towards resilience and sustainability for historic buildings: a review of envelope retrofit possibilities and a discussion on hygric compatibility of thermal insulations", International Journal of Architectural Heritage 15, 5, 807-823.

Ranesi, A., Faria, P., Veiga, R. 2021. "Eco-efficiency of plasters for rehabilitation and new buildings". Proceedings of the 2nd International Conference on Sustainable, Environmentally Friendly Construction (ICSEFCM2021), E. Horszczaruk, P. Brzozowski (Eds.), Poland, 91-96. ISBN: 978-83-7663-324-4.

Rode, C., Peuhkuri, R.H., Mortensen, L.H., Hansen, K.K., Time, B., Gustavsen, A., Ojanen, T., Ahonen, J., Svennberg, K., Arfvidsson, J., Harderup, L.E. 2005. "Moisture buffering of building materials". Technical University of Denmark, Department of Civil Engineering (Eds.).

Rosell, J.R., L. Haurie, L., Navarro, A., Cantalapiedra, I.R., 2014. "Influence of the traditional slaking process on the lime putty characteristics", Construction and Building Materials, 55, 423–430.

Santos, A.R., Veiga, M.R., Santos Silva, A., de Brito, J. and Álvarez, J. I., 2018. "Evolution of the microstructure of lime based mortars and influence on the mechanical behaviour: The role of the aggregates", Construction and Building Materials, 187, 907–922.

Santos, T., Faria, P., Silva, V., 2019. "Can an earth plaster be efficient when applied on different masonries?", J. Build. Eng., vol. 23, pp. 314–323.

Santos, T., Almeida, J., Silvestre, J.D., Faria, P., 2021. "Life cycle assessment of mortars: A review on technical potential and drawbacks", Construction and Building Materials, 288, 123069. https://doi.org/10.1016/j.conbuildmat.2021.123069.

Shen, J., Gao, Z., 2018. "Ozone removal on building material surface: a literature review", Building and Environment 134, 205-217. https://doi.org/10.1016/j.buildenv.2018.02.046.

Trasande, L., Thurston, G.D., 2005. "The role of air pollution in asthma and other pediatric morbidities", Journal of Allergy and Clinical Immunology 115:4, 689-699. https://doi.org/10.1016/j.jaci.2005.01.056.

Veiga, R., 2017. "Air lime mortars: What else do we need to know to apply them in conservation and rehabilitation interventions? A review", Construction and Building Materials, 157, 132–140.

Veiga, R., Faria, P., 2018. "O papel das argamassas na durabilidade das alvenarias antigas," CirEA2018 - Conferência Int. sobre Reabil. Estruturas Antigas Alvenaria, pp. 1–15.

Wargocki, P., Wyon, D.P., 2013. "Providing better thermal and air quality conditions in school classrooms would be cost-effective", Building and Environment 59, 581-89. DOI: 10.1016/j.buildenv.2012.10.007.

Weschler, C.J., 2000. "Ozone in indoor environments: concentration and chemistry", Indoor Air 10, 269-288. https://doi.org/10.1034/j.1600-0668.2000.010004269.x.

Weschler, C.J., 2006. "Ozone's impact on public health: contributions from indoor exposures to ozone and products of ozone-initiated chemistry", Environmental Health Perspectives 114, 10. https://doi.org/10.1289/ehp.9256.

Wolkoff, P., 2018. "Indoor air humidity, air quality, and health – An overview", International Journal of Hygiene and Environmental Health 221, 376-90. DOI: 10.1016/j.ijheh.2018.01.015.

Xiong, J., Lian, Z., Zhou, X., You, J., Lin, Y., 2015. "Effects of temperature steps on human health and thermal comfort", Building and Environment. 94, 144-154. https://doi.org/10.1016/j.buildenv.2015.07.032.

Yang, Y., Shen, Z., Wu, W., Zhang, H., Ren, Y., Yang, Q., 2022. "Preparation of a novel diatomite-based PCM gypsum board for temperature-humidity control of buildings", Building and Environment. 226, 109732, ISSN 0360-1323. https://doi.org/10.1016/j.buildenv.2022.109732.

# ANNEX

## A.1 List of publications disseminating the work

PEER-REVIEWED JOURNAL ARTICLES

1. **Ranesi, A.**; Faria, P.; Freire, M.T.; Gonçalves, M.; Veiga, M.R. (2023). "Gypsum plastering mortars with Acacia dealbata biowaste additions: Effect of different fractions and contents on the relative humidity dependent properties". *Construction and Building Materials,*404, 133283. https://doi.org/10.1016/j.conbuildmat.2023.133283
2. **Ranesi, A.**; Faria, P.; Correia, R.; Freire, M.T.; Veiga, R.; Gonçalves, M. (2022). "Gypsum Mortars with Acacia dealbata Biomass Waste Additions: Effect of Different Fractions and Contents". *Buildings*,12, 3, 339. https://doi.org/10.3390/buildings12030339.
3. **Ranesi, A.**; Posani, M.; Veiga, R.; Faria, P. (2022). "A Discussion on Winter Indoor Hygrothermal Conditions and Hygroscopic Behaviour of Plasters in Southern Europe". *Infrastructures* ,7, 3, 38. https://doi.org/10.3390/infrastructures7030038.
4. **Ranesi, A.**; Faria, P.; Veiga, R. (2021). "Laboratory characterization of relative humidity dependant properties for plasters: a systematic review". *Construction and Building Materials,* 304, 124595. https://doi.org/10.1016/j.conbuildmat.2021.124595.
5. **Ranesi, A.**; Veiga, R.; Faria, P. (2021). "Traditional and Modern Plasters for Built Heritage: Suitability and Contribution for Passive Relative Humidity Regulation". *Heritage*, 4, 2337–2355. https://doi.org/10.3390/heritage4030132.

PEER-REVIEW BOOK CHAPTER (from an abstract presented in a conference)

1. **Ranesi, A.**; Faria, P.; Veiga, R. (2023). "Moisture buffering value of plasters: the influence of two different test methods". Chastre, C.; Ribeiro, Á.; Ribeiro, D.; Neves, J.; Pinho, F.F.S.; Neves, M.G.; Biscaia, H.; Faria, P.; Micaelo, R. (Eds.). Testing and Experimentation in Civil Engineering - From Current to Smart Technologies. Springer and RILEM.

FULL-LENGTH PEER-REVIEWED CONFERENCE ARTICLES AND EXTENDED ABSTRACTS

1. **Ranesi, A.**; Gall, E.T.; Veiga, R.; Faria, P. (2023). "Clay-based plasters for passive air pollutant removal: the case of ozone". *Submitted and accepted* at 2nd International Conference on Construction, Energy, Environment and Sustainability (CEES2023), Itecons (Eds.), Portugal.
2. **Ranesi, A.**; Faria, P.; Veiga, R. (2022). "Moisture buffering value of plasters: the influence of two different test methods". Chastre, C.; Ribeiro, Á.; Ribeiro, D.; Neves, J.; Pinho, F.F.S.; Neves, M.G.; Biscaia, H.; Faria, P.; Micaelo, R. (Eds.). Proceedings – Extended Abstracts – of the 3rd Conference on Testing and Experimentation in Civil Engineering. NOVA School of Science and Technology, 55-56. ISBN: 978-972-99923-5-3, https://doi.org/10.34619/ycjz-atxf.
3. **Ranesi, A.**; Posani, M.; Veiga, R.; Faria, P. (2021). "A study on hygrothermal conditions in intermittently heated or unheated bedrooms in southern Europe". Proceedings of the 1st International Conference on Construction, Energy, Environment and Sustainability (CEES2021), Itecons (Eds.), Portugal. ISBN: 978-989-54499-1-0.
4. **Ranesi, A.**; Faria, P.; Veiga, R. (2021). "Eco-efficiency of plasters for rehabilitation and new buildings". Proceedings of the 2nd International Conference on Sustainable, Environmentally Friendly Construction (ICSEFCM2021), E. Horszczaruk, P. Brzozowski (Eds.), Poland, 91-96. ISBN: 978-83-7663-324-4.
5. **Ranesi, A.**; Veiga, R.; Faria, P. (2020). "Plasters for rehabilitation – relevant requirements and characteristics (Rebocos interiores para reabilitação – requisitos e características importantes)", in Portuguese. Proceedings of the ENCORE2020 – 4°Encontro de conservação e reabilitação de edifícios. https://doi.org/10.34638/yzys-hn57.

## A.2 Laboratories where the work took place

- National Laboratory for Civil engineering (LNEC), Building, Coatings and Thermal Insulation Unit (NRI), Building Department.
- National Laboratory for Civil engineering (LNEC), Organic Materials Unit (NMO), Materials Department.
- NOVA University Lisbon, NOVA School of Science and Technology, Department of Civil Engineering (DEC).
- NOVA University Lisbon, NOVA School of Science and Technology, Department of Chemistry (DQ).

- Portland State University (PSU), Healthy Buildings Research Lab (HRBL), Department of Mechanical and Materials Engineering.
- SIVAL- Gessos Especiais Lda, Department of Research and Development.

⟨2023⟩ ALESSANDRA RANESI ECO-EFFICIENT PLASTERS FOR INCREASED INDOOR AIR QUALITY AND COMFORT

NOVA SCHOOL OF SCIENCE & TECHNOLOGY

⟨2023⟩

# ECO-EFFICIENT PLASTERS FOR INCREASED INDOOR AIR QUALITY AND COMFORT

UNIVERSIDADE NOVA DE LISBOA